REPUBLIC OF BENIN

------000------

MINISTRY OF HIGHER EDUCATION AND SCIENTIFIC RESEARCH

------000------

UNIVERSITY OF ABOMEY - CALAVI

------000------

DOCTORAL SCHOOL OF LIFE AND EARTH SCIENCES

------000------

Registered under N°: 491

A DISSERTATION

Submitted

In partial fulfillment of the requirements for the degree of

DOCTOR of Philosophy (PhD) of the University of Abomey-Calavi

In the framework of the

Graduate Research Program on Climate Change and Water Resources (GRP-CCWR)

By

Albert Elikplim AGBENORHEVI

Public defense on: 30/12/2025

Subject: Hydrology
Specialty: Climate Change and Water Resources

======

ASSESSING LAND USE/COVER DYNAMICS AND RAINFALL EXTREMES IN THE PRA CATCHMENT, GHANA: A CATCHMENT-SCALE BASELINE FOR FUTURE WATER RESOURCE IMPACT ASSESSMENT

======

Supervisors:		
Nelly Carine KÈLOMÉ	Full Professor	University of Abomey-Calavi, Benin
Leonard Kofitse AMEKUDZI	Full Professor	KNUST, Ghana.
German Advisor		
Julian KLAUS	Full Professor	University of Bonn, Germany
Reviewers:		
Philip Gbenro OGUNTUNDE	Full Professor	Federal University of Technology, Nigeria
Kwaku Amaning ADJEI	Full Professor	KNUST, Ghana
Mathieu Maurice Ahouansou	Associate Professor	University of Abomey-Calavi, Benin

JURY

Julien ADOUNKPE	Full Professor, University of Abomey-Calavi, Benin	President
Philip Gbenro OGUNTUNDE	Full Professor, Federal University of Technology, Nigeria	Reviewer
Kwaku Amaning ADJEI	Full Professor, KNUST, Ghana	Reviewer
Mathieu Maurice AHOUANSOU	Associate Professor, University of Abomey-Calavi, Bénin	Reviewer
Aymar BOSSA	Associate Professor, University of Abomey-Calavi, Bénin	Examiner
Nelly Carine KELOME	Full Professor,University of Abomey-Calavi, Bénin	Supervisor
Leonard Kofitse AMEKUDZI	Full Professor, KNUST, Ghana	Co-supervisor
Julian KLAUS	Full Professor, University of Bonn, Germany	Advisor

WASCAL West African Science Service Centre on Climate Change and Adapted Land Use
With funding from the: Federal Ministry of Research, Technology and Space

REPUBLIQUE DU BENIN

------ooo------

MINISTERE DE L'ENSEIGNEMENT SUPERIEUR ET DE LA RECHERCHE SCIENTIFIQUE

------ooo------

UNIVERSITY OF ABOMEY - CALAVI

ECOLE DOCTORALE SCIENCES DE LA VIE ET DE LA TERRE

------ooo------

Enregistrée sous N°: 491

THESE

Soumise pour obtenir le grade de

DOCTEUR de l'Université d'Abomey-Calavi

Dans la Spécialité:

Changement climatique et Ressources en Eau

Par

Albert Elikplim AGBENORHEVI

Soutenue publiquement le : 30/12/2025

Discipline: Hydrologie
Spécialité: Changements Climatiques et Ressources en Eau

======

ASSESSING LAND USE/COVER DYNAMICS AND RAINFALL EXTREMES IN THE PRA CATCHMENT, GHANA: A CATCHMENT-SCALE BASELINE FOR FUTURE WATER RESOURCE IMPACT ASSESSMENT

======

Directeurs de thèse:		
Nelly Carine KÈLOMÉ	Professeur Titulaire	Universite d'Abomey-Calavi, Benin
Leonard Kofitse AMEKUDZI	Professeur Titulaire	KNUST, Ghana.
Conseiller Allemand:		
Julian KLAUS	Professeur Titulaire	University of Bonn, Germany
Rapporteurs:		
Philip Gbenro OGUNTUNDE	Professeur Titulaire	Federal University of Technology, Nigeria
Kwaku Amaning ADJEI	Professeur Titulaire	KNUST, Ghana
Mathieu Maurice Ahouansou	Maître de conférences	University of Abomey-Calavi, Benin

JURY

Julien ADOUNKPE	Professeur Titulaire, University of Abomey-Calavi, Benin	President
Philip Gbenro OGUNTUNDE	Professeur Titulaire, Federal University of Technology, Nigeria	Rapporteur
Kwaku Amaning ADJEI	Professeur Titulaire, KNUST, Ghana	Rapporteur
Mathieu Maurice AHOUANSOU	Maître de conférences, University of Abomey-Calavi, Bénin	Rapporteur
Aymar BOSSA	Maître de conférences, University of Abomey-Calavi, Bénin	Examinateur
Nelly Carine KELOME	Professeur Titulaire,University of Abomey-Calavi, Bénin	Superviseur
Leonard Kofitse AMEKUDZI	Professeur Titulaire, KNUST, Ghana	Co-superviseur
Julian KLAUS	Professeur Titulaire, University of Bonn, Germany	Membre équipe d'encadrement

WASCAL West African Science Service Centre on Climate Change and Adapted Land Use
With funding from the: Federal Ministry of Research, Technology and Space

Dedication

This book is dedicated to God Almighty and my late father, Mr. Stanley Yao Agbenorhevi, whose guidance and selflessness have brought me thus far.

Acknowledgment

This PhD research was carried out within the framework of the West African Science Service Center on Climate Change and Adapted Land Use (WASCAL) and was funded by the German Ministry of Education and Research (BMBF), in collaboration with the Benin Ministry of Higher Education and Scientific Research (MESRS). I also gratefully acknowledge the Argelander Scholarship for PhD students from the Global South and the Hochschulrechenzentrum of the University of Bonn for enabling international collaboration and for providing access to high-performance computing facilities that supported this research. Without this support, completing this challenging and rewarding journey would not have been possible.

I would like to express my sincere gratitude to my supervisors, Prof. Nelly Carine Kèlomé (Université d'Abomey Calavi), Prof. Leonard Kofitse Amekudzi (Kwame Nkrumah University of Science and Technology), and Prof. Julian Klaus (University of Bonn). Your guidance, scientific rigor, and continuous support throughout the study profoundly shaped both this research and my academic development.

I am also thankful to the Hydrology Research Group led by Prof. Julian Klaus and the Climatology Research Group led by Prof. Leonard Amekudzi for providing data, technical support, and constructive feedback that helped strengthen this thesis. I appreciate the valuable comments and suggestions received during regular research and laboratory presentations. My gratitude also extends to the management and colleagues of the WASCAL Doctoral Graduate Study at Université d'Abomey Calavi for their support in many ways throughout my doctoral training.

Finally, and most importantly, I thank my wife, Antoinette Nweakoa Allou, and my son, Ahava Klaus Eyram Agbenorhevi, for their patience, encouragement, and constant support throughout this journey. I am deeply grateful to my mother, Florence Adzo Agbenorhevi, and my siblings for their love and understanding. I also thank Mr. Eben Yevugah, Mr. Agbetawokpor, Mrs. Amma Anto, and my friends Ernest Biney, Patrick Davies, Ernestina Annan, Flavio Odoi Yorke, and Godfred Torsah for their support and encouragement during my time away from home and throughout the course of this study.

Synthèse de la Thèse

Résumé

Dans les bassins versants tropicaux, l'impact combiné du changement climatique (CC) et du changement d'utilisation et de couverture des sols (Land Use/Land Cover, LULC) n'est pas suffisamment analysé, compromettant la gestion durable des ressources en eau et l'atteinte des Objectifs de Développement Durable. Cette étude évalue les effets conjoints du CC et du LULC sur les processus hydrologiques dans le bassin de Pra (PRB), au Ghana, afin d'établir une base de référence scientifique pour la planification et la gestion intégrée de l'eau. Une approche méthodologique intégrée a été adoptée. Elle combine (i) une revue systématique selon la méthode PRISMA, appuyée par des analyses bibliométriques et VOSviewer, pour évaluer l'état des connaissances sur les interactions climat-LULC-hydrologie à l'échelle du bassin ; (ii) l'analyse des changements historiques du LULC pour les années 2007, 2015 et 2023, ainsi que des projections futures à l'horizon 2030 et 2063, à l'aide de Google Earth Engine, Idrisi® Selva et ArcMap ; (iii) l'analyse des tendances climatiques et la projection des précipitations extrêmes selon les scénarios SSP1-2.6 et SSP3-7.0 pour la période 2021-2100 ; et (iv) l'évaluation de l'impact combiné du CC et du LULC sur le bilan hydrique du PRB. Les performances des données et des modèles ont été évaluées à l'aide d'indicateurs statistiques incluant la précision globale, le coefficient de Kappa, le NSE, le MBE et le coefficient de corrélation.
Les résultats révèlent une croissance annuelle estimeé de 9,25 % des recherches sur les liens entre climat, utilisation des terres et hydrologie, ainsi qu'une intensification de la déforestation et de la perte de végétation naturelle au profit des terres agricoles (+13 %) et des zones bâties (+3 %). Les projections climatiques indiquent un allongement potentiel des saisons des pluies, une incertitude accrue des dates de début et de fin, et une intensification des événements pluviométriques de courte durée. Sous le scénario SSP3-7.0, l'effet combiné du CC et du LULC entraînerait des pertes hydriques annuelles accrues, avec des variations mensuelles pouvant atteindre ±24 %. Ces résultats soulignent la nécessité urgente de stratégies de gestion intégrées pour renforcer la sécurité hydrique d'un bassin qui soutient les moyens de subsistance de plus de 6,2 millions de personnes au Ghana.

***Mots clé*:** Changement climatique, extrêmes hydrologiques, changement d'utilisation et de couverture des sols (LULC), bassin de Pra (PRB), Gestion des Ressources en Eau.

Introduction

La croissance démographique rapide et l'expansion urbaine en Afrique subsaharienne ont accru la demande en eau et en ressources alimentaires, entraînant une conversion généralisée de la végétation naturelle en terres agricoles (Olofintoye et al., 2022). Parallèlement, les régimes pluviométriques de la région présentent une forte variabilité spatio-temporelle, exacerbant les pressions sur les écosystèmes et les ressources en eau (Bibi et al., 2014; Owusu & Waylen, 2013). Dans ce contexte, l'utilisation et la couverture des sols jouent un rôle central dans le contrôle des processus hydrologiques des bassins tropicaux. La compréhension de la dynamique spatio-temporelle du LULC, en interaction avec le changement climatique, est ainsi essentielle pour appuyer une planification agricole efficace et une gestion durable des ressources en eau de surface et souterraines.

Problématique

Le bassin du fleuve Pra, au Ghana, constitue le quatrième bassin versant prioritaire du pays et approvisionne environ 6,2 millions d'habitants, avec un taux de croissance démographique annuel estimé à 2,2 % (Water Resource Commission, 2012). Les études récentes indiquent que ce bassin connaît une transformation rapide de l'occupation des sols, associée à l'émergence de stress hydrologiques croissants (Dossou et al., 2021; Obodai et al., 2019) , faisant de l'expansion démographique et de ses impacts une préoccupation majeure à l'échelle nationale (Attiogbe & Nkansah, 2017).

Des études antérieures indiquent que le bassin du fleuve Pra a connu six phases distinctes d'évolution de l'utilisation et de la couverture des sols (LULC), caractérisées par une augmentation marquée des zones de peuplement, des terres agricoles et des zones minières, estimée respectivement à 130 %, 198 % et 304 % entre 1986 et 2016 (Awotwi et al., 2018). Par ailleurs, Awotwi et al. (2019) ont analysé les variations saisonnières du bilan hydrique, tandis que Kankam-Yeboah et al. (2013) ont projeté une diminution du débit des cours d'eau de 22 % et 46 % à l'horizon 2020 et 2050, respectivement. De leur côté, Owusu et al. (2017) ont mis en évidence une augmentation soutenue de la demande en eau domestique et agricole entre 2000 et 2050.

Ces dynamiques ont contribué à des modifications significatives des conditions hydrométéorologiques du bassin, notamment une tendance à la réduction des précipitations durant les périodes de transition saisonnière, avant le début et après la cessation des pluies

(Awotwi et al., 2017). Toutefois, ces études ont été menées de manière isolée et se sont principalement concentrés sur le bassin versant supérieur, où sont situés les barrages de Berekese et d'Owabi, laissant le bassin versant inférieur, voire l'ensemble du bassin, largement sous-étudié (Darko et al., 2022; Loh et al., 2022; Osei et al., 2021a; 2021b; 2019). Ces études représentent une avancée significative dans la compréhension de la dynamique de l'utilisation et de la couverture des sols, des réponses hydrologiques et de la demande en eau dans le bassin.

Malgré les avancées récentes, des lacunes scientifiques majeures persistent dans l'étude des interactions entre le changement climatique, l'utilisation des terres et l'hydrologie du bassin du fleuve Pra. À titre d'exemple, Bessah et al. (2020) ont souligné la nécessité de recourir à des approches innovantes et multi-outils, intégrant la télédétection et les techniques d'apprentissage automatique, en remplacement des modèles de surface terrestre à méthode unique couramment utilisés pour la classification de l'utilisation et de la couverture des sols. Par ailleurs, la caractérisation des précipitations extrêmes et l'analyse détaillée des événements n'ont pas été systématiquement intégrées dans les études existantes portant sur les tendances pluviométriques à long terme du bassin (Awotwi et al., 2017; Bessah et al., 2020; Osei & Amoakowaah, 2021; Owusu et al., 2017; Owusu & Waylen, 2009)

En outre, les analyses des impacts du changement climatique réalisées à ce jour reposent exclusivement sur des projections issues de l'ensemble CMIP5 et de modèles climatiques régionaux, sans considérer les nouvelles données du CMIP6, qui offrent une résolution spatiale améliorée et une meilleure représentation des processus climatiques (Awotwi et al., 2021; Osei & Amoakowaah, 2021). Par conséquent, les implications des scénarios socio-économiques partagés (Shared Socioeconomic Pathways, SSP) pour le bassin du fleuve Pra demeurent largement inexplorées.

Ces insuffisances méthodologiques et conceptuelles ont des implications significatives pour la planification de l'approvisionnement en eau, la préparation aux inondations et le développement des infrastructures urbaines. En l'absence d'une évaluation rigoureuse des précipitations extrêmes et d'une compréhension approfondie des interactions terre–atmosphère fondée sur des approches avancées, les évaluations des risques hydrologiques restent limitées. Il apparaît donc nécessaire de conduire une étude intégrée à l'échelle de l'ensemble du bassin versant, portant simultanément sur les précipitations extrêmes et la dynamique de l'utilisation et de la couverture des sols, afin de renforcer la base scientifique de la gestion hydrologique, de

la réduction des risques d'inondation, de la mise en œuvre à long terme de la Gestion Intégrée des Ressources en Eau (GIRE) et des stratégies d'adaptation au changement climatique.

Zone d'étude

Le bassin de Pra est situé dans le sud-ouest du Ghana, entre les longitudes 2°30′ O et 0°30′ O et les latitudes 5° N et 7°30′ N. Il couvre une superficie d'environ 23 200 km² et présente une altitude moyenne de 300 m au-dessus du niveau de la mer, avec des valeurs extrêmes variant de 2 m à 830 m (Amekudzi et al., 2015; Awotwi et al., 2019; Bessah et al., 2020a; Osei & Amoakowaah, 2021). Administré comme le quatrième bassin prioritaire du Ghana par la Commission des ressources en eau (Water Resources Commission, WRC), le bassin englobe 41 districts administratifs répartis entre les régions Ashanti, Est, Centre et Ouest. Sur le plan géologique, le bassin est dominé par des formations précambriennes, tandis que les sols sont majoritairement constitués d'acrisols sableux limoneux, qui représentent plus de 75 % de la superficie totale (Kusimi et al., 2015; Leube et al., 1990). Le bassin est couvert principalement par une forêt humide semi-décidue et se caractérise par une forte pression anthropique liée à l'exploitation aurifère intensive, aux activités agricoles et à l'urbanisation rapide (Agbenorhevi et al., 2024). Il comprend trois principaux sous-bassins versants Offin, Birim et Main Pra ainsi qu'un lac naturel d'importance hydrologique et écologique, le lac Bosomtwe. Le climat du bassin est de type subéquatorial à influence de mousson, avec un régime pluviométrique bimodal contrôlé par la migration saisonnière de la discontinuité intertropicale (ITD). Les précipitations annuelles moyennes varient entre 1200 et 1400 mm, tandis que le débit moyen annuel est estimé à environ 214 $m^3 s^{-1}$. Les températures moyennes annuelles oscillent entre 21 °C et 32 °C, reflétant les conditions climatiques typiques des zones tropicales humides.

Matériel et méthodes

Afin d'atteindre les objectifs de l'étude, une combinaison intégrée de ressources documentaires, de données satellitaires, climatiques et de méthodes de modélisation a été réalisée. La revue systématique de la littérature a d'abord été conduite à partir de quatre bases de données scientifiques majeures ProQuest, Scopus, Web of Science et Google Scholar afin d'identifier des articles pertinents publiés entre 2006 et 2023 dans des revues à facteur d'impact élevé. La sélection des études a suivi un cadre méthodologique en quatre étapes comprenant la délimitation du champ d'étude, la planification, la recherche et la sélection des articles. La littérature relative au bassin du fleuve Pra a été examinée afin d'identifier les tendances

dominantes, les lacunes critiques et les stratégies de gestion applicables, sur la base de mots-clés et de leur pertinence directe pour le climat, l'utilisation et la couverture des sols (LULC) et l'hydrologie.

Les changements d'utilisation et de couverture des sols, classés en cinq catégories (forêt, terres cultivées/agricoles, zones bâties ou sols nus, plans d'eau et végétation naturelle), ont été analysés pour les années 2007, 2015 et 2023. Les images satellitaires Landsat 7, 8 et 9, ainsi que les données de référence au sol, ont été traitées à l'aide de l'algorithme Random Forest (RF) implémenté dans Google Earth Engine. La précision de la classification a été évaluée à l'aide de la précision de l'utilisateur (UA), de la précision du producteur (PA) et de la précision globale (OA) (Fung & LeDrew, 1988), puis améliorée par l'intégration d'indices spectraux, notamment le NDVI, le MNDWI et le BSI. Les projections du LULC à l'horizon 2030 et 2063, selon un scénario de statu quo, ont été réalisées à l'aide du modèle CA-Markov dans Idrisi® Selva.

L'évaluation de l'impact du changement climatique s'est appuyée sur les données de précipitations CHIRPS-v2, les réanalyses ERA5 du Centre européen pour les prévisions météorologiques à moyen terme (CEPMMT) et les projections multi-modèles du Climate Model Intercomparison Project Phase 6 (CMIP6) selon les scénarios SSP1-2.6 et SSP3-7.0. Les données CHIRPS-v2 et ERA5 ont été validées, tandis que les projections CMIP6 ont été réduites d'échelle et corrigées des biais à l'aide de la méthode de cartographie quantile (Quantile Mapping, QM). Les analyses statistiques incluent la corrélation (r) et l'erreur de biais moyenne (MBE). Cinq modèles climatiques CMIP6 ACCESS-CM2, EC-Earth3-Veg-LR, IPSL-CM6A-LR, MIROC-ES2L et MPI-ESM1-2-LR ont été retenus pour l'analyse des impacts et des projections climatiques. Cinq indices de précipitations extrêmes ont été utilisés pour caractériser les événements saisonniers, après vérification de la non-stationnarité des séries à l'aide des tests de Mann–Kendall modifié et de LOESS. Les dates de début et le centre de masse (Center of Mass, COM) des précipitations ont ensuite été déterminés à partir des analyses de tendances et des projections climatiques.

Enfin, le modèle hydrologique pluie-débit HBV-light a été utilisé pour évaluer les réponses du débit fluvial aux changements climatiques et à la dynamique du LULC. Le modèle a été appliqué sous une forme globalisée, calibré et validé à partir de données observées, puis évalué à l'aide de plusieurs critères de performance, notamment l'efficacité de Nash–Sutcliffe (NSE), l'efficacité de Kling-Gupta (KGE), le biais relatif (PBIAS) et le coefficient de détermination

(R^2), avant d'estimer l'impact combiné du changement climatique et du LULC sur le débit des cours d'eau.

Résultats et discussion

Résultats

L'analyse systématique et bibliométrique des publications sur le bassin du fleuve Pra révèle une moyenne de 23,63 citations par article, avec un âge moyen de 7,45 ans, illustrant une croissance annuelle rapide de 9,25 % de la production scientifique. La co-auteurisation internationale représente 32,31 %, avec un pic de publication attendu vers 2039. Les thèmes centraux incluent la qualité de l'eau, le changement climatique, la détection des changements par SIG et l'utilisation et la couverture des terres (UTCATF). Toutefois, la recherche sur l'adaptation, la résilience socio-écologique et les options d'assainissement reste limitée. Les principaux groupes thématiques UTCATF, pollution et gestion des risques hydriques montrent une intégration progressive, mais certaines lacunes persistent.

L'analyse de l'UTCATF indique qu'environ un tiers de la couverture terrestre du bassin a changé entre 2007 et 2023, avec une déforestation marquée et des pertes de végétation naturelle (NV) au profit des terres cultivées (CU/FL, +13 %) et des zones bâties (BU/BL, +3 %). Ces changements sont concentrés le long des berges et dans le nord-est (Haut et Bas Offin, Twifo Praso) ainsi que dans le nord (Oda et Haut Pra), avec une déforestation intensive dans le nord-ouest (Haut Pra, Anum et Birim). Les projections LULCC pour 2030 et 2063 indiquent que les pertes de NV et de forêt (FO) resteront les principaux contributeurs au changement net, avec des superficies de -3300 km² et ~ -2200 km² respectivement pour BU/BL et CU/FL.

L'évaluation du changement climatique montre que les années plus humides tendent à retarder le centre de masse des précipitations (CoM). Les événements extrêmes prévoient un raccourcissement de 15 à 18 jours pour le R95P et un seul pic de précipitations à l'avenir. Le Rx5day indique une augmentation des précipitations extrêmes (de 50-100 mm à 150-200 mm) surtout entre septembre et novembre (SON). Les projections futures suggèrent une intensification des sécheresses et des fortes pluies (+20 %), une incertitude accrue sur le début et la fin des saisons et une hausse des températures de 2 °C (SSP1-2.6) à 3–4 °C (SSP3-7.0).

L'impact combiné du changement climatique et du LULC sur le débit fluvial montre que l'évapotranspiration constitue le principal facteur de perte d'eau (864,88 mm, ~60 %), suivie

du ruissellement de surface (185,85 mm, ~13 %), soulignant le rôle critique des processus hydrologiques dans la gestion de l'eau du bassin.

Discussion

Les résultats révèlent une évolution de la recherche au sein du bassin du fleuve Pra (PRB), passant des évaluations de la qualité de l'eau à des études intégrées sur le changement climatique, l'utilisation et la couverture des sols (LULC) et la modélisation hydroclimatique, avec un taux de croissance annuel de 9,25 %. Cette dynamique favorise l'adoption de données satellitaires et de méthodologies avancées, telles que la télédétection et l'apprentissage automatique, pour réduire les incertitudes liées au paramétrage et à la validation des modèles (Atiah et al., 2020; Awotwi et al., 2019; Bessah et al., 2020).

Les analyses du LULC montrent un lien étroit entre les activités économiques et la dégradation environnementale. L'expansion des zones bâties et des terres agricoles au détriment des forêts et de la végétation naturelle illustre la pression exercée par l'urbanisation et l'exploitation des ressources. Les projections à moyen et long terme indiquent que la perte continue de végétation naturelle et de forêt contribuera fortement aux changements nets de couverture terrestre, soulignant l'urgence de politiques de gestion durable des terres et de renforcement de la conservation, notamment le long des berges riveraines (Agodzo et al., 2023; Bessah et al., 2020; Winkler et al., 2021).

L'analyse des impacts climatiques, basée sur les modèles CMIP6, montre leur capacité à représenter les événements extrêmes, bien que des biais pluviométriques persistent, nécessitant un affinage des méthodes de réduction d'échelle (Fuso et al., 2024; Kim & Kim, 2020). Les projections indiquent une augmentation de la fréquence et de l'intensité des sécheresses et des fortes pluies, ainsi qu'une hausse des températures pouvant atteindre 2–4 °C selon les scénarios SSP1-2.6 et SSP3-7.0. Ces conditions exacerbent les défis hydrologiques et agricoles et soulignent l'importance de stratégies adaptatives, telles que l'irrigation améliorée et les systèmes d'alerte précoce (Atiah & Muthoni, 2023; Hounkpè et al., 2022). Les simulations hydrologiques montrent que le débit moyen du bassin suit les cycles de la mousson africaine, avec des crues pendant la saison des pluies (JJA) et un débit faible en saison sèche (DJF). D'ici la fin du XXIe siècle, le débit moyen devrait diminuer de 20,8 % dans le scénario SSP1-2.6 et de 28,2 % dans le SSP3-7.0, reflétant l'impact combiné du changement climatique et du LULC.

Dans l'ensemble, ces résultats fournissent une base de référence pour comprendre l'évolution environnementale du PRB et renforcent la nécessité de politiques intégrées conciliant gestion durable des terres, adaptation au changement climatique et développement socio-économique.

Conclusion

Cette étude évalue la dynamique de l'utilisation et de la couverture des sols (LULCC) et des précipitations extrêmes dans le bassin du fleuve Pra, en examinant les tendances historiques et en projetant les évolutions futures afin de fournir une base de référence pour l'évaluation des impacts sur les ressources en eau.

Les résultats révèlent que la recherche sur le bassin est en pleine expansion, avec une croissance annuelle d'environ 9 %, bien que l'intégration des études sur le climat et le LULCC reste limitée.

L'analyse du LULCC montre une forte déforestation et une perte de végétation naturelle (NV) au profit des terres cultivées (CU/FL, +13 %) et des zones bâties (BU/BL, +3 %). Les projections futures indiquent une conversion continue de NV et de forêts (FO) en terres cultivées et zones bâties, renforçant le risque de ruissellement et de dégradation des sols.

Les analyses pluviométriques suggèrent un allongement des saisons des pluies, lié au retard du centre de masse des précipitations dans les stations clés, ainsi que des dates de début et de fin incertaines dans les zones forestières, avec une intensification des événements de courte durée.

Enfin, le débit moyen du bassin devrait diminuer au XXIe siècle, principalement en raison de l'évapotranspiration et du ruissellement de surface, augmentant potentiellement la vulnérabilité aux inondations. Ces résultats fournissent une base scientifique pour la planification de la gestion intégrée des ressources en eau et la mise en œuvre de stratégies d'adaptation au changement climatique dans le bassin du fleuve Pra.

Table of Contents

CHAPTER 1: GENERAL INTRODUCTION 1

1.1 Context and Problem Statement 1

1.2 Justification for the study 2

1.3 Literature Review 4

1.3.1 Land Use and Land Cover Changes Modelling 4

1.3.2 General Overview of the West African Rainfall Regime 7

1.3.3 Climate Change Modelling 9

1.3.4 Water Balance Modelling in a Watershed 11

1.3.5 Challenges in Water Balance Modelling and Assessment 13

1.3.6 Governance and Climate Change Management 14

1.4 Research Questions 15

1.5 Thesis Objectives 15

1.5.1 Specific Objectives 15

1.6 Hypothesis 16

1.7 Novelty 16

1.8 Scope of the Thesis 16

1.9 Expected Results and Benefits 17

1.10 Outline of the Thesis 17

CHAPTER 2: STUDY AREA 18

2.1 Basin Relief and Topography 18

2.2 Hydrology and Water Discharge 19

2.3 Hydrogeology, Aquifer Characteristics, and Groundwater Yield 20

2.4 Climate 20

2.5 Vegetation and Land Cover 21

2.6 Demography, Environmental, Social, and Economic Activities 23

2.7 Partial Conclusion 23

CHAPTER 3: DATA, MATERIALS, AND METHODS 24

3.1 Data And Materials 24

3.1.1 Metadata 24

3.1.2 Land Use Land Cover Data 25
3.1.3 Climate Data 26
3.1.4 Observed Data 27
3.1.5 CHIRPS Data 27
3.1.6 ERA 5 Data 28
3.1.7 CMIP6 data 28
3.2 Methods 29
3.2.1 State of the Art Assessment 29
3.2.2 Land Use Land Cover Change 33
3.2.3 Climate Change 41
3.2.4 Calibration and Validation of Hydrological Model 48
3.2.5 Methodological Justification and Coherence 49
3.3 Partial Conclusion 50
CHAPTER 4: STATE OF THE ART OF BASIN 52
4.1 Results 52
4.1.1 Overview of Bibliometric Parameters and Article Production 52
4.1.2 Life Cycle of Scientific Production 54
4.1.3 Country Network Collaboration on Trend Topics 55
4.1.4 Word Cloud of the Most Occurring Keywords and Trend Topics 56
4.1.5 Thematic Mapping, Evolution, and Their Factorial Analysis of Keywords 57
4.1.6 Research Interest Identified 60
4.2 Discussion 64
4.2.1 Bibliometric Parameters and Article Production 64
4.2.2 Impact of the Life Cycle of Scientific Production 65
4.2.3 Relevance of Collaboration Network on Research 66
4.2.4 Significance of Keywords to Trend Topics 66
4.2.5 Implication of Thematic Mapping, Evolution, and Factorial Analysis of Keywords 67

4.2.6 Research Trends, Gaps, Implications, and Perspectives of the State of the Basin .. 69
4.3 Partial Conclusion 70
CHAPTER 5: EVALUATION OF SPATIO-TEMPORAL LAND USE LAND COVER CHANGE 71
5.1 Results 71
5.1.1 Mapping LULC in the Basin 71
5.1.2 Accuracy Assessment 72
5.1.3 Change Detection in LULC 74
5.1.4 Transition Probability Matrix of LULC 75
5.1.5 Future land use land cover prediction 77
5.2 Discussion 81
5.2.1 Assessment of the Spatio-temporal LULC Change 81
5.2.2 Regional Comparison with the Volta Basin 81
5.2.3 Hydrological Implications of LULC Change 82
5.2.4 Environmental and Socioeconomic Implications 83
5.2.5 Policy Implications on Transition Probability 84
5.2.6 Management Implications for Water Resources 85
5.2.7 Classification Accuracy and Challenges 86
5.2.8 Partial Conclusion 87
CHAPTER 6: CLIMATE CHANGE IMPACT ON BASIN 88
6.1 Results 88
6.1.1 Validation of Datasets 88
6.1.2 Rainfall Trends (shifts-onset and CoM) 92
6.1.3 Centre of Mass and Total Annual Rainfall Correlation Analysis Across Stations .. 94
6.1.4 ENSO Impacts on Onset and CoM 96
6.1.5 Seasonal variability and trends in rainfall extreme indices over the Pra River Basin 97
6.1.6 Evaluation of the Performance of CMIP6 Models 99

6.1.7 Climate Change Projections under SSP1-2.6 and SSP3-7.0 100
6.1.8 Rainfall-PDF Characteristics Under Observed and Future Scenarios 103
6.1.9 Projected Rainfall Variability and Extreme Indices Trend (2015-2100) 105
6.1.10 Precipitation Anomaly Indices 109
6.2 Discussion 111
6.2.1 Correlation Analysis Between the Centre of Mass and the Total Annual Rainfall 111
6.2.2 Nonlinear Rainfall Onset Dynamics and Spatial Heterogeneity 112
6.2.3 ENSO Controls on Catchment Hydrology 113
6.2.4 Performance of Bias Correction 114
6.2.5 Implications of Rainfall-PDF Trends (Extremes under Future Climate Scenarios) 114
6.2.6 Impact of Change in Rainfall Seasonality and Climate Scenarios 116
6.2.7 Impact of seasonal variability and trends in rainfall extreme indices 117
6.2.8 GCMs Performance and Climate Change Implications 118
6.2.9 Precipitation Anomaly Index Implications 119
6.2.10 Implications for Basin Management 119
6.2.11 Climate Extremes and Socio-Economic Outcomes: Interconnected Risks and Implications 119
6.2.12 Adaptation Strategies for Extreme Indices 121
6.2.13 Adopting the RAI Concept for the Climatic Water Balance 121
6.2.14 Research Contributions and Future Directions 122
6.3 Partial Conclusion 122
6.4 Limitations of the Study 123
CHAPTER 7: ESTIMATION OF WATER BALANCE 124
7.1 Results 124
7.1.1 Water Balance 125
7.1.2 Climate Change Impact on Future Streamflow 126
7.2 Discussion 127

7.2.1 Performance of the HBV Model in the Pra River Catchment 127
7.2.2 Representation of Streamflow Dynamics and Hydrological Processes 128
7.2.3 Implications of Projected Climate Change on Streamflow 129
7.2.4 Implications for Water Resources Management and Basin Sustainability 130
7.2.5 Influence of Catchment Characteristics, Data, and Uncertainties in Model Structure 131
7.2.6 Partial conclusion 131
CHAPTER 8: GENERAL CONCLUSION AND RECOMMENDATION 132
8.1 Conclusion 132
8.2 Recommendations 133
8.3 Perspectives or Future Work (AGUA Project) 134
REFERENCES 139
APPENDIX 166
ANNEX 172
Annex 1: List of Publications 172
Annex 2: List of Conferences/Workshops/Training 173

LIST OF ACRONYMS

BAU	Business-As-Usual
BSI	Bare Soil Index
CCD	Cold Cloud Duration
CHIRPS	Climate Hazards Group InfraRed Precipitation with Station data
CMIP	Coupled Model Intercomparison Project
CSIR	Center for Scientific Industrial and Research
DEM	Digital Elevation Model
ECMRWF	European Centre for Medium-Range Weather Forecasts (ERA 5),
ETCCDI	Expert Team on Climate Change Detection and Indices
GCM	Global Climate Model
GEE	Google Earth Engine
GHG	Greenhouse Gas
GIS	Geographic Information Systems
GMet	Ghana Meteorological Agency,
IPCC	Intergovernmental Panel on Climate Change
IWRM	Integrated Water Resources Management
LULC	Land Use and Land Cover
LULCC	Land Use and Land Cover Change
MAE	Mean Absolute Error
MCA	Median Composite Algorithm
MKT	Mann-Kendall Test
ML	Machine Learning
MMKT	Modified Mann-Kendall Test
MNDWI	Modified Normalized Difference Water Index
NASA	National Aeronautics and Space Administration
NDVI	Normalized Difference Vegetation Index
NOAA	Climate Forecast System,
NSE	Nas–Sutcliffe Efficiency
OA	Overall Accuracy
PA	Producer Accuracy
PBIAS	Percent Bias

PRB	Pra River Basin
PRISMA	Preferred Reporting Items for Systematic Reviews and Meta-Analyses
RAI	Rainfall Anomaly Index
RCM	Regional Climate Model
RF	Random Forest
RMSE	Root Mean Square Error
ROC	Relative Operating Characteristic
SCP	Semi-Automatic Plugin
SDG	Sustainable Development Goals
SLR	Systematic Literature Review
SPI	Standardized Precipitation Index
SRTM	Shuttle Radar Topography Mission
SSP	Shared Socio-economic Pathway
SWAT	Soil and Water Assessment Tool
TM	Thematic Mapper
TOA	Top of Atmosphere
TRMM	Tropical Rainfall Measuring Mission
UA	User Accuracy
WHO	World Health Organization
WMO	World Meteorological Organization
WRC	Water Resources Commission
WRM	Water Resource Management

LIST OF FIGURES

Figure 2.1: DEM of the PRC in southern Ghana (left) with the main river network, the lake, and rainfall gauge stations. West Africa map (right) with Ghana, and the PRC (red) 19
Figure 2.2: Rainfall and temperature climatology plot of PRB (1981-2022) from CHIRPS and ERA5, respectively. (a) mean annual rainfall (b-d) temperature. 21
Figure 2. 3:Agricultural expansion and deforestation coverage in Ghana (2021) 22
Figure 2.4:Key physiographic and hydrological characteristics of the Pra River Basin, Ghana 24

Figure 3.1:Adopted methodological framework (a) data extraction from database (b) Bibliometric analysis process using Bibliometrix (R Studio) and VOSviewer software. 32
Figure 3.2: LULC Classification and RS data analysis Workflow 34
Figure 3.3: A thematic diagram of the method used for data preparation and climate analysis. 47
Figure 3.4: The HBV-light conceptual model 48

Figure 4.1:Overview of bibliometric parameters on the Pra River Basin 52
Figure 4.2:Annual article production trend on the Pra River basin. 53
Figure 4.3:Life Cycle of Scientific Production 55
Figure 4.4:Country Collaboration Network Map of research in the Pra River Basin, Ghana . 56
Figure 4.5:Word Cloud of the top 50 frequent keywords in literature under review 57
Figure 4.6:Thematic Mapping (Four Quadrants) of research keywords from the literature under review 58
Figure 4.7:Thematic Evolution of keywords showing the early phase, expansion phase and recent consolidation phase of the literature under review 59
Figure 4.8:Conceptual structure map using the Multiple Correspondence Analysis (MCA) Approach 60

Figure 5.1: LULCC map of the Pra River catchment for 2007, 2015, and 2023 72
Figure 5.2: A rate of LULC change plot for 2007-2015 and 2015-2023 of the Pra River Basin. 74
Figure 5.3: A rate of change graph for the time series 2007 to 2023 of the Pra River Basin .. 75
Figure 5.4: LULC transition probability heatmap from 2015 to 2023. The diagonal (persistence within the same land use class) and off-diagonal (transitions to other classes). .. 76
Figure 5.5: Gains and losses, and contribution of net change of LULCC in km^2 in the PRB (2015 and 2023) using Land Change Modeller (LCM) in Idrisi®Selva. 76
Figure 5.6: The actual (a) and simulated (b) LULC map of PRB in 2023 78
Figure 5.7: A 3rd cubic polynomial surface trend from forest to cultivated land (a) and Natural Vegetation to built-up/bare land (b) between 2023 and 2030. 79
Figure 5.98: Contribution to the Net change in Built-up/bare land (a) and cultivated/farmland (b) for LULC 2030 in km^2 80
Figure 5.9: LULCC in the Pra River Basin from 2007 to 2063 80

Figure 6.1: Correlation coefficient (r) of ERA 5 against GMet observed data for three gauge stations (a) Dunkwa, (b) Twifo-Praso, (c) Mfensi in the Pra River Basin. 89

Figure 6.2: Trend analysis using Sen's slope with annual precipitation on the y-axis and the duration on the x-axis for all stations 90
Figure 6.3: Rainfall trends using LOESS for all stations 91
Figure 6.4: Normalised cumulative annual rainfall plot for the twelve stations showing the onset and centre of mass (CoM). 92
Figure 6.5: The correlation coefficient of rainfall timing (Centre-of-Mass DOY) and total annual rainfall across individual stations. The red dashed line (the threshold: p = 0.05) 94
Figure 6.6: Annual rainfall onset dates and LOESS-smoothed trends in the forest belt and coastal zones stations of the Pra River catchment from 1981–2022. 95
Figure 6.7: Annual rainfall onset timing and ENSO phases (1981–2022). Red band (El Niño years), and blue bands (La Niña years) with ±0.5-year padding for clarity). 96
Figure 6.8: Seasonal analysis for the historical period (1981-2022 using the extreme rainfall indices 98
Figure 6.9: A correlation coefficient and mean bias error (MBE) of the CMIP6 model against the reference data (1981-2015) 99
Figure 6. 10: A correlation coefficient and mean bias error (MBE) plot of the monthly bias-corrected CMIP6 model against the reference data (1981-2015) 100
Figure 6.11: CMIP6 SSP1-2.6 bias correction plot of historical data showing multimodel ensemble and mean annual rainfall. 101
Figure 6.12: Projected annual rainfall under two scenarios: SSP1-2.6 (blue), SSP3-7.0 (red), and observed (black) for the future period (2015-2100) and observed (1981-2022) 101
Figure 6.13: CMIP6 Historical monthly mean temperature of the PRB (a) SSP1-2.6 (b) CMIP6 SSP3-7.0 102
Figure 6. 14:Future projection (SSP1.26 and SSP3.70) of temperature from (SSP1.26 and SSP3.70). (a) minimum (b) maximum compared to observed data (1981-2015). 103
Figure 6.15:Projected changes in the probability distribution of short- to sub-monthly rainfall at Bunso station, indicating a shift toward more frequent low-rainfall events and altered moderate- to high-rainfall probabilities under future SSP1-2.6 and SSP3-7.0 scenarios relative to observed and historical baselines. 104
Figure 6.16:Seasonal mean rainfall anomalies at each station under future SSP1-2.6 (left) and SSP3-7.0 (right) scenarios relative to observations, illustrating robust wetting in JJA but widespread drying in DJF and MAM with station-dependent SON responses. 106
Figure 6.17: Projected seasonal patterns of future CMIP6 SSP1-2.6 rainfall-extreme indices (R10mm, R20mm, Max5d, R95p, and CWD) over the Pra River Basin for 2015–2100, highlighting spatial contrasts between intensified wet extremes and changes in dry-spell duration 108
Figure 6.18: Projected seasonal patterns of future CMIP6 SSP3-7.0 rainfall-extreme indices (R10mm, R20mm, Max5d, R95p, and CWD) over the Pra River Basin for 2015–2100, highlighting spatial contrasts between intensified wet extremes and changes in dry-spell duration 109

Figure 6. 19: Projected frequency of dry and wet events for the Pra River Catchment during 2015–2100, derived from Rainfall Anomaly Index–based polar plots using the CMIP6 SSP3-7.0 multi-model ensemble. 110
Figure 6. 20: Projected frequency of dry and wet events for the Pra River Catchment during 2015–2100, derived from Rainfall Anomaly Index–based polar drought plots using the CMIP6 SSP3-7.0 multi-model ensemble. 111

Figure 7.1: Graph of Calibration and Validation of HBV model..... 125
Figure 7.2: Average annual water balance components of the Pra Basin 126
Figure 7.3: Change in seasonal streamflow for the (a) near-future (2015-2044) and (b) mid-future (2045-2074) period in relation to the historical period (1985-2014) over the Pra basin. 127

LIST OF TABLES

Table 2.1:Soil types with the corresponding area and percentage coverage 20

Table 3.1: Data acquired for systematic literature review 25
Table 3.2: A summary of data acquired for land use land cover change 26
Table 3.3: A summary of data materials used for the study 26
Table 3.4: Selected Rainfall Stations and their location in the Pra River Basin 27
Table 3.5: CMIP6 GCMS and respective institutions, horizontal resolutions 29
Table 3.6: Description of Land use land cover classes, and in-situ data points 35
Table 3.7: Selected LULC indices used for analysis. 36
Table 3.8: Indicator auxiliary variable ranges for the used LULC classification 36
Table 3.9: Land use/cover change scenarios 40
Table 3.10: Extreme rainfall characteristics indices used for the study 46
Table 3.11: The Precipitation Anomaly Indices Classification Scheme used for extreme projection. 47

Table 4.1: Overview of publication trend from 2006 to 2023. 53
Table 4. 2:Selected summary of key interest areas identified, including methods and findings 62

Table 5.1: Classified Area (km^2) and Percentage Cover of the LULC Classes from 2007 to 2023 71
Table 5.2: Area-based Error Matrix of the 2023 Classified Map with Accuracy Indices presented at 95% Confidence Interval. 72
Table 5.3: Accuracy Assessment of Pra River Basin from 2007 to 2023. 73
Table 5.4: Area statistics of actual and simulated land use/cover map of 2023 77

Table 6.1: Statistical Analysis of Rainfall Trends Using the Modified Mann-Kendall Test and Sen's Slope Method (2000–2022) 89

Table 7.1: Parameters and their ranges used for the Monte Carlo simulations 124
Table 7.2: Average monthly water balance components values (2004-2011) for the Pra basin 125

CHAPTER 1: GENERAL INTRODUCTION

The general introduction provides a general overview of the thesis. It describes the content of the dissertation, beginning with the context and the problem raised in Section 1.1. Section 1.2 justifies why the work is carried out. Section 1.3 is the literature review, detailing land use land cover changes (LULC), characteristics of climate, including rainfall and temperature from the regional to local level, climate change, and governance for climate action. Section 1.4 focuses on the research questions, while sections 1.5 to 1.7 highlight the objectives, hypothesis, and novelty of the research. The scope of the thesis is detailed in Section 1.8, and the expected results are discussed in Section 1.9.

1.1 Context and Problem Statement

The Pra River Basin in Ghana is the second largest catchment, supporting approximately 6.2 million people, with an annual growth rate of 2.2% (Water Resource Commission, 2012). Recent national concerns are that the basin demographic expansion has intensified land use pressure through settlement expansion, agriculture, and mining activities. This has resulted in widespread landscape modification (Agbenorhevi et al., 2024).

Past studies indicate the basin underwent six distinct land use/land cover phases with settlement, cropland, and mining areas increasing by 130%, 198% and 304%, respectively, between 1986 and 2016 (Awotwi et al., 2018). The report of Attiogbe & Nkansah (2017) identified deforestation and land degradation as dominant impacts arising from intensified surface mining in the Birim North subcatchment. These changes have contributed to significant shifts in hydrometeorological conditions, including a decreasing trend in post-cessation and pre-onset rainfall during February and March across the basin (Awotwi et al., 2017).

Other existing research at the PRB has addressed LULC dynamics, water balance modelling, and rainfall trends analysis in isolation. Awotwi et al. (2019) modelled water balance changes showing reduced runoff during dry seasons and increased baseflow during wet seasons. Kankam-Yeboah et al. (2013) projected 22% and 46% streamflow declines for the 2020s and 2050s, respectively, using SWAT modelling. Additionally, Owusu et al. (2017) reported an increasing domestic and agricultural water demand from 2000 to 2050, with pronounced pressure around the Kumasi Metropolitan Area. However, these studies are concentrated on the upper catchment, where the Berekese and Owabi dams are located, leaving the lower catchment,

or the entire catchment, understudied (Darko et al., 2022; Loh et al., 2022; Osei et al., 2021a; 2021b; 2019).

These findings indicate a basin undergoing rapid land surface transformation, coupled with emerging hydrological stress driven by unregulated land use activities (Dossou et al., 2021; Obodai et al., 2019). However, critical gaps remain. Most classifications relied on single-method land surface models rather than multi-tool approaches combining remote sensing with machine learning, and accuracy assessments were often inadequate (Bessah et al., 2020). Unregulated settlement expansion and intensified mining activities have contributed to recurrent flooding driven by short-duration and high-intensity rainfall events (Fowler et al., 2021). However, rainfall event analysis and flood forecasting remain understudied. Also, existing rainfall studies focus predominantly on long-term trend analysis rather than rainfall extreme characterisation, despite reported increases in annual totals across parts of the basin (Awotwi et al., 2017; Bessah et al., 2020; Osei & Amoakowaah, 2021; Owusu et al., 2017; Owusu & Waylen, 2009). Furthermore, other studies show inconclusive findings regarding rainfall variability trends, with some either indicating increases or decreases (Awotwi et al., 2021; Kankam-Yeboah et al., 2013). There is also limited research on future climate change impacts in the basin (Awotwi et al., 2021; Osei & Amoakowaah, 2021). This is because the climate impact studies done about the basin focused mainly on high flows and rely on CMIP5-based projections and regional climate models. The newer CMIP6 ensemble (Eyring et al., 2016) offers higher spatial resolution than many regionally downscaled CMIP5 products, including CORDEX RCM outputs, but its implications for the basin remain unknown.

These gaps have significant consequences for water supply planning, flood preparedness, and municipal infrastructure development. Without robust rainfall extreme assessment and an improved understanding of land-atmosphere interactions from advanced methodological approaches, hydrological risk assessments remain weak. A comprehensive, catchment-scale investigation of rainfall extremes alongside LULC dynamics is therefore required to strengthen the scientific basis for hydrological management, flood risk reduction, and long-term IWRM policy implementation and climate adaptation.

1.2 Justification for the study

The Pra River Basin (PRB) is experiencing increasing hydroclimatic pressure arising from population growth, expansion of artisanal and industrial mining, agricultural intensification,

and rapid urban development. These pressures are occurring within a climatically sensitive basin that plays a critical role in Ghana's water supply, energy production, and ecosystem services. Under such conditions, water planners and managers require reliable, basin-specific hydrological and climatic information to support sustainable development and climate-resilient infrastructure planning.

Despite the basin's importance, significant gaps remain in the integrated assessment of land use and land cover (LULC) change and rainfall extremes at the catchment scale. Existing studies have often examined these drivers in isolation or at broader spatial scales, limiting their relevance for basin-level flood risk assessment, drought preparedness, and water resources management. By explicitly examining LULC–rainfall extreme interactions within the PRB, this study addresses a critical gap in understanding how land transformations and changing rainfall characteristics jointly influence hydrological behaviour.

The establishment of a basin-specific rainfall extreme baseline using robust statistical techniques provides an essential reference for flood forecasting, peak flow estimation, and drought early warning. In addition, the application of multi-tool approaches combining remote sensing, machine learning classification, and comprehensive accuracy assessment addresses limitations associated with earlier single-method LULC studies, thereby improving the reliability of land surface representation.

This study further responds to the need for a robust historical baseline before the application of CMIP6-based climate projections and hydrological simulations. Meaningful impact assessment and scenario analysis depend on a sound characterisation of historical LULC dynamics and rainfall variability against which future changes can be evaluated. Without such a baseline, hydrological model outputs and climate impact assessments remain poorly constrained.

Overall, this work provides a spatially explicit, multi-period foundation that strengthens basin-scale hydroclimatic understanding and directly supports future hydrological modelling, climate impact studies, and evidence-based adaptation planning for one of Ghana's most critical river basins. The study aligns with national water resources management priorities, including the objectives of the Integrated Water Resources Management (IWRM) framework.

1.3 Literature Review

The literature overview focused on land use changes, the general overview of the West African rainfall regime, water availability, climate change data, and analysis. It also reviewed in detail the climate change projections over Ghana, focusing on rainfall and temperature.

1.3.1 Land Use and Land Cover Changes Modelling

Land use change represents one of the most visible transformations in cultural landscapes worldwide, primarily influenced by anthropogenic activities and global climate dynamics (Bormann et al., 2009; Kim, 2016). Land use and land cover (LULC) play a crucial role in the global carbon cycle, acting as both sources and sinks of carbon (Kim, 2016). Understanding LULC dynamics, particularly within water basins, is essential for promoting sustainable ecosystem development (Hegazy & Kaloop, 2015; Lambin et al., 2003; Obodai et al., 2019; Penman, 2003). The Intergovernmental Panel on Climate Change (IPCC) has established six primary land use categories essential for effective classification: forest land, grassland, cropland, wetland, settlement, and other lands (Allan, 2023). However, these categories may not be sufficient for accurately identifying water bodies within inland water surfaces, highlighting the necessity for more refined classification methodologies (Li et al., 2021)

In recent decades, rapid and unprecedented LULC changes have been particularly pronounced in developing nations, where urban expansion, land degradation, and the repurposing of agricultural land for alternative uses, such as shrimp farming, have intensified. These changes often result in significant environmental consequences, including habitat destruction and soil depletion (Dossou et al., 2021; Ghansah et al., 2021; Lambin et al., 2003; Stanturf, 2015). In conjunction with socio-economic pressures and climate variability, land use changes are expected to significantly impact river catchments, altering water balances and affecting ecosystem resilience (Bormann et al., 2009).

Accurate LULC data is essential for informed land use planning to meet growing demands for natural resources while ensuring human welfare and environmental sustainability (Guidigan et al., 2019). Within land change science, integrating Remote Sensing (RS) and Geographic Information Systems (GIS) has emerged as a robust approach to land and resource management (Roshani et al., 2022). By utilising satellite imagery and advanced data processing techniques, researchers can effectively monitor and reconstruct human activities on Earth's surface. This hybrid assessment system integrates diverse environmental indicators into a comprehensive analytical framework (Dossou et al., 2021).

Long-term remote sensing imagery provides invaluable insights into LULC changes, making it an indispensable tool for assessing both the positive and negative impacts of human activities on the environment (Li et al., 2023; Obodai et al., 2019; Sridhar & Sathyanathan, 2020). Numerous studies emphasise the efficacy of GIS and RS in tracking LULC changes, particularly in regions experiencing intensive mining operations, where environmental degradation poses significant concerns (Aleissaee et al., 2023; Awotwi et al., 2018; Duncan et al., 2018; Obodai et al., 2019; Wemegah et al., 2020). As global environmental pressures and human demands continue to rise, accurately tracking and managing LULC is becoming increasingly vital for sustainable development. The application of advanced tools like GIS and RS facilitates comprehensive land use analysis, fostering informed decision-making processes that balance human needs with ecosystem conservation.

Classification of Land Use and Land Cover

Advancements in Remote Sensing (RS) and Geographic Information Systems (GIS) have significantly enhanced the ability to monitor dynamic changes in the Earth's surface, including alterations in LULC. LULC classification involves the categorisation of land surface features represented as pixels in satellite imagery based on their spectral properties through computational algorithms. This classification provides critical insights into environmental dynamics and ecosystem transformations.

Two primary approaches to LULC classification exist: Supervised Classification and Unsupervised Classification (Sathya & Abraham, 2013). In supervised classification, the process is guided by user-defined parameters, including the specification of LULC categories and the selection of reference areas known as training data or ground truth data (Lillesand et al., 2015). Given its reliance on user-defined training data, supervised classification typically yields highly accurate and detailed LULC maps. Conversely, unsupervised classification utilises algorithms to independently detect LULC categories without predefined training data (He et al., 2017; Maxwell et al., 2018). While this method is generally less precise than supervised classification, it is particularly useful for exploratory analyses.

LULC Datasets and Classification Algorithms

Satellite imagery serves as the fundamental input for LULC classification, varying based on the governing organisation, intended application, and spatial and temporal resolutions. The development and deployment of various satellite missions have facilitated improved LULC data

acquisition. One of the most extensive and longest-running satellite programs for land and coastal area monitoring is the Landsat series, jointly managed by the United States Geological Survey (USGS) and the National Aeronautics and Space Administration (NASA). launched in 1972, the Landsat program has since launched multiple satellites, with spectral bands extending up to 11 (excluding the failed sixth band). Landsat imagery is widely used in global LULC mapping, offering moderate spatial resolutions of 15 m, 30 m, and 60 m, depending on the specific satellite. Another notable dataset is the Copernicus Global Land Service (CGLS), operated under the European Union's flagship Copernicus program in collaboration with the European Space Agency (ESA). CGLS provides biophysical variables such as the Leaf Area Index and Soil Water Index to monitor land surface evolution, including vegetation and water bodies. It offers spatial resolutions ranging from 50 m to over 1 km. Additionally, the Global Land Cover Characterisation Database, maintained by USGS, provides LULC classification at a spatial resolution of 1 km with 24 predefined categories, widely utilised in West Africa (Olofintoye et al., 2022).

LULC classification employs various computational algorithms, including Maximum Likelihood Classification (MLC), Support Vector Machines (SVM), and Decision Trees, such as Random Forests. The Random Forest algorithm is an ensemble learning technique that enhances classification accuracy, particularly on complex and non-linear datasets (Belgiu & Drăgu, 2016). It constructs multiple decision trees using randomly sampled data and determines the final classification based on the aggregate decision of these trees. Random Forest is less prone to overfitting and efficiently processes large datasets, even when handling missing data. However, its accuracy is contingent upon the quality of input data, including satellite imagery and training datasets.

The training dataset is typically partitioned into two subsets: training data (approximately 70%) and validation data (30%), with the latter reserved for accuracy assessment. The performance of LULC classification is evaluated using metrics such as Overall Accuracy (OA), Producer's Accuracy (PA), and User's Accuracy (UA). Additionally, error quantification methods, including quantity disagreement and allocation disagreement, have been proposed to complement traditional metrics like the kappa statistic, which has been found inadequate for accuracy assessments (Gilmore Pontius et al., 2011; Obodai et al., 2019).

When analysing multiple classified maps, changes in LULC categories over time and space can be quantified using measures such as absolute change, relative change, and rate of change. These assessments provide critical insights into land transformation trends and facilitate effective environmental planning and resource management.

1.3.2 General Overview of the West African Rainfall Regime

The West African climate is known for its instability, exhibiting significant interannual and multi-decadal variability (Owusu & Waylen, 2009). A strong or weak Tropical Easterly Jet (TEJ) or African Easterly Jet (AEJ) influences rainfall in West Africa by promoting upper-level divergence and sustaining a robust Hadley-type overturning circulation (Nicholson & Grist, 2001). Studies have shown that positive or negative phases of these jets result in increased or decreased rainfall over West Africa, respectively (Camberlin et al., 2001; Nicholson & Grist, 2001).

This variability poses serious threats to livelihoods in countries like Ghana, which rely primarily on rain-fed agriculture and are dependent on rainfall for all socioeconomic activities. The impact of rainfall variability on Ghanaian climate indices has revealed a decreasing trend in consecutive wet days across the Savannah, Transition, and Coastal zones. In contrast, an increasing trend is observed in the Forest zone (Atiah et al., 2020). Furthermore, these trends in wet indices over Ghana have been positively correlated with Atlantic Ocean sea surface temperature variability and negatively correlated with Pacific and Indian Ocean sea surface temperature variability (Aryee et al., 2018; Atiah et al., 2021).

Water Availability

In light of global warming, it is vital to estimate the influence of climate change on evapotranspiration to develop realistic water and energy budgets (Ajjur & Al-Ghamdi, 2021). Despite broad recognition of Africa's widespread water shortages, accurate spatial and temporal data on freshwater availability are still scarce (Schuol et al., 2008). Domestic drinking water supplies are also susceptible to disruptions, and low per capita domestic water supply has been widely documented among African homes. Although international monitoring frameworks increasingly incorporate water availability indicators, the methodologies applied to measure and track freshwater availability in Africa remain inconsistent and insufficiently defined (Thomas et al., 2020).

Although there is a significant positive trend in the temperature time series, it is anticipated that the entire rainy season would be shortened in West Africa (Kunstmann et al., 2004). anticipated that the entire duration of the rainy season would be shortened in West Africa. Ajjur & Al-Ghamdi (2021) applied Penman and Budyko techniques to climate data from the sixth phase of the Coupled Model Intercomparison Project (CMIP6) to examine evapotranspiration and water availability evolutions throughout the Middle East and North Africa (MENA) in the twenty-first century. The results indicate that the MENA region is sensitive to temperature increases, which can lead to higher evapotranspiration losses and decreased water availability. The analysis predicted a lack of available water (precipitation minus actual evapotranspiration), which is concerning for most MENA regions. Under SSP2-4.5, the annual water availability drop could reach 26 mm by 2100 compared to the reference period (1981-2010), and under SSP5-8.5, it could reach 62 mm.

Jankowska et al. (2012) conducted a spatial modelling of water availability, malnutrition, and livelihoods in Mali, Africa, linking 14,238 children to livelihoods and each malnutrition indicator in the Demographic and Health Survey (DHS), as well as to connect climate and stunting. If morbidity levels remain constant, projections indicate that by 2025, nearly 250,000 children in this increasingly desertified zone will be stunted, close to 200,000 will be malnourished, and more than 100,000 will suffer from anemia. Faramarzi et al. (2013) highlight the impact of climate change on freshwater availability in Africa at the sub-basin scale for 2020-2040, showing that uncertainties are greater in dry regions than in wet regions. This adds further pressure on agriculture in already water-stressed areas, where irrigation will become increasingly vital to stabilize and enhance food production. Ahmed et al. (2014) report several key findings: (1) large parts of Africa are experiencing statistically significant changes in terrestrial water storage (TWS), ranging from +44 mm/yr to -15 mm/yr, due to natural and anthropogenic factors; (2) warming in the tropical Atlantic Ocean has intensified monsoons and increased precipitation and TWS over western and central Africa; (3) warming in the central Indian Ocean has reduced precipitation and TWS over eastern Africa; (4) flooding has increased TWS in the Zambezi and Okavango basins; (5) fossil groundwater extrction has decreased TWS in the Saharan aquifers; (6) deforestation has reduced TWS in three sub-basins. Collectively, these trends raise serious concerns for the continent’s water security.

Falkenmark (1989) stressed the urgent need to improve the quality of life and food security in Africa's semiarid countries, despite the environmental constraints of hydroclimatically-driven

water scarcity and significant interannual variability in freshwater supply. Furthermore, water is unlikely to meet the needs of Africa's growing population in the medium term. Strengthened awareness and understanding among African leaders are therefore essential to guide development policies under severe water constraints. Without such measures, the continent risks falling into a multi-risk spiral, with recurrent collapses during drought years.

1.3.3 Climate Change Modelling

Climate change and population increase have significantly stressed surface water resources in recent decades. To examine future climatic conditions, scientists employ both theoretical and observational models, with General Circulation Models (GCMs) being among the most reliable physics-based theoretical models (O'Neill et al., 2016). Although GCMs are comprehensive, their large scale presents certain drawbacks. To address this, various downscaling procedures, including dynamic and statistical methods, are used to adapt these models to smaller scales (Guo & Wang, 2016; Wilby & Wigley, 1997). Dynamic downscaling often employs tools like Ferret, Jupyter Notebook, or CDO, while statistical downscaling can be effectively performed using the Statistical Downscaling Model (SDSM) developed by Wilby et al. (2014) and Wilby & Dawson (2013), which considers daily minimum and maximum temperatures, precipitation, and sunshine hours or solar radiation.

For a deeper understanding of climate change, the Coupled Model Intercomparison Project Phase 6 (CMIP6) has produced the most recent simulations of past, present, and future climates. These models offer significant improvements over the CMIP5 models, including higher resolution and enhanced physics (Xin et al., 2020). Recent developments in climate research have led to the creation of new pathway scenarios, known as Shared Socio-economic Pathways (SSPs). These scenarios illustrate changes in climate and global socio-economic conditions, categorised from SSP1 to SSP5, and are depicted as SSPx-y, where x represents the SSP and y indicates the radiative forcing in 2100 (Gupta et al., 2020; O'Neill et al., 2016). SSP1 represents Sustainability (the green road to low challenges to mitigation and adaptation). SSP2 represents the Middle of the road (where challenges to mitigation and adaptation are neither low nor high). SSP3 also represents Regional rivalry (a rocky road with high challenges to mitigation and adaptation). SSP4 is for Inequality (a road divided into low challenges to mitigation, high challenges to adaptation), and SSP5 represents Fossil-fueled development (taking the highway where high challenges to mitigation, low challenges to adaptation). To standardise GCM designs and distribute simulated models, various organizations have collaborated to utilize

groups of climate model outputs, which have become essential in guiding global climate research (Thorne et al., 2017). Rapid population growth and industrial expansion significantly impact greenhouse gas (GHG) emissions, necessitating the continuous update of emission scenarios. Most climate studies have traditionally used CMIP3 or CMIP5 outputs to assess regional climate changes. However, the current study focuses on CMIP6, aiming to address key questions about Earth's response to various pressures, the origins and effects of organized models, climate change quantification, and scenario uncertainty. Compared to CMIP5, CMIP6 models feature more vertical layers, leading to more accurate stratosphere simulations and a broader range of potential scenarios, including new ones such as SSP1-1.9, SSP4-3.4, and SSP3-7.0, alongside updates of CMIP5 scenarios (Gupta et al., 2020).

Climate Change Projections

The Intergovernmental Panel on Climate Change (IPCC) has predicted with high confidence that global mean temperatures will rise by 1 to 3°C above 1990 levels by the end of this century due to increasing GHG emissions from human activities (Houghton, 2000). This temperature rise will benefit some regions while causing significant damage and costs in others. Africa, in particular, is highly vulnerable to the impacts of climate change, attributed to its high poverty levels, low adaptive capacity, reliance on rain-fed agriculture, and weak institutional and economic structures (Antwi-Agyei et al., 2015).

Projections from the Coordinated Regional Climate Downscaling Experiment (CORDEX) ensemble indicate temperature increases of 1.5°C and 2°C in Africa under different global warming levels (Nikulin et al., 2018). Simulations using CORDEX-Africa and COSMO-CLM models demonstrate high agreement between GCMs and Regional Climate Models (RCMs) (Dosio & Panitz, 2016). Additionally, CORDEX estimates suggest a decrease in the number of wet days across most of Africa during the twenty-first century, with Eastern Africa, the Central and Eastern Sahel, and the Sahel showing a tendency for wetter conditions (Tamoffo et al., 2019). This underscores the new significance of climate change research in Africa, where temperatures are expected to rise faster than the global average, coupled with notable regional anomalies (Lennard et al., 2018).

Climate Projections over Ghana

Ghana signed the United Nations Framework Convention on Climate Change (UNFCCC) during the Rio de Janeiro Earth Summit in June 1992, after the Convention was established on

May 9, 1992, to address climate change (Asante & Amuakwa-Mensah, 2015). Three primary physical effects of climate change in Ghana have been identified: temperature change, rainfall change, and sea level rise (Asante & Amuakwa-Mensah, 2015).

Temperature Change Projections

The Ghanaian Ministry of Environment, Science, Technology, and Innovation (MESTI) projected an average temperature increase of 0.6°C by 2020, 2.0°C by 2050, and 3.9°C by 2080 (Asimah, 2013). Similarly, the World Bank (2010) forecasted a steady temperature rise across all regions of Ghana between 2010 and 2050, with the northern sector experiencing the highest increases of up to 2.2–2.4°C, resulting in average temperatures reaching approximately 41°C. Additional studies support these projections, indicating continuous temperature increases through 2050 and 2080 (Stanturf, 2015). These national trends align with global estimates from the Intergovernmental Panel on Climate Change (IPCC), which emphasises that the warming of the climate system is unequivocal, backed by extensive evidence of rising global air and ocean temperatures (Field et al., 2012).

Rainfall Change Projections

Unlike temperature projections, rainfall projections exhibit significant variability, with some models predicting reductions and others indicating potential increases (Mcsweeney et al., 2010). The World Bank (2010) anticipates that Ghana will experience annual rainfall variations ranging from a 9% decline under a global wet scenario to a 14% reduction under a Ghana dry scenario across all agroecological zones. Amekudzi et al. (2015) observed rainfall fluctuations, reporting a 2- to 8-year variability in the onset and cessation of rainy seasons across Ghana's coastal, forest, and transition zones, highlighting the increasing unpredictability of precipitation patterns.

1.3.4 Water Balance Modelling in a Watershed

Hydrological models are essential for understanding watershed processes because direct measurements are often limited by scale mismatches, data gaps, and measurement errors (Beven, 2001). These models support the analysis of water balance components and enable scenario-based assessments such as flood forecasting and climate change impact studies. Numerous models have been developed to address different water resources questions. However, their performance is constrained by uncertainties arising from input data quality,

model structure, parameter estimation, and human-related errors, which limit the accurate representation of watershed processes (Cornelissen et al., 2013).

Types of Hydrological Models

Hydrological models differ in structure and complexity, which influences their suitability for specific applications. Based on their mathematical formulation, models are commonly classified as deterministic or stochastic. Deterministic models produce a unique output for a given input, whereas stochastic models account for randomness and may generate varying outputs for the same input conditions. Models are also distinguished by how physical processes are represented. Physically based models describe hydrological processes using physical laws, while conceptual models rely on simplified representations of these processes. Quasi-physical models combine elements of both approaches. With respect to spatial representation, hydrological models may be lumped, distributed, or semi-distributed. Lumped models treat the watershed as a homogeneous unit with spatially averaged parameters. Distributed models explicitly represent spatial variability in basin characteristics and processes, while semi-distributed models divide the basin into sub-units that are treated individually but internally lumped (Hounkpè & Diekkrüger, 2018). Although distributed models provide greater spatial detail, they require extensive data and computational resources and often introduce higher uncertainty due to increased complexity (Jajarmizad et al., 2012).

Hydrological Models Applied in West Africa

Several hydrological models have been applied in West Africa to support water resources assessment. The Soil and Water Assessment Tool (SWAT) is a widely used continuous semi-distributed model designed to simulate surface and groundwater processes and assess the impacts of land use and climate variability (Arnold et al., 1998). It requires meteorological, soil, elevation, and land use data as core inputs. Other models include the UHP HRU model developed for application in Benin (Cornelissen et al., 2013) and the Water Flow and Balance Simulation Model (WaSiM), a fully distributed model that simulates hydrological processes above and below the land surface using gridded meteorological, soil, and land use data (Schulla, 2014). WaSiM has been applied in climate and land use change impact studies. The Water Evaluation and Planning System (WEAP) has been used primarily for water allocation and demand assessment in transboundary river basins (Höllermann et al., 2010). Conceptual models such as GR4J, one-dimensional SVAT models, and event-based models such as HEC HMS have also been applied across African watersheds. These models generally rely on rainfall,

temperature, evapotranspiration, soil properties, topography, and discharge data (Nounangnonhou et al., 2018).

More recently, Artificial Intelligence approaches, including machine learning techniques, have been introduced into hydrological modelling. These methods are particularly useful for pattern recognition and prediction in data-limited regions and have been applied in soil and water quality assessments, where conventional modelling approaches are constrained (Werther et al., 2021)

1.3.5 Challenges in Water Balance Modelling and Assessment

Challenges in Water Balance Modelling

Despite its importance, water balance modelling is affected by several limitations. A major challenge is the limited availability of long-term, high-resolution observational data for key hydrological variables such as precipitation, streamflow, soil moisture, evapotranspiration, and land use. Available datasets are often inconsistent due to equipment limitations and human errors, which reduce model reliability. Remote sensing products have improved environmental monitoring and data availability (Odusanya et al., 2021). However, their use introduces additional uncertainties related to spatial resolution, temporal coverage, and retrieval biases. Integrating satellite products with ground observations can improve model performance, but uncertainties remain (Bodjrènou et al., 2023). The choice of spatial and temporal scale also influences water balance assessment. Large-scale assessments capture broad trends but may overlook localised processes relevant for basin-level management. Similarly, long-term analyses provide insights into variability and stability that may not be evident in short-term assessments.

Uncertainties in Water Balance Assessment

Uncertainty in water balance assessment arises from model structure, parameterisation, and input data. In models such as SWAT, simplified assumptions about catchment processes may lead to deviations from observed conditions (Bailey et al., 2020). Model sensitivity to climate inputs further complicates calibration and validation, particularly in data-scarce regions. These uncertainties are amplified by rapid climate and land use changes in West Africa. Climate models differ in their representation of future emissions, precipitation, and temperature trends, leading to divergent projections (Lawin et al., 2019). As a result, long-term assessments of water balance and hydrological responses remain subject to considerable uncertainty.

1.3.6 Governance and Climate Change Management

Although climate change is a global concern, its local consequences are particularly severe in developing nations like Ghana. The country, classified as a lower-middle-income economy (Federal Ministry for Economic Cooperation and Development, n.d.), is one of Africa's most vulnerable nations to climate change impacts (World Bank, 2021). Ghana's vulnerability stems from a combination of political, geographic, and socioeconomic factors, ranking 109th out of 181 nations in the 2020 ND-GAIN Index (World Bank, 2021). Despite emitting approximately 42 million tonnes of greenhouse gases (a modest fraction of Africa's 4% contribution to global emissions), Ghana has experienced substantial climate-related disasters over the past five decades. Water-related events, including floods and droughts, have been the most frequent, with at least three major droughts and 19 floods affecting over 16 million people and causing at least 444 deaths, excluding undocumented drought-related fatalities (Armah, 2010; Government of Ghana, 2007; Okyere, 2018). From EM-DAT, the financial losses due to extreme weather events in Ghana exceeded $119.6 million between 1968 and 2016, with unreported damages further exacerbating the situation (Shen & Hwang, 2019).

Historically, Ghana has relied on organizational, infrastructural, and engineering approaches to address climate and water-related challenges, often overlooking the role of effective governance in managing natural resources (Young et al., 2020). Weak governance structures, influenced by internal and external political economy complexities, have contributed to inefficient climate change and water management responses. Studies highlight governance failures as a primary driver of water insecurity and ineffective climate change adaptation in Ghana. Key issues include insufficient government prioritization of water management, weak regulatory frameworks, ineffective institutional coordination, inadequate stakeholder engagement, and poor service delivery (Cooper, 2018; Young et al., 2020).

Recent research increasingly frames climate change and water security as governance challenges rather than purely technical or infrastructural issues. Water experts, policymakers, and practitioners emphasise the importance of governance in mitigating climate-related risks (Araral & Wang, 2013; Özerol et al., 2018). The World Water Development Report (WWAP, 2020) underscored the strong interconnection between climate change and water management, identifying poor governance as a critical barrier to sustainable water access and climate adaptation. Governance failures limit the availability of freshwater resources and obstruct access to climate adaptation resources, disproportionately affecting marginalized communities

and low-priority economic sectors (Sinharoy et al., 2019). In many developing nations, ineffective governance has intensified debates around economic water scarcity, where access to water is hindered not by physical shortages but by institutional, economic, and political barriers. Addressing these governance deficiencies is essential for ensuring long-term climate resilience and sustainable water resource management in Ghana and other vulnerable regions.

1.4 Research Questions

To achieve these goals, the study answers the following questions:

i. What key drivers (past, present, and future) are significant to the Pra River Basin management?
ii. What LULC changes have taken place in the PRB in the past under different scenarios?
iii. How do the probability distributions, as well as the onset and cessation of seasonal rainfall and standard extreme rainfall indices, vary over time in the basin?
iv. How are these LULCC dynamics and rainfall extremes projected to change under future climate and LULC scenarios?
v. Based on existing hydrological-impact studies, what are the likely implications of the observed and projected LULCC and rainfall extremes for hydrological processes, hydrological extremes, and water-resources planning in the Pra River Basin?

1.5 Thesis Objectives

This study identifies and examines the drivers of hydrological change at a catchment scale to establish a clear baseline of their impact on hydrological processes and water resources.

1.5.1 Specific Objectives

To test these questions, we pursued three specific objectives:

1. To assess current knowledge on the drivers of hydrological change at a basin scale in an Anthropogenic climate change era, with a focus on establishing the basis for testing whether the basin exhibits significant changes.
2. To evaluate the spatio-temporal changes in historical LULC and projected future patterns for the catchment
3. To assess climate change impacts on rainfall extremes, seasonal variability, onset–cessation behaviour linked to ENSO, and future rainfall shifts under projected climate scenarios.
4. Assess the combined effect of LULC and climate change on water balance.

1.6 Hypothesis

To achieve the objectives, the following hypotheses linked to the research objectives were tested.

i. LULC in the PRB has changed significantly over the study period, with measurable shifts among classes, and similar trajectories are projected under future scenarios.
ii. Land use and land cover changes significantly vary spatiotemporally within the basin, with projected trends indicating further disruption under future scenarios.
iii. The distributions of short-duration rainfall extremes, as well as the onset and cessation dates and seasonal rainfall indices, exhibit statistically significant temporal changes consistent with regional climate variability and change.
iv. What changes in water balance have been influenced by LULC and climate change?

1.7 Novelty

The main novelty of this research lies in providing the first integrated, catchment-scale baseline for the Pra River Basin that couples detailed multi-temporal LULC dynamics with a systematic characterisation of rainfall extremes using the CMIP6 model. This serves as a scenario-based driver baseline that future models can directly adopt. Additionally, the work as a catchment-scale baseline for future water resource impact assessment is in line with the national calls for better data to support river basin planning in Ghana (Agodzo et al., 2023). This further goes to directly bridge the diagnostic gap between scattered academic studies and the information that basin managers need for anticipatory, scenario-informed decision-making.

1.8 Scope of the Thesis

This thesis examines the impact of Global Change on a nested tropical ecosystem, and insights from the Pra River Basin in Ghana, West Africa. A conceptual understanding of the basin was developed through state-of-the-art research to identify key areas of interest, research gaps, and recommendations for future studies. Building upon this foundation, trends in land use and land cover (LULC) changes are evaluated and also forecasted using an integrated multi-tool approach, which incorporates high-resolution satellite imagery, remote sensing techniques, and machine learning-based classification. The study further projects the implications of rainfall variations on the basin by examining future hydro-climatic extremes under two shared socio-economic pathways (SSP1-2.6 and SSP3-7.0). This research contributes to understanding the interactions between climate and land dynamics, offering a data-driven approach to enhance climate resilience and sustainable water management strategies for all basins in the tropical region.

1.9 Expected Results and Benefits

The study's findings will include (i) identifying the research interests on the basin and gaps for future research. (ii) spatio-temporal trends of the land use land cover changes. (iii) forecast of land use land cover changes under scenarios (business-as-usual) (iv) shifts in rainfall seasonality trends and forecasting of extremes (v) assess the reliability of CMIP6 and satellite data for a data-scarce nested tropical environment, and (vi) performance of CMIP6 data in extreme projection (vii) determine the impact of CC and LULC on water balance.

1.10 Outline of the Thesis

This thesis is systematically structured into eight chapters.

Chapter 1 provides the background, problem statement, literature review, research questions, goals and objectives, hypotheses, novelty of the research, scope of the study, expected outcomes, and the overall thesis structure.

Chapter 2 describes the study area, detailing its physical characteristics, including geographical location, vegetation, climate, hydrogeology, soil, land use, and the environmental, social, and economic activities within the region.

Chapter 3 presents the data sources, data collection procedures, and the methodologies adopted for the study, including the analytical frameworks employed.

Chapters 4 to 7 discuss the results and findings, focusing on metadata analysis, land use land cover change analysis, climate impact assessment, and water balance results.

Chapter 8 presents the general conclusions and provides recommendations for policy, management, and future research directions, and lastly, the various references, including annexes, publications, and conference or workshop materials, during the research period are presented.

CHAPTER 2: STUDY AREA

Chapter 2 describes the research areas. The first section discusses the relief and topography of the basin. The second covers the hydrology and water discharge. The third section addresses the hydrogeology, aquifer characteristics, and groundwater yield. The climate of the basin is the fourth section. The fifth focuses on vegetation and land use, while the final section outlines the demography, environmental, social, and economic activities in the basin.

2.1 Basin Relief and Topography

The Pra River Basin covers an area of approximately 23,200 km² in the south-west part of Ghana (2°30′ W and 0°30′ W, and 5°N and 7°30′ N, Fig. 2.1). The basin exhibits a varied topography that reflects its geological history and drainage dynamics. The southern section of the basin is relatively flat, characterised by low-relief terrain and gentle slopes. In contrast, the mid to northern sections consist of a few peaks with broad river valleys, indicating a more undulating landscape with greater relief variation. The basin's relief is situated primarily at a mean elevation of 300 m.asl, ranging from 2 to 840m, with the upper portions originating from the Kwahu Plateau in the Eastern Region asl (Amekudzi et al., 2015; Bessah et al., 2020a). The upper part of the Pra River Basin in the west is relatively flat, while the topography of its lower reaches is close to that of the Densu Basin, creating a transition from flat to undulating terrain as one moves downstream.

The main Pra River flows for approximately 240 km before joining the Atlantic Ocean near Shama in the Western Region, after traveling through four administrative regions (Eastern, Ashanti, Western, and Central, (Water Resource Commission, 2012)). The basin has four major tributaries: the Birim, Offin, Anum, and Oda rivers, along with the densest network of streams in Ghana. The basin also contains one notable natural freshwater Lake (Bosomtwe), which plays a significant role in the basin's hydrology and water resources.

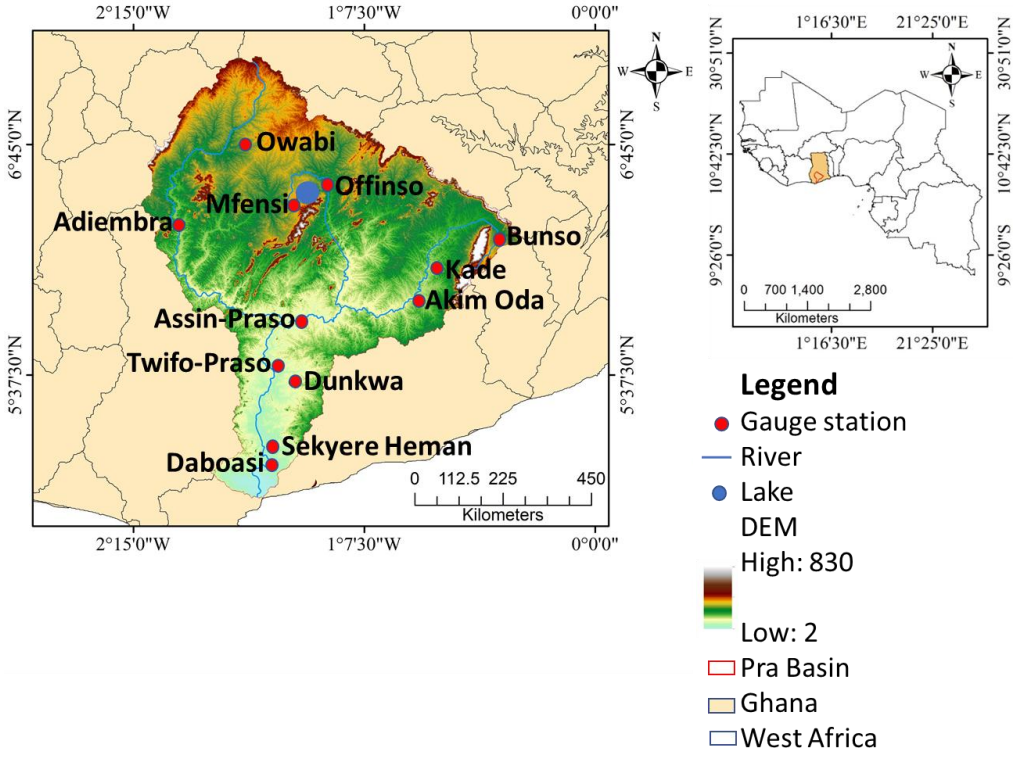

Figure 2.1: DEM of the PRC in southern Ghana (left) with the main river network, the lake, and rainfall gauge stations. West Africa map (right) with Ghana, and the PRC (red)

2.2 Hydrology and Water Discharge

The Pra River Basin exhibits a bimodal rainfall pattern with the main season between April and July and a minor season from September to the first dekad of November (Amekudzi et al., 2015). The mean accumulated annual rainfall climatology based on 39 (1981-2019) years of CHIRPS datasets, indicating values ranging between 1200 and 1700 mm, with precipitation patterns increasing from north to south (Fig. 2.2a; Osei et al., 2021). Hydrologically, the basin demonstrates characteristic tropical basin dynamics with a mean annual river discharge of 214 m^3/s at the Daboase gauge station, the outlet of the PRB.

The basin's hydrology is influenced by its soil characteristics, particularly the dominance of acrisols (covering over 75% of the PRB), along with luvisols, lixisols, fluvisols, leptosols, and reclaimed soil (Kusimi et al., 2015; Table 2.1). These soil types directly influence infiltration, runoff generation, and streamflow responses. The hydrological response of the basin suggests that annual water runoff in the basin has increased over the long-term (1970-2010) period (Awotwi et al., 2017a). Hydrological modelling research also confirmed good simulation of the basin's hydrology, with calibration and validation statistics showing Nash-Sutcliff efficiency

(NSE) and coefficient of determination (R^2) values exceeding 0.75, with percent bias (PBIAS) within ±10% (Awotwi et al., 2017c; Bessah et al., 2020b; Osei et al., 2021).

Table 2.1:Soil types with the corresponding area and percentage coverage

Soil Type	Area (km^2)	%
Acrisols	18,328.8	78.9
Alisols	213.4	0.92
Arenosols	1.2	0.0052
Ferralsols	1.4	0.0060
Leptosols	206.2	0.889
Lixisols	3,564.9	15.36
Fluvisols	854.1	3.68
Luvisols	11.0	0.047

2.3 Hydrogeology, Aquifer Characteristics, and Groundwater Yield

The basin is underlain by two main granitoid formations: the Cape Coast granitoids and the Dixcove granitoids, alongside rock units of the Birimian Supergroup and Tarkwaian rock groups. These granitoids are referred to us as basin and belt types, respectively (Kusimi et al., 2015; Leube et al., 1990; Manu et al., 2021). Hydrochemical facies analysis identified two dominant water types, Ca-Mg-HCO3 and Na-HCO3, along with minor types such as Ca-Mg-Cl and Na-Cl (Tay, 2015). Additionally, the principal mechanisms influencing groundwater chemistry include silicate $(SiO4)^{4-}$ weathering, ion-exchange reactions, sea aerosol spray, and the leaching of biotite, chlorite, and actinite. Groundwater studies show that borehole yields in the lower basin are generally low, ranging between 0.4 m^3/hr to 51.7 m^3/hr, at depths of 22 to 96 m (Tay, 2015; 2017). Groundwater occurrence is closely linked to regolith and fissure development. Borehole yield from a schist area in the basin averages 91.03 l/m, 89.12 l/m for gneiss, while granites produce the lowest yield of 3.33 l/m (Manu et al., 2021; Tay et al., 2017). These results confirm that groundwater is primarily stored in fractures and faults, and that deeper boreholes are more likely to intercept significant water-bearing zones.

2.4 Climate

The climate in the basin is sub-equatorial and monsoonal, and the rainfall is modulated by the seasonal movement of the inter-tropical discontinuity (ITD). Figures 2.2b-d illustrate the

minimum, maximum, and mean temperatures of the catchment based on ERA5 data (Bell et al., 2021; Hersbach et al., 2020) from 1981 to 2019. The basin experiences characteristic tropical temperature conditions. The minimum temperature varies between 19 and 20°C, with the lowest values observed in the mountainous and forested regions in the northeast, northwest, and southern parts of the catchment (Fig. 2.2b). The central region experiences moderate minimum temperatures of 20–21°C, whereas the extreme south records the highest minimum temperatures (21–22°C). The maximum temperature (Fig. 2.2c) ranges from 28 to 36°C, following a distinct latitudinal decline from south to north. The mean temperature (Figure 2.2d) remains relatively low (~25°C) in mountainous and forested areas, while the northernmost section of the catchment experiences slightly higher values, peaking at approximately 27°C. These temperature conditions, combined with the double rainy season precipitation pattern, create a humid tropical climate regime that sustains the High Forest Zone vegetation. Previous studies provide detailed assessments of the basin's climate (Agodzo et al., 2023; Amekudzi et al., 2015; Awotwi et al., 2017c; Bessah et al., 2020b; Osei et al., 2021).

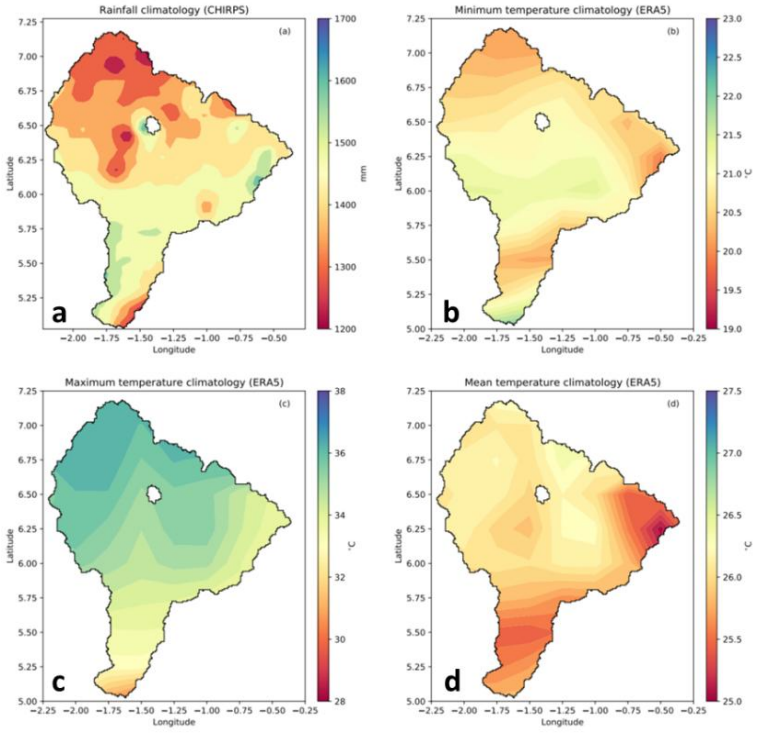

Figure 2.2: Rainfall and temperature climatology plot of PRB (1981-2022) from CHIRPS and ERA5, respectively. (a) mean annual rainfall (b-d) temperature.

2.5 Vegetation and Land Cover

The Pra River Basin is located within Ghana's High Forest Zone, characterised by tropical forest ecosystems interspersed with agricultural land use. The basin is predominantly covered by

semi-moist deciduous forest. Its vegetation coverage is moderately closed trees with dense herbs located centrally in the basin and patches of closed forest within the basin. The basin's vegetation has experienced significant changes due to anthropogenic activities (Awotwi et al., 2019). More specifically, according to Ghana Green Growth PASA (Ghana Country Forest Note, 2023), cocoa plantations cover 27.1% of the basin's total area (approximately 644,000 hectares), representing the dominant land use across much of the PRB. Oil palm cultivation covers 1.2% of the basin (roughly 28,000 hectares), predominantly along the coastal strips. Undisturbed forest covers approximately 9.04% of the total basin area (roughly 211,000 hectares), representing remnants of the original forest ecosystem (Abu et al., 2021; Vancutsem et al., 2021; Fig. 2.3)

The basin's vegetation has undergone rapid deforestation attributable to anthropogenic activities, including settlement expansion, mining, agriculture, and logging. Between 2015 and 2021, studies show the Pra Basin experienced notable changes in land cover, with closed forests decreasing by 27.9% and grasslands decreasing by 64.3%, while cropland increased by 358.1%, shaded cocoa by 15.5%, and settlements by 24.5% (Awotwi et al., 2019; Bessah et al., 2020b). This pattern reflects the conversion of forest (dense and open) to cropland and settlement as the major historical land use change in the basin, driven primarily by agricultural expansion, particularly cocoa cultivation, and resource extraction activities.

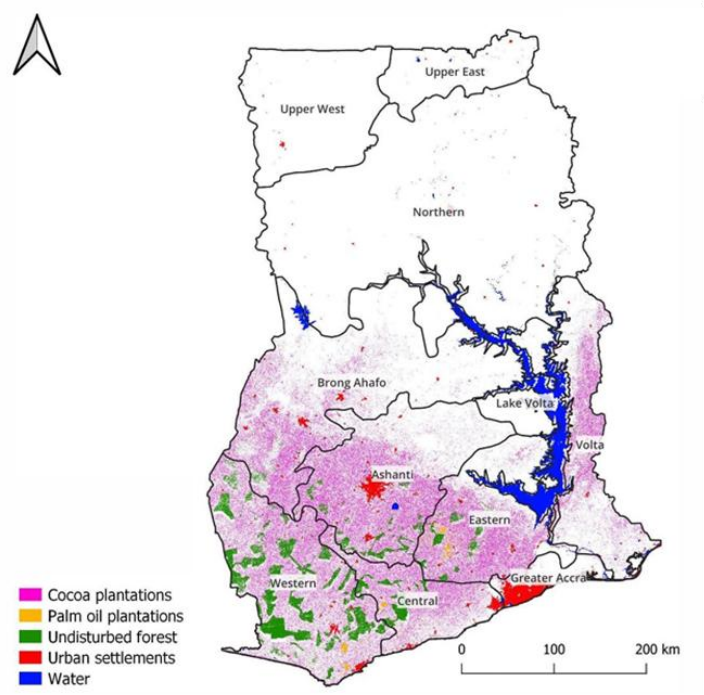

Figure 2. 3:Agricultural expansion and deforestation coverage in Ghana (2021)

2.6 Demography, Environmental, Social, and Economic Activities

The Pra River Basin is one of the most widely and severely altered river basins in Ghana due to expansion in settlement, mining, agriculture, and logging activities. The basin is divided into 41 administrative districts, with 4 in the Western Region, 6 in the Central Region, 11 in the Eastern Region, and 20 in the Ashanti Region. According to the Water Resource Commission, the river and its tributaries provide water to settlements in the basin through two major reservoirs (Barekese and Owabi dams). The population is largely engaged in cash crop farming, like cocoa and palm oil. In addition, Gold and other mineral deposits are heavily mined in the upper basin by both small and large-scale operators (AngloGold Ashanti), reflecting both an economic asset and a source of land use change pressure. These anthropogenic pressures have resulted in uncontrolled, rapid, illegal, and small-scale mining activities, leading to major pollution of most river bodies. The basin has become one of the fastest water-declining river basins globally (Water Resource Commission, 2012). This degradation reflects the combined impacts of climate variability, land use change, and direct human water withdrawals for agricultural, industrial, and domestic uses. The basin's favorable farming environment and high mineral deposits have attracted significant human settlement and economic activity, further accelerating the need for integrated water resources management strategies that balance development needs with ecosystem preservation.

2.7 Partial Conclusion

The Pra River Basin illustrates a tropical West African drainage system with distinct characteristics: a relatively flat southern section transitioning to more rugged terrain in the mid to northern portions, dense forest and agricultural ecosystems undergoing rapid transformation, and sub-equatorial climate conditions supporting high precipitation and streamflow. The basin's dominant acrisol soils influence its hydrological response characteristics, with annual discharge averaging 214 m^3/s and marked seasonal variability tied to the double rainy season pattern. Understanding these physical characteristics is essential for developing sustainable water resources management strategies that address both the basin's ecological functions and the water security needs of its substantial human population, particularly in the context of ongoing land use change and anthropogenic pressures. Figure 2.4 shows the summary of the key physiographic and hydrological characteristics of the basin.

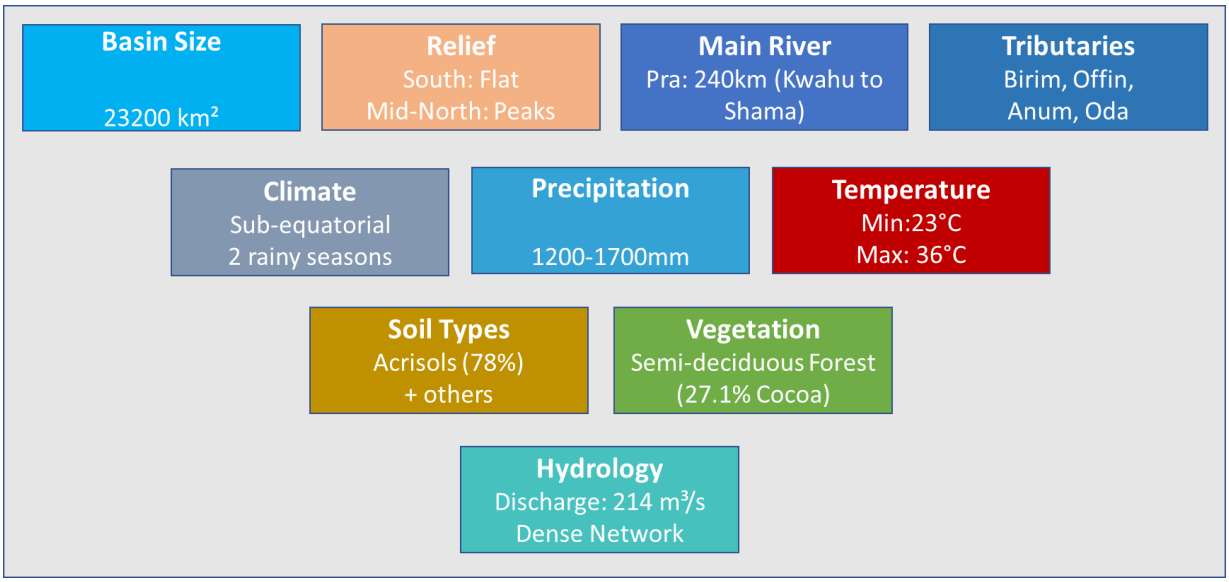

Figure 2.4:Key physiographic and hydrological characteristics of the Pra River Basin, Ghana

CHAPTER 3: DATA, MATERIALS, AND METHODS

This chapter presents the data, materials, and methods used in this study. It is divided into two main sections: the first details the data sources and materials employed, while the second outlines the methodology applied to achieve each research objective.

3.1 Data And Materials

3.1.1 Metadata

The conceptual understanding of the basin response in the anthropogenic climate change era required a systematic literature review using metadata from five major web engines: *Web of Science, Google Scholar, ProQuest, Scopus, and Grey Literature databases* (Table 3.1). The selection focused on peer-reviewed articles published between 2006 and 2023 and written in English. The metadata collected includes publication title, authorship, publication year, journal or source, keywords, and abstract summaries. These elements facilitate an analysis of thematic coverage, research trends, and knowledge gaps about the basin. Additionally, the metadata captures the geographical focus, trends in topics and interest, methodological approaches,

conceptual structures on thematic mapping, and extent of collaboration among researchers, ensuring a balanced representation of the environmental and socio-economic aspects of the basin.

Table 3.1: Data acquired for systematic literature review

Database	Total data
Web of Science	30
Google Scholar	24
ProQuest	20
Scopus	65
Grey literature	3
Total	**142**

3.1.2 Land Use Land Cover Data

The land use and land cover (LULC) data describe the spatial datasets used to analyse land cover variations over time (Table 3.2). The datasets were obtained from Landsat imagery for the years 2007, 2015, and 2023, with a 30-meter spatial resolution, accessed via the USGS Earth Explorer platform in July 2023. Three (3) cloud-free Landsat 8 (OLI/TIRS) images (row 193 path 56, row 194 path 56, and row 194 path 55) were downloaded from the United States Geological Survey Website. The period of imagery chosen was to balance the need to capture meaningful changes in LULC with the availability of high-quality satellite images. Although a 10-year interval was the initial plan, limitations in image quality and access, especially for the early millennium years, required some adjustments. The choice of 2007 reflects the availability of clearer images with minimal cloud cover. The year 2015 aligns with the global shift from the Millennium Development Goals (MDGs) to the Sustainable Development Goals (SDGs), both central to environmental sustainability efforts. Finally, including 2023 ensured that the most recent LULC conditions were captured, strengthening the study's relevance for current and future planning. Additionally, the study incorporated a digital elevation model (DEM) derived from the Shuttle Radar Topography Mission (SRTM) and shapefiles sourced from EarthExplorer. The Landsat datasets used include Landsat 7 (LE07/C02/T1_L2) and Landsat 8 OLI/TIRS sensors, with specifications ensuring data quality and consistency. These datasets provide structured and reproducible information essential for assessing land cover dynamics in the PRB.

Table 3.2: A summary of data acquired for land use land cover change

No	Data	source
1	DEM	Shuttle Radar Topography Mission (SRTM) EarthExplorer (usgs.gov)
2	Shapefile	EarthExplorer (usgs.gov)
3	landsat/LE07/C02/T1_L2	https://developers.google.com/earth-engine/guides/landsat
	Landsat 8 OLI/TIRS	EarthExplorer (usgs.gov)
	Landsat 8 OLI/TIRS	EarthExplorer (usgs.gov)

*OLI: Operational land imager, LE07/CO2/T1: Landsat 07, level 2, collection 2. Tier 1

3.1.3 Climate Data

The climate datasets used in this study comprise observed data, satellite and reanalysis datasets, and global climate model (GCM) projections (Table 3.3). Rainfall data from the Ghana Meteorological Agency (GMet) and Climate Hazards Group InfraRed Precipitation with Station data (CHIRPS), Temperature data from the European Centre for Medium-Range Weather Forecasts (ERA 5), and climate projections data from the Coupled Model Intercomparison Project Phase 6 (CMIP6) under SSP1-2.6 and SSP3-7.0 scenarios.

Table 3.3: A summary of data materials used for the study

Data type	Resolution	Sources
Observed data Daily rainfall (mm), Daily Runoff (mm) Max and Min temperature (°C)		Ghana Meteorological Agency (GMET) Ghana Hydrological Services (Kumasi)
CHIRPS Rainfall (1981-2022)	0.05°	https://data.chc.ucsb.edu/products/CHIRPS2.0-/global_daily/netcdf/p05/?C=D;O=A
Reanalysis (ERA5) (Max, Min, and Mean Temp)	0.25°	https://cds.climate.copernicus.eu/cdsapp#!/-dataset/projections-cmip6?tab=form
CMIP6 Precipitation, Max, Min, Mean, temperature	Non-uniform	https://github.com/ClimateImpactLab/-downscaleCMIP6
Soil data (km)	10	https://www.fao.org/soils-portal/data-hub/soil-maps-and-databases/en/ CSIR-Soil Research Institute, Ghana, Harmonized World Soil Database (Dewitte et al., 2013)

3.1.4 Observed Data

Rainfall data at daily and monthly scales from twelve weather stations distributed across the PRB (Table 3.4) were obtained from the GMet for the period 1981-2015. GMet, as Ghana's primary weather service provider, ensures adherence to the rainfall measurement standards set by the World Meteorological Organization (WMO). Due to data quality and inconsistencies in the obtained data, CHIRPS data at high spatial resolution (0.05° × 0.05°) were used to directly fill the missing rainfall data. The reliability of the CHIRPS datasets has been validated in previous studies (Amekudzi et al., 2008; Aryee et al., 2018; Quansah et al., 2014) through statistical assessments such as Pearson's correlation coefficient, bias, and root mean square error (RMSE), and found to be in good agreement with the observed station. For this reason CHIRPS dataset was the preferred rainfall data.

Table 3.4: Selected Rainfall Stations and their location in the Pra River Basin

Station_names	Latitude	Longitude
Dunkwa	5.59	-1.47
Mfensi	6.45	-1.47
Offinso	6.54	-1.39
Adiembra	6.36	-2.02
Akim Oda	5.57	-0.55
Kade	6.05	-0.50
Daboasi	5.1	-1.38
Sekyere Heman	5.19	-1.58
Twifo-Praso	5.36	-1.33
Assin-Praso	5.56	-1.22
Bunso	6.29	-0.47
Owabi	6.75	-1.71

3.1.5 CHIRPS Data

The CHIRPS-v2 was selected as the primary precipitation dataset for this study. CHIRPS-v2 provides quasi-global precipitation estimates at high spatial resolution (0.05° × 0.05°) between latitudes 50°S and 50°N, integrating infrared Cold Cloud Duration (CCD) observations with in-situ station data, as well as data from the Tropical Rainfall Measuring Mission (TRMM) and NOAA's Climate Forecast System (Didi Sacré Regis et al., 2020; Dinku et al., 2018; Funk et al., 2015; Pitman & Bailey, 2021). The 42-year period establishes a robust baseline that exceeds the WMO 30-year climate standard, enabling reliable trend detection and climate characterisation over the basin. Although meteorological station observation extends to 2015 with gaps and CMIP6 historical simulations end in 2014, CHIRPS-v2 provides complete spatial-temporal

coverage through 2022 with validated performance over the study region (correlation r > 0.8, Aryee et al., 2018; Atiah et al., 2020). For this study, CHIRPS-v2 daily rainfall data available spanning 1981-2022 were analysed, although CHIRPS data, while valuable for Ghana's data-sparse regions, exhibit limitations including overestimation of consecutive dry days (CDD) in northern savannah zones and poor detection of heavy/violent rainfall events (POD near 0%), rendering it less suitable for flood analysis (Atiah & Muthoni, 2023) . The extended timeframe captures multiple decadal oscillations necessary to distinguish long-term climate change signals from natural variability. CHIRPS-v2 hybrid methodology overcomes the limitation of sparse ground-based networks, ensuring gridded rainfall estimates across the entire basin, including previously ungauged areas. An overlapping validation period (1981-2014/2015) was used to establish consistency between CHIRPS-v2 and meteorological station data, after which the analysis extended through 2022 using satellite-derived estimates. CMIP6 historical simulations (1981-2014) were retained separately for model validation and bias correction of future projection (2015-2100)

3.1.6 ERA 5 Data

ERA5, the fifth-generation reanalysis dataset, provides hourly atmospheric variables, including surface air temperature and precipitation, at a spatial resolution of 0.25° × 0.25° (Bell et al., 2021; Tarek et al., 2020). The hourly data on both single and pressure levels span from 1950 to the present (Hersbach et al., 2020), integrating satellite and ground-based observations to generate high-quality climate datasets. A 4D-Var assimilation method is used to produce global daily hourly estimates of climate variables at a 31 km horizontal resolution and 137 vertical levels extending from the surface to 0.01 hPa. In this study, ERA5 datasets were accessed in November 2023, ensuring the inclusion of the latest data updates. The datasets are quality-controlled during the assimilation process, while the physical laws allow for the estimation of data in sparse locations. Also, it is worth noting that ERA5 temperature shows persistent warm biases over northern Ghana and Sahelian margins, alongside underrepresentation of extreme heat waves due to model resolution constraints (Ousmane et al., 2024).

3.1.7 CMIP6 data

The CMIP6 dataset provides long-term climate projections under different greenhouse gas emissions scenarios (Shared Socioeconomic Pathways, SSPs). For this study, precipitation and temperature projections from both low and high emissions scenarios (SSP1-2.6, SSP3-7.0) from historical records (1981–2014) to future projections (2015–2100) were analysed (Eyring et al.,

2016). These pathways reflect international efforts to mitigate climate change and a business-as-usual scenario regionally, respectively (Grose et al., 2020; O'Neill et al., 2016). Whereas the SSP1-2.6 informs the Paris Agreement target of 1.5 °C above pre-industrial, the SSP3-7.0 fills a gap in the medium to high end of the range of future forcing pathways with a new baseline scenario, assuming no additional mitigation beyond what is currently in force. Using SSP1-2.6 and SSP3-7.0 ensures coverage of both stringent mitigation and plausible no-additional-mitigation futures, giving a clearer "range of outcomes" for hydrological and climate-impact analyses while controlling ensemble size (Lu et al., 2022; Soares et al., 2024; Tebaldi et al., 2021). This choice aligns with IPCC AR6-era framing and with many regional downscaling efforts, which can improve comparability of your results with other CMIP6-based studies and assessments (IPCC et al., 2021). The selection of the 5 models (Table 3.5) was chosen based on several recent studies, which documented their ability to reproduce key features of the Ghana and regional (West Africa) climate characteristics reasonably well after bias correction and are frequently retained in impact studies (Kabo-Bah et al., 2025; Mensah et al., 2022; Schürmann et al., 2025) . Also, models like MPI-ESM1-2-LR and EC-Earth3-Veg-LR, in particular, have been ranked among the better performers for precipitation or temperature in regional evaluations, supporting their inclusion (Azad & Ahmadi, 2024).

Table 3.5: CMIP6 GCMS and respective institutions, horizontal resolutions

Model Number	Model name (GCM)	Modelling Institutions	Horizontal resolution (lat. x lon.)
1	ACCESS-CM2	Commonwealth Scientific and Industrial Research Organization/Australia	1.25° x 1.875°
2	EC-Earth3-Veg-LR	EC-Earth-Consortium	0.703125° x 0.703125°
3	IPSL-CM6A-LR	L'Institut Pierre-Simon Laplace/France	1.26° x 2.5°
4	MIROC-ES2L	National Institute for Environmental Studies, and Riken Center for Computational Science/Japan	2.8° x 2.8°
5	MPI-ESM1-2-LR	Max Planck Institute for Meteorology (MPI-M) - Germany	0.9375° x 0.9375°

3.2 Methods

3.2.1 State of the Art Assessment

This study adopted the Preferred Reporting Items for Systematic Reviews and Meta-Analyses (PRISMA) approach to conduct a systematic literature review. PRISMA provides a standardised, evidence-based methodology for reporting systematic reviews and meta-analyses

(Page et al., 2021). Its primary focus is to ensure transparency and replicability in systematic reviews by outlining clear inclusion and exclusion criteria. The guidelines followed in the PRISMA approach are illustrated in Figure 3.1.

The literature review on the Pra River Basin aimed to identify key research themes, emerging trends, critical gaps, and potential management strategies for the basin. A structured five-step approach was employed, comprising scoping, planning, searching or identifying, screening, and scanning. A preliminary literature search was conducted to assess the breadth and availability of studies on the Pra River Basin. A search string expression *((Pra Basin OR Pra River OR Pra Catchment) AND (Climate Change OR Climate Variability) OR (Water OR Streamflow OR Discharge) OR (Land Use Land Cover OR Land Use) OR (Modelling))* was developed and tested across multiple databases to ensure comprehensive coverage.

Given the large number of search results, inclusion and exclusion criteria were applied to establish clear boundaries for the systematic review. The selection focused on peer-reviewed articles published between 2006 and 2023 and written in English. The period set was to cover nearly two decades of research development. The year 2006 marked a point climate change studies gained academic visibility, partly due to the IPCC's Third Assessment Report and the policy that highlighted climate adaptation and mitigation. This period also overlaps with the Millennium Development Goals era (2000-2015). Ending the review in 2023 allowed the inclusion of the most recent studies and provided a broad, up-to-date view of developments in the field. All data were extracted and downloaded on January 25, 2024. Non-peer-reviewed sources, such as books, theses, and letters, were excluded to maintain data reliability and authenticity. However, grey literature, including policy briefs, technical reports, and research studies, was selectively incorporated to enhance the depth and applicability of the review. A total of 142 articles were initially retrieved across four major databases: 30 from Web of Science, 24 from Google Scholar, 20 from ProQuest, 65 from Scopus, and 3 from grey literature sources. After a rigorous screening and scanning process based on relevance to the study objectives, 65 articles formed the basis for bibliometric and systematic analyses.

For the bibliometric analysis, the study employed the Bibliometrix package (version 4.3.2) within R Studio (version 4.4.0) and VOSviewer (version 1.6.20). Bibliometrix is used for initial data processing, statistical analysis, and identifying key trends (Aria & Cuccurullo, 2017). On the other hand, the VOSviewer was used to visualise these trends and relationships in a network format (Cui et al., 2024; Kumar et al., 2024). It is worth noting that these two software tools

were selected due to their complementary strengths compared to other bibliometric platforms. For instance, visualisations created with VOSviewer have better clarity and user-friendliness than CiteSpace (Markscheffel & Schröter, 2021)

The Bibliometrix was employed to conduct the following quantitative analyses: (i) annual publication trends, (ii) geographic distribution of research trend topics production, (iii) international collaboration networks, (iv) keyword frequency and trend topics, and conceptual structure on thematic mapping, factorial, and evolution analysis. Additionally, the VOSviewer software generated network visualisations that clustered keywords into thematic nodes, revealing the conceptual structure and intellectual connections within the field. To complement the quantitative bibliometric results, the most relevant papers were reviewed using a standardised selection protocol that captured their methods, key findings, theoretical approaches, innovations, relevance, and research gaps. This mixed-methods approach was preferred to strengthen analytical rigour and ensure both quantitative extent and qualitative depth. Nevertheless, a few limitations remained. Using four search engines and databases has excluded relevant publications indexed in other databases. Limiting to English-language papers may have biased coverage against non-English-speaking regions. In addition, the bibliometric outputs depend inherently on keyword choices and database indexing practices, which can influence how clusters are formed.

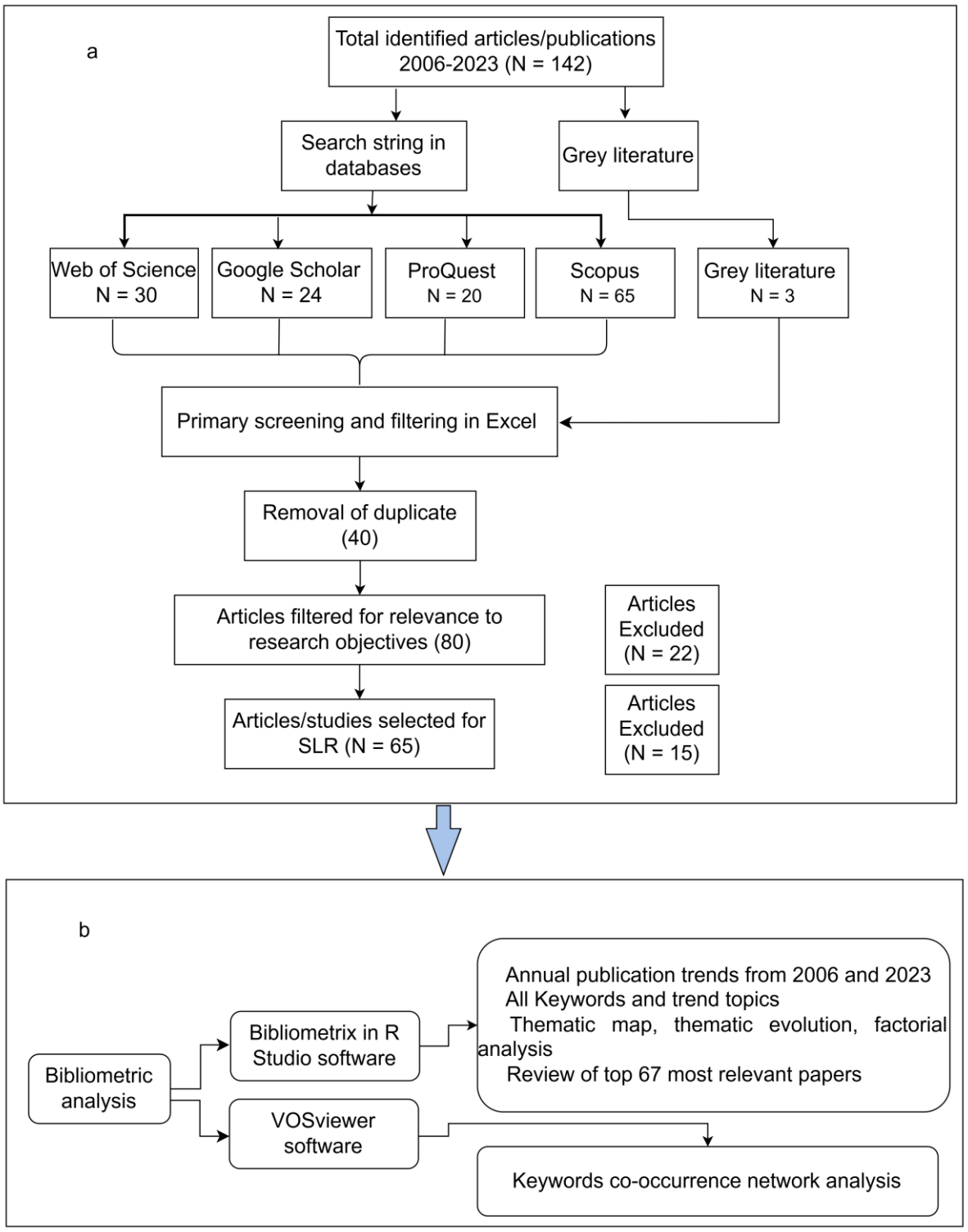

Figure 3.1:Adopted methodological framework (a) data extraction from database (b) Bibliometric analysis process using Bibliometrix (R Studio) and VOSviewer software.

3.2.2 Land Use Land Cover Change

3.2.2.1 Remote Sensing

Landsat 7 and Landsat 8+9 satellite images were used to analyse land use and land cover (LULC) changes in the PRB. Figure 3.2 illustrates the stepwise approach adopted for the analysis. Landsat 7 images were pre-processed and retrieved as cloud-free images from the Google Earth Engine (GEE) catalogue, while Landsat 8+9 images were obtained from EarthExplorer (usgs.gov). These images were clipped, mosaicked, and masked to extract the PRB study area before being imported into GEE for analysis. Three time series-2007, 2015, and 2023 were selected for this study to assess LULC changes over time. The images of 2007 and 2015 were selected from 1st January to 31st March and extended to 30th April, where the quality was insufficient. The 2023 images, captured between August and November, coincided with ground-truth and field data collection efforts to ensure the composite image accurately represented land cover conditions. To minimise atmospheric distortions and enhance image quality, the median composite algorithm (MCA) was applied. MCA computes the median value of corresponding bands and pixels across the image stack, reducing the effects of cloud cover and shadows (Dube et al., 2024). The GEE script used for this processing is available at doi: 10.17632/9hcwfgf6rs.1.

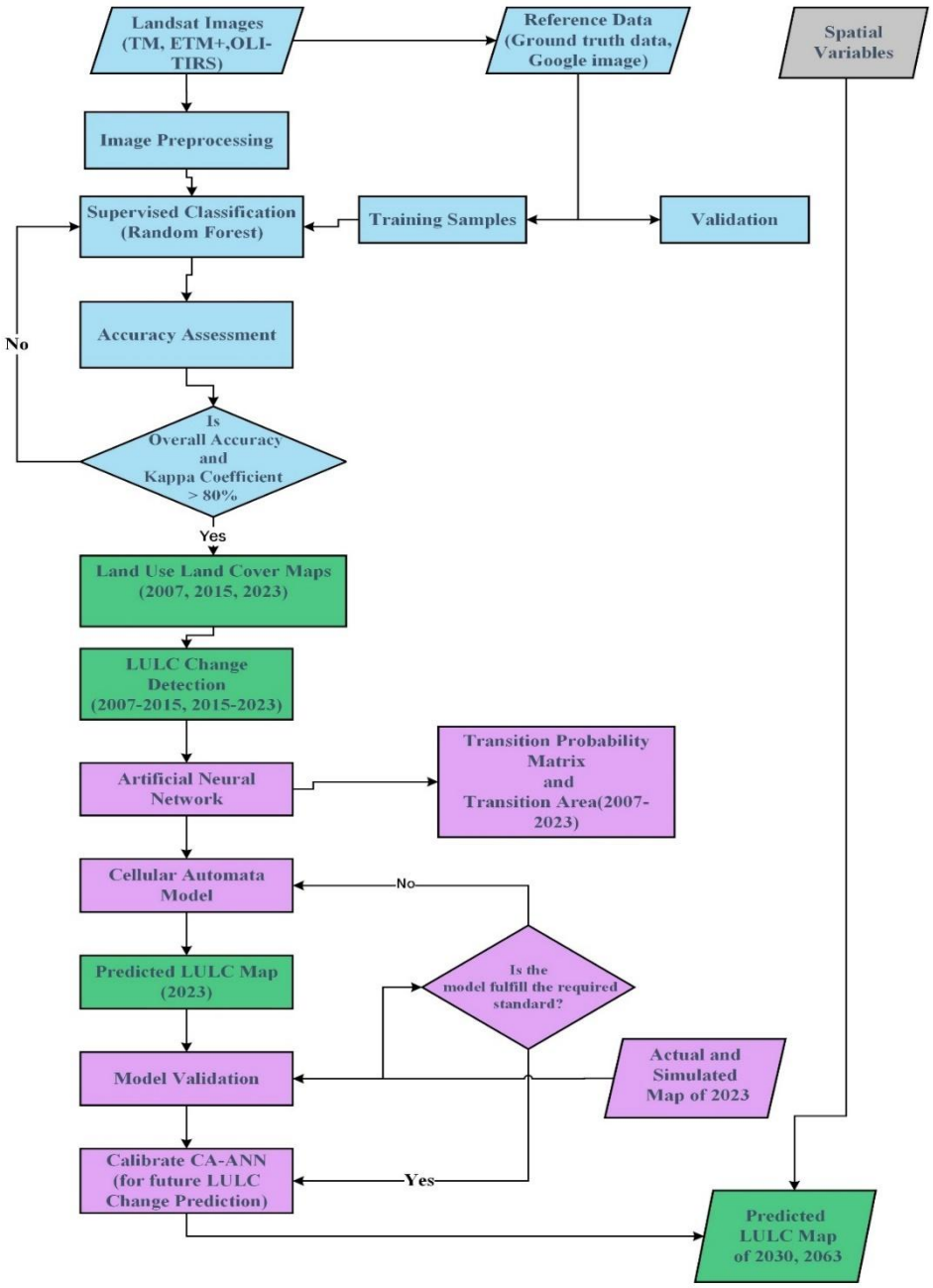

Figure 3.2: LULC Classification and RS data analysis Workflow

3.2.2.2 Determination of Land Use Classification System

The second step involved selecting training samples (polygons) to generate decision trees for classification. Five land cover classes were defined to ensure a representative and reliable classification system. These categories were selected based on their distinct spectral characteristics to minimise classification errors and avoid potential overlaps or omissions. Table 3.6 provides details on each land cover class.

Table 3.6: Description of Land use land cover classes, and in-situ data points

Types	Description	Ground-truth points	Training points
Forest	Forest reserves, sparse forests, and trees creating dense areas	42	29
Cultivated lands/farmlands	Agricultural land, cropland	130	91
Built-up/ bare lands	Includes settlement in cities, towns, and villages, Infrastructure (roads, schools, etc), and bare areas	102	71
Water	Lake, river, reservoir, dams, depression pit from a mining area	65	46
Natural Vegetation	Grasses, bushes, shrubs	340	238

3.2.2.3 Land Use Land Cover Index

To improve classification accuracy, three spectral indices computed from the median composite image: (i) Normalized Difference Vegetation Index (NDVI): used to assess vegetation health and differentiate vegetated areas from non-vegetated surfaces, (ii) Modified Normalised Difference Water Index (MNDWI): applied to enhance water body detection while suppressing noise from built-up areas and soil, and (iii) Bare Soil Index (BSI): used to distinguish bare land and built-up areas from vegetation (https://en.wikipedia.org/wiki/Normalized_difference_water_index). The index equations and band combinations used for different years are presented in Table 3.7. Calculations followed standard spectral formulations, where *NIR corresponds to B4 in 2000 and B5 in 2015 and 2023. Red is represented by B3 in 2000 and B4 in 2015 and 2023. Green by B2 in 2000 and B3 in 2015 and 2023. SWIR by B5 in 2000 and B6 in 2015 and 2023. Blue by B1 in 2000 and B2 in 2015 and 2023.*

In addition, the NIR+MLC method (Sheng et al., 2008) was applied in a two-step process. First, a threshold value of 0.25 was set for the near-infrared (NIR) band to separate water bodies from other land cover types. Secondly, the maximum likelihood classifier (MLC) was used to classify water, built-up areas, vegetation, and bare soil. The MNDWI enhanced water features by suppressing vegetation and built-up area noise, while NDVI quantified vegetation density and distribution. Results are summarised in Table 3.8. The final image classification was performed using the Random Forest (RF) machine learning algorithm, integrated into the Google Earth Engine (GEE) cloud platform (Dube et al., 2024).

Table 3.7: Selected LULC indices used for analysis.

Land Use Index & Reference	Formula	2007	2015/2023
NDVI (Turker, 1979)	$\frac{NIR - RED}{NIR + RED}$	$\frac{B4 - B3}{B4 + B3}$	$\frac{B5 - B4}{B5 + B4}$
MNDWI (Xu, 2006)	$\frac{GREEN - SWIR}{GREEN + SWIR}$	$\frac{B2 - B5}{B2 + B5}$	$\frac{B3 - B6}{B3 + B6}$
BSI (Diek et al., 2017)	$\frac{(RED + SWIR) - (NIR + BLUE)}{(GREEN + SWIR) + (NIR + BLUE)}$	$\frac{(B3 + B5) - (B4 + B1)}{(B2 + B5) + (B4 + B1)}$	$\frac{(B4 + B6) - (B5 + B2)}{(B4 + B6) + (B5 + B2)}$

Table 3.8: Indicator auxiliary variable ranges for the used LULC classification

Spectral Reflectance LULC Class	BSI	NDVI	MNDWI
Forest	value < 0	value > 0.5	value <0.1
Cultivated lands/ Farmlands	value > 0.5	value > 0.2	value < 0.1
Built-up/ Bare lands	value > 0.4	value < 0.2	value < 0
Water	value < 0.2	value < 0.2	value > 0.2
Natural Vegetation	value < 0.1	value > 0.4	value < 0

3.2.2.4 Random Forest Model Validation

This study evaluated the effectiveness of the RF algorithm for LULC analysis compared with other machine learning techniques such as regression trees, support vector machines, and artificial neural networks (Hengl et al., 2015; Kuhn & Johnson, 2013). While RF can be constrained by the covariate ranges in training data, many studies highlight its advantage over linear regression (Ahmad et al., 2010; Kuhn & Johnson, 2013). Unlike linear regression, RF accommodates complex non-linear relationships without requiring assumptions about the target variable's probability distribution, making it well-suited for high-dimensional datasets (Kuhn & Johnson, 2013). RF was selected due to its proven success in diverse research fields across Ghana (Caie et al., 2020; Dahan et al., 2024; Forkuor et al., 2017; Ghansah et al., 2021). It is simple to implement and computationally efficient, as it generates multiple "basic" decision trees during training and aggregates predictions through majority voting (mode) for classification. The RF model was trained using a 70% random split of the ground-truth data. A total of 300 Global Positioning System (GPS) and 379 random sample ground-truth data points from Google Earth Pro imagery were used to validate the classification outputs. Model

validation employed three error matrices: User Accuracy (UA, Eq. 3.0), Producer's Accuracy (PA, Eq. 3.1), and Overall Accuracy (OA, Eq. 3.2) (Fung & LeDrew, 1988). UA measures how accurately map classes represent actual ground conditions. PA reflects the probability that a ground feature is correctly classified. OA indicates the proportion of correctly classified reference points across all classes. Additionally, the Kappa Coefficient (T), one of the widely used statistics for testing inter-rater reliability, was calculated (García-Álvarez et al., 2022). The remaining 30% of ground-truth data was used to compute the error matrix, which also aided in identifying the most influential variables in the RF model.

$$\boldsymbol{UA} = \frac{\boldsymbol{Number\ of\ correctly\ classified\ pixels\ in\ each\ category\ (diagonal)}}{\boldsymbol{Total\ number\ of\ reference\ pixels\ in\ each\ category\ (row\ total)}} \times \mathbf{100} \tag{3.0}$$

$$\boldsymbol{PA} = \frac{\boldsymbol{Number\ of\ correctly\ classified\ pixels\ in\ each\ category\ (diagonal)}}{\boldsymbol{Total\ number\ of\ references\ pixels\ in\ each\ category\ (column\ total)}} \times \mathbf{100} \tag{3.1}$$

$$\boldsymbol{OA} = \frac{\boldsymbol{Total\ number\ of\ corrected\ classified\ pixels\ (diagonal)}}{\boldsymbol{Total\ number\ of\ references\ pixels}} \times \mathbf{100} \tag{3.2}$$

$$(\boldsymbol{T}) = \frac{\boldsymbol{Total\ number\ of\ Sample \times Total\ number\ of\ corrected\ sample - \sum (col.tot \times row.tot)}}{\boldsymbol{(Total\ number\ of\ sample)^2 - \sum (col.tot \times row.tot)}} \times \mathbf{100} \tag{3.3}$$

3.2.2.5 Image Classification and Change Detection

To enhance classification accuracy and change detection, an if-then rule incorporating elevation and slope data was implemented as a post-classification refinement (Hutchinson, 1982; Janssen & Partee, 1997). All image processing was conducted within the Google Earth Engine (GEE) platform to ensure computational efficiency and accuracy.

Change detection in LULC is a critical aspect of remote sensing (RS) and environmental monitoring, facilitating the management of natural resources and supporting informed decision-making on land use policies, zoning regulations, and resource allocation. To quantify land cover changes between different time periods, the Semi-Automatic Classification Plugin in QGIS was used for post-classification change detection. A change matrix was generated to establish a historical baseline for LULC transformations and to support long-term trend analysis. Additionally, a transition probability matrix was estimated to assess the likelihood of different land cover transitions. The transition probability is based on area-based changes between two classified images, capturing how land cover categories evolve. The conversion rule for the land

use was set between 0 and 1. As the value approaches 1, land use conversion becomes more challenging, while a value closer to 0 indicates a higher likelihood of conversion. To quantify the extent and rate of LULC changes, three key metrics were computed: (i) Absolute Change (AC) (Eq. 3.4) – Measures the net change in land cover area between two time periods. (ii)Relative Change (RC) (Eq. 3.5) – Expresses land cover change as a percentage relative to its initial extent. (iii) Rate of Change **(q)** (Eq. 3.6) – Estimates the annual rate of LULC change.

Absolute change, $AC = A_2 - A_1(km^2)$ (3.4)

Relative change, $RC = \frac{A_2 - A_1}{A_1}(\%)$ (3.5)

Rate of change, q = $RC = (\frac{A_2}{A_1})^{\frac{1}{t_2 - t_1}} - 1(\%/y)$ (3.6)

Where A_2 and A_1 are the Areas of LULC classes of the final and initial years, and t_1 and t_2 are the respective separate years.

These computations provided insights into the pace and direction of landscape transformations within the PRB, contributing to a more comprehensive understanding of the basin's land cover dynamics and environmental implications (García-Álvarez et al., 2022).

3.2.2.6 Future LULC Change

This section projected the possible future LULC changes based on a business-as-usual (BAU) scenario derived from the classified maps in Objective 2. The classified LULC maps were used as input into the Cellular Automata-Markov (CA-Markov) model in Idrisi® Selva software to analyse land cover transitions (Lin et al., 2014). The analysis involved validating the most recent LULC map and subsequently projecting future LULC changes for 2030 and 2063. These years were selected in alignment with the Sustainable Development Goals (SDGs-2030) and the Agenda 2063: The "Africa We Want", providing a framework for evaluating projected changes against regional and global development objectives.

The BAU assumptions incorporated the potential impacts of geopolitical influences on the management of the Pra River Basin. The presence of alluvial gold deposits has led to exponential small-scale and illegal mining activities (Galamsey), influencing land use dynamics. Additionally, migration patterns and urban expansion were considered in assessing future LULC trends (Table 3.9). Given data limitations, this study primarily relied on geophysical factors such as built-up areas, digital elevation models (DEM), and slope as key

drivers of land use transitions. The influence of the surrounding natural environment was also accounted for in predicting land use changes.

Validation of Projected 2023 LULC Map

Accurate LULC projections require validation of the projection methodology. The CA-Markov model was employed to predict future LULC, leveraging transition probabilities derived from historical land cover changes (Hamdy et al., 2017; Lin et al., 2014). The Markov transition matrix was used to estimate the likelihood of LULC types transitioning between different categories or persisting over time (Equation 3.7). The CA-Markov model enhances LULC projections by incorporating both spatial patterns of land use change (from the Cellular Automata component) and the probability of transitions (from the Markov model, Gilmore Pontius et al., 2011; Pontius & Malanson, 2005). The future state of each land cover class was determined based on its current state and the neighboring land cover types (Equation 3.8). This approach allowed for a dynamic simulation of LULC evolution, accounting for both spatial autocorrelation and temporal trends in land cover transformation.

$$S_{i,j}(t+1) = f(S_{i,j}(t), (t), T) \quad (3.7)$$

Where:

$s_{i,j}(t+1)$ is the future state (LULC class) of the cell at location (i,j) at time t+1 from the CA-Markov projection

$S_{i,j}(t)$ is the current state of the neighbouring cells

T is the probability of transitioning from LULC class i to j

$$T = \begin{matrix} P_{ij} & \dots & P_{in} \\ \vdots & \ddots & \vdots \\ P_{nj} & \dots & P_{nn} \end{matrix} \quad (3.8)$$

Pij is the probability of transitioning from LULC class i to j

n is the number of LULC classes, each row summing to 1 as the total probability of transitioning from one class must equal 1.

The transition probabilities and areas were first estimated using the Markov transition in IDRISI Selva with the 2007 and 2015 maps and the time between them as input. The estimated

transition probabilities and areas were used as input into the CA-Markov tool to simulate the LULC for the year 2023. The simulated 2023 map was assessed against the classified 2023 LULC map for its overall agreement, as well as quantity and location agreement.

Uncertainty Management in LULC Projections

Management of LULC projection uncertainty while using the CA-Markov model in Idrisi®Selva environment was rigorously addressed at different stages to enhance reliability. Validation of the model's predictive performance combined categorical accuracy measures (overall accuracy, user's and producer's accuracy, Kappa coefficients) and advanced disagreement metrics. validation compared simulated future maps to observed LULC using the relative operating characteristics (ROC), and Kappa indices and that isolates agreement due to total agreement, K-standard, and K-location following best practices established by Pontius and others. The ROC value ranges from $0 < ROC < 1$, where 1 indicates a perfect fit, and 0.5 indicates a random fit. To further quantify uncertainty, the study minimised input data errors by selecting high-quality satellite imagery and harmonising classification methods. Limitations remain, including the model's assumption of stationary transition probabilities and its limited treatment of external socio-economic drivers, which can result in spatial misallocation of predicted change or under- or over-estimation of some transitions. This was also addressed by reporting the quantity and allocation disagreement, not just overall agreement, as these provide a more nuanced view of uncertainty.

Table 3.9: Land use/cover change scenarios

Scenario type	Description
Business as Usual (BAU)	A scenario, representing a continuous exponential Anthropocene with political interest interference preventing basin management and worsening environmental degradation, with high unemployment that leads to migration and a rise in illegal mining (Galamsey) in alluvial gold-rich river basins.

Future LULC Maps

The CA-Markov projection of the 2023 LULC map demonstrated a reasonable ability to learn from earlier LULC scenarios and make predictions. However, it also highlighted some deviations from reality. Hence, the 2023 classified map was used as a baseline to project future LULC for 2030 and 2063 to enhance the credibility and reliability of future projections and

reduce error propagation from the simulated 2023 map, as recommended (Foody, 2010; Padial-Iglesias et al., 2021). The 2015 and 2023 classified LULC maps were used to project the 2030 LULC map, and the 2023 and 2030 maps were used to estimate LULC for 2063.

3.2.3 Climate Change

3.2.3.1 Data Validation

The reliability of CHIRPS data against GMet's observed data needed no validation because it has been validated at both the daily and monthly scales and assessed through statistical comparisons with gridded datasets using Pearson's correlation coefficient, bias, and root mean squared error (RMSE) (Amekudzi et al., 2008; Aryee et al., 2018; Atiah et al., 2020; Quansah et al., 2014). Additionally, reanalysis data from ERA5 were validated at the daily scale by evaluating their correlation with observed station data. Using ERA5 and CHIRPS satellite datasets as references, the performance of bias correction techniques applied to Global Climate Model (GCM) outputs was assessed. The validation involved three statistical performance indicators: (i) Pearson Correlation Coefficient (Eq. 3.9) – Measures the strength and direction of association between datasets. (ii) Mean Absolute Error (MAE) (Eq. 3.10) – Evaluate the magnitude of error between observed and modelled values. (iii) Bias (Eq. 3.11) – Quantifies systematic over- or under-estimation in the model output. Smaller errors indicate improved performance of bias correction techniques (Pearson & Lee, 1903; Peng et al., 2023). To ensure comparability, all datasets were converted to daily, monthly, and yearly means before statistical evaluation.

$$r = \frac{N\sum_{i=0}^{N} O_i P_i - \sum(O_i)\sum(P_i)}{\sqrt{\left(N\sum O_i^2 - \sum\left(O_i^2\right)\right)\left(N\sum P_i^2 - \sum\left(P_i^2\right)\right)}} \quad (3.9)$$

$$MAE = \frac{\sum_{i=0}^{n} |P_i - O_i|}{n} \quad (3.10)$$

$$Bias = \frac{\sum_{i=0}^{n} P_i}{\sum_{i=0}^{n} O_i} \quad (3.11)$$

3.2.3.2 Trend Analysis

Modified Mann-Kendall (MMK) Test

The Modified Mann-Kendall (MMK) test was utilised to detect monotonic trends in both daily precipitation and extreme indices, considering autocorrelation in the datasets (Mann, 1945; Yue et al., 2002). The MMK test statistic (S), variance (V(S)), and z-statistic (Z) were computed as (Eqn. 3.12):

$$S = \sum_{i=1}^{n-1} * \sum_{j=i+1}^{n} sgn(X_j - X_i) \tag{3.12}$$

where:

(X_j) and (X_i) represent daily rainfall measurements at times (j) and (i), respectively, and (n) denotes the total number of observations (Wei & Zhao, 2024) and sgn (x, Eqn. 3.13)

$$sgn(x) = \begin{Bmatrix} 1 & if\ x > 0 \\ 0 & if\ x = 0 \\ -1 & if\ x < 0 \end{Bmatrix} \tag{3.13}$$

To account for autocorrelation, which is critical when analysing hydrological time series (Patakamuri et al., 2020; Yue et al., 2002), the variance of (S) is adjusted appropriately (Eqn 3.14):

$$V\ (S) = \frac{n(n-1)(2n+5)}{18} - \sum_{k-1}^{n-1} \frac{(2k+5)}{18} * \rho_k \tag{3.14}$$

where $(\rho_{k)}$ denotes the autocorrelation coefficient at lag (Ghanim et al., 2023).

The corresponding z-statistic is then computed (Eqn. 3.15):

$$Z = \begin{Bmatrix} \frac{S-1}{\sqrt{V(S)}} & if\ S > 0 \\ 0 & if\ S = 0 \\ \frac{S+1}{\sqrt{V(S)}} & if\ S < 0 \end{Bmatrix} \tag{3.15}$$

Sens Slope

To quantify the magnitude of identified trends, Sen's slope estimator (Q, Sen, 1968) was implemented as follows (Eqn 3.16):

$$Q = median\left(\frac{X_j - X_i}{j - i} : j > i\right) \tag{3.16}$$

Where X_i, X_j are observations at times *i* and *j*. *Q also represents the trend magnitude (slope) in units per time step.*

This method provides an estimate of the rate of change in the time series data (Yagbasan et al., 2020). Furthermore, Kendall's tau (τ) was calculated to assess the strength and direction of the monotonic relationship between the data points (Eqn. 3.17):

$$\tau = \frac{S}{\frac{n(n-1)}{2}} \quad (3.17)$$

Where S: Mann-Kendall's tau (τ) statistic, n: Number of observations, $\tau \in [-1, 1]$: $values\ near + 1\ or - 1\ indicate\ strong\ monotonic\ trends$

Locally Weighted Scatterplot Smoothing (LOESS)

Locally Estimated Scatterplot Smoothing (LOESS) is a nonparametric method used to smooth noisy datasets and detect trends by fitting simple models to localised subsets of data (Green & Finlay, 2008; Wanishsakpong & Notodiputro, 2018). Unlike global regression models, LOESS adapts to local data structures, making it well-suited for analysing non-linear and irregular hydrological time series.

In this study, LOESS was applied to rainfall data to reveal underlying temporal trends that may be obscured by short-term variability and measurement noise. Its flexibility allows for effective visualisation of rainfall dynamics across different timescales and topographic conditions. Previous studies have demonstrated its utility in identifying seasonal and decadal trends, as well as in complex terrains like the Loess Plateau (Green & Finlay, 2008; Irizarry, 2001; Mu et al., 2022; Wu et al., 2018). The method supports improved interpretation of rainfall variability and strengthens the validation process for hydrological modelling.

3.2.3.3 Rainfall Trends (Shifts-onset and centre of mass)

To investigate changes in precipitation distribution, the onset and centre of mass of rainfall for each station were assessed. The onset of rainfall was defined according to the World Meteorology (WMO) as the first occurrence of significant rainfall of at least 20 mm in 3 consecutive days, with no dry spell (5+ dry days) in the next 10 days, while the center of mass (for 50% accumulated rainfall) was calculated using the following formula (Eqn. 3.18):

$$Center\ of\ Mass\ (CoM) = \frac{\sum_{t=1}^{n} t \times P_t}{\sum_{t=1}^{n} P_t} \quad (3.18)$$

whereP_t is the daily precipitation at time (t), and (n) is the total number of days in the analysis period. This methodology enables the identification of potential shifts in rainfall patterns over time. Understanding the variability in rainfall onset timing is essential for informed decision-

making in agriculture, particularly in regions that rely heavily on rain-fed systems. Accurate information on the spatial distribution of rainfall supports the effective planning and management of infrastructure, such as drainage systems, to reduce flood risk. These considerations highlight the importance of analysing rainfall dynamics, specifically onset timing and the centre of mass, for the development of robust risk assessments and climate adaptation strategies in vulnerable areas (Kim & Kim, 2020; Maybee et al., 2023; Saini et al., 2022). Furthermore, correlation analyses were performed between the onset and centre of mass of rainfall to investigate their interrelationships and potential shifts, providing insights into how changes in the rainfall distribution affect hydrological responses in the area.

3.2.3.4 Correlation Analysis

To investigate the relationship between the timing of rainfall and annual rainfall totals, the Centre of Mass (CoM) of rainfall was computed for each hydrological year at all monitoring stations. CoM represents the day of the year by which 50% of the total annual rainfall has been accumulated. This metric provides insight into the temporal distribution and concentration of rainfall events. Pearson's correlation coefficient (r) was used to quantify the strength and direction of the relationship between CoM and total annual rainfall. Positive values of r indicate that higher rainfall totals are associated with later CoM dates, suggesting longer rainy seasons. Statistical significance was assessed at the 5% level ($p < 0.05$) to determine whether the correlations observed were likely due to chance.

3.2.3.5 ENZO-Rainfall Onset Analysis

The influence of ENSO on rainfall onset was assessed by superimposing major El Niño and La Niña years, identified from NOAA's Oceanic Niño Index (ONI), onto station-level onset time series. Annual onset dates were expressed as day of year (DOY) for each gauge and stratified into two climatic zones: (i) coastal/forest-belt and (ii) forest/intra-zonal stations. ENSO years were categorized as El Niño (1982, 1983, 1987, 1991, 1992, 1997, 1998, 2002, 2009, 2015) and La Niña (1988, 1999, 2000, 2007, 2008, 2010, 2011, 2016, 2020) and highlighted in red and blue, respectively, on onset plots. For each station, onset DOY series were visualised using scatter plots with locally weighted scatterplot smoothing (LOESS) to extract non-linear temporal trends. ENSO years were overlaid as vertical bands to facilitate visual identification of co-occurring anomalies in onset timing. Plots were arranged in standardised 3×4 grids with common axes to support inter-station comparison. Centre-of-mass (CoM) of seasonal rainfall

was similarly analysed, with smoothed CoM trajectories examined alongside ENSO phases to evaluate shifts in the timing of seasonal rainfall concentration.

3.2.3.6 Probability Density Function (Rainfall Analysis)

Rainfall probability density function (PDF) plots offer insights into how frequently different rainfall amounts occur over a given period. A shift in the curve to the right signals an increase in heavy rainfall events, while a shift to the left or a flattening curve implies lighter rainfall or a more even distribution. These shifts carry important implications for water resource management and climate adaptation planning. The PDFs were generated by aggregating rainfall over four temporal windows (1-day, 5-day, 15-day, and 20-day), and then applying kernel density estimation to compute the probability density of rainfall amounts for each period. This method enables direct comparisons between the observed baseline and future projections under SSP1-2.6 (low-emission pathway) and SSP3-7.0 (high-emission pathway).

3.2.3.7 Model Evaluation (Bias Correction and Downscaling)

To improve the reliability of climate projections, bias correction, spatial disaggregation, and downscaling of GCM outputs were conducted. Following the approach of Wood et al. (2004), probability density functions (PDFs) of climate variables were mapped onto gridded reference datasets aggregated at the required resolution (Vandal et al., 2017, 2019).

- Bias Correction – CHIRPS (for precipitation) and ERA5 (for temperature) served as reference datasets for bias correction of CMIP6 outputs under SSP1-2.6 and SSP3-7.0 scenarios. Quantile Mapping (QM) was applied to align CMIP6 data with historical observations by transforming statistical distributions to match reference data (Enayati et al., 2021; Grillakis et al., 2017; Katiraie-Boroujerdy et al., 2020; Maraun, 2013; Thrasher et al., 2012).
- Spatial Disaggregation CMIP6 data were bilinearly interpolated to match the spatial resolution of reference datasets, with correction factors applied to improve accuracy.

3.2.3.8 Analysis of Extreme Rainfall Indices

Long-term rainfall trends, intensity, and extreme events were analysed using indices developed by Sillmann et al. (2013) and the Expert Team on Climate Change Detection and Indices (ETCCDI). Table 3.10 details the five indices used in the study. Calculations were conducted for both historical (1981–2022) and future (2015–2100) periods using CMIP6 projections under SSP scenarios. The analysis was implemented using Python-based interfaces (Spyder and

Jupyter Notebook), which are available for free download from (https://www.anaconda.com/products/navigator)

Table 3.10: Extreme rainfall characteristics indices used for the study

Index	Descriptive name	Definition	units
R10mm	Number of heavy precipitation days	Annual count of days when PRCP > = 10 mm	mm
R20mm	Number of very heavy precipitation days	Annual count of days when PRCP > = 20 mm	mm
R95p	Very wet days	Annual total PRCP when RR > 95th percentile	mm
RX5day	Max-5-day precipitation amount	Monthly maximum consecutive 5-day precipitation	mm
CWD	Consecutive wet days	Maximum number of consecutive days with R > =1mm	day

3.2.3.9 Precipitation Anomaly Indices Classification

To assess precipitation anomalies and their impact on the Pra River Basin (PRB), the Rainfall Anomaly Index (RAI) and Standardised Precipitation Index (SPI) were applied to quantify the frequency of wet and dry years from 2015 to 2100 under SSP1-2.6 and SSP3-7.0 climate scenarios (Okpara et al., 2017; Okpara & Tarhule, 2015; Türkeǵ et al., 2009). The RAI ranks precipitation totals relative to historical records, providing insights into anomaly detection, while the SPI calculates standardised deviations of precipitation over multiple temporal scales, correcting for variability and long-term mean values. SPI was computed at 1-, 3-, 5-, and 12-month timescales to evaluate flood and drought risks, following the methodology outlined by Okpara et al. (2017). All analyses were conducted in Python, with wet and dry conditions classified based on the scheme proposed by Guttman (1998) and Raziei (2021). Negative RAI and SPI values indicated drought conditions, whereas positive values denoted wet conditions. The World Meteorological Organisation (WMO, 2012) recognises SPI as a global standard for assessing precipitation variability and intensity, ensuring consistency in the interpretation of

extreme hydrological events within the PRB (https://www.droughtmanagement.info/standardized-precipitation-index-spi/)

Table 3.11: The Precipitation Anomaly Indices Classification Scheme used for extreme projection.

RAI/SPI values	Classification
≥3	Extremely wet
2.00 to 2.99	Very wet
1.00 to 1.99	Wet
-0.99 to 0.99	Normal (wet to dry)
-1.99 to -1.00	Dry
-2.99 to 2.00	Very dry
≤-3	Extremely dry

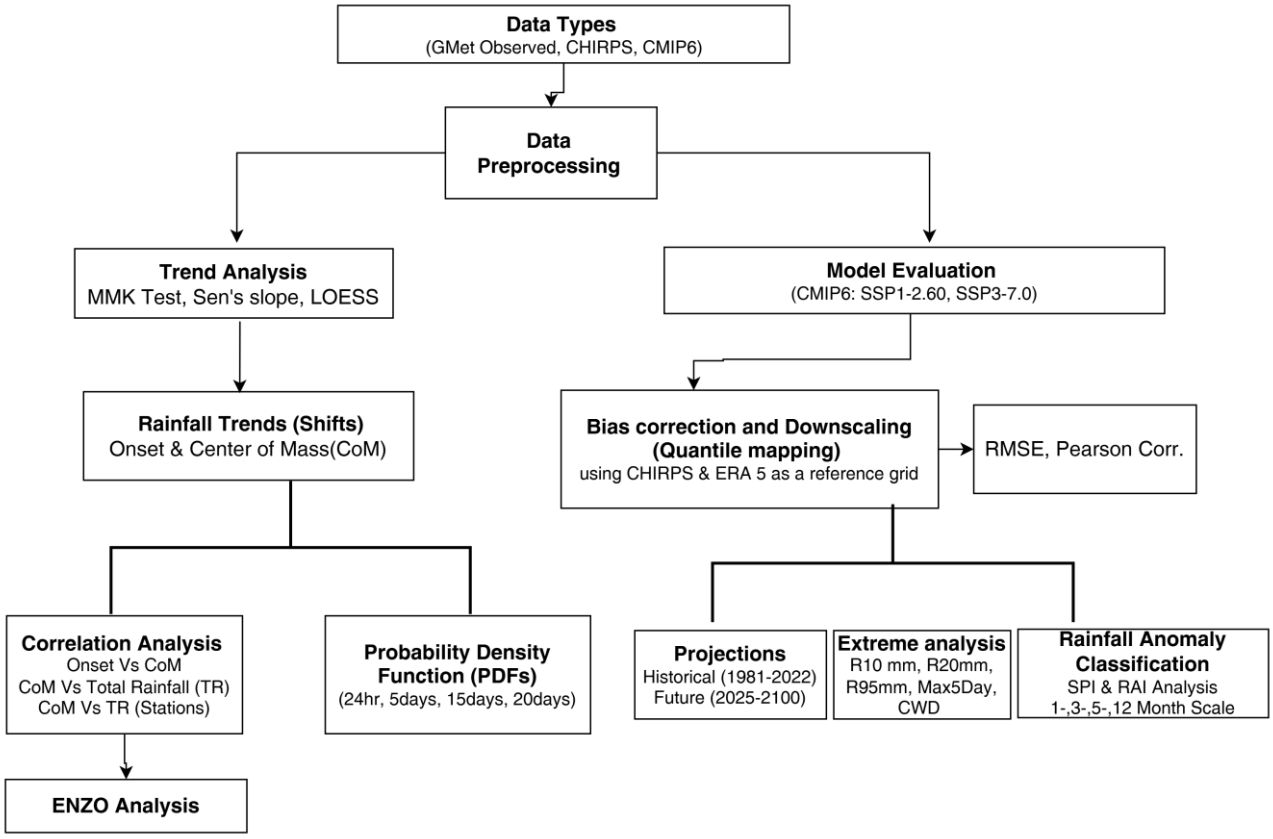

Figure 3.3: A thematic diagram of the method used for data preparation and climate analysis.

3.2.4 Calibration and Validation of Hydrological Model

3.2.4.1 Hydrological Model and Setup

The Hydrologiska Byråns Vattenbalansavdelning (HBV) model (Bergström, 1976), is a conceptual, semi-distributed hydrological model designed to simulate catchment-scale water balance processes. The HBV light version 4.0.0.24 (Fig. 3.4) used in this study is a simplified implementation developed by Seibert and Vis (2012). Owing to its relatively low data requirements and robust performance, the model has been widely applied and evaluated across catchments with contrasting climatic and physiographic conditions (Ahmad et al., 2020; Hakala et al., 2018; Meresa & Gatachew, 2019; Usman et al., 2021). HBV light represents hydrological processes through routines that account for snow accumulation and melt, soil moisture dynamics, groundwater storage, and runoff generation. Precipitation, air temperature, and potential evapotranspiration are spatially distributed within the model using elevation and vegetation zones. This model was used in this study to simulate the daily streamflow of the Pra catchment.

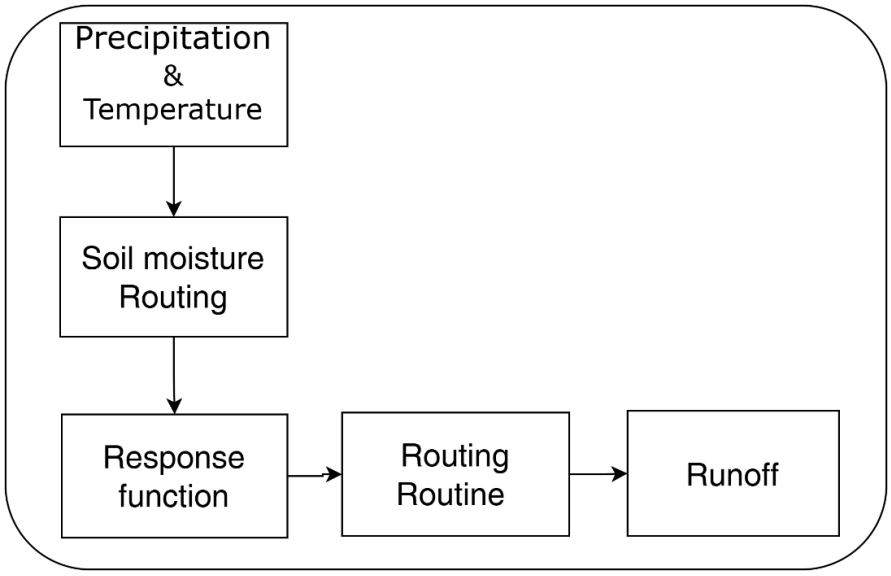

Figure 3.4: The HBV-light conceptual model

Model calibration and validation were conducted to ensure that simulated streamflow adequately represents observed catchment responses. Before calibration, the model was initialised using a warm-up period from 2004 to 2005 to reduce the influence of initial conditions. This ensured that soil moisture, groundwater, and snow routines (not needed in this study) reached a quasi-steady state before calibration. The calibration period spanned 2005 to 2009. The model parameters were first estimated using the Genetic Algorithm and the Powell

optimisation method (GAP; Seibert & McDonnell, 2002), which iteratively selects and recombines high-performing parameter sets to maximise objective functions. Parameter ranges proposed in previous HBV-light studies were used as initial bounds. Manual trial-and-error adjustments were also applied to refine the final parameter set.

Following GAP calibration, Monte Carlo (MC) simulations were performed to explore parameter uncertainty and support multi-criteria optimisation. A total of 500,000 MC simulations were generated, assuming parameter sets followed a normal distribution. For multi-criteria evaluation, parameter ranges were constrained based on GAP-derived sets that yielded a Nash–Sutcliffe efficiency (Reff) greater than 0.3. Model simulations were then ranked according to objective functions, and the best-performing parameter sets were identified. Sensitivity and uncertainty analyses were performed using these sets to assess model robustness and reliability. The model was then validated for the period 2009 to 2011 using the parameter sets obtained during calibration. Validation ensured that the model could reproduce observed streamflow without additional tuning.

3.2.4.2 Model performance evaluation

Model performance was quantified using statistical metrics that assess agreement between observed and simulated streamflow. The Nash–Sutcliffe efficiency (Reff) was the primary objective function:

$$Reff\ (NSE)\ = 1 - \frac{\sum(Q_{obs} - Q_{sim})^2}{\sum(Q_{obs} - Q_{obs})^2} \quad (3.19)$$

Additional metrics included the Kling-Gupta efficiency (KGE; Gupta et al., 2009), coefficient of determination (R^2), and per cent bias (PBIAS).

$$KGE = 1 - \sqrt{(r-1)^2 + (\alpha - 1)^2 + (\beta - 1)^2} \quad (3.20)$$

$$R^2 = \frac{(\sum(Q_{obs} - \overline{Q_{obs}})\,(Q_{sim} - \overline{Q_{sim}})\,)^2}{\sum(Q_{obs} - \overline{Q_{obs}})^2 \sum(Q_{sim} - \overline{Q_{sim}})^2} \quad (3.21)$$

$$PBIAS = \frac{\sum_{i=1}^{n} s_i - o_i}{\sum_{i=1}^{n} o_i} \times 100 \quad (3.22)$$

3.2.5 Methodological Justification and Coherence

The methodological framework adopted in this study was designed to capture the interacting influences of climate variability, LULC change, and hydrological processes within the PRB, while remaining consistent with data availability and the study objectives. An integrated

approach was necessary to ensure that both physical drivers and knowledge gaps were systematically addressed.

A systematic literature review was undertaken to provide a structured synthesis of existing research on climate, land use, and hydrology in the Pra River Basin. Given the dispersed nature of prior studies, the use of multiple scientific databases and a transparent four-step review framework ensured methodological rigour and reduced selection bias. This review informed the identification of key research trends, gaps, and management-relevant themes, thereby strengthening the conceptual basis of the empirical analyses. Land use and land cover analysis were incorporated to explicitly represent anthropogenic surface changes that influence hydrological response through modifications in infiltration, evapotranspiration, and runoff generation. The selected land cover classes reflect dominant and hydrologically distinct surface types within the basin. The use of multi-temporal Landsat imagery and a Random Forest classifier enables consistent change detection in a heterogeneous tropical environment, while accuracy assessment using multiple metrics enhances confidence in classification reliability. Future LULC projections were included to explore plausible development pathways rather than to produce deterministic predictions.

The climate change assessment combines satellite observations, reanalysis data, and CMIP6 multi-model ensembles to characterise historical variability and future uncertainty in rainfall dynamics. Bias correction and downscaling ensure suitability for hydrological impact analysis, while the selection of contrasting SSP scenarios allows evaluation across a range of plausible future conditions. The HBV-light model was selected for its suitability in data-limited basins and its ability to reproduce seasonal and interannual streamflow variability. Its conceptual structure and parsimony support scenario-based assessment of combined climate and LULC impacts at the basin scale.

3.3 Partial Conclusion

This chapter outlined the types of data, materials, collection processes, and methodologies used for data processing and analysis. For the systematic literature review, data were sourced from four major databases: ProQuest, Scopus, Web of Science, and Google Scholar, along with selected grey literature. A four-step framework involving scoping, planning, searching, screening, and then forming the basis for bibliometric and systematic analyses. After rigorous screening, 65 relevant articles were selected from an initial pool of 142 for detailed analysis.

For the land use and land cover (LULC) analysis, satellite images from Landsat 7, 8, and 9 were retrieved and processed using Google Earth Engine (GEE). A Median Composite Algorithm (MCA) was applied to minimise atmospheric distortions. To align with SDG targets and Agenda 2063 (Africa We Want), images were analysed for three key time points: 2007, 2015, and 2023. LULC was classified into five categories: forest, cultivated lands, built-up/bare lands, water, and natural vegetation. Spectral indices such as NDVI, MNDWI, and BSI were computed to improve classification accuracy. A Random Forest (RF) machine learning algorithm was used for classification, with data split into 70% for training and 30% for validation. Model performance was assessed using the user's accuracy, producer's accuracy, overall accuracy, and the Kappa coefficient, ensuring reliable classification. Change detection was performed using absolute, relative, and rate of change indicators, providing insights into long-term land cover transformations. The CA-Markov model was also applied to project future LULC changes for 2030 and 2063, under a business-as-usual (BAU) scenario, to evaluate the impact of unregulated small-scale mining (Galamsey), political interference, and limited basin management on land use.

For the climate change assessment, data sources included ground station data, high-resolution satellite datasets (CHIRPS), reanalysis datasets (ERA5), and CMIP6 climate projections. Data validation involved statistical comparisons between observed station data and reanalysis datasets (ERA5, CHIRPS), using metrics such as correlation coefficients, mean absolute error (MAE), and bias correction techniques. The quantile mapping approach was used to bias-correct CMIP6 projections, ensuring their comparability with historical climate observations. These methodological approaches facilitated an in-depth evaluation of seasonality, extreme events, and long-term climate change projections for the PRB.

The adopted HBV modelling framework combined robust calibration, multi-criteria evaluation, and uncertainty assessment to ensure reliable streamflow simulation. This integrated approach provides a sound basis for analysing hydrological processes and interpreting subsequent results for the Pra catchment.

Overall, this chapter described the materials and tools needed to achieve the objectives of the study. It also systematically provides the methods and framework to be adopted for analysis and results.

CHAPTER 4: STATE OF THE ART OF BASIN

This chapter presents the findings and discussion from a systematic literature review analysis of the Pra River Basin in Ghana, West Africa, from 2006 to 2023. The chapter is in 2 main sections: Section 4.1 (results and findings of articles under review), the Section 4.2 (discussion of Section 4.1, implications, and perspectives). The study aims to identify prevalent research interests, gaps, and trends during the specified timeframe.

4.1 Results

4.1.1 Overview of Bibliometric Parameters and Article Production

Figure 4.1 displays the overview of bibliometric data on the Pra River Basin research extracted from the four databases from 2006 to 2023. The corpus comprises 65 documents from 47 distinct sources, with an annual growth rate of approximately 9.25%. Co-authorship metrics indicate substantial international engagement: the dataset includes 216 authors, with an average of 4 co-authors per document, 32.31% international co-authorship, only 4 single-authored documents (6.2% of total publications), and 280 author-supplied keywords. Document citation patterns show an average of 23.63 citations per article, with documents averaging 7.45 years in age at the time of analysis, indicating a mix of foundational and recent scholarship.

Annual article production on hydroclimatic change, land-use/land-cover (LULC) and water quality in the Pra River Basin, Ghana, demonstrates a clear four distinct periods (Fig. 4.2). From 2006 to 2011, publication output was sparse and irregular (no or 1 article per year). Between 2012 and 2015, a modest increase, with 2 and 4 annual. The period 2016 - 2019 recorded the highest publication (16 articles). The final period, 2020-2023, showed 9 publications per annually.

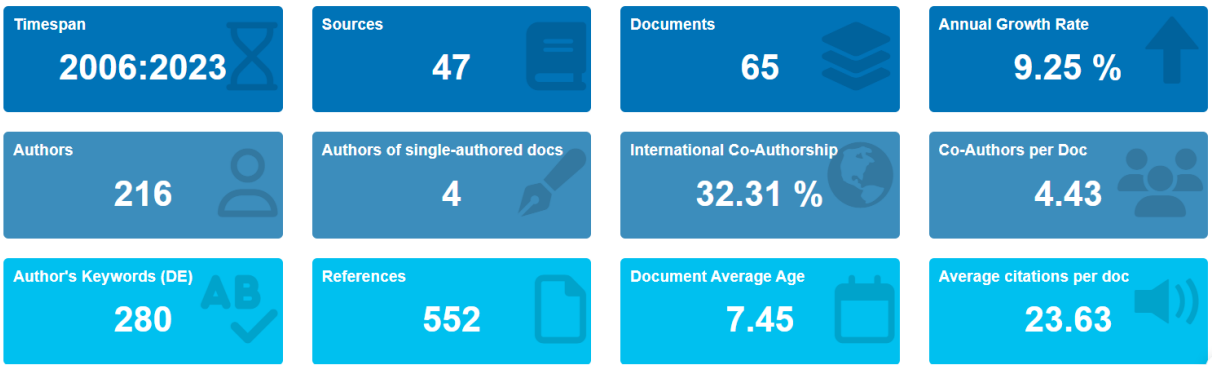

Figure 4.1:Overview of bibliometric parameters on the Pra River Basin

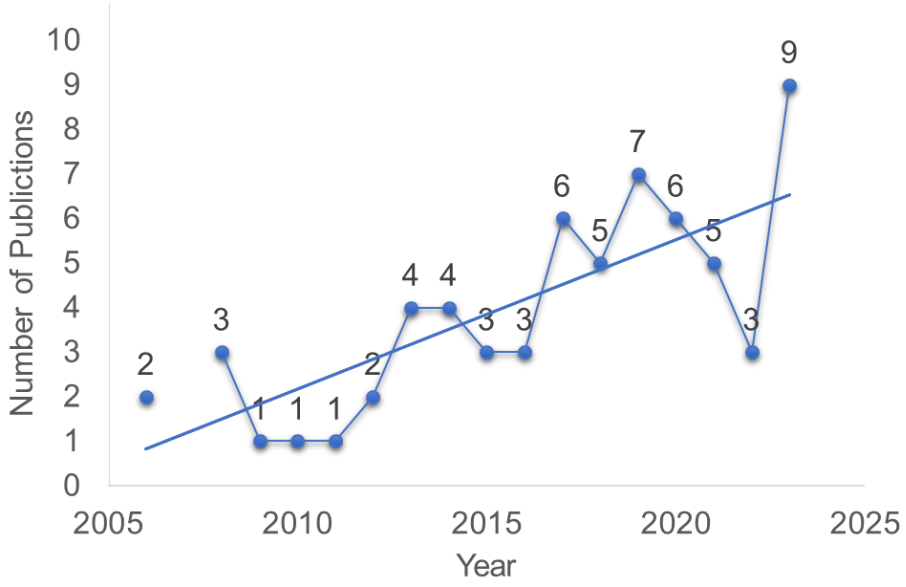

Figure 4.2:Annual article production trend on the Pra River basin.

Table 4.1: Overview of publication trend from 2006 to 2023.

Year	Articles
2006	2
2007	0
2008	3
2009	1
2010	1
2011	1
2012	2
2013	4
2014	4
2015	3
2016	3
2017	6
2018	5
2019	7
2020	6
2021	5
2022	3
2023	9
Total	142

4.1.2 Life Cycle of Scientific Production

The logistic life-cycle model (Fig. 4.3) applied to Pra River Basin research publications reveals a characteristically sigmoidal growth trajectory, with the fitted curve achieving a coefficient of determination (R^2) of 0.728. Observed data points show minimal publication output in the mid-2010s, increasing steadily through the late 2010s, and accelerating into the early 2020s, with several publications reaching or approaching 9 per year. The logistic regression projects a maximum (peak) annual production of approximately 22 publications, expected to occur around 2039 (specifically in July 2038). Following this projected peak, the modelled curve forecasts a gradual and progressive decline in annual publication rates through the mid to late 21st century, with output asymptotically approaching zero by approximately 2080. The R^2 value of 0.728 indicates adequate fit to the observed data, though some residual variance remains unexplained, suggesting occasional high-volatility years or external perturbations not captured by the pure logistic model. The current position of observed data points (as of 2023) places the field in the steep ascending limb of the S-curve, approximately 60% of the way toward the projected 2039 peak, indicating that research production is still in a phase of rapid acceleration rather than stabilisation or decline.

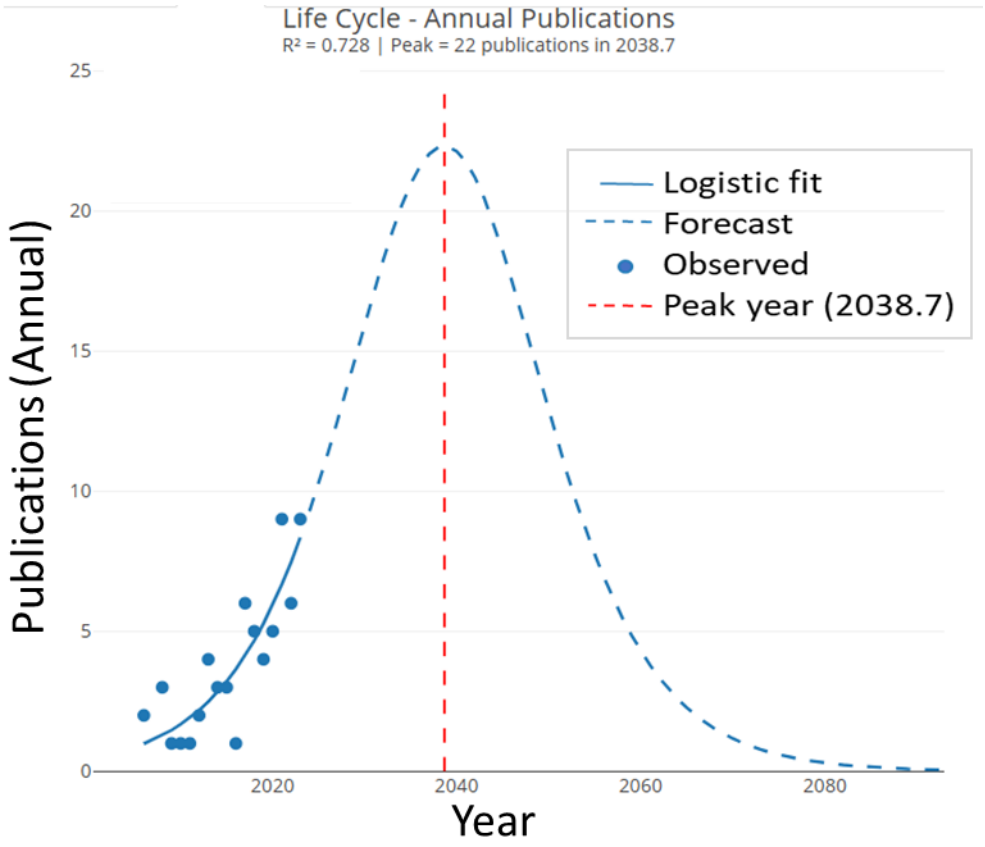

Figure 4.3:Life Cycle of Scientific Production

4.1.3 Country Network Collaboration on Trend Topics

The collaboration network map (Fig.4.4) illustrates international research partnerships centred on the Pra River Basin, with Ghana prominently positioned as a hub from which collaboration lines extend to a global set of partners. The visual representation shows nodes (representing countries) and connecting lines (representing collaborative linkages between institutional authors). Ghana appears centrally located with multiple outgoing connections to partner nations, including North America (Canada, United States), Europe (United Kingdom, EU member states), Asia (China, India), Australia, and African (Nigeria and South Africa). The thickness and density of connecting lines vary, with notably robust connections between Ghana and several European nations, the United Kingdom, and the United States, indicating frequent multi-country co-authorship on research publications. The network exhibits a hub-and-spoke topology, with Ghana as the dominant hub and peripheral nodes representing partner countries with fewer inter-partner connections. This suggests that most international collaboration is bilateral or involves Ghana as a linking partner rather than forming fully integrated regional or global research networks. The geographic dispersal of collaborating nations and the absence of

dense clustering among Global North partners indicate that collaboration is organised around the Pra Basin as the focal geographic and scientific object rather than around pre-existing research consortia or international networks.

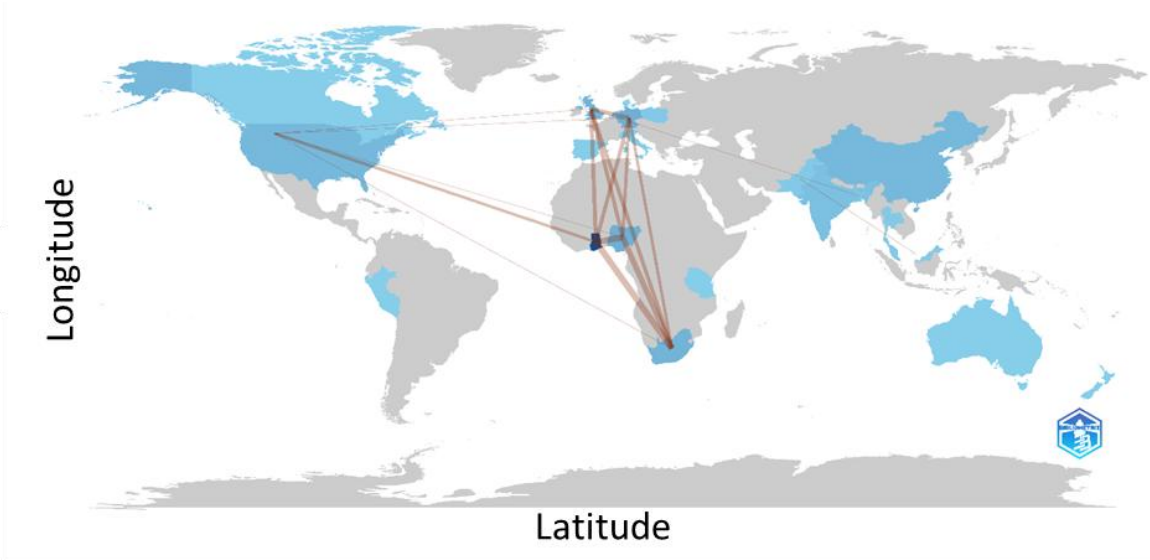

Figure 4.4:Country Collaboration Network Map of research in the Pra River Basin, Ghana

4.1.4 Word Cloud of the Most Occurring Keywords and Trend Topics

Figure 4.5 shows the word cloud analysis of the top 50 keyword frequencies of articles under review, organised by word size corresponding to occurrence frequency in The largest terms were "Pra River Basin" and “Ghana”, representing the central organising concepts of the research corpus. Followed by "climate change," and "water quality", and at medium font size include "vulnerability," "adaptation," "water pollution". "GIS", "remote sensing," "risk assessment," and "change detection" reflect a diverse methodological toolkit. Smaller-font keywords such as "small-scale mining," "illegal mining," and "heavy metals" appear with lower frequency. The structure of the word cloud demonstrates that while research operates within a common conceptual framework (climate-change impacts on basin water resources), it branches into specialised thematic areas reflecting specific environmental stressors, geographic sub-units, and methodological approaches.

Figure 4.5:Word Cloud of the top 50 frequent keywords in literature under review

4.1.5 Thematic Mapping, Evolution, and Their Factorial Analysis of Keywords

The thematic map (Fig. 4.6) classifies research keywords according to two dimensions: relevance degree (centrality, horizontal axis) and development degree (density, vertical axis), organised into four quadrants. Motor themes (upper right) address high centrality and growing research areas within the field, suggesting "Pra River Basin," "change detection," "GIS", and "climate change". Basic themes (lower right) with high centrality but lower development density include "water quality" and "irrigation," indicating recognised known concepts not currently a primary research focus. Niche themes (upper left) with low centrality but high development density include "estuaries," which represent specialised topics investigated in depth by research subgroups but not yet a mainstream research focus. Emerging or declining themes (lower left) with low centrality and low development include "risk assessment" and "temperature", suggesting these represent either nascent research directions or topics declining in prominence.

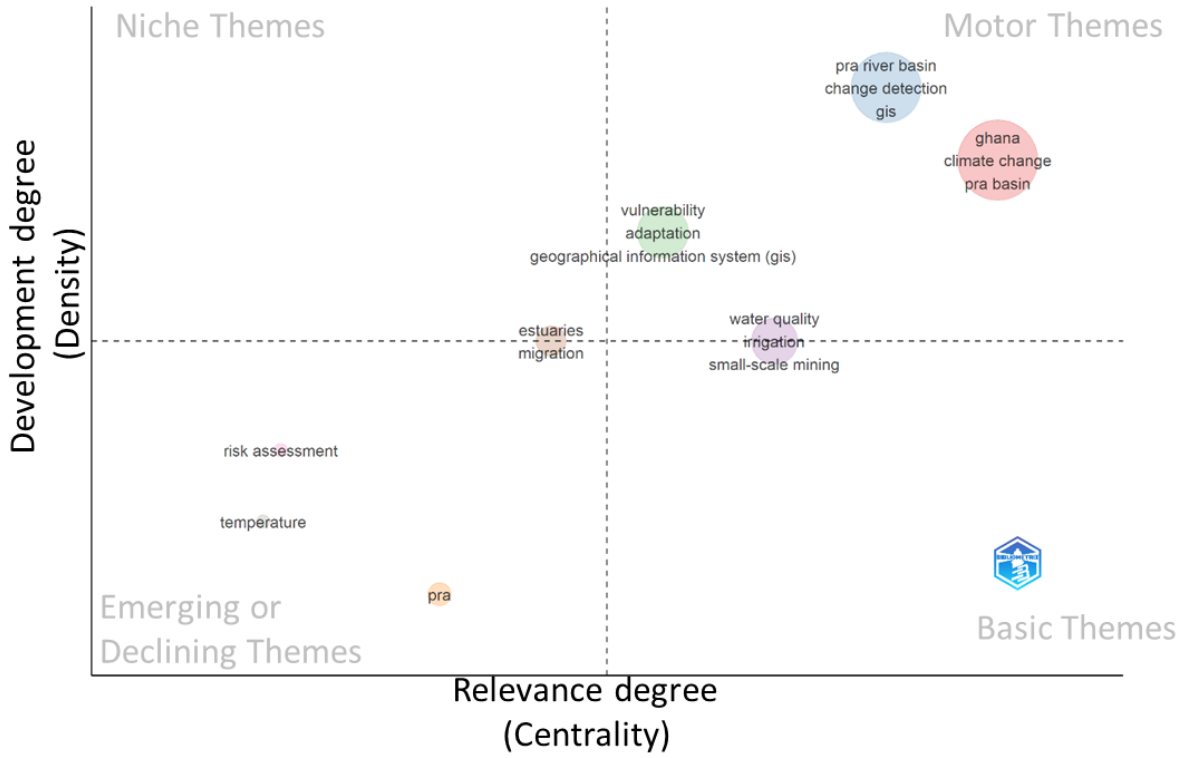

Figure 4.6:Thematic Mapping (Four Quadrants) of research keywords from the literature under review

Additionally, the thematic evolution diagram (Fig. 4.7) tracks keyword prominence across three temporal periods: 2006-2017 (early phase), 2018-2021 (expansion phase), and 2022-2023 (recent consolidation phase). During 2006-2017, the research landscape was sparsely dominated by a single large red bar, "climate change" as the overarching conceptual frame, with minimal contributions from "risk assessment" and "ecological impact." From 2018-2021, "Ghana" became the geographically grounded research, followed by "climate change," "irrigation," "rivers," and "disasters," reflecting thematic diversification and recognition that climate variability interconnects with water demand, riverine ecology, and hazard risks. This also shows "climate change" themes still of interest from the early period, while irrigation and disasters emerge as new branches. The 2022-2023 period shows dominance for "Pra River Basin", indicating an explicitly named, focused research object, followed by "climate change", though relatively diminished, and emergence of "quality control" and reappearance of "risk assessment," signalling transition toward specialised basin-specific research with elevated analytical rigour and systematic risk characterisation.

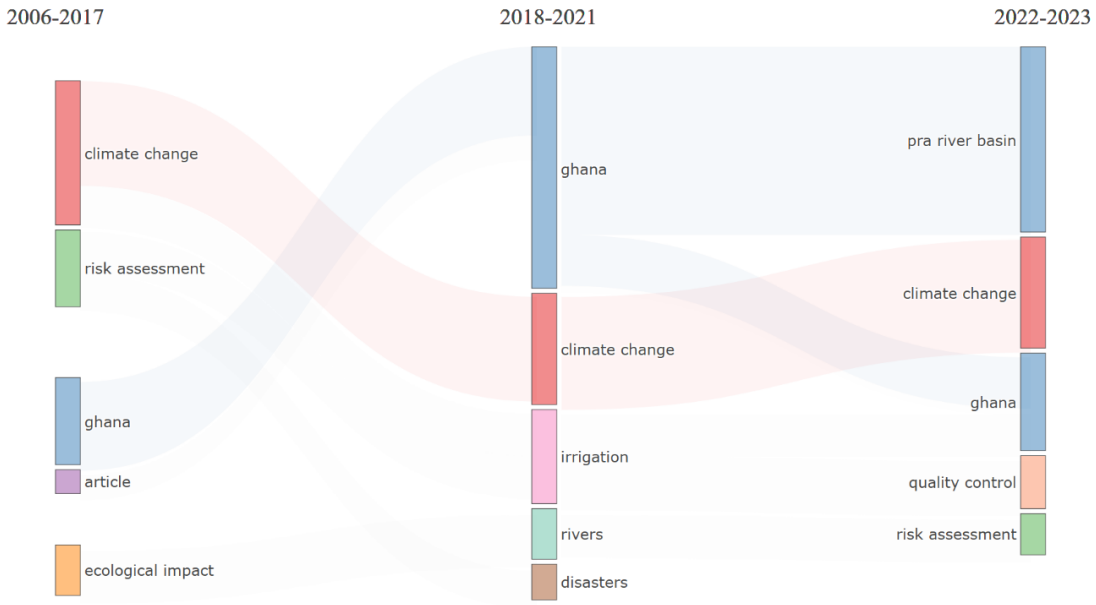

Figure 4.7:Thematic Evolution of keywords showing the early phase, expansion phase and recent consolidation phase of the literature under review

Also, the factorial analysis conducted via multiple correspondence analysis (MCA) reveals the underlying dimensional structure of Pra Basin research, projected onto two principal factorial axes (Fig. 4.8). The red cluster (upper right) represents land-use and land-cover (LULC) research, including "land-use change", "Pra River Basin", "adaptation," and "climate change". This demonstrates the focus on landscape transformations and spatiotemporal drivers. The blue cluster (left and lower-left) represents water quality and pollution monitoring with terms like "water sampling", "heavy metals", "sediment pollution", "environmental monitoring and methodological-analytical terms. This also reflects contaminant characterisation and monitoring protocols. The green cluster (lower-right and right) represents water-resources management and hazard assessment, which indicates integrated water availability and risk governance research. Terminologies such as "remote sensing", "vulnerability", "agriculture", "water management", "groundwater resources", "probabilistic risk assessment," and "population statistics" make up this cluster. The horizontal axis (Dim 1, 61.41% inertia) separates water quality or biophysical characterisation (left) from management and adaptive-response research (right), while the vertical axis distinguishes large-scale LULC drivers and basin-level patterns (upper) from fine-scale hydrogeological processes and socioeconomic

outcomes (lower). Keywords near the origin (e.g., "Ghana", "climate change", "Pra Basin") serve as bridging concepts connecting distinct research domains.

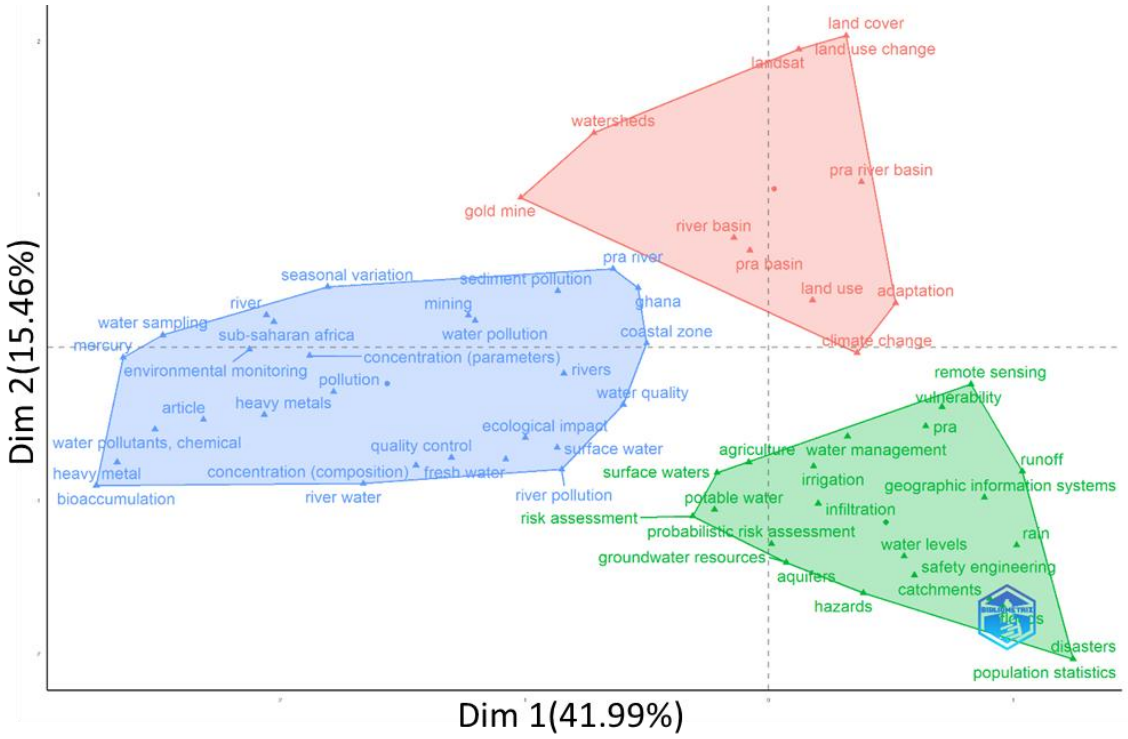

Figure 4.8:Conceptual structure map using the Multiple Correspondence Analysis (MCA) Approach

4.1.6 Research Interest Identified

Based on the motor themes and the most occurring keywords, five key interests identified are water quantity, water quality, land-use land cover change, hydroclimatic modelling, human health and aquatic ecosystem, summarised in Table 4.2. Studies on water quantity in the Pra River Basin focus on streamflow dynamics, runoff variations, and hydrological modelling (Arthur et al., 2020; Awotwi et al., 2017a, 2019; Bessah et al., 2020a; Kankam-Yeboah et al., 2013). The quality of the water is generally acidic, with low pH values in all seasons and high levels of total suspended solids (TSS), turbidity, and colour in the river basin (Darko et al., 2023; Dorleku et al., 2018; Duncan et al., 2018). Additionally, population growth and migration, availability of mineral resources, and response to socio-economic conditions and policies as the main drivers for land use changes within the basin (Akrasi & Ansa-Asare, 2008; Boakye et al., 2020). There are a few studies on hydroclimatic modelling which focused on evapotranspiration, extreme events and rainfall variability (Nsiah et al., 2021; Osei & Amoakowaah, 2021; Owusu & Waylen, 2009)

Studies on human health and aquatic ecosystems assess pollution exposure and biodiversty changes (Okyere, 2018; Oppong et al., 2010). Findings show mercury exposure risks from fish consumption and fish diversity due to improved estuarine conditions (Kortei et al., 2020; Okyere & Nortey, 2018)

Table 4. 2:Selected summary of key interest areas identified, including methods and findings

Author(s)/Year	Method	Findings and Conclusion
		Water quantity
Kankam-Yeboah et al. (2013)	Hydroclimatic analysis: SWAT with ECHAM4 & CSIRO GCMs	Streamflow declines of ~ 22% by 2020 and ~ 46% by 2050.
Awotwi et al. (2017a)	Trend & time-series analysis; Mann–Kendall test.	Runoff reduced during 1987–2000, but increased in 2001–2004 and 2005–2010, linked to anthropogenic drivers.
Awotwi et al. (2019)	SWAT hydrological simulations	A drop in surface runoff and water yield in the dry season, but increased baseflow and evapotranspiration in the 2025 wet season.
Arthur et al. (2020)	SWAT Flow Duration Curves (FDC), Power Duration Curves (PDC).	Ten potential hydropower sites identified; mean annual flows across sites ranged from 5.3 m^3/s to 172.9 m^3/s
Bessah et al. (2020a)	Integrated Valuation of Ecosystem Services and Trade-offs model	The warming scenario projected annual water yield change of +44% (local), -46% (regional), -48% (sub-regional), and -35% (ensemble mean).
		Water quality
Donkor et al. (2006)	Sampling of water, sediment, soil, and biota in wet/dry seasons.	Rainfall influences hydrology, flow, and mercury (Hg) levels; wet season sediments are moderately-severely polluted; dry season shows low contamination; Hg is higher in dry hair samples.
Tay et al. (2014)	Hydrochemical and stable isotopes (^{18}O, 2H)	Groundwater chemistry is shaped by silicate weathering, ion exchange, sea aerosols, and sulfide oxidation; dominant ions: $Na^+ > Ca^{2+} > Mg^{2+} > K^+$ and $HCO3^- > Cl^- > SO4^{2-}$ respectively.
Adukpo et al. (2015)	Gamma-ray spectrometry; ORTEC MAESTRO-32.	^{238}U, ^{232}Th, and ^{40}K detected in water; annual dose 0.35 to 3.91 µSv/yr^{-1}, average 1.82 µSv/yr^{-1}, within WHO safety levels.
Tay (2015)	Q-mode Hierarchical Cluster Analysis (HCA)	Ion-exchange drives shift from Ca-Mg-HCO3/Na-HCO3 to Ca-Mg-Cl water, limited recharge from Na-Cl local rainwater.
Klubi et al. (2018)	New ^{210}Pb-based TERESA model and sediment accumulation rates (SAR).	Sediment accumulation of 2.73 ± 0.06 g $cm^{-2}y^{-1}$ in mining areas; radionuclide levels show no major ecological or health risks.
Essumang et al. (2017)	Water Sampling, Liquid chromatography-mass spectrometry analysis	Tap water treatment fails to remove PFOA, PFOS, PFHxA, PFDA, and PFPeA. The Pra River has 398 ng/L of ∑PFAAs in the river, 200 ng/L in treated water.

Duncan et al. (2018)	Two-season sampling; Nemerow's Pollution Index (NPI)	Metals such as Pb, Cd, Cr, Ni, Fe, and Zn were dominant pollutants, and Mn, As, and Cu minor.
	Land use land cover change impact	
Awotwi et al. (2019)	LULC maps + SWAT analysis	LULC change increased runoff (124.51%) and water yield (40.13%) with reduced baseflow (30.8%) and ET (13.25%); This resulted in less water during the dry season and more during the wet season, as well as in 2025.
(Osei & Amoakowaah, (2021)	SWAT analysis	Topography and forest influenced water loss; evapotranspiration and runoff controlled flow; RCP projections show a decline in rainfall and streamflow.
Awotwi et al. (2018)	SWAT analysis	Small-scale mining boosted runoff (44%) and cut baseflow (23%). Galamsey raised runoff (52%) and sediment (161.9 t/yr); large-scale mining decreased runoff but raised baseflow.
	Hydroclimatic Modelling	
Owusu et al. (2019)	point-to-pixel method, correlation coefficient (r), and per cent bias (%Bias)	The TMPA 3B42 rainfall showed the best performance.
Gyamfi et al. (2021)	CORDEX RCA4 Regional Climate Model simulations.	Four GCMs (CanESM2, IPSL, CNRM-CM5, and HadGEM2-ES) reproduced modest annual biases (0.8%–18.4%); the ensemble correlated strongly ($r > 0.75$).
Nsiah et al. (2021)	SEBAL methodology	Averaged ET 5.63 mm/day, higher over water (5.51–7.81) and uncultivated forests (5.10–7.71); lower over settlements (~2.1)
Oriakhi et al. (2021)	Groundwater Modelling System	Model well calibrated (RMSE = 3.32, $R^2 = 0.99$, and ME = 0.07)
Osei & Amoakowaah, (2021)	the Gumbel extreme value distribution	Projected changes in rainfall maxima, wet/dry spells, and floods under rising due to climate/anthropogenic factors.
Osei et al. (2021)	The R-package hyfo, for CHIRPS and MPI-ESM-MR rainfall datasets.	Short rainfall spells are more frequent than long. Projections suggest increases in both wet and dry events.
	Human Health and Aquatic Ecosystems	
Oppong et al. (2010)	Cold Vapour Atomic Absorption Spectrometry	Fish are unlikely to cause significant mercury exposure when consumed.
Okyere, (2018)	Cast net plus water quality checker	Fish diversity and dissolved oxygen increased across 23 months in the estuary.
Okyere & Nortey, (2018)	Physicochemical factors and macrozoobenthic Bioindicators.	Low benthic macroinvertebrate density (<300 individual/m) indicated low organic contamination.
Kortei et al., (2020)	Atomic Absorption Spectrophotometer	Cd, Pb, As, and Hg levels in fish are within safe hazard quotient limits (HQ <1); no major non-carcinogenic risks.

4.2 Discussion

4.2.1 Bibliometric Parameters and Article Production

The annual growth rate from the articles suggests the rapid focus and attention on the basin in the Anthropogenic era challenges. The study over the basin implies that about one-third of publications involve cross-border collaboration. This also indicates the basin has experienced a moderate collaborative approach in research, though not as extensive as some basins of national interest, like the Volta Basin. The volume of references also indicates a comprehensive literature engagement and a rigorous academic foundation. The average citation rate of the basin research demonstrates a scholarly impact, influence and relevance that the PRB is facing in the Anthropogenic era, including climate challenges from the local perspective. The Author's keywords suggested the diversity in research areas and interests within the basin. This represents multiple subtopics and approaches to addressing the arising challenges. These metrics suggest that the identified research interest on water quality, climate change, land use change, hydroclimatic modelling, and human and aquatic ecosystems has evolved from a niche research area to a substantial interdisciplinary field with growing international collaboration networks. The diversity in co-authorship suggests prospects for more cross-border partnerships, particularly as hydroclimatic-LULC issues increasingly rise above local boundaries and necessitate coordinated global responses.

The trends in annual publications imply that the interest areas remained at a niche stage until 2010, with a single-digit or no publication annually (Table 4.1). The low and irregular output during 2006-2011 reflects the emerging state of coordinated climate-LULC-water research in the basin, occurring parallel to early implementation of Ghana's 2007 National Water Policy. The modest expansion between 2012 and 2015 aligns with the maturation of geospatial tools (GIS, remote sensing) and the growing regional recognition of land-use impacts on hydrology. The sharp acceleration post-2016 directly corresponds to global endorsement of the Paris Agreement (2016) and Sustainable Development Goals (2015), which catalysed climate and water-security research funding and policy prioritisation across Africa. The sustained high production from 2020-2023, coupled with elevated international co-authorship (32.31%) and multi-author collaboration, reflects the basin's integration into competitive international research partnerships and funding mechanisms aligned with climate adaptation and SDG implementation. However, the notable drop in 2022 can be attributed to the many factors and not solely drop in scholarly interest in the field. For example, bibliometric datasets are noted

for delays in indexing in recent years. This often leads to an incomplete representation of publications between 2022 to 2023. Also, backlog of unpublished papers as a result of the COVID-19 Pandemic may have projected the significant output in 2020-2021. Similarly, funding cycles and evolving policy agenda, as the post-COVID-19 economic recovery could have influenced the short-term publication patterns, despite the growing relevance in these interest areas. Regardless, the broader trajectory shows a continued global interest in hydroclimatic-LULC.

Nevertheless, the high citation rate (23.63 per document) suggests that Pra Basin research is increasingly cited and incorporated into broader regional and global scholarship on African water systems and climate impacts. Together, these patterns indicate that Pra Basin research has transitioned from a peripheral, exploratory topic into a recognised focus within African global-change science, attracting substantive institutional and financial support.

4.2.2 Impact of the Life Cycle of Scientific Production

The logistic model's projection of a peak around 2039 suggests that Pra Basin research will reach maximum visibility and intensity within approximately 14-16 years from 2023, assuming current growth trajectories persist. This peak timing aligns plausibly with expected consolidation of methodological approaches, completion of major national and donor-funded research programs initiated during the 2015-2025 decade, and potential saturation of core scientific questions regarding basin hydroclimatic dynamics and LULC impacts. The subsequent projected decline does not imply diminished policy or environmental relevance but rather a transition from rapid discovery and capacity-building research toward embedded, implementation-oriented studies integrated into basin management plans and national water-policy frameworks. The R^2 of 0.728 indicates moderate predictive power; the unexplained variance may reflect funding volatility, policy shifts affecting research priorities, or the emergence of competing research foci. For current researchers and policymakers, the ascending limb of the curve represents a critical window to leverage growing scientific capacity, establish long-term monitoring infrastructure, translate findings into decision-support tools, and institutionalise knowledge systems that will remain valuable after publication rates stabilise, ensuring that the transition from high-volume discovery research to more selective, impact-oriented investigation occurs without loss of scientific rigor or policy engagement.

4.2.3 Relevance of Collaboration Network on Research

Ghana's central position in the collaboration network reflects its status as the basin country and host to major research institutions, government agencies and field-research sites, making it an indispensable partner for any externally-led Pra Basin research. The prominence of connections to European, UK, and North American institutions reflects long-standing North-South research partnerships, capacity-building initiatives, and the availability of competitive funding for African water resources and climate research from entities such as the EU Horizon Europe programmes. The relatively sparse inter-partner connections among non-Ghanaian countries suggest limited regional South-South collaboration or direct partnerships between European and Asian research groups on Pra Basin topics, indicating room to strengthen intra-regional (West African) and inter-regional (African-to-Asian) research networks. While North-South partnerships have been instrumental in building research capacity and providing access to advanced tools and funding, they have sometimes perpetuated asymmetries in which African partners. They provide data and field access while Global North institutions lead publication, methodology development and funding acquisition. Strengthening Ghana-led research leadership, fostering direct partnerships between African research institutions (Nigeria, South Africa, and other West African nations), and creating research funding mechanisms that prioritise African-led teams would enhance research equity, deepen South-South knowledge sharing, and ensure Pra Basin research is aligned with African development and adaptation priorities rather than primarily serving Global North research agendas.

4.2.4 Significance of Keywords to Trend Topics

The dominance of "Pra River Basin", "Ghana", establishes the foundation of the research under review. "Climate change" and "water quality" indicate a growing awareness of the need to understand how climate variability affects water-resource quality and availability in a specific, named geographic system. The substantial representation of "vulnerability" and "adaptation" suggests that research increasingly engages risk-assessment and response-strategy frameworks. This demonstrates a shift from merely understanding the impact of global change to practically developing management strategies toward social-ecological resilience and adaptive management perspectives. The clustering of mining-related keywords ("small-scale mining", "illegal mining", "heavy metals") emphasises real response mechanisms to ecosystem challenges within the Anthropogenic stressors, with mining industries as primary drivers of water-quality degradation and must be studied alongside climate impacts. The prevalence of

remote-sensing and GIS suggests the growing role of technology and data analytics in climate research, enabling basin-scale monitoring and change detection over decadal timescales. This is essential for tracking hydroclimatic and LULC dynamics in data-scarce regions. The presence of participatory rural appraisal terminology alongside remote sensing reflects a growing integration of social and technical dimensions, acknowledging that effective water-resource management requires both biophysical monitoring and stakeholder engagement. Collectively, these patterns demonstrate that Pra Basin research has achieved sophistication in addressing coupled climate-land-water-mining dynamics using diverse methodologies, positioning the basin as an exemplary global-change system where scientific advances can directly inform policy and management actions.

4.2.5 Implication of Thematic Mapping, Evolution, and Factorial Analysis of Keywords

4.2.5.1 Thematic Mapping

The positioning of climate change, change detection, vulnerability, and geospatial methodologies as motor themes indicates that the research field is currently driven by efforts to map and quantify how hydroclimatic and land-cover dynamics unfold across the basin, and is analysed with remote-sensing and GIS capabilities. The classification of water quality as a basic theme shows a central importance, but not intensively developed. This suggests that while water quality degradation is universally recognised as a critical outcome, few studies may focus exclusively on contaminant mechanisms or advanced treatment approaches, representing an understudied frontier. The lack of concentration in niche themes reveals an intellectual gap in Pra Basin studies, indicating both an opportunity to mainstream them and a gap in socio-ecological resilience research. The emergence of estuaries and migration as niche themes signals growing recognition of downstream ecosystem concerns and climate-mobility linkages, reflecting evolving policy priorities under the SDGs. The positioning of risk assessment in the emerging or declining quadrant raises concerns: if emerging, it reflects expected scientific progression from characterisation toward quantitative risk frameworks; if declining, it may indicate saturation or shift toward adaptive-response research rather than hazard documentation. For advancing Pra Basin science, a strategic priority should be transitioning LULC changes and climate change interaction to niche through deliberate funding and capacity-building initiatives, ensuring that scientific advances serve equitable, locally appropriate basin management and climate resilient development.

4.2.5.2 Evolution Mapping

The early climate-centric phase (2006-2017) reflects the post-2007 global consensus on climate change significance for African water resources, following major IPCC reports and the establishment of Ghana's National Water Policy framework. The expansion and diversification phase (2018-2021) directly corresponds to global adoption of the Paris Agreement and SDGs, which catalysed donor funding for climate-water-development research and enabled recognition that hydroclimatic impacts cannot be managed in isolation from competing water demands, land-use change and ecosystem health. The emergence of irrigation and rivers as distinct themes reveals the growth in methods toward explicit water-use nexus analysis, such as integrating agricultural demand, riverine ecology, and hydrological variability. The inclusion of disasters reflects global emphasis on hazard and risk reduction, moving research beyond descriptive climate impacts toward quantified risk characterisation supporting adaptation planning. The most recent period's prominence of "Pra River Basin" as an explicitly named research object indicates the basin has achieved recognition as a distinct scientific system worthy of focused, sustained investigation. The growing emphasis on quality control suggests a transition from exploratory discovery toward evidence-based policy support. For future research directions, sustained investment in vulnerability-adaptation frameworks, participatory governance research, and nature-based solutions will be essential to ensure that scientific maturity translates into equitable, effective basin management and community resilience.

4.2.5.3 Factorial Analysis

The factorial analysis used for the multiple correspondence analysis (MCA) structure demonstrates that Pra Basin research addresses three interconnected yet analytically distinct scientific questions: (1) what land-use and climate drivers are transforming the basin (LULC cluster); (2) what contaminants are present and what are their sources (water-quality cluster); and (3) how can resources be managed and hazards mitigated (management cluster). The red cluster's integration of "adaptation" with LULC research indicates emerging recognition that land-use changes often represent adaptive responses to climate variability (e.g., crop diversification, water harvesting), not merely passive outcomes of economic drivers. The blue cluster's tight association of mining-related terms ("mining", "heavy metals", "bioaccumulation") reveals mining as a critical, well-researched water quality threat specific to the Pra Basin context. Additionally, the presence of standardised analytical terms ("quality control", "water sampling", "concentration") within the blue cluster confirms that water quality research has been extensively researched. The green cluster's integration of "probabilistic risk

assessment", "disasters", and "population statistics" reflects an emerging orientation toward quantitative risk frameworks linking hydrological extremes to demographic vulnerability. This suggests a sophisticated, policy-relevant approach. The separation between biophysical characterisation (blue) and management adaptation (green) suggests specialised research subfields with distinct vocabularies. However, it also shows a concept for integrated assessments. To maximise policy relevance, future research should deliberately integrate insights across clusters through coupled-modelling studies, transdisciplinary teams, and decision-support platforms that translate water quality, LULC, and climate change knowledge into adaptive management strategies and risk-informed planning.

4.2.6 Research Trends, Gaps, Implications, and Perspectives of the State of the Basin

The bibliometric analysis of Pra River Basin research during the anthropogenic-climate change era reveals several distinctive trends that characterise the evolution of this scientific field. Thematically, the research about the basin is evolving from climate-centric framing (2006-2017) toward integrated investigations addressing coupled climate-land-use-water-quality dynamics, with motor themes now dominated by change detection, methodologies, and basin-specific characterisation. However, the management of the state of the basin is tied to socio-economic pressures, with population growth, mining activity, and agricultural expansion acting as the core drivers behind observed environmental trends. These socio-economic drivers do not operate in isolation. They interact, amplify each other's impacts, and are poorly regulated, which leaves the Pra Basin increasingly vulnerable to climatic stressors. Without a coordinated governance response that integrates land, water, and socio-economic planning, the basin's future remains at risk. This suggests the urgency for an integrated research on the climate-land use and hydrology nexus.

The study has identified gaps and future research perspectives that need to be prioritised for management decisions.

- Using satellite and reanalysis data for reliable and conclusive outcomes constrained by the scarcity and reliability of available data.
- Adopting advanced approaches (remote sensing and physically distributed hydrological models) that offer huge potential in overcoming the challenges in trend uncertainties. Such models can establish basins' baseline hydrological behavior, especially in data-scarce environments, and provide ensemble projections for various change scenarios.

- Research studies on groundwater resources of the basin, the interaction between surface and groundwater, water availability and allocation under anthropogenic activities, and socio-hydrology should be the new trends.
- The factorial structure revealing distinct research clusters (LULC, water quality, climate change, and resource management) underscores the necessity of transdisciplinary synthesis and integrated assessment platforms to inform coherent policy responses.

4.3 Partial Conclusion

The investigation into research on the Pra River Basin in Ghana under the Anthropogenic-climate change era extracted 65 documents from 47 distinct sources across four databases from 2006 to 2023. The findings demonstrated an annual growth rate of approximately 9.25%, thematic expansion, and increasing international collaboration. The marked acceleration in annual publications, particularly since 2016, underscores the basin's emergence as a focal point in African and global water-climate research, driven by international policy initiatives such as the SDGs and the Paris Agreement. Thematic mapping and factor analyses reveal the evolution from singular climate-centric studies toward more multi-dimensional research addressing land-use change, water quality, pollution, vulnerability, and adaptation. Despite these advances, critical gaps remain. An integrated research on climate-land-use change studies is insufficiently mainstreamed, often confined to a niche status rather than being foundational to basin-scale management discussions. Similarly, the mechanistic understanding and applied solutions for mining-induced pollution, as well as research on estuarine and migration linkages, are underrepresented compared to the basin's pressing environmental needs. These gaps highlight an urgent need for transdisciplinary integration, development of decision-support frameworks, and greater investment in locally led, participatory research that addresses both the biophysical and socio-ecological complexities of the basin.

Pra River Basin research is at a pivotal stage: while major progress has been made in expanding thematic scope and collaboration, future advancements will depend on the field's ability to bridge remaining gaps, foster equitable South–South partnerships, and translate scientific insights into policy and practice. This will ensure that research continues to support sustainable management and climate resilience for Ghana and the wider Sub-Saharan region.

CHAPTER 5: EVALUATION OF SPATIO-TEMPORAL LAND USE LAND COVER CHANGE

In this section, results from the spatio-temporal differences in the LULC type distribution across the three historical LULC maps (2007, 2015, and 2023), as well as their rates of change, are described. The future projected LULC maps for 2030 and 2063 are also described.

5.1 Results

5.1.1 Mapping LULC in the Basin

The results of the LULC mapping in the basin for 2007, 2015, and 2023 revealed that the Pra River Basin was originally covered with natural vegetation in its major parts (Fig. 5.1). The classification accuracy and indices for these LULC maps under a 95% confidence interval revealed natural vegetation covered 72.3% of the River Pra Basin in 2007 and followed by 10.4% of forest cover and 1.2% for cultivated/farmland (Table 5.1). However, in 2023, although natural vegetation still covers most of the basin, it has declined to 57.5%, and cultivated/farmland and built-up/bare land have increased to 14.3% and 7.9% respectively. Forest areas also experienced an increase between 2007 (10.4%) to 23.1% in 2015 before declining to 19.8% in 2023. In addition, water increased by 0.2% in 2023 from 2015 (0.3%).

Table 5.1: Classified Area (km^2) and Percentage Cover of the LULC Classes from 2007 to 2023

LULC Class	**2007**		**2015**		**2023**	
	km^2	**(%)**	**km^2**	**(%)**	**km^2**	**(%)**
Forest	2412.8	10.4	5359.2	23.1	4593.6	19.8
Cultivated/Farmland	2788.4	1.2	1670.4	7.2	3317.6	14.3
Built-up/Bare land	1136.8	4.9	1368.8	5.9	1832.8	7.9
Water	69.6	0.3	69.6	0.3	116	0.5
Natural Vegetation	16792.4	72.3	14732	63.5	13340	57.5
Total	23200	100	23200	100	23223.2	100

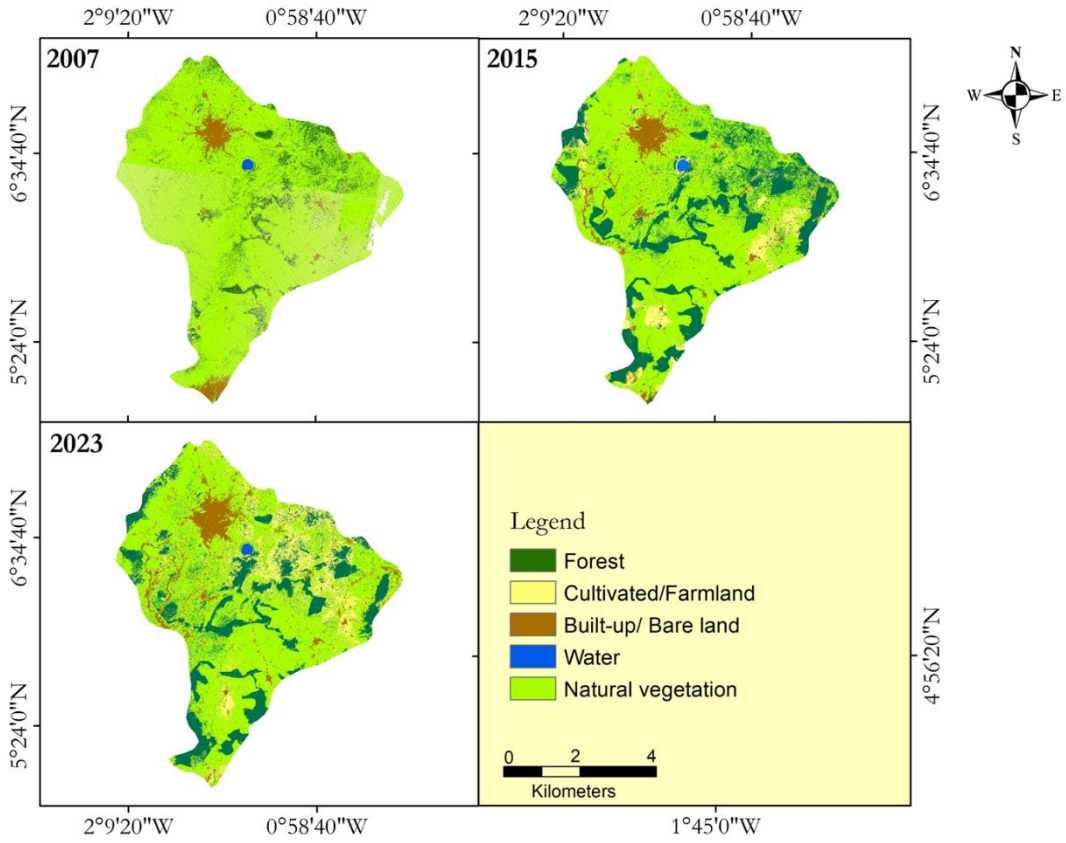

Figure 5.1: LULCC map of the Pra River catchment for 2007, 2015, and 2023

5.1.2 Accuracy Assessment

Findings indicate that natural vegetation constitutes the largest proportion of the classified area, with a row total of 0.5758, while water accounts for the smallest proportion at 0.0046. Minimal misclassification or overlap is evident in the reference data. Forest classification appears relatively accurate, with a minor misclassification rate of 0.0039 against cultivated/farmland and 0.043 against natural vegetation (Table 5.2). However, cultivated/farmland exhibits notable confusion with natural vegetation (0.0986) and, to a lesser extent, forest (0.0279), highlighting challenges in distinguishing agricultural fields from natural landscapes. Built-up areas and bare lands also show considerable misclassification with natural vegetation (0.0232) and cultivated/farmland (0.0063), likely due to spectral similarities in urban-rural transitions.

Table 5.2: Area-based Error Matrix of the 2023 Classified Map with Accuracy Indices presented at 95% Confidence Interval.

Classification	**Reference data**					
	F	**CU/FL**	**BU/BL**	**WA**	**NV**	**Row Total**

Forest (F)	0.1499	0.0039	0.0005	0.0002	0.043	0.1975
Cultivated (CU)/ Farmland (FL)	0.0279	0.0155	0.001	0.0000	0.0986	0.143
Built-up (BU)/ Bare lands (BL)	0.0031	0.0063	0.0464	0.0000	0.0232	0.079
Water (WA)	0.0012	0.0001	0.0004	0.0023	0.0006	0.0046
Natural Vegetation (NV)	0.0553	0.0475	0.0094	0.0000	0.4636	0.5758
Total	**0.2373**	**0.0734**	**0.0578**	**0.0025**	**0.629**	**1**

The supervised classification of LULC for 2007, 2015, and 2023 yielded pixel-based overall accuracy values greater than 90%. Additionally, the producer's accuracy (PA), user's accuracy (UA), and kappa statistics values were all greater than 90% for the three classes (Table 5.3). This indicates that the classification is reliable and of strong accuracy agreement. The area-based accuracy produced an overall accuracy above 90.4% ± 0.4 with total commission and omission errors of 9.6%. Quantity and allocation disagreements were 2.1% and 4.8% respectively. Omission errors in Cultivated/Farmland were equal in magnitude to those in Natural vegetation. This showed a 3% overestimation in Settlements/bare land areas.

Specifically, for the 2007 classified map, the area of proportion analysis indicated an overall accuracy of 93.2% ± 0.6 and a total error of 6.8%. Exchange and shift errors were 2.3 and 1.8%, respectively, and the quantity disagreement was 2.2%. In terms of omission, water bodies had the highest omission error at about 3%, followed by Cultivated/Farmland, Natural vegetation, Built-up/bare lands and Forest areas, which had the lowest of error. This means the areas belonging to these LULC types were either excluded or misclassified. Similar results were found for the 2015 map with an OA of 94.5 % ± 0.5, PA of > 90%, and the 2023 map with an OA of 95.3% ± 0.5, PA > 90%.

Most errors involved confusion between Water bodies and built-up/bare lands, and Natural vegetation and Cultivated/Farmland, were caused by pixel-level similarity. For instance, the appearance of Water bodies resembles bare land in several locations, leading to overestimation.

Table 5.3: Accuracy Assessment of Pra River Basin from 2007 to 2023.

	Producers Accuracy (%)	**Users Accuracy (%)**
Year (2007-2023) LULC Class	**Range**	**Range**

	Pixel-based		
Forest	98-99.5		96.5-97
Cultivated/Farmland	98.6-99.4		96.8-98.5
Built-up/Bare land	90.5-92.8		93.9-94
Water	100		99.7-100
Natural Vegetation	97.4-99.5		95.2-98.7
Kappa Statistic		95-97	
	Overall Area-based		
Overall Accuracy		93-96	

5.1.3 Change Detection in LULC

The rate of LULC changes from 2007 to 2023 was determined for the Pra River Basin (Fig. 5.2). The rate of change is as follows: cultivated/farmland increased by 25% between 2007 and 2015 and further increased by 8% between 2015 and 2023. Similarly, built-up/ bare land increased by 2.5% between 2007 and 2015 and 4% between 2015 and 2023. Forest showed an increase of 10% between 2007 and 2015, but decreased by 2% between 2015 and 2023. Natural vegetation also showed a decreasing trend between 2007 and 2015 and between 2015 and 2023 by 4% and 1% respectively.

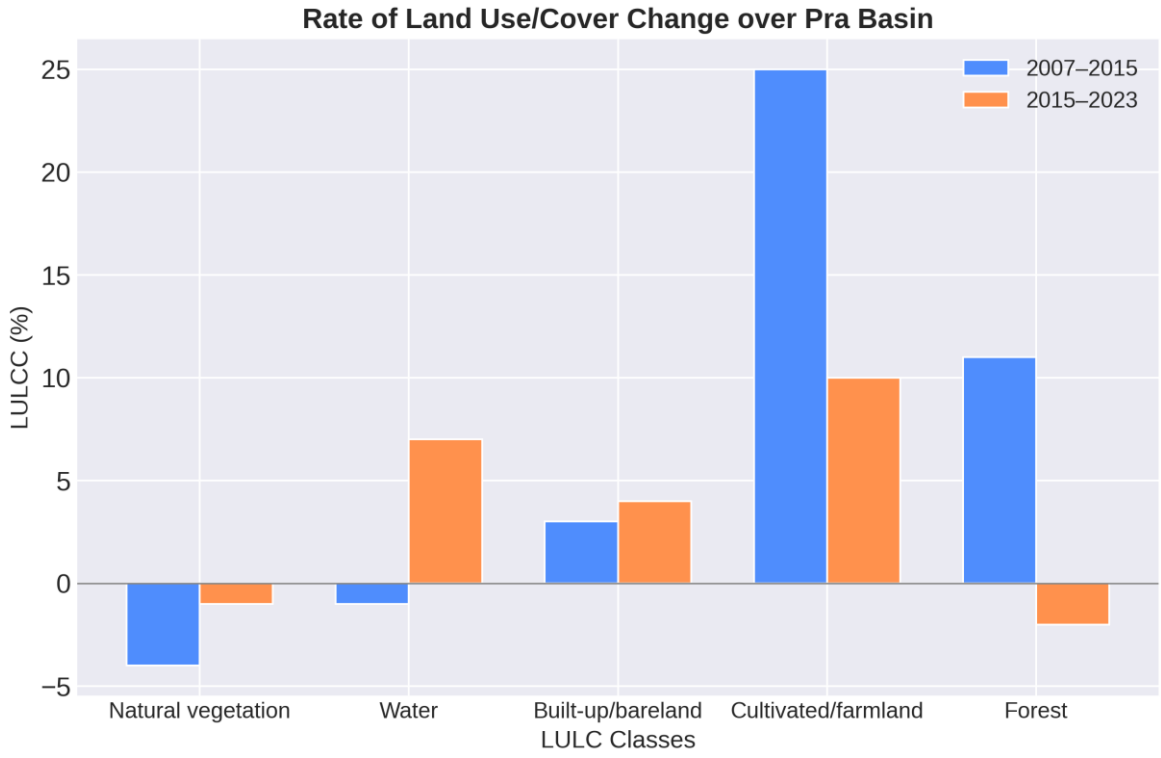

Figure 5.2: A rate of LULC change plot for 2007-2015 and 2015-2023 of the Pra River Basin.

The period from 2015 to 2023 exhibited the fastest rates of losses and gains in LULC, spanning fewer years compared to the periods 2007 - 2015 (Fig. 5.2). Specifically, Natural vegetation

areas have been on a sharp decline from over 80% to 50% within this period, while cultivated lands and built-up/bare lands exhibited sharp increases at from 1% to 15% and 5 to 8% respectively (Fig. 5.3). However, during the periods 2007 - 2015, forest land increased from 10% to 22% but gradually decreasing until 2023 to 20%.

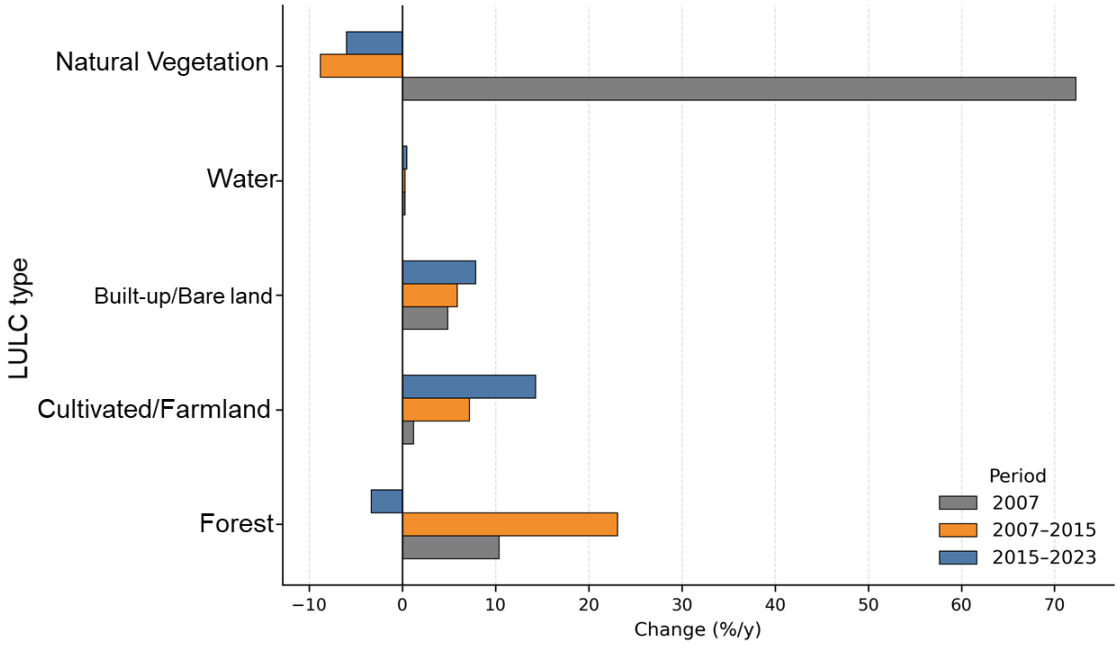

Figure 5.3: A rate of change graph for the time series 2007 to 2023 of the Pra River Basin

5.1.4 Transition Probability Matrix of LULC

A transition probability matrix shows the transfer direction of land use types in the Pra River Basin between 2015 and 2023 (Fig. 5.4). Forest, built-up/bare land, water, and natural vegetation are the most stable with 0.69, 0.84, 0.92, and 0.76 probabilities, respectively. The most dynamic land classes were forest to natural vegetation (0.19) and cultivated land (0.11), cultivated land (0.11) to natural vegetation (0.65), with the latter being the most dynamic in the reverse direction (0.16). These observations are critical transitions for policy attention.

In summary, natural vegetation (> -3300 km^2) and forest (~ -2200 km^2) had losses more than gains from 2007 to 2023 (Fig. 5.5a). However, cultivated/farmland and built-up/bare land gained about 3300 km^2 and 1100 km^2, respectively, compared to losses. Similarly, Figure 5.5b shows that natural vegetation is the most significant contributor to cultivated/farmland, built-up as similar to Figure 5.5c, where forest contribution to land use types changes is significant.

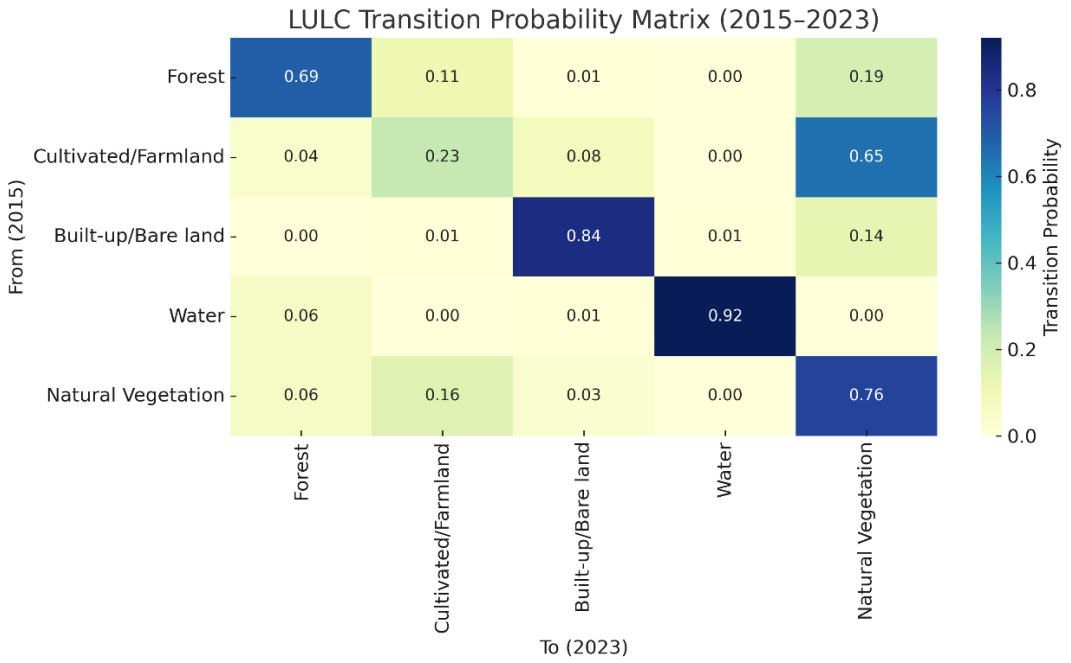

Figure 5.4: LULC transition probability heatmap from 2015 to 2023. The diagonal (persistence within the same land use class) and off-diagonal (transitions to other classes).

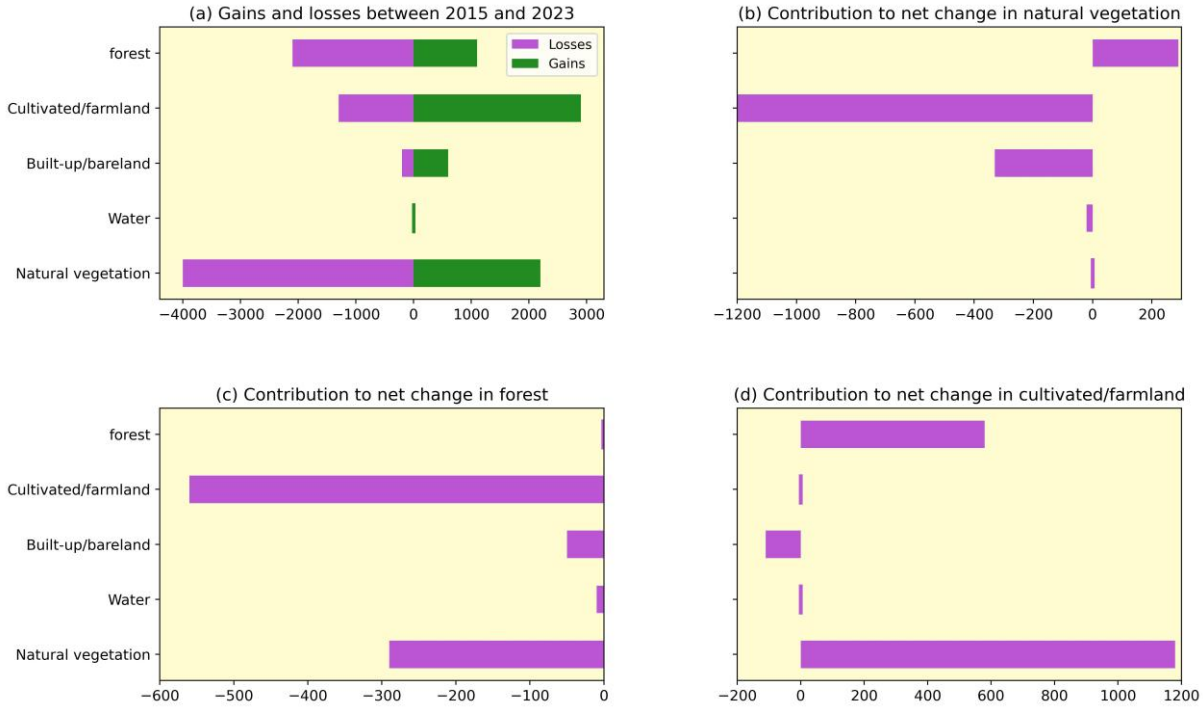

Figure 5.5: Gains and losses, and contribution of net change of LULCC in km^2 in the PRB (2015 and 2023) using Land Change Modeller (LCM) in Idrisi®Selva.

5.1.5 Future land use land cover prediction

5.1.5.1 Validation of 2023 Projected LULC

The 2023 simulated LULC map showed good agreement with the actual map (Fig.5.6). The proportions of total, quantity, and location agreement are presented in Table 5.5. The CA-Markov projection shows fewer changes in cultivated lands in the central part of the basin compared to the actual map (Fig. 5.6). This is observable in how the validation showed a higher location disagreement than quantity disagreement. An overall agreement of greater than 80% depicts acceptable projection performance (Leta et al., 2021). The dominant cover projected in the 2023 simulated map based on the transition trend between 2007 and 2015 is natural vegetation, which is the same as the actual map, but the model underestimated natural vegetation lands by 1 % and overestimated cultivated lands by 4%. The model also projected more Forests than the actual map, while underestimating built-up/bare lands and water.

The relative operating characteristic (ROC) of the CA-Markov model yielded a true positive value of 0.9997, indicating an almost perfect match between the Boolean map of "actual" versus a “simulated” LULC, as well as highly accurate soft prediction. The overall ROC statistic yielded 0.9626, a very strong value indicating prediction accuracy. Kappa values: Kappa standard (0.83), Kno (0.87), and Kappa location (0.88) indicate an over 80% accuracy, demonstrating strong reliability with agreement between the actual and simulated maps. Among the driving factors, slope (0.25), built-up (0.21), and elevation (0.18) exerted a significant influence on LULC change, as indicated by Cramer’s V statistics. In general, variables with Cramer’s V above 0.15 are considered useful predictors, while those above 0.40 are regarded as good.

Table 5.4: Area statistics of actual and simulated land use/cover map of 2023.

	Actual maps		**Simulated maps**		**Difference**	
LULC Type	km^2	%	km^2	%	km^2	%
Forest	4604	19.84	5010	21.59	-406	-1.75
Cultivated /Farmland	3326	14.34	2357	10.16	+966	+4.16
Built-up/ bare land	1833	7.90	1764	7.60	+69	+0.30
Water	105	0.45	93	0.40	+12	+0.05
Natural Vegetation	13833	59.63	14077	60.68	-244	-1.05
Total	23200	100	23200	100		
Performance metrics	**Value**					
Total agreement	0.88					

Quantity agreement	0.79
(disagreement)	0.06
Location agreement	0.80
(disagreement)	0.14

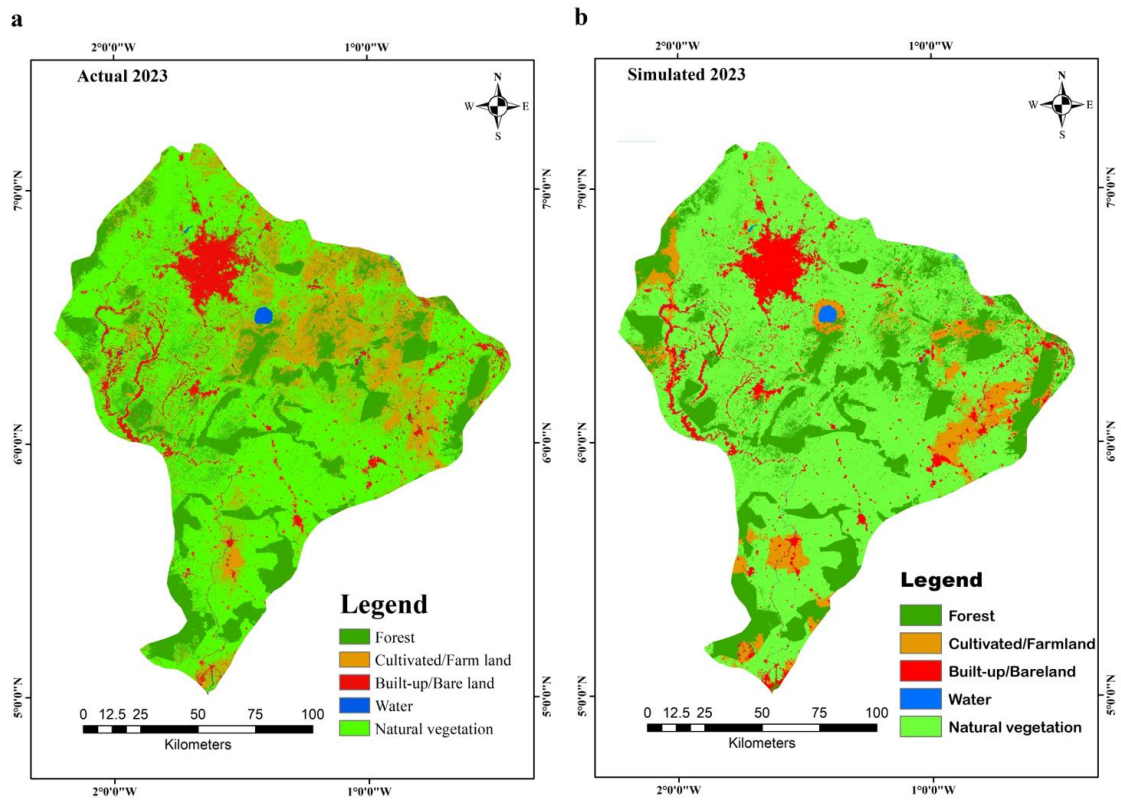

Figure 5.6: The actual (a) and simulated (b) LULC map of PRB in 2023

5.1.5.2 Projected Future Change in LULC

From 2023 to 2030, the third-order cubic polynomial trend surface predicts that human activities will be the dominant driver of land use and land cover (LULC) changes, introducing complexities in transformation patterns. The most notable shifts are forest areas converting to cultivated land and natural vegetation transitioning to built-up and bare lands (Fig. 5.7).

The projected LULC for 2030 and 2063, under the 'business as usual' (BAU) scenario, indicates a continuous decline in natural vegetation, forest cover, and water bodies, while built-up/bare lands and cultivated areas are expected to expand (Fig. 5.8). In 2030, the largest contributions to net change in built-up or bare lands come from natural vegetation (~240 km²), cultivated land (240 km²), and forest (20 km²) (Fig. 5.9, left). Similarly, forest loss (~400 km²) is projected to significantly contribute to cultivated land expansion (Fig. 5.9, right).

Overall, LULC changes across 2007, 2015, 2023, 2030, and 2063 indicate that natural vegetation has been the highest contributor to net land cover transformation, followed by forest

and water bodies. The projected trajectory suggests continued deforestation and expansion of cultivated/farmlands and built-up/bare land through the end of the 21st century, especially if land use continues under the BAU scenario without effective management interventions (Fig. 5.10).

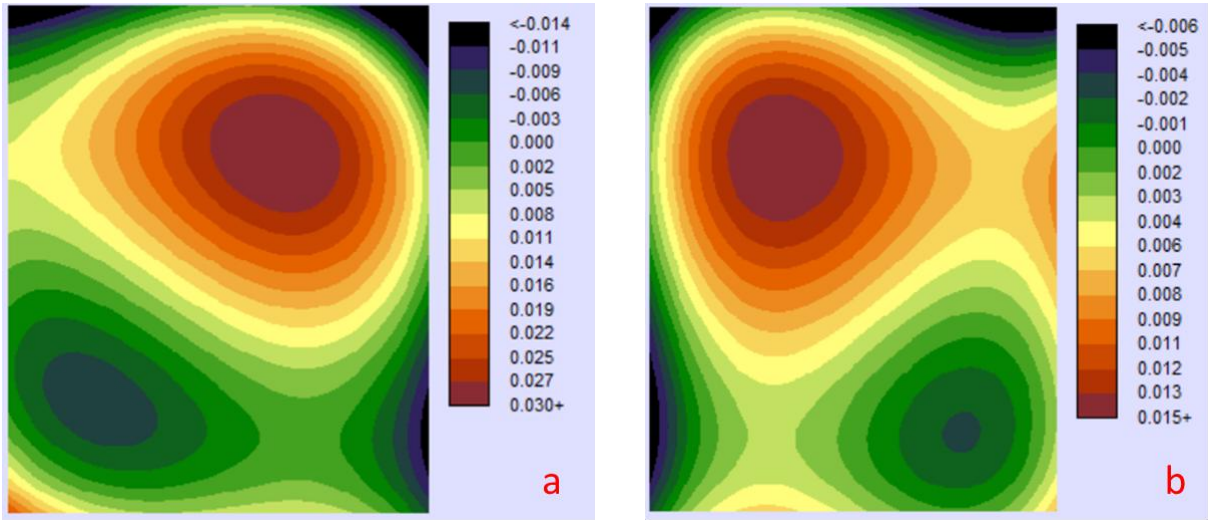

Figure 5.7: A 3rd cubic polynomial surface trend from forest to cultivated land (a) and Natural Vegetation to built-up/bare land (b) between 2023 and 2030.

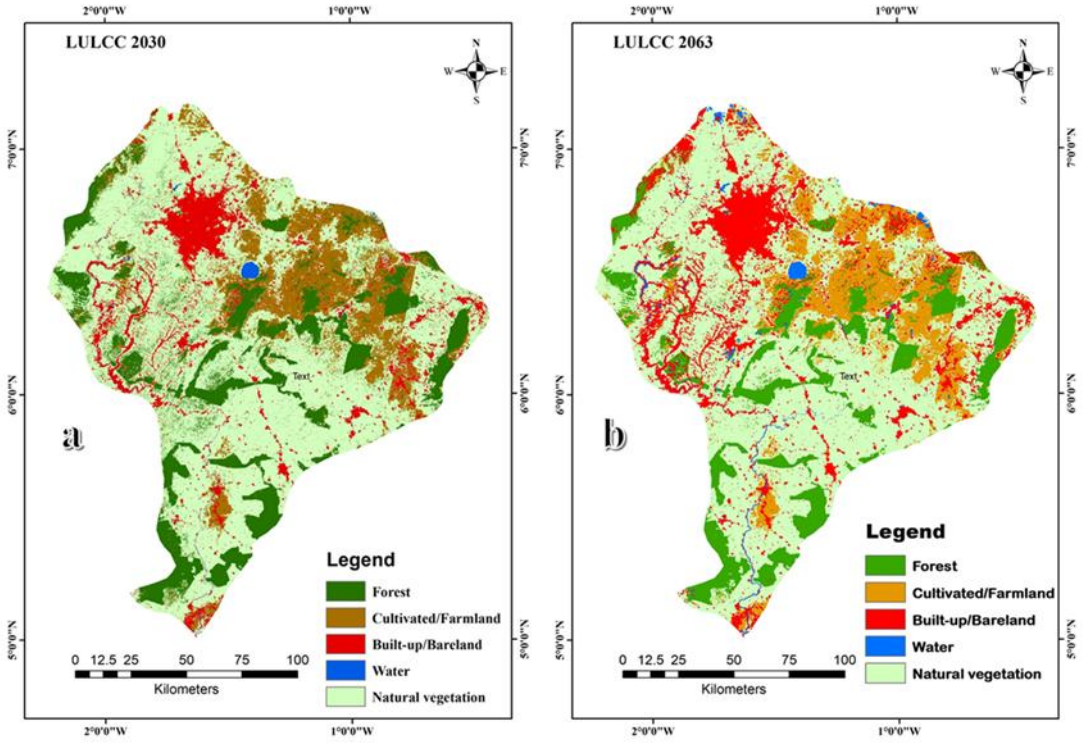

Figure 5.8: Future LULCC prediction (a) LULCC 2030 and (b) LULCC 2063

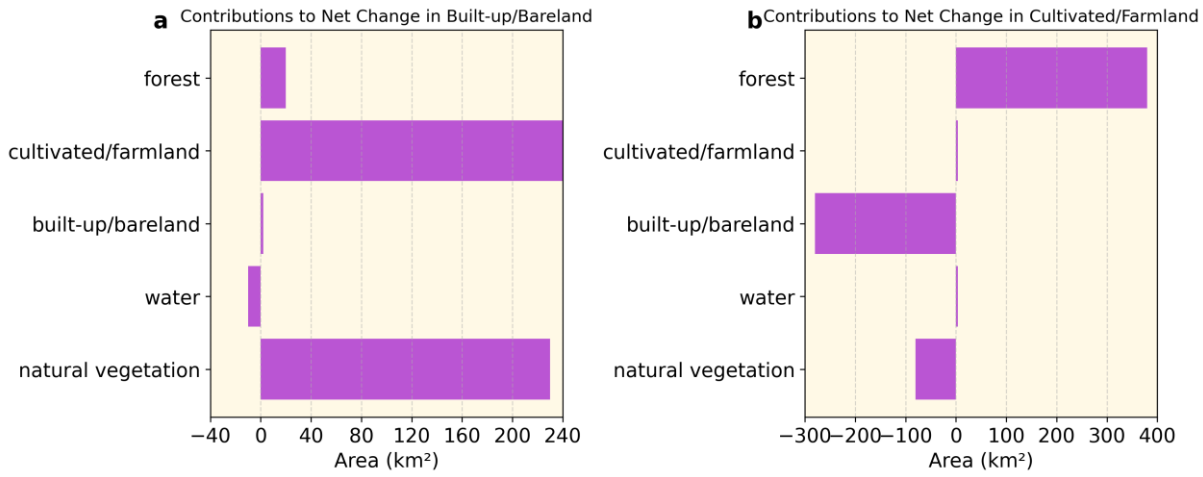

Figure 5.9: Contribution to the Net change in Built-up/bare land (a) and cultivated/farmland (b) for LULC 2030 in km^2.

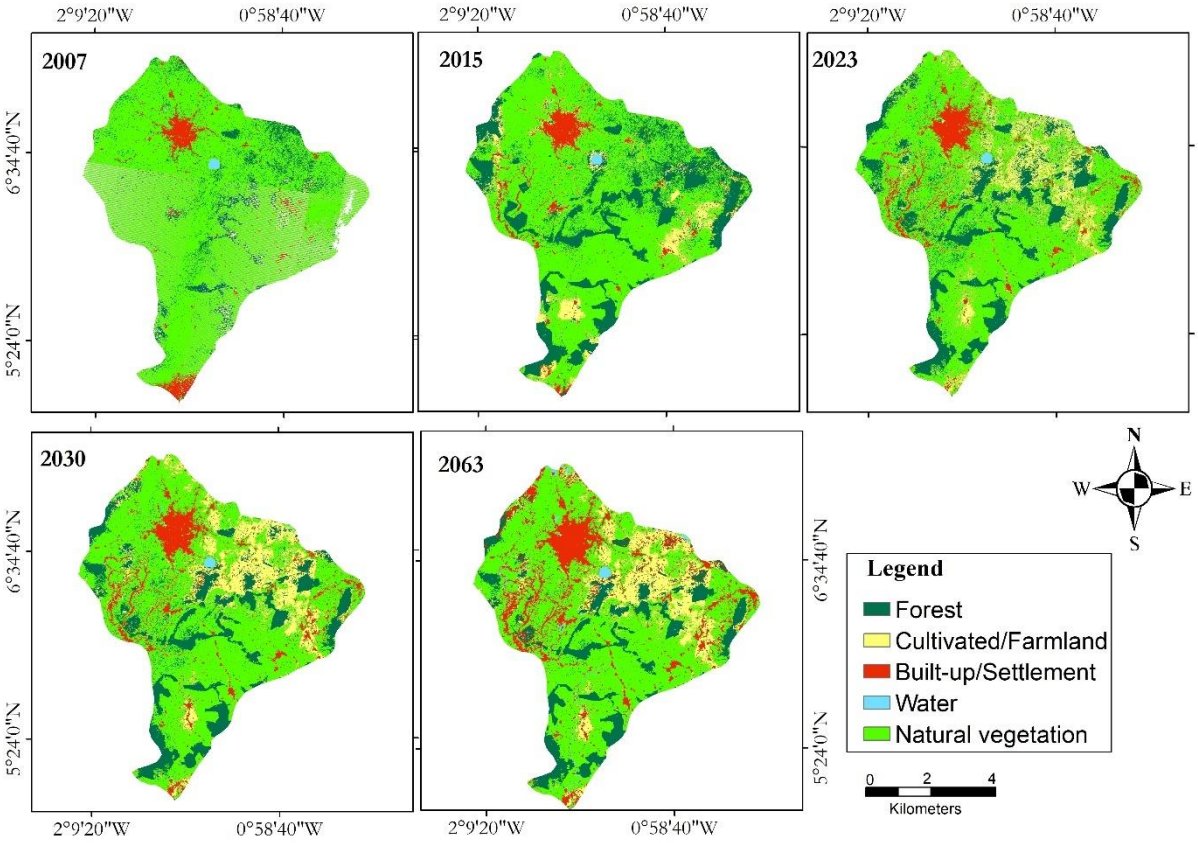

Figure 5.10: LULCC in the Pra River Basin from 2007 to 2063

5.2 Discussion

5.2.1 Assessment of the Spatio-temporal LULC Change

The spatio-temporal analysis of LULC in the Pra River Basin indicates a significant transformation of the landscape over the study period. In 2007, natural vegetation dominated the basin (72.3%), but progressive deforestation and land conversion have led to its decline mainly in favour of cultivated lands and built-up/bare lands. The findings are consistent with earlier works in the basin, which also reported continuous expansion of croplands and urban areas at the expense of forest and natural vegetation (Awotwi et al., 2019; Bessah et al., 2020; Winkler et al., 2021). The spatial pattern of change is heterogeneous: farmland abandonment, deforestation and agricultural expansion are most pronounced in the northwestern sub-basins (Upper Pra, Anum, and Birim). The northeastern zones (Upper and Lower Offin, Twifo Praso) show a stronger riparian deforestation, river encroachment and growth of built-up areas due to mining. Additionally, both the northern (Oda and Upper Pra) and southern (Lower Pra) regions have experienced substantial increases in built-up and bare lands, underscoring basin-wide intensification of human pressure.

5.2.1.1 Socio-economic and Policy Drivers

The Forest shows a distinctive non-monotonic trend: an increase from 10.4% in 2007 to 23.1% in 2015, before declining by 3.3% in 2023. This temporary recovery is plausibly linked to Ghana's National Forest Plantation Development Programme, launched in 2001 with a reforestation target of 20,000 ha per year and to the Modified Taungya System (MTS) introduced in 2002, which incentivised farmers to plant trees alongside food crops. These interventions likely facilitated restoration of degraded forest patches within parts of the PRB before more recent pressures reversed some of these gains. In the later years (2023), intensifying socio-economic drivers, particularly illegal mining (Galamsey), expansion of agricultural land and rapid urbanisation have reinforced deforestation and landscape degradation, contributing to the renewed decline in forest cover. This pattern aligns with studies that link LULC change in the PRB to farmland expansion, mineral exploitation and a roughly 2.2% annual growth rate, as well as rural migration and associated residential and commercial development (Appiah et al., 2015; Boakye et al., 2020; Kankam-Yeboah et al., 2013).

5.2.2 Regional Comparison with the Volta Basin

In a regional context, the PRB's LULC dynamism shows many of the dominant trends observed across the Volta system, while also exhibiting distinctive features. In the White Volta Basin,

Tahiru et al. (2020) report increases in grassland/farmland, settlements, bare land and closed savannah, followed by declines in open savannah and water bodies, indicating a broad shift from natural savannah to more intensively used landscapes. Similarly, several studies in the Black Volta Basin show substantial forest and scrub decline, expansion of cropland and settlements, and strong growth in bare lands, particularly in mining-affected areas (Abungba et al., 2022; Akpoti et al., 2016; Amproche et al., 2020; Dayinday, 2023). At the sub-catchment scale, Nyadzi et al. (2021) show that in the Nasia catchment of the White Volta, shrubland and settlement/bare lands increased over 2000-2020, whereas cropland, forest, grassland and water bodies declined overall. These Volta studies demonstrate a consistent regional signal where conversion of natural vegetation (closed and open savannah, scrub, forest, wetlands) into cropland, bare land and settlements.

Building on this, the PRB shares the overarching pattern of natural vegetation loss and expansion of agricultural and built-up/bare lands, but differs in three important ways. First, the temporary recovery of the forest between 2007 and 2015 is more successful in Pra than in most Volta case studies. This reflects the stronger imprint of national plantation and Taungya programmes in a historical forested basin. Second, while bare lands and settlements also expand in the Volta Basin, these classes are more linked to intensive and often illegal mining as well as to urban growth along key river banks. Third, the forested headwaters and dense riparian zones of the PRB make it particularly vulnerable to riverbank encroachment and riparian deforestation. Much of the Volta system, by contrast, sits within the savannah landscape where dominant degradation pressure arises from woodland and scrub, rather than closed forest. These contrasts suggest that shared regional drivers such as population growth, agricultural expansion, weak land use regulation with basin-specific biophysical conditions and sectoral pressures lead to different patterns of LULC change in forest-dominated landscapes compared with savannah systems.

5.2.3 Hydrological Implications of LULC Change

The LULC changes observed have significantly altered key components of the water balance, especially towards a more “runoff-dominated” regime. Some studies indicate that land cover changes have increased surface runoff by about 124.5%, reduced baseflow by 30.8%, and lowered evapotranspiration by 13.3% (Awotwi et al., 2019; Osei et al., 2019). This reflects the combined effects of forest loss, soil disturbance, and urbanisation. As a result, water loss from the basin is now increasingly governed by topography and the spatial distribution of remaining

forest cover, while evapotranspiration and runoff dynamics shape how rainfall is split between quickflow and delayed subsurface flow. The slight 0.2% increase in water extent or water level observed in 2023 is consistent with this shift, where reduced canopy cover and infiltration capacity have raised the frequency of runoff into the persistently wet regime over southern Ghana.

By 2030 and 2063 in reference to the SDG and Africa's Agenda 2063, respectively, the prevailing trajectory considering the BAU scenarios shows that forest decline, agricultural expansion, mining-related bare land growth and urbanisation are expected to sustain, and potentially intensify, these hydrological shifts. Continued reduction in deep-rooted vegetation and soil structural integrity will likely maintain elevated runoff and reduce baseflow, limiting the basin's capacity to buffer intra-/inter-annual variability in rainfall. This is a concern for long-term water resource sustainability, including reduced reliability of dry-season flows which aligns with findings by Awotwi et al. (2019) and Osei et al. (2019).

5.2.4 Environmental and Socioeconomic Implications

The findings indicate that deforestation and agricultural expansion have accelerated significantly in recent years, particularly between 2015 and 2023. This pattern aligns with broader land use assessments in West Africa, such as the U.S. Geological Survey's study in Benin, which identified the region as experiencing high rates of agricultural land expansion (Tappan et al., 2016).

The rapid loss of tree cover has profound ecological and climatic consequences, given that forests serve as crucial carbon sinks (Wheeler et al., 2016). In particular, forest degradation in the northeastern region is driven by the expansion of mining industries, including large-scale mining, small-scale mining, and illegal 'galamsey' activities. This degradation exacerbates carbon emissions, further contributing to climate change (McNicol et al., 2018).

Additionally, deforestation intensifies the basin's vulnerability to extreme climate events, particularly flooding. Several studies have highlighted the increasing flood risks associated with vegetation loss (Diatta et al., 2020; Dossou et al., 2021; Hounkpè et al., 2019, 2022a; Osei & Amoakowaah, 2021). The implications of population growth within and around the basin are also evident, with the Upper West region experiencing high rates of built-up and cultivated land expansion due to migration patterns (Agariga et al., 2021; Gbedzi et al., 2022).

Population increases drive higher demand for food, water, and settlements, accelerating the transformation of cultivated lands and built-up areas. However, the middle belt of the basin has seen land abandonment, raising concerns about sustainable resource management and long-term ecosystem productivity. Furthermore, forest degradation around the Kwahu Plateau is particularly concerning. The plateau's forests primarily cover mountain tops, and continued deforestation is expected to increase runoff and evaporation rates due to the loss of canopy cover and displacement of topsoil. This underscores the need for enhanced land management strategies to mitigate the negative hydrological and environmental impacts of LULC changes in the Pra River Basin.

5.2.5 Policy Implications on Transition Probability

Over the eight years (2015-2023), some land cover types demonstrated significant stability. Water bodies, for instance, exhibited the highest level of persistence, with a probability of 0.92, suggesting minimal encroachment or transformation. Similarly, built-up and bare land areas remained largely unchanged, with a persistence probability of 0.84. Natural vegetation and forested areas also showed relatively high stability, with probabilities of 0.76 and 0.69, respectively, indicating moderate pressure from external forces such as human activity or natural changes. On the other hand, cultivated or farmland areas showed a much lower probability of remaining unchanged (0.23). This low stability is counterbalanced by a notably high transition probability of 0.65 into natural vegetation. Such a pattern could suggest a widespread occurrence of land abandonment, fallowing practices, or natural regeneration of previously farmed land. Additionally, a portion of cultivated land (8%) was converted to built-up or bare land, indicating urban expansion and encroachment into agricultural zones.

Transitions from forest to other land cover types are particularly critical for environmental management. Approximately 11% of forested areas transitioned to cultivated/farmland, and 19% transitioned to natural vegetation. These changes may point to deforestation driven by agricultural activities or a reclassification due to thinning forest canopies. Similarly, 16% of natural vegetation was converted into farmland, highlighting potential human-induced pressures on ecosystems. Although these conversions might support agricultural livelihoods, they also pose threats to biodiversity and long-term ecological sustainability.

Overall, the transitions from forest to farmland, farmland to natural vegetation, and natural vegetation to farmland represent some of the most critical dynamics in the matrix. These shifts

have important implications for land management, urban planning, and environmental conservation policies, including attaining the UN Sustainable Development Goals:

- SDG 4 - Enhancing public awareness of environmental sustainability and water resource management.
- SDG 6 - Ensuring clean water and sanitation by regulating land use practices that impact water quality.
- SDG12-Promoting sustainable agricultural practices for responsible production and consumption.
- SDG 13 - Supporting climate adaptation and mitigation strategies to combat environmental degradation.
- SDG14 - Protecting aquatic ecosystems and ensuring sustainable water resource management (life below water).
- SDG 15 - Promoting biodiversity conservation and land restoration (life on land).

Additionally, the Business-As-Usual (BAU) scenario serves as a reference case, illustrating the potential consequences of unregulated socio-economic trends, including population growth, deforestation, and land degradation (Fig. 5.9). This calls for the urgent implementation of stringent policy frameworks and regulations to manage river basins and mitigate anthropogenic activities, particularly artisanal and small-scale mining (ASM) along riverbanks. Addressing these challenges requires the promotion of sustainable agricultural and mining practices through: (i) Stronger environmental regulations, (ii) Enhanced enforcement mechanisms, and (iii) Community-driven conservation initiatives.

5.2.6 Management Implications for Water Resources

These findings underscore the need to integrate land use regulation and water resources management more explicitly in the PRB. Given that topography and forest cover are primary controls on water loss (Awotwi et al., 2019; Osei et al., 2019). Protecting and restoring forest in headwater and steep-slope areas, together with enforcing riparian buffer zones, should be central to any strategy that aims to stabilise baseflow and moderate peak runoff. The government must build on the forest restoration initiative targeted at areas in critical recharge zones could help partially reverse the observed declines in baseflow, evapotranspiration and soil erosion. Curbing illegal mining and reclamation requirements is essential to limit the

proliferation of bare lands and disturbed soils that accelerate runoff generation and sediment delivery to streams (Akpoti et al., 2016)

Additionally, a coordinated basin-scale planning that recognises the essence of coupling between LULC, water balance components and hydrological extremes will be critical if the PRB is to maintain both ecological integrity and socio-economic functions under continuing land use intensification and a changing climate.

To reduce pressure on forests, sustainable agriculture practices must be promoted. These include conservation agriculture, agroecology, and climate-smart techniques that enhance yields without expanding farmland. Capacity-building and incentives for farmers will be essential for widespread adoption.
environmental risks can foster stewardship. Participatory land use planning can ensure that interventions reflect local needs and realities.

5.2.7 Classification Accuracy and Challenges

The accuracy assessment of the classified LULC maps demonstrated high agreement with reference datasets, confirming the reliability of Landsat Surface Reflectance data and Random Forest classification algorithms in Google Earth Engine (GEE) for LULC evaluation. However, some classification challenges remain, particularly in distinguishing:

- Built-up areas and bare lands often share spectral characteristics with cultivated lands during the dry season.
- Bare land and water bodies, where mining activities contribute to spectral confusion (Li et al., 2023; Li et al., 2021; Lobo et al., 2016; Snapir et al., 2017).

Furthermore, cloud cover and Landsat's spatial resolution also influenced classification accuracy, underscoring the need for higher-resolution satellite imagery and advanced classification techniques (Dube et al., 2024; Fisher et al., 2018; Momeni et al., 2016)

5.2.8 Partial Conclusion

The spatio-temporal analysis of land use and land cover changes in the Pra River Basin between 2007 and 2023 highlights a rapidly shifting landscape shaped by deforestation, agricultural expansion, urbanisation, and mining. This transition reveals not only extensive ecological transformation but also pressing socio-environmental challenges. The high rate of conversion from forests and natural vegetation to agricultural and built-up areas reflects the growing influence of human activity, driven by population growth, economic development, and land-based livelihoods.

Despite these challenges, the transition probabilities offer a nuanced view of the landscape's dynamics, revealing both vulnerabilities and potential. The notable reversion of farmland to natural vegetation suggests areas of opportunity for ecosystem restoration and sustainable land use. However, persistent land degradation driven by artisanal mining, unsustainable farming, and weak land use regulation continues to undermine progress toward environmental sustainability.

The proposed policy responses and interventions are grounded in the observed patterns and transition dynamics, offering actionable pathways to mitigate further degradation. By integrating spatial planning, community-based governance, sustainable agriculture, and robust monitoring, stakeholders can address current pressures while safeguarding the basin's ecological and hydrological integrity. Ultimately, addressing these issues in a coordinated, multi-level approach that balances development needs with environmental sustainability is essential for advancing the UN Sustainable Development Goals, achieving climate resilience, and ensuring a sustainable future for the region.

CHAPTER 6: CLIMATE CHANGE IMPACT ON BASIN

This chapter focused on characterising rainfall and temperature for both baseline and future projections in terms of extreme indices. It also focuses on the performance of CMIP6 in future projections using SPI and RAI.

6.1 Results

6.1.1 Validation of Datasets

The trend of rainfall from the observed stations of the Pra River Basin from 1981 to 2022 shows an annual range between 750 mm and 1400 mm. While there are some variations, many stations display similar trend patterns in terms of the timing of peaks and troughs, indicating a relatively consistent regional rainfall behaviour across the Pra River Basin. Across the multiple stations, the lowest rainfall events or peaks were recorded in 1994 and 2014, and the highest in 2000, 2008, and 2011.

The Modified Mann-Kendall test and Sen's slope (Fig. 6.2) estimator were applied to analyse long-term trends in rainfall across twelve monitoring stations within the study area (Mann, 1945; Yue et al., 2002). The results indicated statistically significant trends at four locations. Bunso exhibited the strongest decreasing trend ($p < 0.001$), with a Sen's slope of -4.024. Similar decreasing trends were observed at Sekyere Heman ($p = 0.007$, slope = -3.676) and Daboasi ($p = 0.017$, slope = -2.021). Conversely, Adiembra showed a significant increasing trend ($p = 0.006$) with a slope of +2.958. At the remaining stations, no statistically significant trends were detected ($p > 0.05$), although Mfensi approached the 5% significance threshold ($p = 0.052$), indicating a possible weak upward trend. Other stations such as Kade, Twifo-Praso, Dunkwa, and Assin-Praso showed low Tau values and non-significant p-values, reflecting stable or inconsistent long-term patterns (Table 6.1).

In addition, the correlation between the observed data for three selected stations and the reanalysed data (ERA 5) was strong (0.7 to 0.8) for each selected station data signifying the reliability of the ERA 5 data and confidence in using the data as a reference data (Fig. 6.1). These results highlight the spatial variability of trends across the basin, with certain locations exhibiting pronounced hydrological changes likely influenced by climatic variability or land use dynamics.

Table 6.1: Statistical Analysis of Rainfall Trends Using the Modified Mann-Kendall Test and Sen's Slope Method (2000–2022)

Station	Trend	p_value	S	z	Tau	Sens Slope	Intercept
Kade	NT	0.756	-9	-0.311	-0.010	-0.287	1471.540
Twifo-Praso	NT	0.762	-9	-0.303	-0.010	-0.259	1392.457
Owabi	NT	0.331	33	0.973	0.038	1.469	1514.949
Daboasi	decreasing	0.017	-75	-2.391	-0.087	-2.021	1192.806
Assin-Praso	NT	0.216	-35	-1.237	-0.041	-1.162	1500.458
Bunso	decreasing	4.098e-6	-121	-4.606	-0.141	-4.024	1524.902
Adiembra	increasing	0.006	97	2.762	0.112	2.958	1337.186
Akim Oda	NT	0.204	45	1.271	0.052	1.368	1071.538
Dunkwa	NT	0.498	-23	-0.677	-0.027	-0.742	1550.052
Mfensi	NT	0.052	65	1.944	0.075	2.557	1626.942
Offinso	NT	0.265	39	1.115	0.045	1.565	1432.213
Sekyere Heman	decreasing	0.007	-121	-3.752	-0.141	-3.676	1413.611

*NT = no trend

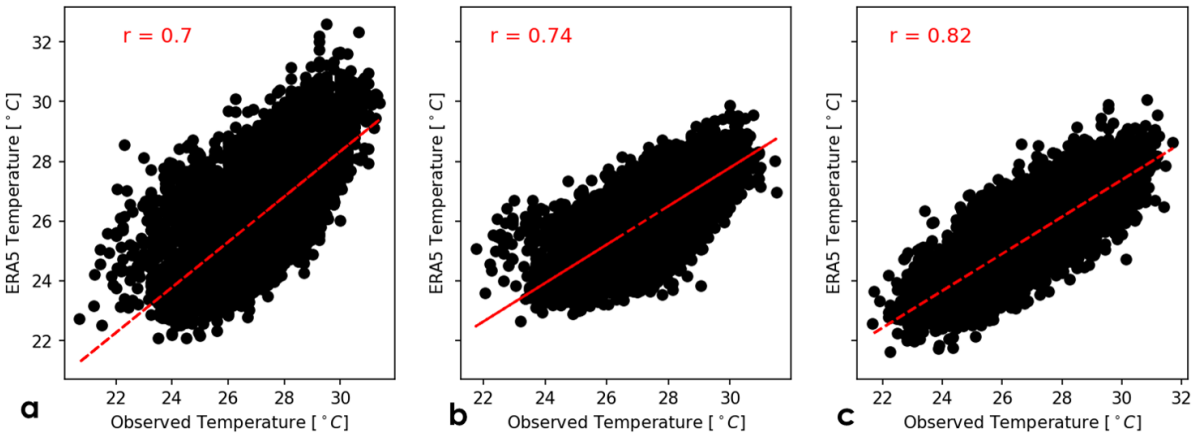

Figure 6.1: Correlation coefficient (r) of ERA 5 against GMet observed data for three gauge stations (a) Dunkwa, (b) Twifo-Praso, (c) Mfensi in the Pra River Basin.

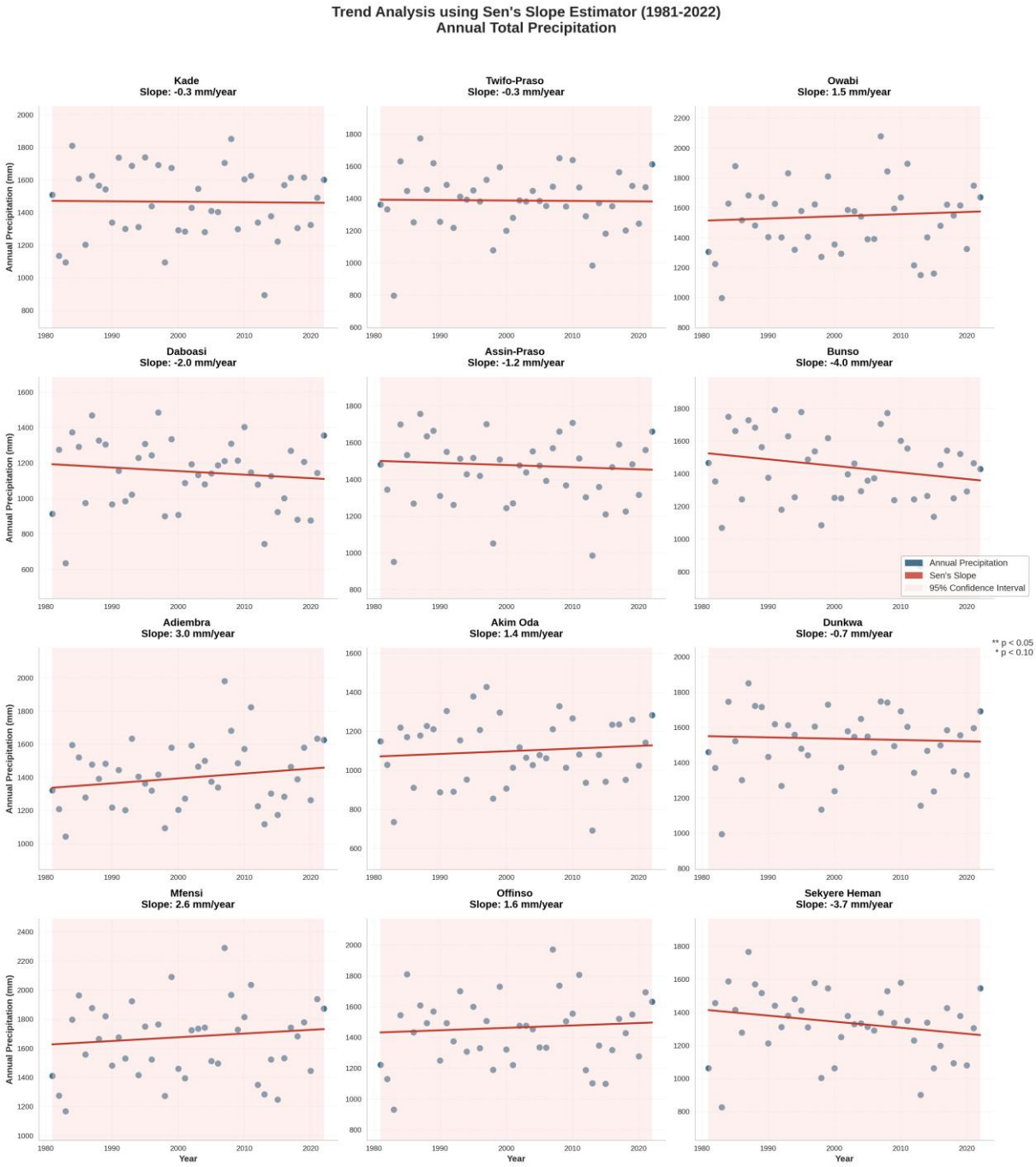

Figure 6.2: Trend analysis using Sen's slope with annual precipitation on the y-axis and the duration on the x-axis for all stations

The LOESS smoothing analysis of annual precipitation from 1981 to 2020 reveals station-specific trends in rainfall (Fig. 6.3). Of the 12 stations, most show weak to moderate trends, with several reaching statistical significance. Increasing trends were observed at Adiembra (+3.3 mm/year, p = 0.041), Mfensi (+2.7 mm/year, p = 0.017), Owabi (+1.9 mm/year, p = 0.010), and Sekyere Heman (+2.6 mm/year, p = 0.026). Decreasing trends occurred at Bunso (−3.8 mm/year, p = 0.045), Daboasi (−1.3 mm/year, p = 0.007), and Twifo-Praso (−2.6

mm/year, p = 0.001). Some stations, such as Akim Oda and Assin-Praso, show minimal trends (±0.5 mm/year), with low R^2 values indicating weak linear relationships. The highest explained variance (R^2 = 0.414) occurred at Mfensi, suggesting more consistent temporal variation, while others had lower R^2 values (mostly < 0.1), indicating high inter-annual variability. Overall, the results show mixed rainfall trends, with localised increases and decreases, but generally weak trends in magnitude. This indicates high spatial variability and modest changes in annual precipitation over the 40-year period.

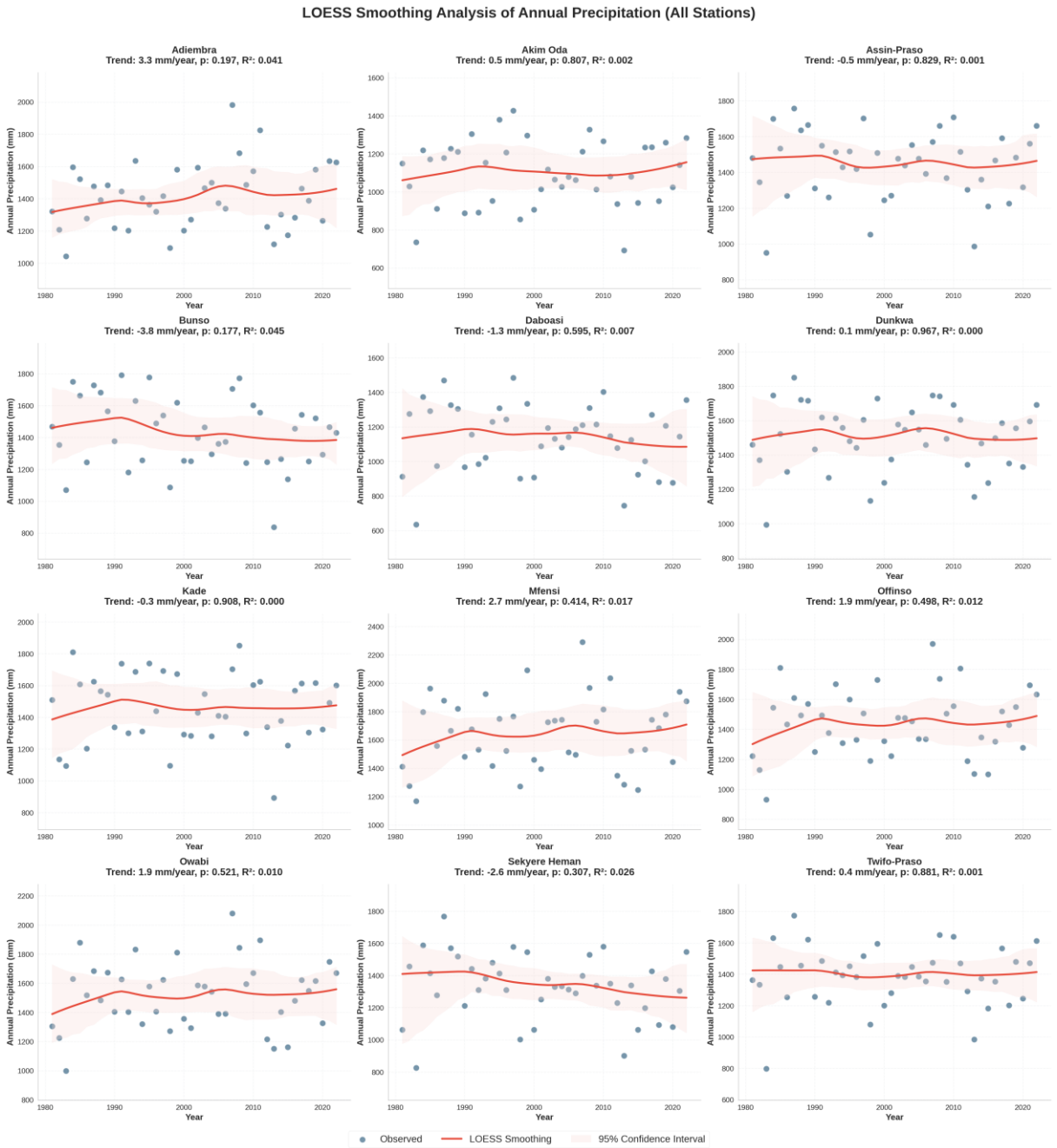

Figure 6.3: Rainfall trends using LOESS for all stations

6.1.2 Rainfall Trends (shifts-onset and CoM)

The normalised cumulative rainfall plots across 12 stations reveal consistent intra-annual rainfall distribution patterns (Fig. 6.4). Most stations exhibit an unimodal to weakly bimodal accumulation curve, with rainfall gradually increasing from the onset to the center of mass (CoM). The onset of the rainy season (red triangles) occurs between Day 50 and 110, while the CoM (black triangles) typically appears between Day 130 and 180, indicating a consistent lag between the start of rains and the point where 50% of annual rainfall is reached.

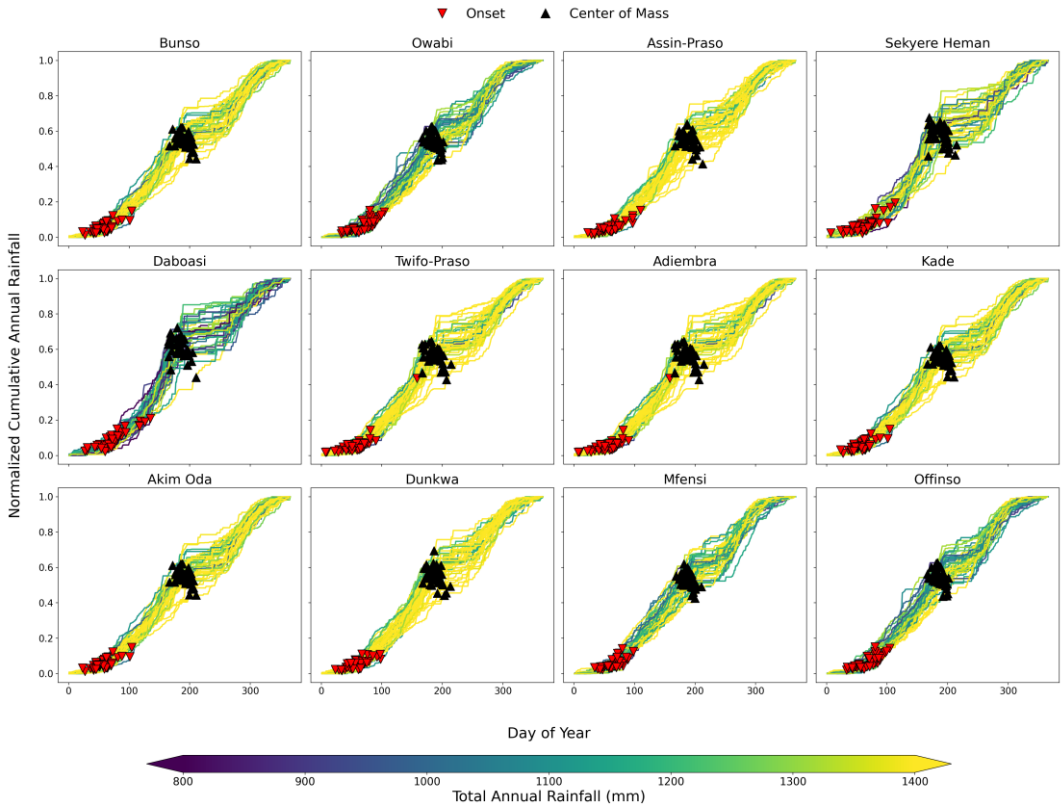

Figure 6.4: Normalised cumulative annual rainfall plot for the twelve stations showing the onset and centre of mass (CoM).

In the coastal zone, Daboasi and Sekyere Heman recorded early and consistent onsets (DOY 07-140) with CoM between DOY 164 and 215 and totals of 1000-1300 mm. In the forest zone, interior stations such as Owabi, Offinso, and Mfensi showed more variability, with onset between DOY 36 and 104 and CoM between DOY 166 and 211. At the same time, Assin-Praso often exceeded 1300 mm despite broader onset ranges (DOY 22-111). Twifo-Praso and Adiembra displayed the widest onset spread (DOY 07-158), yet their CoM values remained concentrated (DOY 166-214).

Stations near the forest boundary (Bunso, Akim Oda, Kade, and Dunkwa) had onset between DOY 23 and 104 and CoM between DOY 166 and 214. Among them, Kade, Akim Oda, and Owabi maintained relatively stable accumulation patterns, while Offinso and Mfensi showed steeper slopes during wetter years, reflecting sharper mid-season rainfall concentration.

Year-specific patterns highlighted interannual variability. The forest zone recorded early onsets in the mid-1990s and delays in the early 1990s, while boundary stations shifted earlier in 2017 but later in the late 1990s. At Twifo-Praso and Adiembra, the onset advanced in 2021 but was delayed in the early 1980s. Coastal stations also showed contrasts, with early onsets in 2011 (Daboasi, Sekyere Heman) and delayed ones in 1983, 2009, and 2021. Across most stations, CoM shifted earlier in wetter years and later in drier years.

Trend analysis using the MK test confirmed spatially variable changes (Table 6.2). Three stations (Sekyere Heman, Adiembra, and Twifo-Praso) showed significant shifts toward earlier onset ($p < 0.05$). Sekyere Heman advanced by ~8 days per decade (Sen's slope -0.78 days/year, $p = 0.0079$), while Adiembra and Twifo-Praso showed comparable advances (~8 days/decade, $p = 0.0328$). A second group (Akim Oda, Bunso, Kade) showed marginally significant earlier trends (-0.394 days/year, $0.05 \leq p < 0.1$), suggesting emerging regional signals. Five stations showed non-significant trends, with slight advancement (Assin-Praso, Dunkwa, Daboasi) or minor delays (Mfensi, Offinso, Owabi). Daboasi showed the most stable pattern (-0.08 days/decade, $p = 0.914$), and Mfensi alone indicated a weak positive slope. Overall, rainfall timing displayed marked spatial and temporal variability, with clear interannual and intra-zonal contrasts in onset, CoM, and annual totals.

*Figure 6.2: Spatiotemporal trends in rainfall onset across the stations in the Pra Catchment based on Mann-Kendall and LOESS Analyses. ** shows the MK significant trend*

Station	Trend	Slope days per year	Trend Direction	MK p_value	R^2
Sekyere Heman	Significant	-0.7836	Earlier	0.0079**	0.181
Adiembra	Significant	-0.8076	Earlier	0.0328*	0.1638
Twifo-Praso	Significant	-0.8076	Earlier	0.0328*	0.1638
Assin-Praso	No	-0.3971	Earlier	0.1064	0.0603
Akim Oda	No	-0.3936	Earlier	0.1087	0.0849
Bunso	No	-0.3936	Earlier	0.1087	0.0849
Kade	No	-0.3936	Earlier	0.1087	0.0849
Dunkwa	No	-0.3291	Earlier	0.179	0.0504
Mfensi	No	0.1237	Later	0.6884	0.0095
Offinso	No	0.0153	Later	0.8709	0.0001

Owabi	No	0.0153	Later	0.8709	0.0001
Daboasi	No	-0.0788	Earlier	0.9137	0.0017

6.1.3 Centre of Mass and Total Annual Rainfall Correlation Analysis Across Stations

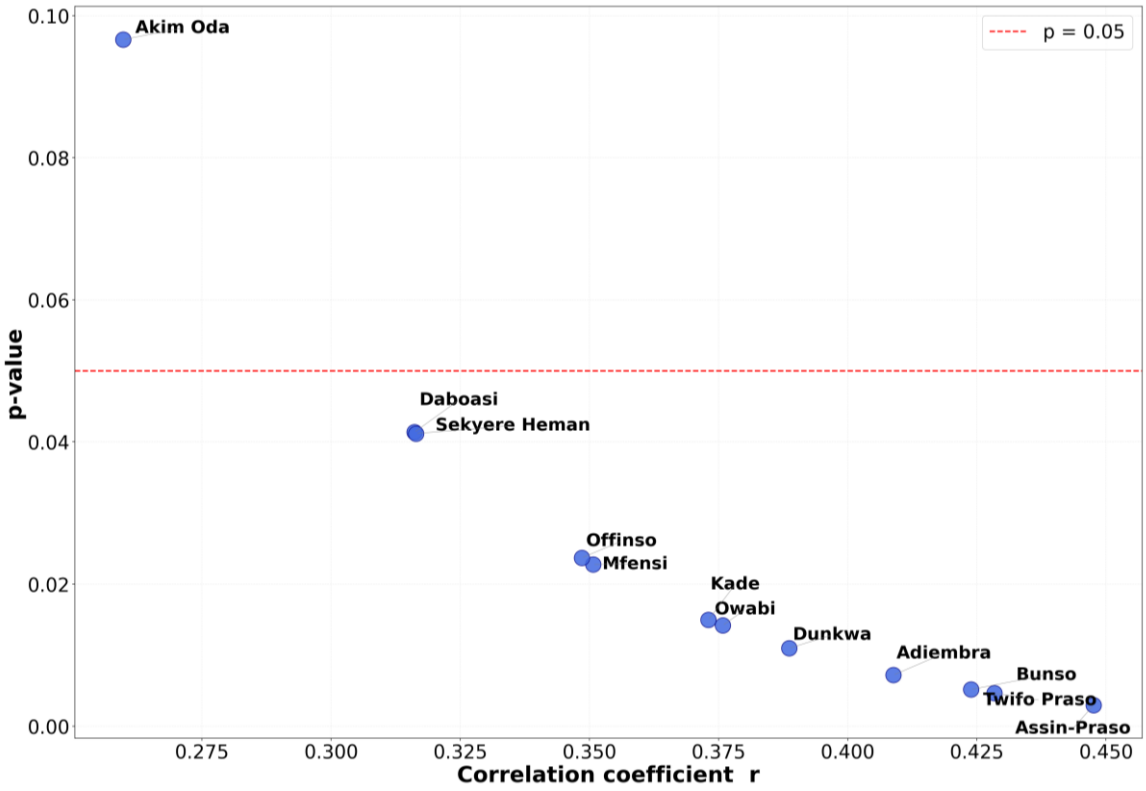

Figure 6.5: The correlation coefficient of rainfall timing (Centre-of-Mass DOY) and total annual rainfall across individual stations. The red dashed line (the threshold: p = 0.05)

The analysis revealed that all stations exhibited positive correlations between CoM and total annual rainfall, indicating that wetter years generally coincide with later seasonal midpoints (Fig. 6.5). This pattern suggests that in years with higher rainfall, precipitation tends to be more spread out, extending the rainy season and delaying the CoM. Most correlations were statistically significant ($p < 0.05$), affirming that the observed relationships are unlikely to be random. The strongest correlations were recorded at: Assin-Praso ($r = 0.448$, $p = 0.003$), Twifo-Praso ($r = 0.428$, $p = 0.005$), Bunso ($r = 0.424$, $p = 0.005$).

These stations demonstrated moderate to strong positive correlations, implying that interannual rainfall variability has a pronounced and consistent influence on the timing of rainfall at these locations. This may be attributed to relatively uniform rainfall patterns with lower intra-seasonal variability. Conversely, the weakest correlation was found at Akim Oda ($r = 0.260$, $p = 0.097$), which was not statistically significant. This suggests that the CoM at Akim Oda is

less sensitive to annual rainfall variability, possibly due to higher intra-seasonal variability, bimodal rainfall distribution, or the influence of local factors such as land use, topography, or dominant convective systems. These findings point to a spatially variable relationship between rainfall timing and magnitude across the study area, with some stations showing strong coherence while others reflect more complex rainfall dynamics.

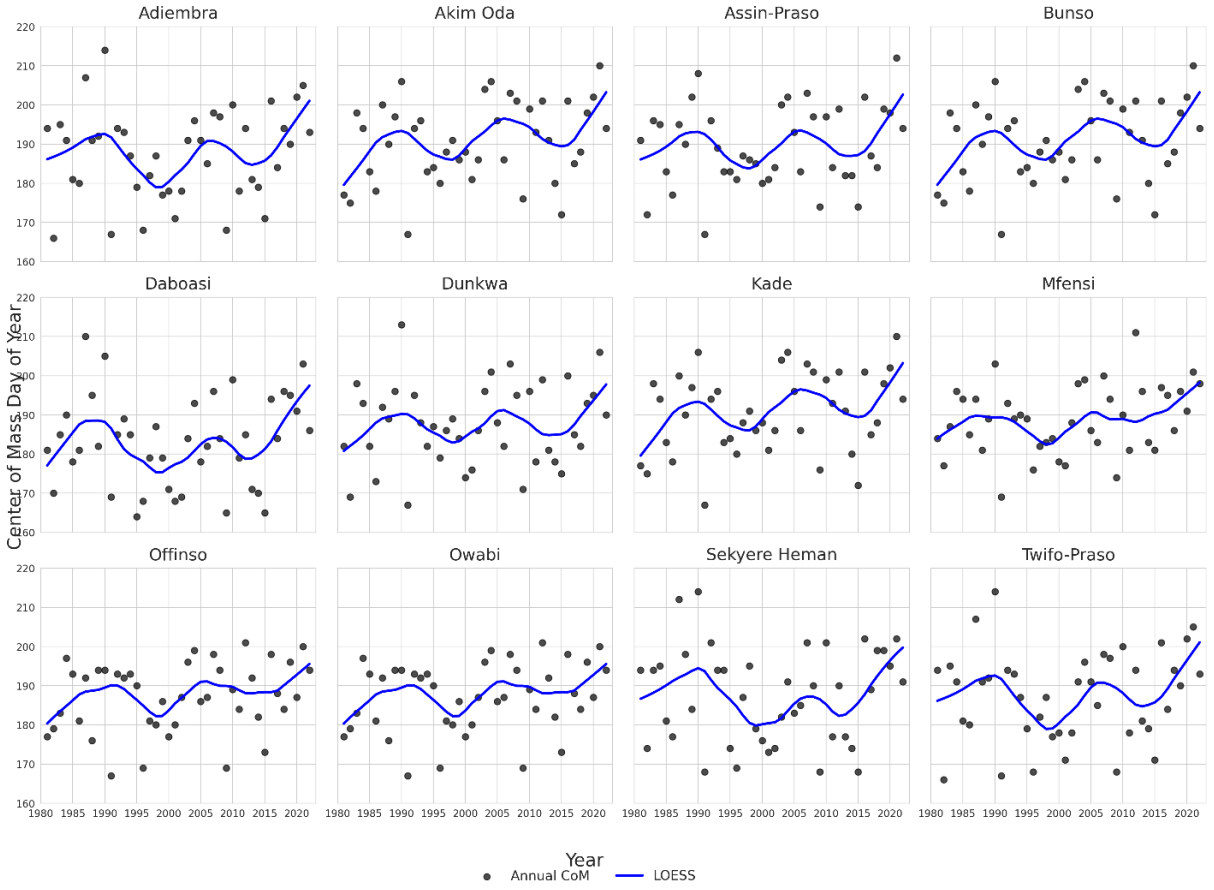

Figure 6.6: Annual rainfall onset dates and LOESS-smoothed trends in the forest belt and coastal zones stations of the Pra River catchment from 1981–2022.

In identifying the climate change signal in rainfall onset timing, the LOESS-smoothed time series plots reveal distinct temporal patterns and regional contrasts across the catchment between 1981 and 2022 (Fig. 6.6). Nearly all stations show a general shift toward earlier rainfall onset. In the forest zone, Bunso and Akim Oda maintain relatively stable onsets, with LOESS slopes close to zero and only minor interdecadal variation. Onsets generally fall between DOY 70 and 90, with occasional outliers between DOY 60 and 110. At Akim Oda, which straddles the forest–coastal transition, a modest positive trend of +1.4 DOY·dec^{-1} translates into an approximate two-week delay over a century.

Interior forest stations show stronger variability. At Mfensi, the onset shifts later at a rate of +2.1 DOY·dec⁻¹, equivalent to one day every five years. Sekyere Heman records a near-zero linear slope, yet the LOESS curve rises in the early 2000s, indicating a temporary delay. Onset dates at these stations spread more widely, ranging from DOY 75 to 150.

6.1.4 ENSO Impacts on Onset and CoM

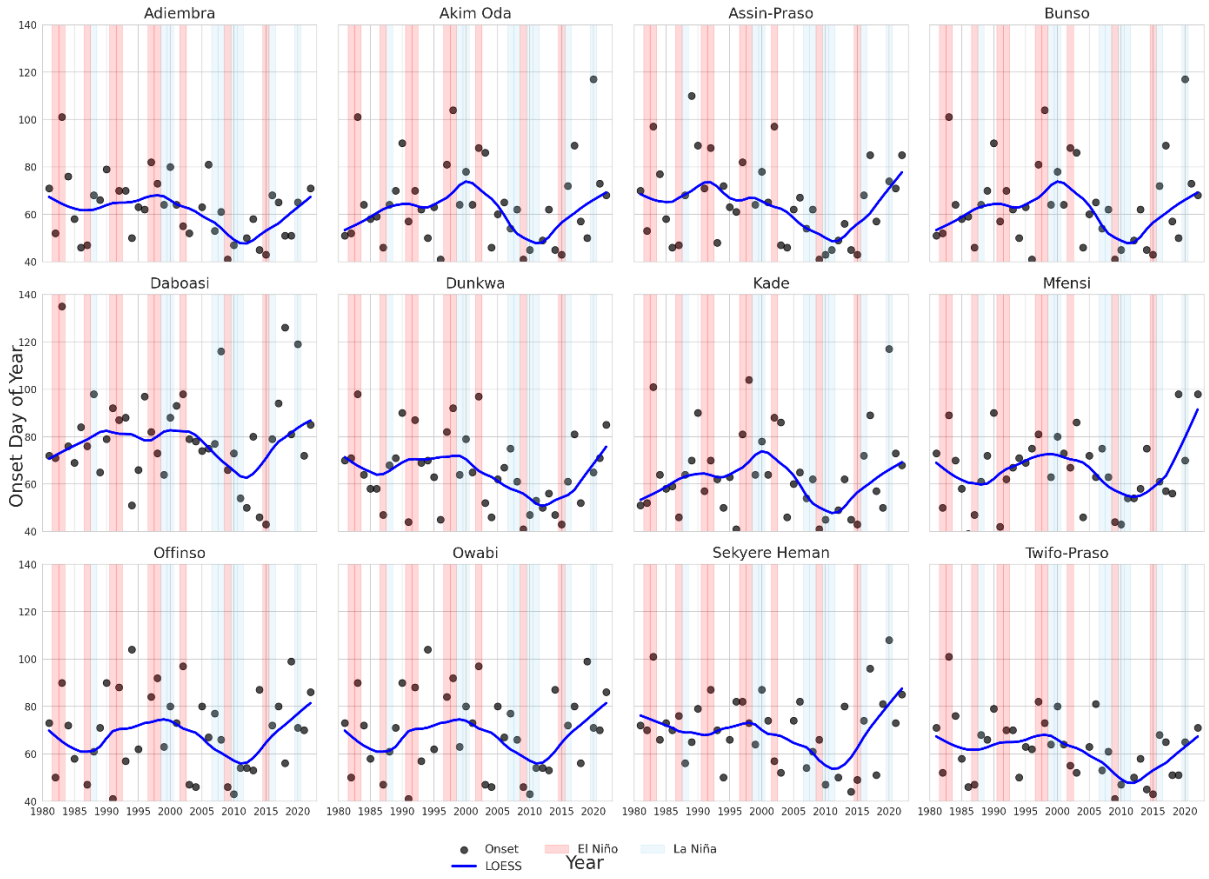

Figure 6.7: Annual rainfall onset timing and ENSO phases (1981–2022). Red band (El Niño years), and blue bands (La Niña years) with ±0.5-year padding for clarity).

In Figure 6.7, Forest-zone stations such as Assin-Praso and Akim Oda showed systematic onset delays during El Niño years, especially in the early-mid 1990s, reflected as upward deviations in LOESS curves. La Niña phases generally coincided with earlier onset at Bunso and Akim Oda, visible as downward excursions in smoothed trends. Coastal stations displayed pronounced fluctuations but smaller extreme deviations than northern interior sites. In interior forest locations such as Mfensi and Sekyere Heman, strong El Niño years (e.g., 1983, 1998) produced onset delays exceeding 50 days relative to preceding years, while La Niña years (e.g., 1988, 2000) were associated with markedly earlier onset.

Onset variability was highest in the northern interior, where Assin-Praso and Mfensi alternated frequently between early and late onset, and Bunso and Daboasi exhibited steeper LOESS slopes, indicating strong interannual variability. Akim Oda maintained comparatively flat onset trends, indicating more stable timing. CoM analyses showed that forest-belt stations (Bunso, Daboasi) consistently peaked near DOY 150-170 with minimal long-term drift. In contrast, Mfensi's CoM shifted from around DOY 160 in the 1980s to beyond DOY 190 recently, implying a three-week delay over four decades. A positive association was observed between delayed onset and higher seasonal rainfall totals, indicative of more intense and prolonged wet seasons.

6.1.5 Seasonal variability and trends in rainfall extreme indices over the Pra River Basin

The study analysed the seasonal variability of extreme rainfall indices in the PRB from 1981 to 2022, focusing on R10mm, R20mm, R95p, RX5day, and CWD (Fig. 6.6). The results reveal distinct seasonal patterns in rainfall intensity and distribution.

Rainfall Intensity (R10mm & R20mm)

SON (September–November) recorded the highest rainfall intensities, with a uniform distribution of R10mm values ranging from 1.50 to 7.75 mm. For R20mm, the highest rainfall intensities (2.7 to 3.0 mm) were observed during JJA (June–August), particularly in the central and northeastern PRB. DJF (December–February) consistently recorded the lowest rainfall intensities (<0.3 mm). R10mm occurrences were more frequent and widespread than R20mm, with the southern, central, and northeastern PRB being most vulnerable to intense rainfall during SON.

Extreme Rainfall Events (R95p & RX5day)

R95p (very wet days contributing 95% of annual precipitation) remained below two days across all seasons, with the highest occurrences in MAM (March-May) and JJA. DJF recorded the lowest R95p values, while the distribution of extreme precipitation events was relatively even during SON and DJF. RX5day (maximum 5-day cumulative rainfall) was generally below 28 mm during DJF but peaked at 76 mm during JJA, indicating increased flood risk during the wet season.

Wet Periods (CWD)

MAM recorded the highest number of consecutive wet days (~5), followed by SON (2 to 5). DJF consistently exhibited the lowest values (<2 days), reinforcing its status as the driest period

in the PRB. These findings underscore the seasonal and spatial heterogeneity of rainfall patterns across the PRB, highlighting distinct periods of high vulnerability to extreme rainfall.. The results are critical for hydrological planning, flood risk assessment, and climate adaptation strategies within the basin.

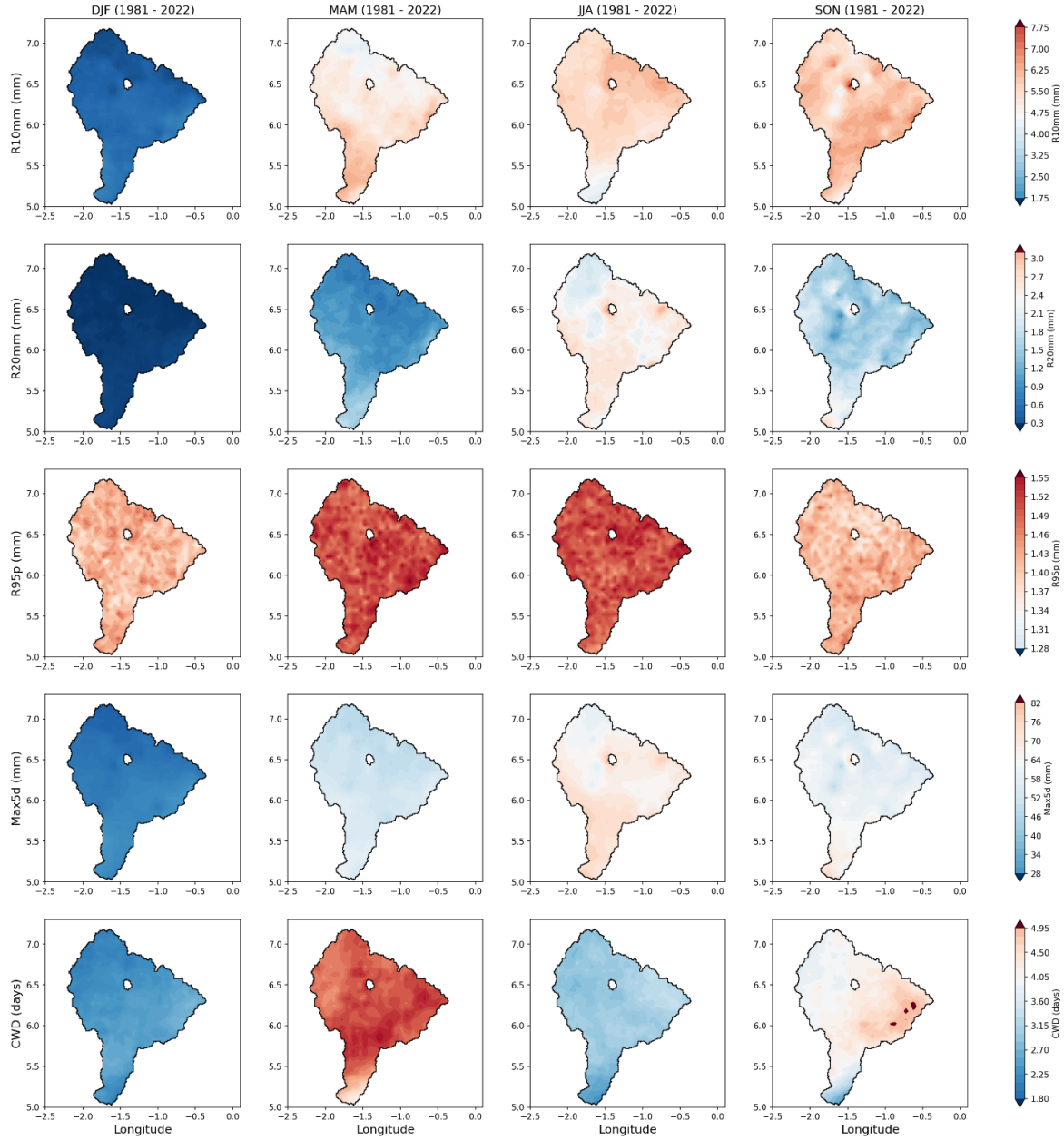

Figure 6.8: Seasonal analysis for the historical period (1981-2022 using the extreme rainfall indices.

6.1.6 Evaluation of the Performance of CMIP6 Models

Comparison of bias correction models

The changes after bias correction of selected CMIP6 models for precipitation and temperature showed that the quantile approach performed well (Fig. 6.7 & 6.8). For instance, ACCESS-CM2 (Fig. 6.7) showed a correlation (r) = 0.8 and a mean bias error (MBE) of -30.41. Similarly, all other models (EC-Earth3-Veg-LR, IPSL-CM6A-LR, MIROC-ES2L, MPI-ESM1-2-LR) showed a correlation ranging from 0.83 to 0.86 and MBE from -11.57 to 49.83, except for their multi-model ensemble mean correlation of 0.89 and an MBE of 5.33. However, for Fig. 6.4, the correlation (r) and MBE for ACCESS-CM2 are 0.78 and -1.41. In addition, the other models r and MBE range from 0.77 to 0.83 and -0.86 to 1.35, respectively. The ensemble mean of the models also showed an r of 0.77 to 0.86 of MBE

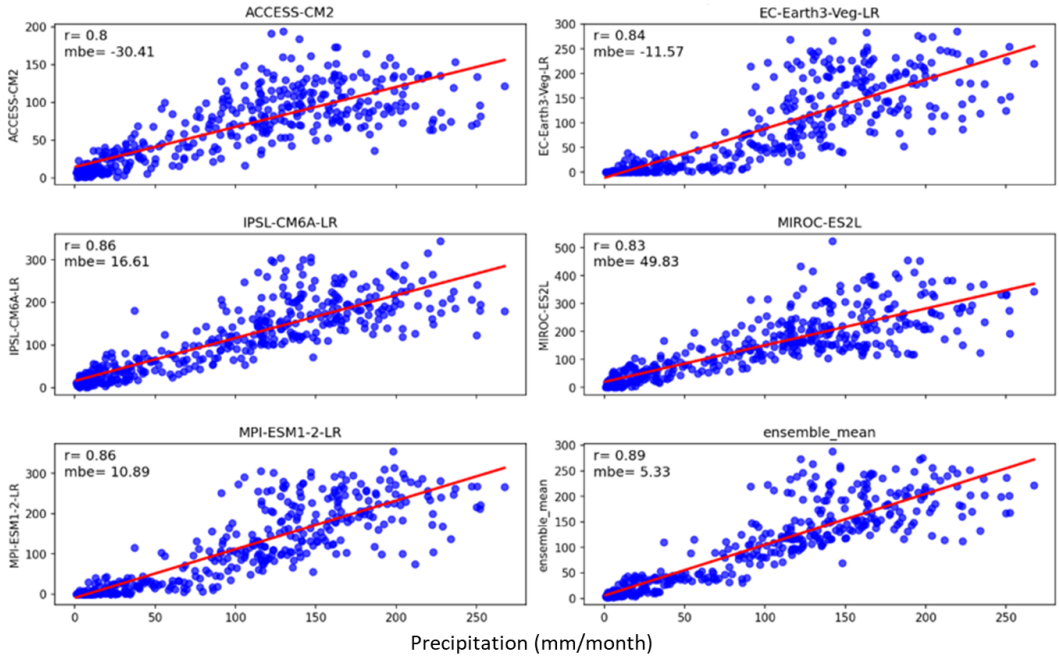

Figure 6.9: A correlation coefficient and mean bias error (MBE) of the CMIP6 model against the reference data (1981-2015).

Figure 6.9 shows the performance of the bias-corrected GCM and the uncorrected GCM relative to the baseline for historical temperature. The results show that the uncorrected GCM underestimated the minimum temperature under SSP1-2.6 by 4-6 °C for all the selected models and overestimated the maximum temperature under SSP3-7.0 by 3-4°C. However, bias correction shows a good fit relative to the baseline for both scenarios. In addition, for precipitation under SSP1.2-6, the uncorrected GCMs show either an overestimation from 1600

mm to 2000 mm or an underestimation from 700 mm to 900 mm relative to the baseline (1200-1400 mm, Fig. 6.10).

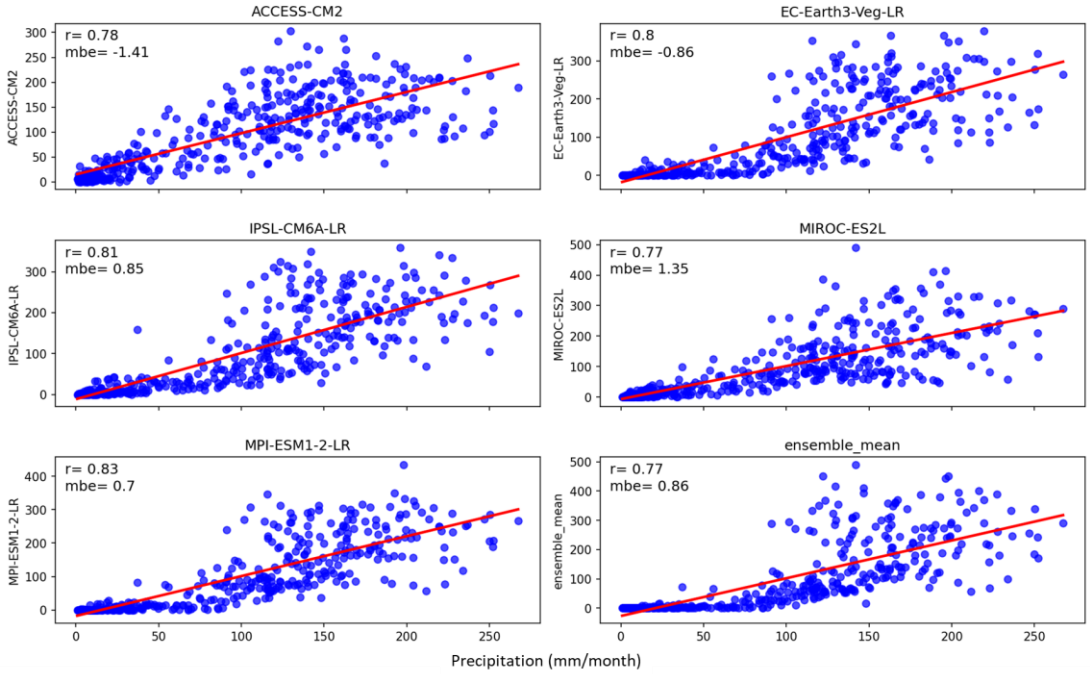

Figure 6. 10: A correlation coefficient and mean bias error (MBE) plot of the monthly bias-corrected CMIP6 model against the reference data (1981-2015)

6.1.7 Climate Change Projections under SSP1-2.6 and SSP3-7.0

6.1.7.1 Rainfall

Average precipitation across scenarios and periods (near term (2021-2040), mid-term (2041-2040), and long term (2081-2100) over the basin is presented in Fig. 6.11. Also, the spatial-temporal projections of major and minor rainy seasons under both scenarios are shown in Fig. 6.9. The average precipitation of the baseline (historical) data (1995-2014) was 1200 mm. Relative to the baseline, precipitation is projected to increase with uncertainties under the SSP1-2.6 and SSP3-7.0 scenarios across seasons and the basin. In the near term, there is a higher increase in precipitation under SSP3-7.0 than under SSP1-2.6, similar to the long term.

However, during the mid-term, SSP1-2.6 precipitation is higher than SSP3-7.0. The precipitation under SSP1 2.6 generally falls within the near-term to long-term ranges between 1200 mm to 1300mm, but 1200 mm to 1400 mm for SSP3-3.70. In addition, the spatial rainfall distribution for the multi-model ensemble mean (Fig. 6.12) showed a high-intensity precipitation amount from the northwestern compared to the northeastern regions for both SSP1-2.6 and SSP3-70 for the minor rainy seasons, but the southern region experienced a lesser

precipitation amount for the long-term period. For the major rainy season, both scenarios (SSP1-2.6 and SSP3-7.0) projected lower precipitation and intensity only in the northwestern region of the basin.

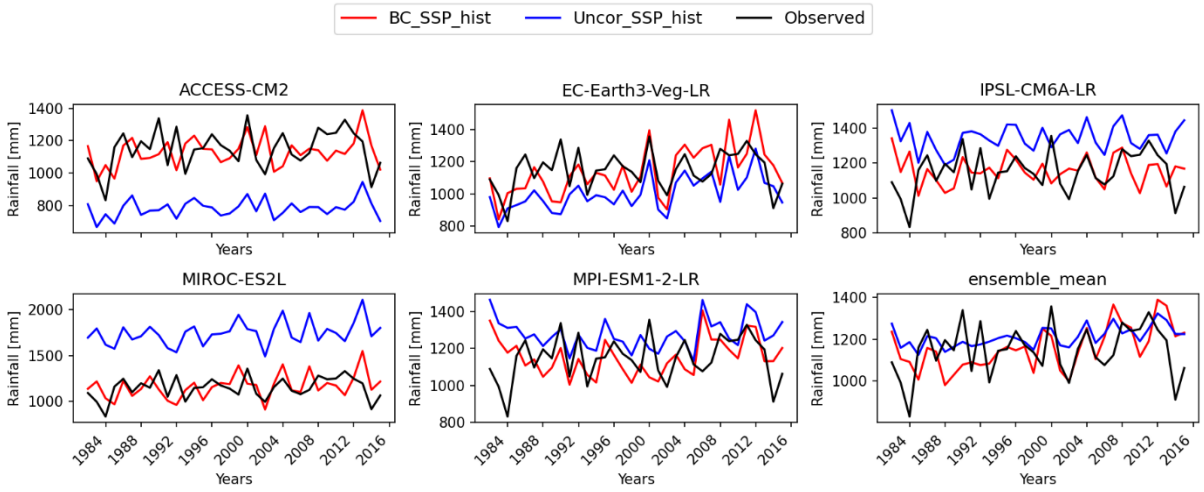

Figure 6.11: CMIP6 SSP1-2.6 bias correction plot of historical data showing multimodel ensemble and mean annual rainfall.

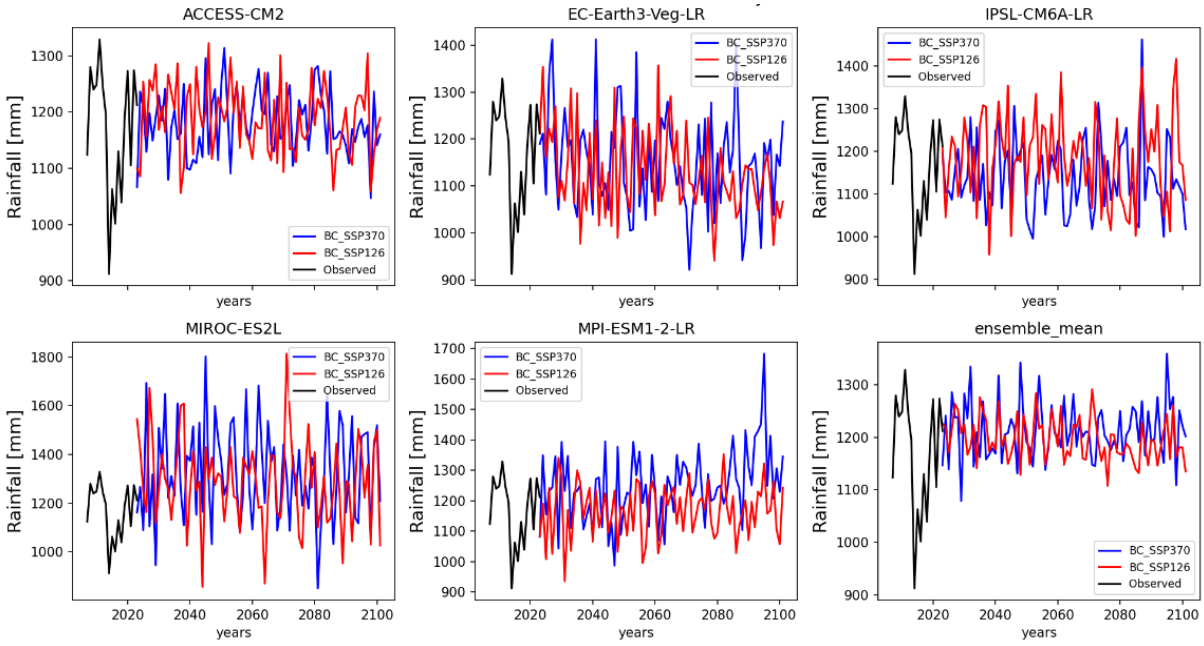

Figure 6.12: Projected annual rainfall under two scenarios: SSP1-2.6 (blue), SSP3-7.0 (red), and observed (black) for the future period (2015-2100) and observed (1981-2022)

6.1.7.2 Temperature

Projections under SSP1-2.6 and SSP3-7.0 scenarios showed divergent trends for rainfall and temperature. Maximum temperatures rose most significantly in northern regions, while southern areas showed modest increases (Fig. 6.13). Temperature projections indicated

increases of 1-2°C under SSP1-2.6 and 3-4°C under SSP3-7.0 by 2100. These trends emphasise the intensification of the hydrological cycle under higher emissions scenarios.

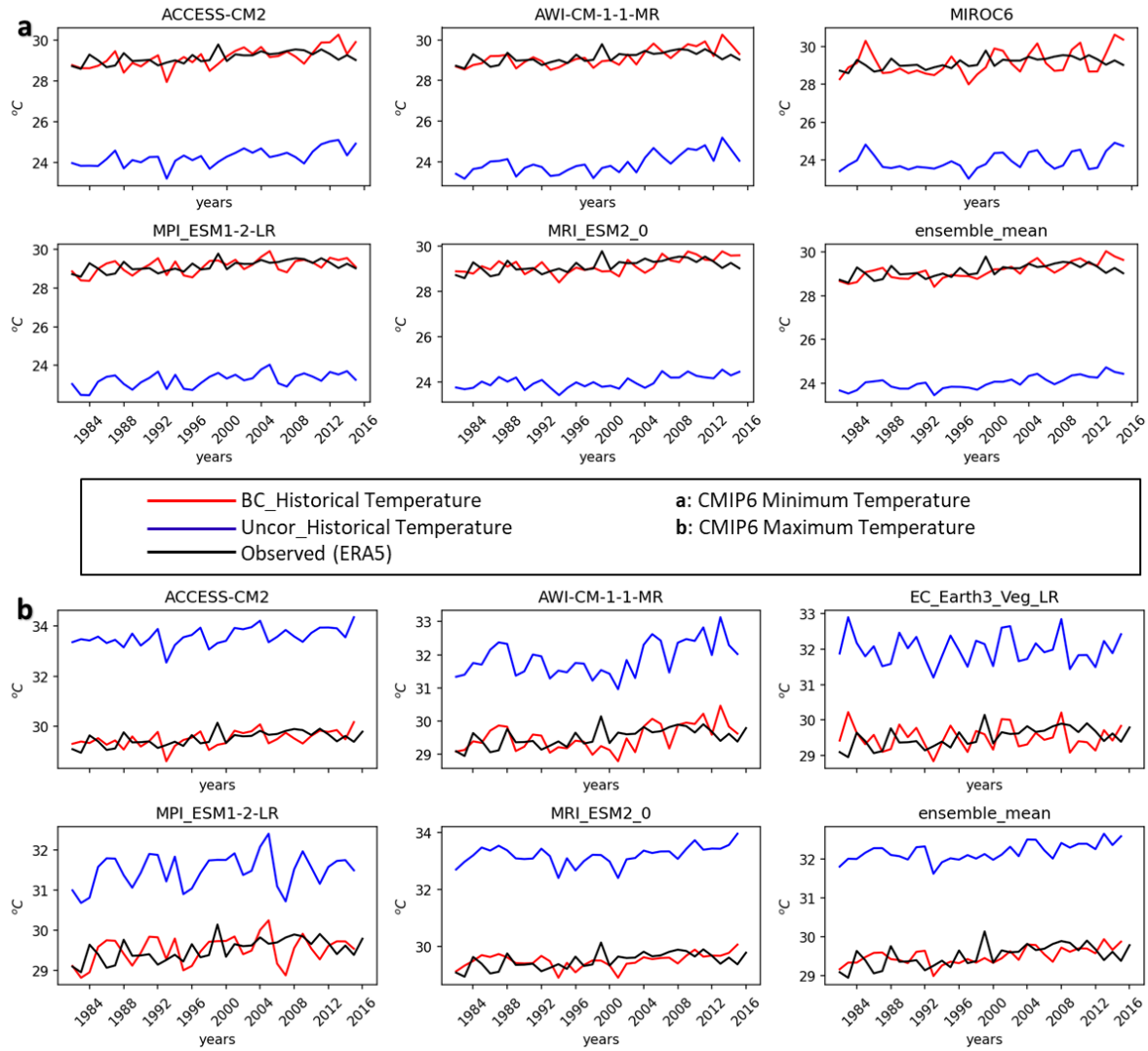

Figure 6.13: CMIP6 Historical monthly mean temperature of the PRB (a) SSP1-2.6 (b) CMIP6 SSP3-7.0

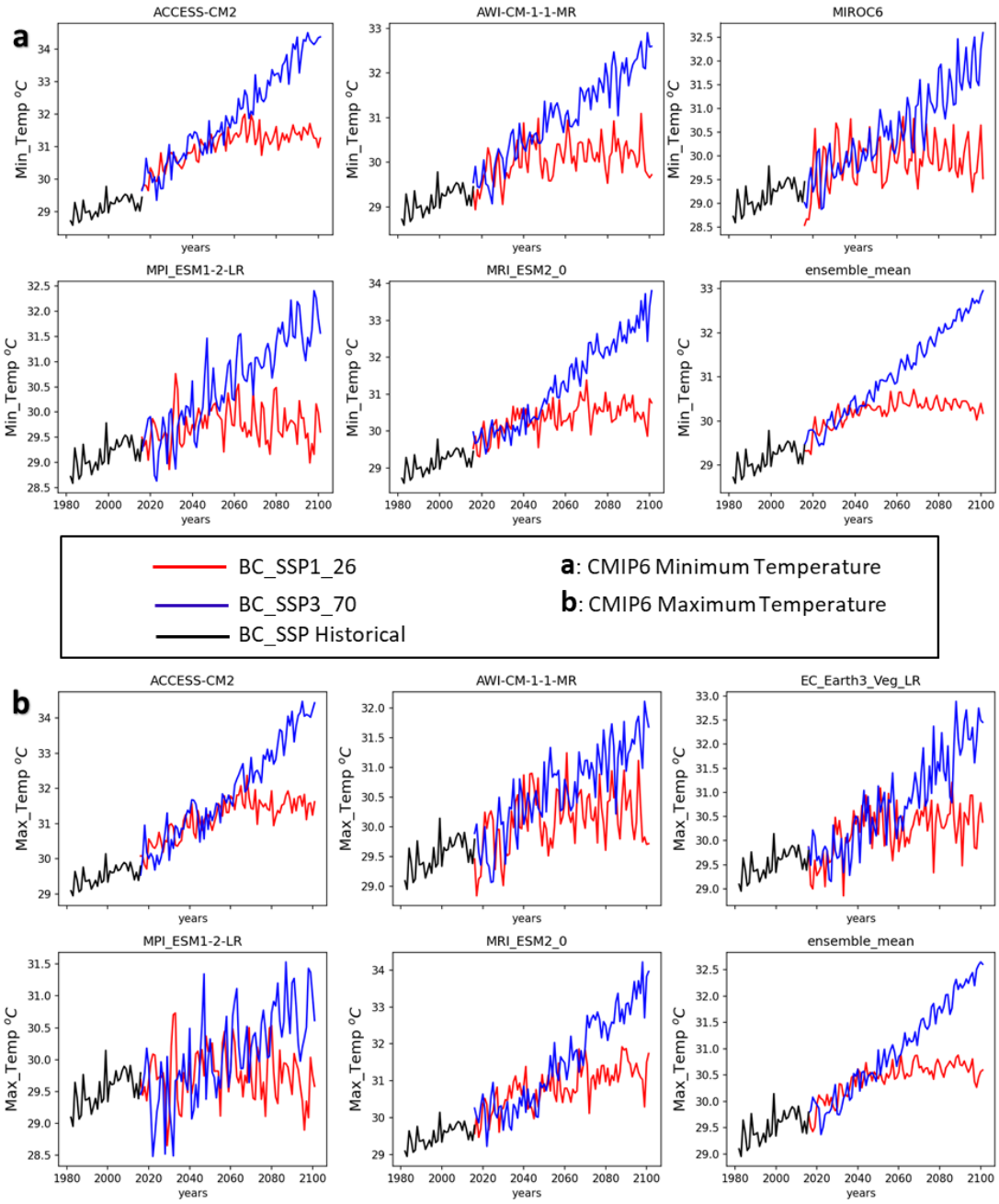

Figure 6. 14:Future projection (SSP1.26 and SSP3.70) of temperature from (SSP1.26 and SSP3.70). (a) minimum (b) maximum compared to observed data (1981-2015).

6.1.8 Rainfall-PDF Characteristics Under Observed and Future Scenarios

The probability density functions (PDFs) for rainfall across all stations were assessed using observational data and CMIP6 simulations (historical and future projections under SSP1-2.6 and SSP3-7.0 scenarios). Across most stations, the SSP1-2.6 (green) curve closely follows the observed (blue) curve, showing only a slight rightward shift. In contrast, the SSP3-7.0 (red) curve is shifted further to the right and displays a fatter upper tail, indicating increased frequency and intensity of extreme rainfall under the high-emission scenario. The most

pronounced shifts were observed in the 1-day and 5-day rainfall durations, suggesting that short-duration, high-intensity rainfall events are projected to increase more strongly than longer-duration totals. The 15-day and 20-day windows showed relatively smaller shifts, indicating lesser changes in moderate multi-week events.

The historical CMIP6 simulations (black) aligned reasonably well with the observed data up to the 90th percentile for most stations. However, in some cases, the models slightly underestimated heavy-rainfall probabilities. Stations such as Kade, Dunkwa, and Offinso (Appendix, Fig. 3A-K) showed the greatest widening of the upper tail under SSP3-7.0, while Sekyere Heman and Mfensi (Appendix, Fig. 3A-K) exhibited smaller shifts. At Akim Oda and Bunso, the SSP1-2.6 and SSP3-7.0 curves were nearly parallel but offset, indicating consistent distribution shapes with increased magnitude under higher emissions.

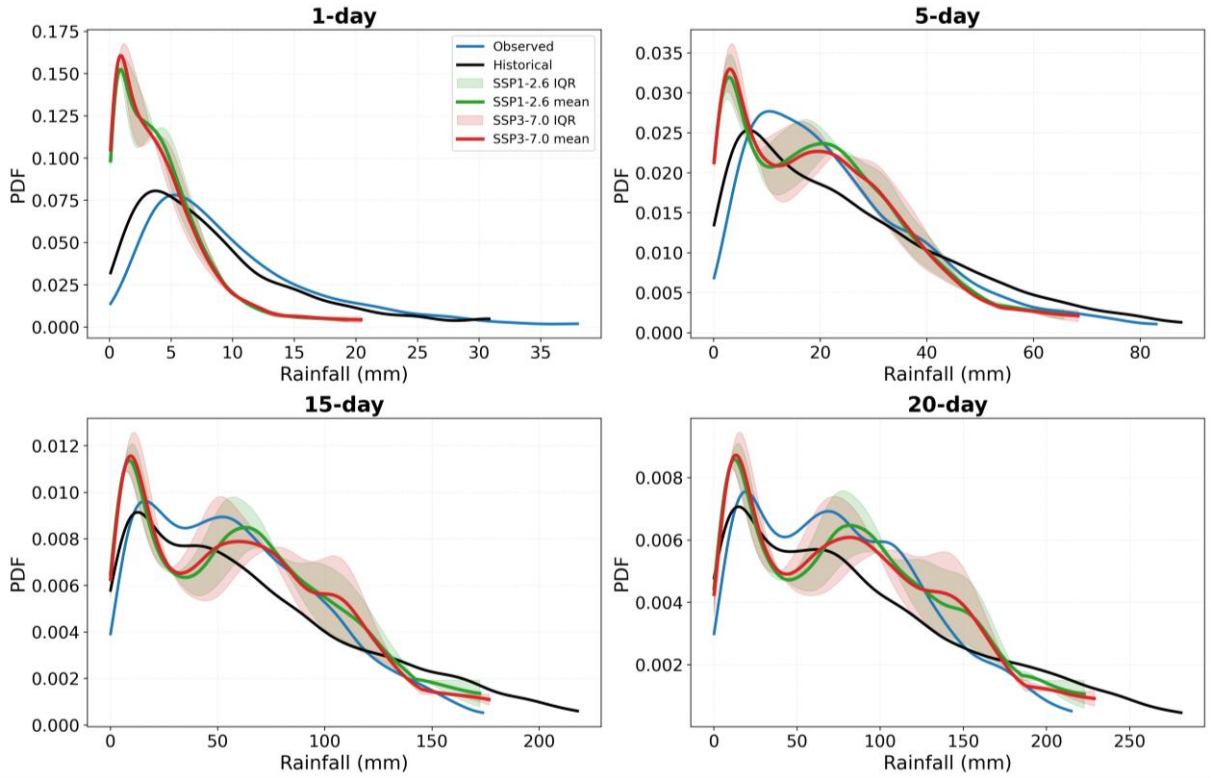

Figure 6.15:Projected changes in the probability distribution of short- to sub-monthly rainfall at Bunso station, indicating a shift toward more frequent low-rainfall events and altered moderate- to high-rainfall probabilities under future SSP1-2.6 and SSP3-7.0 scenarios relative to observed and historical baselines.

6.1.9 Projected Rainfall Variability and Extreme Indices Trend (2015-2100)

Future projections under SSP1-2.6 and SSP3-7.0 for the period 2015-2100 indicate significant shifts in the seasonality, intensity, and spatial distribution of extreme rainfall indices across the Pra River Basin.

6.1.9.1 Seasonal Rainfall Changes under SSP1-2.6 and SSP3-7.0 Scenarios

The analysis of seasonal mean rainfall changes under future climate scenarios (SSP1-2.6 and SSP3-7.0) reveals distinct shifts in rainfall distribution across the studied stations (Fig. 6.16). The December to February (DJF) season exhibits the most severe reductions in rainfall, with percentage decreases ranging from approximately 60% to over 85% across nearly all stations. This consistent decline indicates a potential intensification of the dry season in the future.

During the March to May (MAM) season, rainfall decreases are generally moderate, with reductions typically between 20% and 40%. These losses could affect the onset of the minor rainy season. In contrast, the June to August (JJA) season displays mixed patterns, with several stations, particularly Akim Oda, Daboasi, and Dunkwa, experiencing significant increases in rainfall. At these locations, rainfall increases from 40% to over 110%, depending on the scenario, suggesting potential shifts in the intensity and timing of the major rainy season. The September to November (SON) season also shows a general trend of decreasing rainfall, though the reductions are less severe compared to DJF and MAM, ranging between 1% and 21% in most cases. Despite some variability across the stations, the overall direction of seasonal change is consistent between SSP1-2.6 and SSP3-7.0, with the latter scenario often associated with slightly greater reductions. This consistency across scenarios highlights the robustness of the projected seasonal rainfall changes.

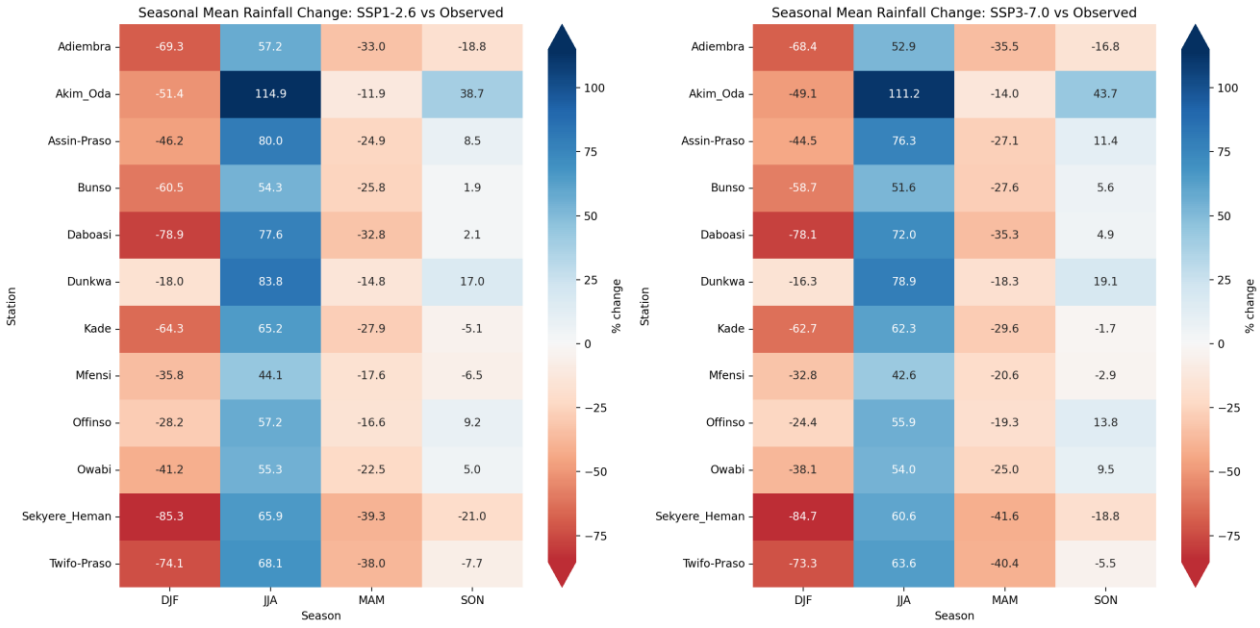

Figure 6.16:Seasonal mean rainfall anomalies at each station under future SSP1-2.6 (left) and SSP3-7.0 (right) scenarios relative to observations, illustrating robust wetting in JJA but widespread drying in DJF and MAM with station-dependent SON responses.

6.1.9.2 Rainfall Intensity (R10mm & R20mm)

For SSP1-2.6, the R10mm index (days with rainfall ≥10mm) ranged between 0.4 and 4.5 mm, with the highest values (4.0-4.05 mm) occurring during SON (September-November). However, the spatial concentration was primarily in the northern and northwestern regions of the basin (Offin, Anum, Oda, and Upper Pra), deviating from the historical distribution. Similarly, under SSP3-7.0, R10mm followed a comparable pattern, with SON still recording the highest values, but with lower intensity and a more limited spatial extent than SSP1-2.6.

For R20mm (days with rainfall ≥ 20mm), projections indicate JJA (June-August) as the most vulnerable season in the northwestern region (Lower Offin), while MAM (March-May) and SON showed lower intensities. However, in SSP3-7.0, MAM exhibited the highest number of rainfall days in the southern basin (Twifo Praso, Lower Pra), whereas JJA and SON followed the same distribution pattern observed in SSP1-2.6.

6.1.9.3 Extreme Rainfall Events (R95 & R95p)

A significant shift in extreme rainfall events was observed in both SSP1-2.6 and SSP3-7.0, with DJF (December–February) emerging as the most vulnerable season for R95 (very wet days contributing to 95% of annual precipitation), followed by JJA. There was a notable decrease in extreme precipitation events (R95p), with fewer than two days of extreme rainfall annually

across all seasons. Localised extremes dropped to 1.43 mm under both scenarios, compared to 1.55 mm in the historical period.

6.1.9.4 Maximum Consecutive Rainfall (RX5day)

The RX5day index (maximum 5-day cumulative rainfall) exhibited substantial reductions in precipitation totals for both scenarios compared to the historical period. Despite the longer projection period (85 years) compared to the 39-year historical period, RX5-day rainfall amounts decreased by 37 mm, ranging from 25 to 44 mm in the future projections, compared to 28 to 82 mm historically. However, localised increases in RX5day were detected in the northern to northwestern PRB (Offin, Oda, Upper Pra, and Anum) across all seasons, in contrast to the historically uniform precipitation distribution observed only during JJA. This suggests a shift toward more intense but shorter-duration rainfall events, raising concerns about increased flood risks due to higher peak intensities over shorter timeframes.

6.1.9.5 Wet Periods (CWD)

The CWD (Consecutive Wet Days) index revealed a seasonal shift in the wettest period: Historically, MAM was the wettest season, whereas JJA emerged as the wettest season in future projections under both SSP1-2.6 and SSP3-7.0. MAM and SON recorded 15-29 consecutive wet days in future projections, compared to just 1-5 days historically during JJA and SON. These findings indicate a major restructuring of seasonal precipitation patterns, with longer wet spells during MAM and SON, coupled with more localised and intense rainfall bursts in the northern PRB. Such shifts could have profound implications for agriculture, water resource management, and flood mitigation strategies in the basin.

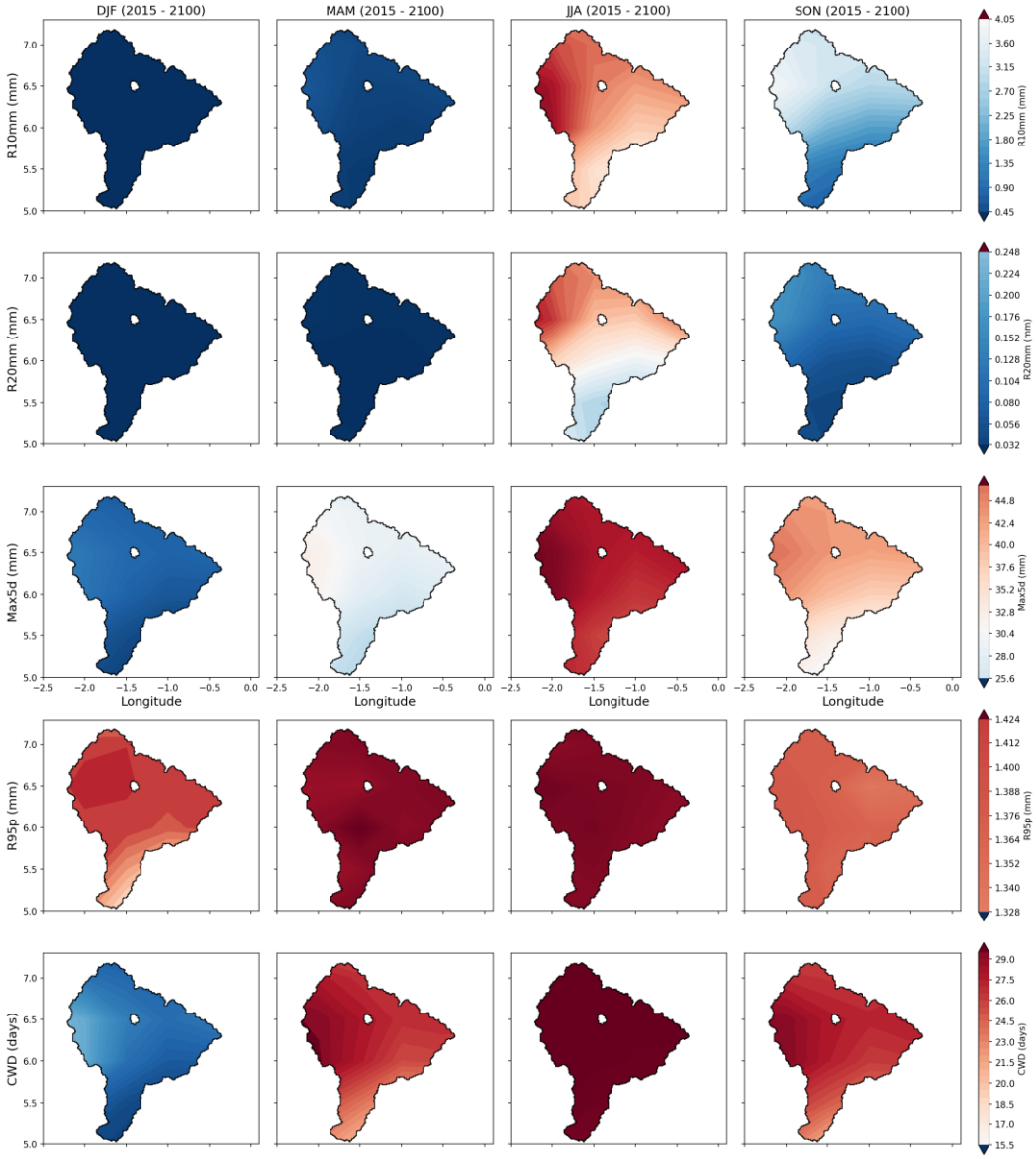

Figure 6.17: Projected seasonal patterns of future CMIP6 SSP1-2.6 rainfall-extreme indices (R10mm, R20mm, Max5d, R95p, and CWD) over the Pra River Basin for 2015–2100, highlighting spatial contrasts between intensified wet extremes and changes in dry-spell duration.

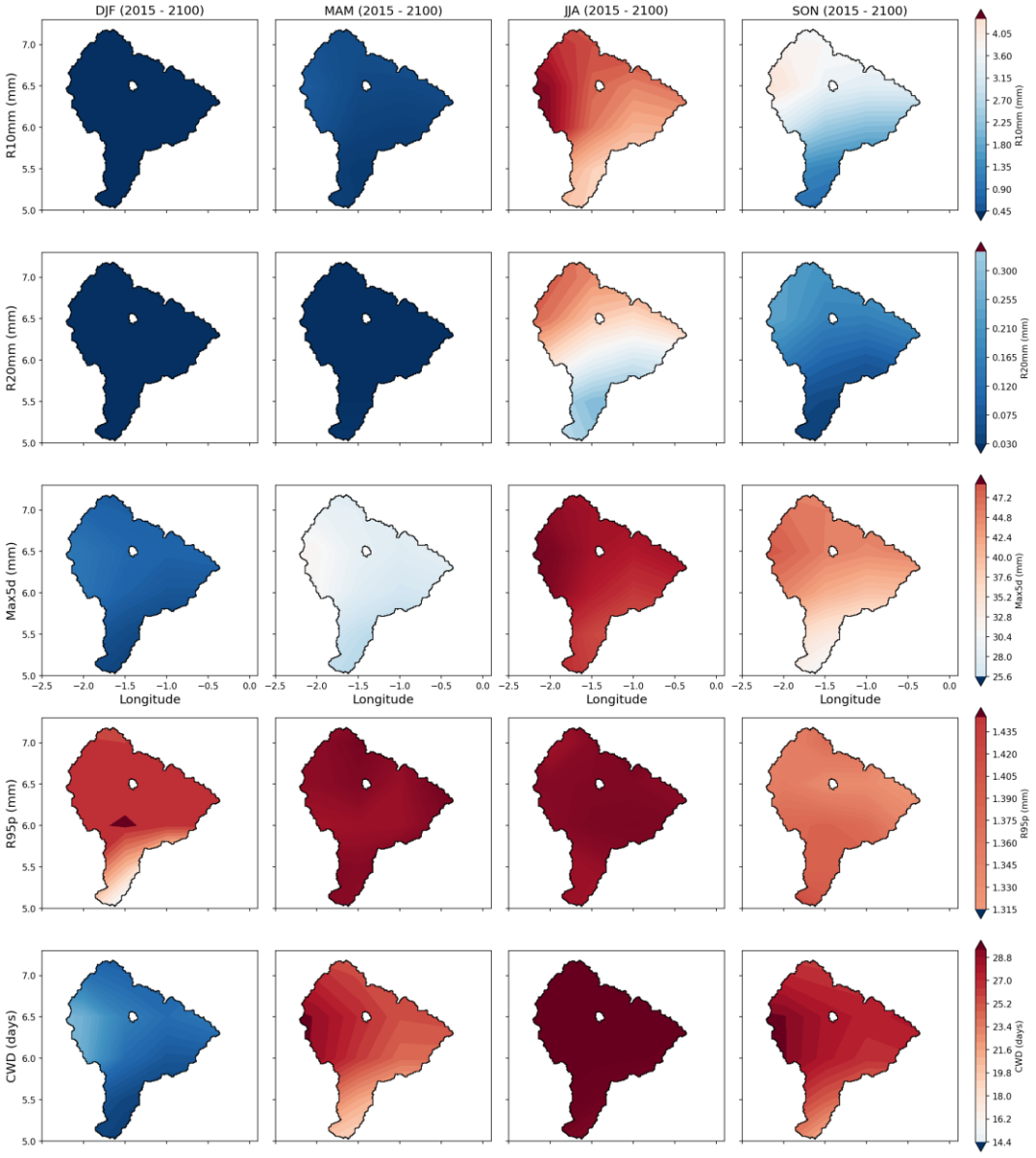

Figure 6.18: Projected seasonal patterns of future CMIP6 SSP3-7.0 rainfall-extreme indices (R10mm, R20mm, Max5d, R95p, and CWD) over the Pra River Basin for 2015–2100, highlighting spatial contrasts between intensified wet extremes and changes in dry-spell duration.

6.1.10 Precipitation Anomaly Indices

Rainfall anomaly index (RAI) and standard precipitation index (SPI) were calculated and projected under the two scenarios (SSP 1-26 and SSP3.70, Appendix Fig. 2A) for the period 2015-2100. The index values and trends averaged over the study area were compared to ease the display and interpretation of the selected model ensemble results. RAI analysis under SSP3-7.0 (Fig. 6.19) revealed distinct patterns of wet and dry periods across the PRB from 2015 to 2100. Dry years, characterised by negative RAI values, showed 10-20% of occurrences. These

dry years frequently registered RAI values below -2, indicating "very dry" to "extremely dry" conditions, with some areas in the northern PRB experiencing the most severe drought intensities. In contrast, wet years with positive RAI values showed less than 20%. RAI values during these years occasionally exceeded +2, classifying them as "very wet" or "extremely wet." The basin also showed less than 50% of normal rain occurrences for the long term (2015 -2100). Spatially, the northern PRB consistently showed higher vulnerability to dry anomalies, while southern areas recorded more intense wet anomalies in the early-century projections. These spatial variations highlight the uneven impacts of climate change across the basin, with southern regions benefiting from early wet periods and northern areas experiencing prolonged drought.

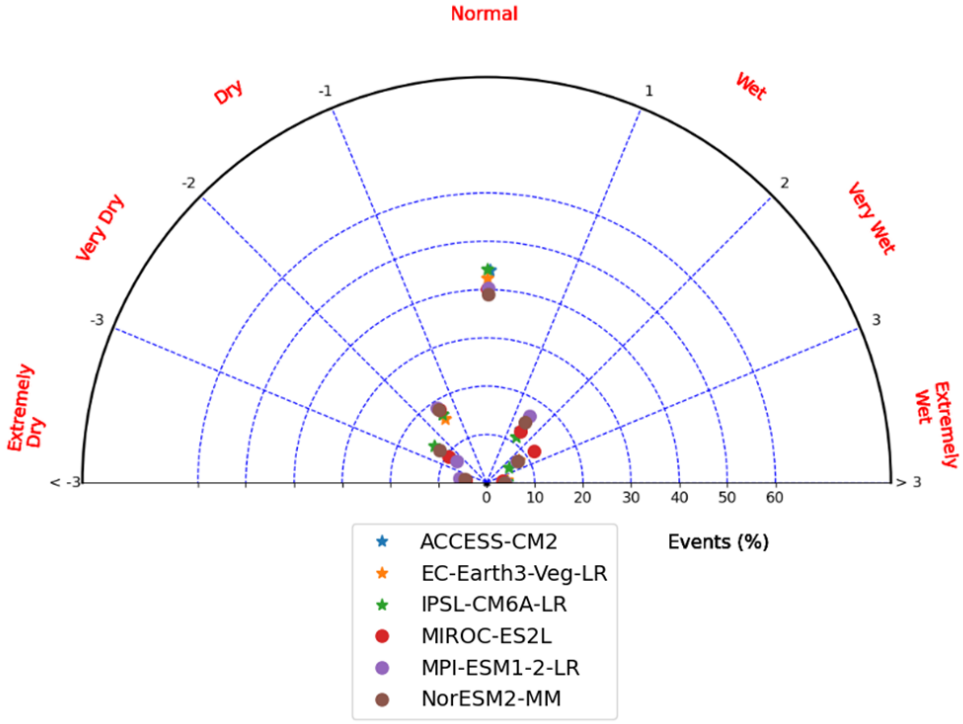

Figure 6.19: Projected frequency of dry and wet events for the Pra River Catchment during 2015–2100, derived from Rainfall Anomaly Index–based polar plots using the CMIP6 SSP3-7.0 multi-model ensemble.

The SPI calculated for 5-month timescales (SPI-5) revealed notable shifts in the frequency and intensity of wet and dry conditions across the Pra River Basin under SSP3-7.0 from 2015 to 2100 (Appendix Fig. 4A-F). The polar drought index projection (Fig. 6.20) indicates a predominance of dry conditions, with most CMIP6 models and the multi-model ensemble mean projecting SPI values clustered in the "Dry" (-1) and "Very Dry" (-2) zones. Approximately 10 - 20% of events fall within the "Dry" category, while less than 10% are classified as "Very Dry." Wet and Extremely Wet events are projected to occur infrequently, with a limited

percentage of events exceeding SPI thresholds of +1 or greater. Normal conditions dominate, accounting for the highest frequency of events, as reflected by the dense clustering of projections near the center of the plot. The Standard Precipitation Index (SPI) analysis under SSP3-7.0 (Fig. 6.20) revealed distinct patterns of wet and dry periods across the PRB from 2015 to 2100. Dry years, characterised by negative SPI values, showed 10-20% of occurrences. The agreement among models highlights the robustness of the projections under the SSP3-7.0 scenario. Notably, extremely dry events (SPI < -3) are rare, occurring in less than 5% of cases, while very wet and extremely wet events (SPI > +2) are even less frequent.

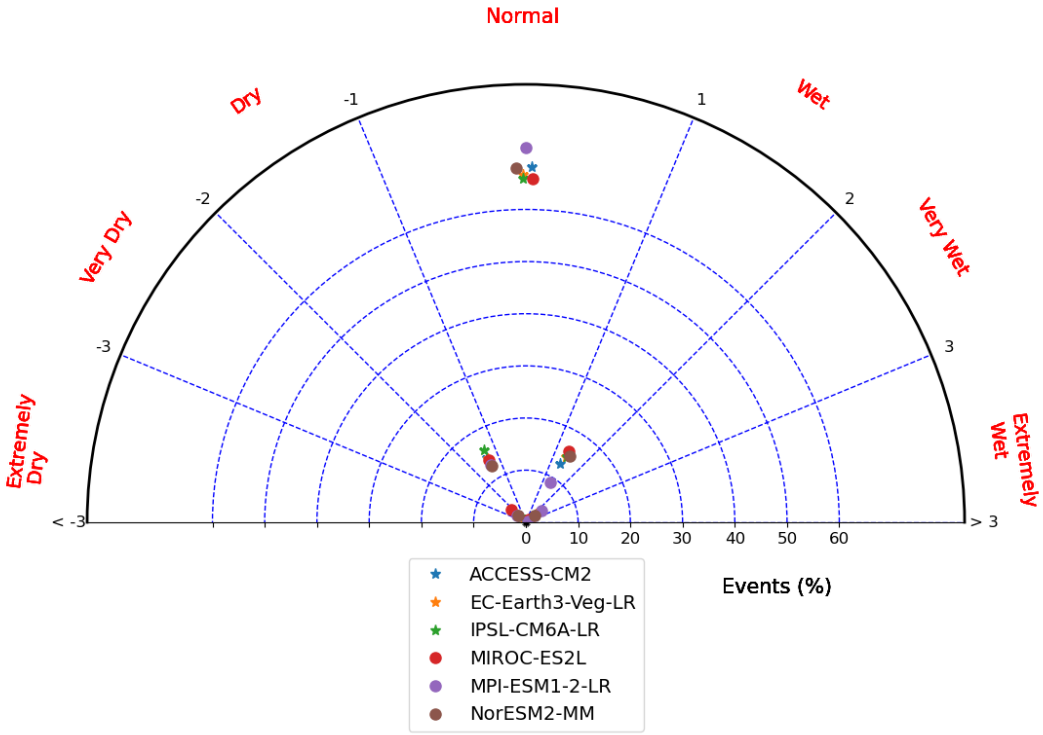

Figure 6.20: Projected frequency of dry and wet events for the Pra River Catchment during 2015–2100, derived from Rainfall Anomaly Index–based polar drought plots using the CMIP6 SSP3-7.0 multi-model ensemble.

6.2 Discussion

6.2.1 Correlation Analysis Between the Centre of Mass and the Total Annual Rainfall

The findings from the correlation between the Center of Mass (CoM) of rainfall and total annual precipitation in the Pra River Basin reflect patterns that align with broader research on rainfall dynamics and their implications for hydrology (Fig. 6.5). The consistent positive correlation observed at various locations within the basin, particularly in areas like Assin-Praso, Twifo-Praso, and Bunso, reinforces the projections that wetter years often coincide with a delayed

CoM, indicating a more extended rainy season. This phenomenon is consistent with broader climatological insights that link increased seasonal precipitation to prolonged rainy events rather than early-season accumulations.

Research by Cai et al. (2024) emphasises that spatial and temporal variations in rainfall significantly influence hydrological responses, notably in urban environments where impermeability exacerbates runoff conditions. The findings from the Pra River Basin align with this, as they suggest that the dynamics of rainfall timing may be closely tied to spatial variations throughout the catchment. Similarly, studies by Smith et al. (2024) on rainfall frequency analysis highlights the critical role of localised climatic conditions on precipitation distribution, further supporting the evidence from the Pra River analysis.

The distinct variability observed at Akim Oda, where a weaker and non-significant correlation was found, illustrates that local factors such as land use, topography, and microclimatic conditions can decouple the relationship between seasonal rainfall volume and its temporal distribution. This observation resonates with the work of Hsu et al. (2017) indicating that precipitation locations significantly depend on varying soil moisture patterns, offering insights into the complexities of hydrological processes at fine spatial scales (Hsu et al., 2017).

Moreover, the spatial coherence observed in regions with robust CoM-rainfall linkages provides a sense of predictability that can be advantageous for water management and agricultural planning. In contrast, findings that indicate weaker correlations imply that reliance on CoM metrics alone may lead to inaccurate forecasts, a view supported by studies examining spatial rainfall heterogeneity and its implications for environmental management (Tetzlaff & Uhlenbrook, 2005). These insights underscore the importance of localised rainfall characterisations and stress that precipitation spatial variability can heavily influence hydrological modelling, particularly at small catchment scales (Saharia et al., 2021). The complexities observed in rainfall dynamics necessitate the integration of multiple variables in hydrological and agricultural assessments to capture the nuances of interannual variability effectively.

6.2.2 Nonlinear Rainfall Onset Dynamics and Spatial Heterogeneity

Rainfall onset across the catchment exhibits non-linear patterns and substantial interannual variability, as revealed by LOESS fits and Sen's slope estimates (Fig. 6). Forest-zone stations show larger shifts in onset timing and a broader interannual spread, indicating a less predictable

seasonal rainfall regime than at the coast. Coastal stations maintain relatively stable onset patterns, consistent with the buffering effect of nearby oceanic conditions on the West African monsoon flow. This spatial heterogeneity aligns with the study that link localized climate variability to elevated hydrological risk (Ghelani et al., 2017).

At the station level, Mfensi displays a U-shaped evolution, with delayed onset in the 1980s, further delays in the 1990s-early 2000s, and earlier onsets after 2010, plausibly reflecting combined microclimatic, land-surface, and topographic influences (Veldhuis et al., 2022) . Bunso and Kade show gradual declines that steepen after 2010, consistent with a shift toward earlier rains that has been reported for parts of southern Ghana (Sanogo et al., 2015). Assin-Praso and Akim Oda exhibit delayed onset with upward LOESS inflections after 2010, highlighting episodic reversals that linear models may overlook. Adiembra shows a steady decline with a moderate negative Sen's slope, while Twifo-Praso maintains a nearly flat trend. Coastal stations are mostly flat up to the early 2000s, followed by sharper downward shifts that are consistent with changing Atlantic SST patterns and their influence on coastal convection.

Most stations record onset dates between about DOY 50 and 100, with occasional late onsets near DOY 130-140, broadly compatible with documented March-April onsets in Ghana's forest and coastal zones. Such variability is known to complicate agricultural decisions and water-resources management. Stations like Bunso, Adiembra, and Daboasi display pronounced LOESS curvature and relatively steep Sen's slopes, whereas Akim Oda and Twifo-Praso show flatter trends with lower explained variance. Recent trend reversals and non-linear behaviour at Mfensi and Assin-Praso are consistent with evidence that rainy-season characteristics in West Africa can respond non-linearly to large-scale forcing, underscoring the limits of purely linear trend analyses (Gomes et al., 2025). These findings support the need for localized, flexible adaptation strategies that explicitly account for spatially heterogeneous and non-linear onset dynamics.

6.2.3 ENSO Controls on Catchment Hydrology

The results indicate that ENSO is a first-order control on rainfall onset and CoM timing in the Pra River Catchment, particularly in interior forest stations. El Niño phases delay onset and shift CoM later in the season, consistent with ENSO-driven weakening of the Walker circulation and West African monsoon inflow, which reduces low-level moisture convergence and convective activity (Biasutti, 2019; Sow et al., 2025). La Niña phases exert the opposite effect, advancing onset and CoM by strengthening monsoon westerlies and enhancing moisture

transport into inland Ghana reflecting the global patterns (Dogar et al., 2017; Losada et al., 2012; Ndehedehe et al., 2020).

Interior stations exhibit larger onset anomalies than coastal sites, implying stronger sensitivity to ENSO-modulated monsoon dynamics away from direct oceanic buffering. This heightened sensitivity leads to delayed soil-moisture recharge, truncated growing windows in El Niño years, and abrupt swings in streamflow regimes between seasons. Shifts in CoM, particularly the gradual delay at Mfensi, suggest a redistribution of rainfall toward later in the season, which can affect groundwater recharge timing, reservoir operation, and ecosystem phenology (Hernandez et al., 2022; Ni & Hsu, 2018).

The positive correlation between delayed onset and higher seasonal totals indicates a tendency toward shorter but more intense wet seasons, enhancing the likelihood of hydrological extremes. Such nonstationary teleconnections, documented to evolve under climate change, underscore the need to incorporate ENSO diagnostics into seasonal forecasting, water-resources planning, and region-specific adaptation strategies for the Pra basin (Haszpra et al., 2020).

6.2.4 Performance of Bias Correction

The outcome of the bias-corrected CMIP6 models demonstrates the effectiveness of the quantile mapping approach adopted in reducing systematic biases, as reported in similar studies (Gosling et al., 2017; Peng et al., 2023). Temperature projections revealed that uncorrected GCMs underestimated Tmin by 2.5°C and overestimated Tmax by up to 3°C during the historical period (1984–2014, Fig. 6.6). This corroborates findings by (Almazroui et al., 2021, 2020a, 2020b; Kamruzzaman et al., 2021) on CMIP6 and their bias-corrected. Similarly, precipitation projections reveal that the uncorrected GCMs either underestimated or overestimated for each model, depicting the uncertainty in rainfall estimation (Fig. 6.6). This result further confirms the findings of Ajibola et al. (2020) on the performance of CMIP6 HighResMIP on West African precipitation. Bias correction brought these estimates closer to observed values, validating the reliability of the process for future projections. This improvement relates to findings from Magang et al. (2024) and Rubel & Kottek (2010).

6.2.5 Implications of Rainfall-PDF Trends (Extremes under Future Climate Scenarios)

The observed results of the probability density functions (PDFs) for rainfall over varying durations (1, 5, 15, and 20 days) reveal critical insights into the potential impacts of climate change on extreme rainfall events. The evident rightward shift and fattening of the SSP3-7.0

curves distinctly indicate an intensification of extreme rainfall occurrences under high-emission scenarios. This phenomenon is particularly pronounced at shorter durations, especially in the 1- to 5-day range, confirming that these short bursts of intense rainfall are more sensitive to warming than longer-duration totals. This finding aligns with growing evidence that extreme precipitation events are increasing in both frequency and intensity across various climatic conditions (Adib et al., 2022; Donat et al., 2016; Madsen et al., 2014; Peng et al., 2023)

The relatively modest changes observed under SSP1-2.6 reflect the potential for stabilising rainfall extremes through the adoption of low-emission pathways. This result is consistent with the argument presented by Van Lanen et al. (2016), who highlighted the critical role of emission scenarios in moderating hydrological responses. These outcomes reinforce the view that proactive efforts to maintain lower emissions can mitigate the severity of future climate impacts, emphasising the importance of climate mitigation strategies. In contrast, the pronounced changes associated with SSP3-7.0 serve as a stark reminder of the risks linked to inaction. The consistent widening of the distribution tails at high-intensity stations such as Kade, Dunkwa, and Offinso (Appendix, Fig. 3A-K) echoes existing studies that associate extreme rainfall intensification with urban runoff and flash flooding, particularly in humid tropical basins, as documented by Taye et al. (2011). This alignment signifies an increased flood risk and reiterates the need for adaptive urban infrastructure and comprehensive flood risk management strategies to cope with anticipated climatic shifts (Dyrrdal et al., 2023).

While drier stations also show projected increases in rainfall extremes, these shifts are less dramatic, underscoring the spatial heterogeneity in climate change impacts. This is a concept well-established in hydrological literature (Huang et al., 2011). Notably, at stations such as Akim Oda and Bunso, the SSP1-2.6 and SSP3-7.0 curves are parallel yet offset, indicating that while the underlying climatic processes may remain consistent across scenarios, their amplification under high-emission conditions could result in more severe hydrological events. This supports assertions by climate modellers that similar physical processes drive rainfall extremes across scenarios, but warming amplifies their intensity (Ngoma et al., 2022; Tsunetaka et al., 2024).

Overall, these findings highlight important links between emission scenarios, rainfall extremes, and the associated risks of flooding and urban runoff. They underscore the need to emphasise infrastructure design and flood-risk planning on short-duration rainfall extremes, particularly

under high-emission futures. The results strongly advocate for the urgent development of climate-informed adaptation policies, especially in urban and flood-prone areas, where even marginal increases in short-term rainfall can lead to significant hydrological and socio-economic consequences.

6.2.6 Impact of Change in Rainfall Seasonality and Climate Scenarios

Seasonal mean rainfall analysis across the Pra River Basin under SSP1-2.6 and SSP3-7.0 scenarios reveals critical shifts in precipitation patterns (Fig. 6.16). The December to February (DJF) season exhibits the most severe reductions, with rainfall declining by approximately 60% to over 85% at nearly all stations. This substantial decrease supports the findings by Luna-Aranguré et al. (2025), who identified marked alterations in precipitation regimes under warming conditions. Their work underscores the vulnerability of ecological systems, reflecting similar concerns highlighted by the intensification of the dry season observed in this study. During the March to May (MAM) season, rainfall decreases are generally moderate, ranging between 20% and 40%. Although less severe than DJF, these reductions have significant implications for rain-fed agriculture, particularly affecting the reliability and timing of the minor rainy season. This observation aligns with Pal et al. (2019), who emphasised that even moderate shifts in precipitation can disrupt crop productivity and threaten food security. Such seasonal unpredictability reinforces the sensitivity of agricultural livelihoods to climate variability.

In the September to November (SON) season, rainfall reductions are less pronounced but still notable, typically falling within the 1% to 21% range. Despite the relatively moderate scale, the downward trend aligns with projections by Oti et al., (2020), who reported concerns over diminishing water availability and its effects on long-term agricultural sustainability. These findings signal a progressive weakening of the transitional rainy season, with implications for groundwater recharge and late-season planting cycles. In contrast, the June to August (JJA) season displays spatial variability in rainfall response. While some stations show modest decreases, others, particularly Akim Oda, Daboasi, and Dunkwa, record substantial increases ranging from 40% to over 110% depending on the scenario. These increases are consistent with observations by Katzenberger et al. (2021), who identified localised intensification of monsoon rainfall under future warming, especially in humid regions. This spatial divergence underscores the complexity of climate responses across ecological zones and highlights the necessity for location-specific modelling to guide hydrological and agricultural planning. The consistency of

trends across both SSP scenarios lends credibility to the robustness of the projections. While SSP1-2.6 reflects more stabilised rainfall patterns, SSP3-7.0 exhibits more extreme deviations, reinforcing the argument made by Kankam-Yeboah et al. (2013) on the growing urgency for adaptive strategies. The pronounced changes in rainfall seasonality observed under SSP3-7.0 point to the potential intensification of water stress and disaster risk, particularly in areas already vulnerable to flooding or drought. An Improved understanding of the interactions between climatic drivers and hydrological responses is essential for designing effective, data-informed management strategies. This is consistent with the recommendations of Alam et al. (2018) and Hassan et al. (2015), who emphasised the importance of integrating scientific evidence into regional water governance and climate adaptation policies.

6.2.7 Impact of seasonal variability and trends in rainfall extreme indices

The analyses showed a shift of wetter conditions from the southeastern (Birim, Assin Praso) to the northwestern (Offin) of the PRB under SSP3-7.0. This indicates significant hydrological and agricultural implications for the basin. The findings align with studies in West Africa on the shifts to localised climate feedback mechanisms and global warming-induced changes in atmospheric circulation (Atiah & Muthoni, 2023; Koudahe et al., 2017; Tabari, 2020). It could also disrupt existing cropping systems and water resource plans, necessitating region-specific adaptation strategies.

The seasonal analysis of extreme rainfall indices highlights the dominance of JJA and SON as the primary wet seasons, validating findings from Atiah & Muthoni (2023) and Hounkpè et al. (2022b). The reduction in precipitation during MAM and JJA under SSP3-7.0, compared to historical trends, emphasises the potential for increased agricultural vulnerability, as these seasons are critical for crop production in the basin (Atiah & Muthoni, 2023). We observed the concentration of R20mm in central and southwestern (Twifo Praso, Assin Prason, Bunso) PRB suggests localised vulnerability, requiring targeted adaptation measures. In addition, the distinct seasonal asymmetry in R95p indices emphasises the changing nature of extreme rainfall events (Mason et al., 1999; Westra et al., 2014). The values of R95p in SON and JJA suggest a narrowing window for high-intensity rainfall, which can exacerbate risks of waterlogging and soil erosion in the affected regions.

The projected shifts and increase in RX5day from JJA and SON historically to SON and MAM in the future indicate a redistribution of extreme rainfall events and intensity (Lenderink & Van

Meijgaard, 2009). This could potentially reduce the risk of prolonged and widespread flooding but increase localised flash flood occurrences in the northern and southwestern PRB. These patterns confirm the increasing unpredictability of extreme rainfall in West Africa (Koudahe et al., 2017; Osei & Amoakowaah, 2021). The unexpected increase in extreme rainfall frequency during DJF under both scenarios highlights the growing complexity of seasonal transitions in the PRB. Historically, DJF has been a dry period, but the projected increase in extreme rainfall could disrupt water management strategies and amplify challenges for communities in the West African region who are unprepared for wetter conditions during this season (Hounkpè et al., 2022b).

6.2.8 GCMs Performance and Climate Change Implications

The findings (Fig. 6.8 & 6.10) show that CMIP6 models effectively simulate the global monsoon intensity and precipitation within the West African Monsoon system, despite persistent common biases and significant intermodel variability (Almazroui et al., 2020a; Guo & Wang, 2016). Bias correction proved effective in reducing systematic errors in CMIP6 outputs, improving their applicability for regional climate assessments (Peng et al., 2023; Quansah et al., 2014). This validates the reliability of the quantile mapping approach. However, the persistence of non-linear trends in uncorrected GCMs highlights the need for further refinement of bias correction techniques. Future temperature projections reveal greater warming across the basin during the latter part of the 21st century compared to the baseline climate, under both SSP1-2.6 and SSP3-7.0 scenarios. The temperature increases, particularly under SSP3-7.0, signal significant hydrological implications, including increased evaporation and water stress. For precipitation, the basin shows a wide ensemble spread and considerable interannual variability throughout the 21st century, with no definitive trend emerging similar to Osei & Amoakowaah (2021). The shift in rainfall seasonality, with wetter conditions moving from southeastern to northwestern PRB, raises concerns about the adaptive capacity of local agricultural systems (Atiah & Muthoni, 2023). These results align with similar trends reported for temperature and precipitation in the broader subregion, emphasising the importance of mitigating emissions to reduce long-term climate risks (Almazroui et al., 2020a; Atiah & Muthoni, 2023; Grose et al., 2020; Libanda & Ngonga, 2018; Ongoma et al., 2018; Peng et al., 2023)

6.2.9 Precipitation Anomaly Index Implications

The findings indicate an increased likelihood of dry conditions in the Pra River Basin under the SSP3-7.0 scenario, underlining a significant shift in precipitation patterns due to higher greenhouse gas emissions under regional rivalry business-as-usual in the PRB (Riahi et al., 2017). The dominance of "Dry" and "Very Dry" events suggests prolonged drought periods, potentially driven by reduced precipitation and heightened climate variability. These results align with the SSP3-7.0 narrative, which projects a warmer and more arid future, particularly in vulnerable regions such as the Pra River Basin (Dibi-Anoh et al., 2023; Lavaysse et al., 2006; Osei & Amoakowaah, 2021). The low frequency of wet and extremely wet events reflects a diminished potential for heavy rainfall occurrences, indicating a narrowing distribution of precipitation extremes. Such changes could exacerbate water scarcity and increase reliance on water storage infrastructure to sustain hydrological and agricultural systems during prolonged dry spells (Atiah et al., 2021; Dibi-Anoh et al., 2023; Koudahe et al., 2017; Raziei, 2021).

6.2.10 Implications for Basin Management

The results highlight the critical need for integrating climate projections into water and agricultural management strategies in the PRB. The spatial heterogeneity of extreme rainfall indices highlights the importance of localised adaptation measures, such as flood defense systems in the northern and southwestern regions and improved drainage infrastructure in urban centres experiencing an increase in the RX5day events. Additionally, the vulnerability of MAM and JJA to reduced precipitation calls for the promotion of water-saving agricultural practices, such as rainwater harvesting and drought-resistant crop varieties, to mitigate the impacts on food security.

6.2.11 Climate Extremes and Socio-Economic Outcomes: Interconnected Risks and Implications

Climate extremes and projections for the Pra River Basin point to rising temperatures, increasing evapotranspiration, and more erratic precipitation under high-emission scenarios like SSP3-7.0. The interplay between extreme weather events and socio-economic impact is multifaceted. These environmental stressors are closely linked to socio-economic vulnerabilities, particularly in sectors like agriculture, water management, public health, and shifts in labour dynamics, notably exacerbating economic inequalities.

- **Agriculture and Food Security**

Recent research indicates that the frequency and intensity of extreme weather events such as heatwaves, floods, and droughts are increasing due to climate change, resulting in more substantial socio-economic consequences, particularly in developing countries (Lange et al., 2020; Lieber et al., 2022; Yeh et al., 2022). Changes in rainfall timing, intensity, and distribution disrupt traditional planting cycles and reduce the predictability of yields in rain-fed systems. Smallholder farmers, who dominate agriculture in the PRB, are especially at risk of facing a greater incidence of crop failure and heatwaves, thus exacerbating food insecurity. Increased frequency of dry spells and irregular rainfall events will limit crop choices, reduce harvests, and raise the risk of food insecurity and income loss. Areas experiencing rainfall shifts (from southeastern to northwestern zones) may face spatial mismatches between crop suitability and existing land use.

- **Water Access and Resource Conflicts**

Rising temperatures combined with prolonged dry periods increase pressure on water systems. In urban areas, this can stress municipal supplies and sanitation services; in rural areas, it can fuel competition over irrigation and drinking water. In the PRB, where mining, agriculture, and domestic use all depend on shared water sources, the risk of resource conflicts rises during drought years.

- **Livelihoods and Economic Inequality**

Climate extremes will disproportionately impact communities with limited adaptive capacity of those lacking access to irrigation, credit, insurance, or resilient infrastructure. In areas where subsistence farming is a major livelihood, repeated crop failures can drive poverty, force migration, or increase reliance on informal labor. Women and marginalised groups, who often bear the brunt of food and water insecurity, are especially vulnerable.

- **Health and Infrastructure Stress**

Flash floods and intense rain events strain drainage systems, raise the risk of waterborne diseases, and disrupt transport and market access. Heatwaves and longer dry seasons can also exacerbate health conditions like dehydration, heatstroke, and vector-borne diseases, with low-income and peri-urban populations most at risk (Biney et al., 2024; Howe et al., 2019). Moreover, the mental health consequences of climate extremes, as outlined by Cruz et al., (2020) underscore the need for integrated approaches to public health and climate resilience, highlighting the psychological toll alongside physical consequences.

Ultimately, understanding these interconnected risks is vital for adapting socio-economic strategies to mitigate the adverse effects of climate extremes. Effective integrated assessments can aid in prioritising community needs and addressing vulnerabilities, particularly in regions projected to experience the most severe impacts of climate change (Field et al., 2012; Franzke, 2017; Höllermann & Evers, 2017; Kettle et al., 2020). This multilayered understanding of climate extremes and their socio-economic implications is crucial for fostering resilience and ensuring equitable recovery strategies globally.

6.2.12 Adaptation Strategies for Extreme Indices

The persistence of fewer than two extreme precipitation events annually (R95p) and the dominance of CWD during MAM and SON expose critical gaps for water resource planning and agricultural resilience. The variability in MAM and JJA, combined with localised extremes, highlights challenges for rain-fed agriculture, which depends on predictable rainfall patterns. These findings align with the studies by Osei et al. (2021) and Quansah et al. (2014), which emphasise the importance of understanding rainfall seasonality to improve food security. The projected reduction in RX5day under future scenarios, despite localised increases, suggests mixed implications. While reduced prolonged rainfall events may alleviate some flooding risks, the increased frequency of flash floods calls for proactive planning. Integrating satellite-derived rainfall data with CMIP6 projections can support early warning systems and inform sustainable water management practices.

6.2.13 Adopting the RAI Concept for the Climatic Water Balance

Evaluating future drought conditions using precipitation-based indices, such as the Standardised Precipitation Index (SPI) and Rainfall Anomaly Index (RAI), may underestimate the true drought potential. These indices provide accurate drought assessments only when other climate parameters remain stationary, which is often not the case in tropical climates. Rising temperatures in these regions increase evapotranspiration rates, potentially intensifying drought conditions beyond what precipitation data alone can capture. Consequently, comprehensive drought risk evaluations should integrate additional climate variables, particularly temperature. Indices that account for both precipitation and temperature offer a more robust approach to drought analysis. Examples include the Palmer Drought Severity Index (PDSI, Alley, 1984), the Reconnaissance Drought Index (RDI; Tsakiris et al., 2007), and the Standardised Precipitation Evapotranspiration Index (SPEI; Vicente-Serrano et al., 2010). Among these, the SPEI applies a methodology similar to the SPI but incorporates the water balance (P-ET) as the

input variable, making it particularly suited for assessing drought risk under changing climatic conditions.

6.2.14 Research Contributions and Future Directions

By combining high-resolution satellite data with bias-corrected CMIP6 projections, this study provides a more nuanced understanding of rainfall variability and its implications for water resources. The integration of high-resolution satellite data with bias-corrected CMIP6 projections provides a reliable framework for assessing climate impacts. However, further research should focus on incorporating socio-economic and land use factors to refine predictions and enhance their relevance for policy-making. Continued advancements in bias correction methodologies are essential to reduce uncertainties and improve the reliability of climate models for regional applications.

6.3 Partial Conclusion

The rainfall in PRB is dominated by high interannual variability; however, the importance of determining changes in this basin's rainfall regimes can be highlighted by outlining the impacts on extreme rainfall can have on the basin's management. Our study builds on the growing body of evidence for local changes in rainfall. Using a combination of high-resolution satellite data and CMIP6 model data from 2015-2100, we have re-assessed and extended previously documented decadal variability and trends in annual and seasonal rainfall, including monthly and yearly extremes. Five rainfall indices have been calculated in the nested tropical environment from 1981 to 2015 and 2015 to 2100. This has provided insight into whether previously documented trends have strengthened or weakened, and new information about emerging trends. GCM shows uncertainty across the catchment, projecting heavy rainfall in the northwest and dry conditions in the southernmost areas for the medium to long-term period. Temperatures are projected to rise, especially in the northernmost areas, with increases of 1–3°C by the end of the century under SSP3-7.0. The dry season is expected to be hotter than the rainy season. Similarly, the occurrence of hot days (mean temperature > 33°C) and hot nights (minimum temperature > 30°C) is expected to increase significantly under SSP3-7.0.

The results point to a significant increase in surface temperatures and rainfall uncertainty across the catchment, which could greatly impact the population, environment, and agriculture. Additionally, the correlation of CoM with annual precipitation in the Pra River Basin reflects broader climatological patterns that reinforce the significance of spatial heterogeneity in

understanding rainfall behaviour. The convergence of findings across various studies indicates that localised analyses are essential for effective water resource management and agricultural planning in response to complex and variable climatic conditions.

Thus, recommends the use of satellite data in data-scarce tropical environments to improve agro-advisories on the timing of seasonal calendar activities. This study highlights the critical role of integrating high-resolution satellite data with climate models to enhance regional climate forecasting. Future research should focus on improving bias correction methodologies and incorporating socio-economic factors to refine projections and inform adaptive management strategies.

6.4 Limitations of the Study

This study serves as a baseline assessment for the PRB but does not include full hydrological modelling of streamflow, groundwater, or water balance components, which limits the direct quantification of impacts on water resources. Existing hydrological impact results cited are drawn from previous studies rather than generated within this work. Spatial analyses rely on the resolution, quality, and temporal availability of satellite imagery and station rainfall data, which may introduce classification errors, missed small-scale changes, and uncertainty in extreme-rainfall statistics. Scenario design for future LULC and climate conditions is constrained to the limited set of models, pathways, and assumptions that could be processed within the project period, so alternative futures are not exhaustively explored. Finally, the scope of work was restricted by funding and timeframe, which did not permit extensive socio-hydrological surveys or the development, calibration, and uncertainty analysis of a full catchment hydrological model built directly on this baseline.

CHAPTER 7: ESTIMATION OF WATER BALANCE

This chapter focuses on the outcome of the calibration and validation of the HBV model used to determine the water balance and discharge of the study area.

7.1 Results

Daily streamflow simulated by HBV-light during calibration (2005–2009) and validation (2009–2011) is shown in Figure 7.1. The model reproduced observed flow dynamics reasonably well. Performance metrics during calibration were R^2 = 0.64, NSE = 0.64, KGE = 0.68, and PBIAS = 5.6% while for validation R^2 = 0.64, NSE = 0.84, KGE = 0.81, and PBIAS = 2.2%. Monthly streamflow simulations showed improved agreement with observations, reflecting the model's ability to capture aggregate flow patterns. Simulation results indicate that actual evapotranspiration is high throughout both calibration and validation periods, while surface runoff dominates catchment streamflow. Less than 1% of total rainfall contributes to groundwater recharge, highlighting the limited infiltration capacity of the catchment. The parameter ranges used for the MC simulation are given in Table 7.1.

Table 7.1: Parameters and their ranges used for the Monte Carlo simulations

Parameter	Explanation	Minimum	Maximum	Unit
Soil and evaporation routine				
FC	Maximum SM	50	550	mm
LP	SM threshold for reduction of evaporation	0.3	1	
BETA	Shape coefficient	1	6	
Groundwater and response routine				
Perc	Maximum flow from upper to lower GW-box	0	6	mmd^{-1}
UZL	Threshold for K_0-outflow	0	100	mm
K_0	Recession coefficient	0.05	0.5	d^{-1}
K_1	Recession coefficient	0.01	0.3	d^{-1}
K_2	Recession coefficient	0.001	0.1	d^{-1}
MAXBAS	Routing, length of weighting function	1	5	d

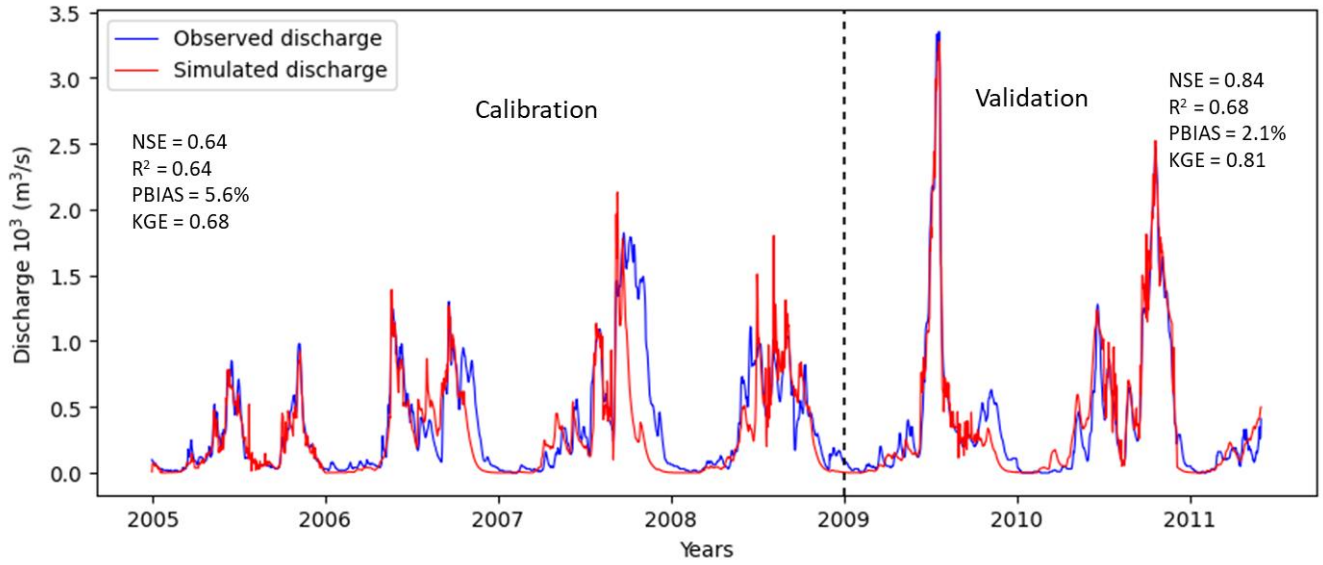

Figure 7.1: Graph of Calibration and Validation of HBV model

7.1.1 Water Balance

The HBV conceptual model, calibrated for the Pra River basin, was used to estimate the main water balance components. The annual and monthly averages of these components are summarized in Table 7.2. Analysis of the annual hydrological components indicates that evapotranspiration dominates water loss within the basin, with an estimated value of 889.45 mm, accounting for approximately 60% of the total water balance. Surface runoff, estimated at 188.67 mm (about 13%), represents the second-largest pathway for water loss. Observations at the basin level suggest that surface runoff is the primary contributor to water yield at the designated outlet. Figure 7.3 shows the average monthly annual distribution of evapotranspiration and surface runoff, where the latter follows a bimodal rainfall pattern characteristic of the Pra basin. This pattern aligns with the seasonal movement of the Intertropical Convergence Zone (ITCZ), consistent with previous findings by Amekudzi et al. (2008) and Osei et al. (2021).

Table 7.2: Average monthly water balance components values (2004-2011) for the Pra basin

Month	Q_{obs} (mm)	Q_{sim} (mm)	AET (mm)	PET (mm)
Jan	2.029	2.035	25.132	156.134
Feb	5.022	5.015	61.640	151.714
Mar	4.065	5.038	162.567	209.793
Apr	2.093	2.089	148.226	190.467
May	19.303	22.214	71.076	171.078
Jun	42.623	42.418	71.682	157.631
Jul	26.770	26.586	65.667	178.561

Aug	9.749	11.732	54.946	170.522
Sep	31.885	31.895	60.854	131.998
Oct	27.852	27.816	67.308	122.115
Nov	8.606	7.409	58.037	138.053
Dec	4.138	4.426	42.319	153.339
Total	**184.135**	**188.673**	**889.454**	**1931.405**

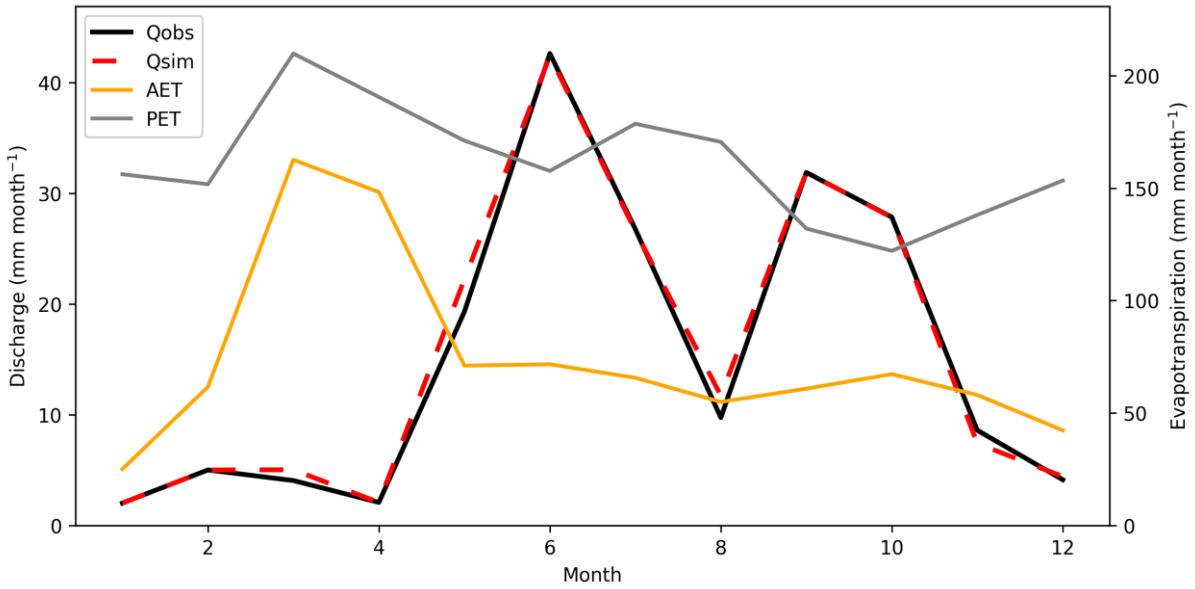

Figure 7.2: Average annual water balance components of the Pra Basin

7.1.2 Climate Change Impact on Future Streamflow

Figure 7.3 presents the seasonal changes in projected streamflow for the near-future (2030s) and mid-century (2050s) periods relative to the historical baseline under two emission scenarios. The results reveal clear seasonal contrasts in both the magnitude and direction of projected streamflow changes. Figures 7.3a and 7.3b show that projected streamflow for both scenarios and time slices exhibits a bimodal seasonal pattern. Two distinct peaks are observed within the annual cycle, corresponding to the major rainy seasons, while lower flows dominate during the dry months. This bimodal structure is maintained across all scenarios and periods considered.

At the basin scale, the bias-corrected CMIP6 ensemble mean indicates an overall reduction in projected streamflow toward the end of the century. Mean streamflow decreases by approximately 20.8% under SSP1-2.6 and 28.2% under SSP3-7.0. Across the ensemble, projected changes range from −32.7% to −7.4% for SSP1-2.6 and from −39.6% to −10% for SSP3-7.0. For the near-future period, projected streamflow changes range between −20.7% and 2.9% under SSP1-2.6 and between −14.3% and 8.6% under SSP3-7.0. In contrast, the mid-

future period shows consistently negative changes, with mean annual streamflow reductions of −19.6% under SSP1-2.6 and −25.54% under SSP3-7.0. Monthly changes during this period range from −34.4% to −3.8% for SSP1-2.6 and from −38.6% to 3.6% for SSP3-7.0.

Seasonally, the largest changes in projected streamflow occur during the rainy season, while smaller changes are observed during the dry season, particularly during December–February (DJF). Greater temporal variability in seasonal discharge is evident during the near-future period (2015–2044) compared to the mid-century period (2045–2074). During 2015–2044, increases in streamflow are limited to June under SSP3-7.0 and January under SSP1-2.6 relative to the historical period. For 2045–2074, all seasons show reductions in projected streamflow, indicating a basin-wide decline in annual discharge.

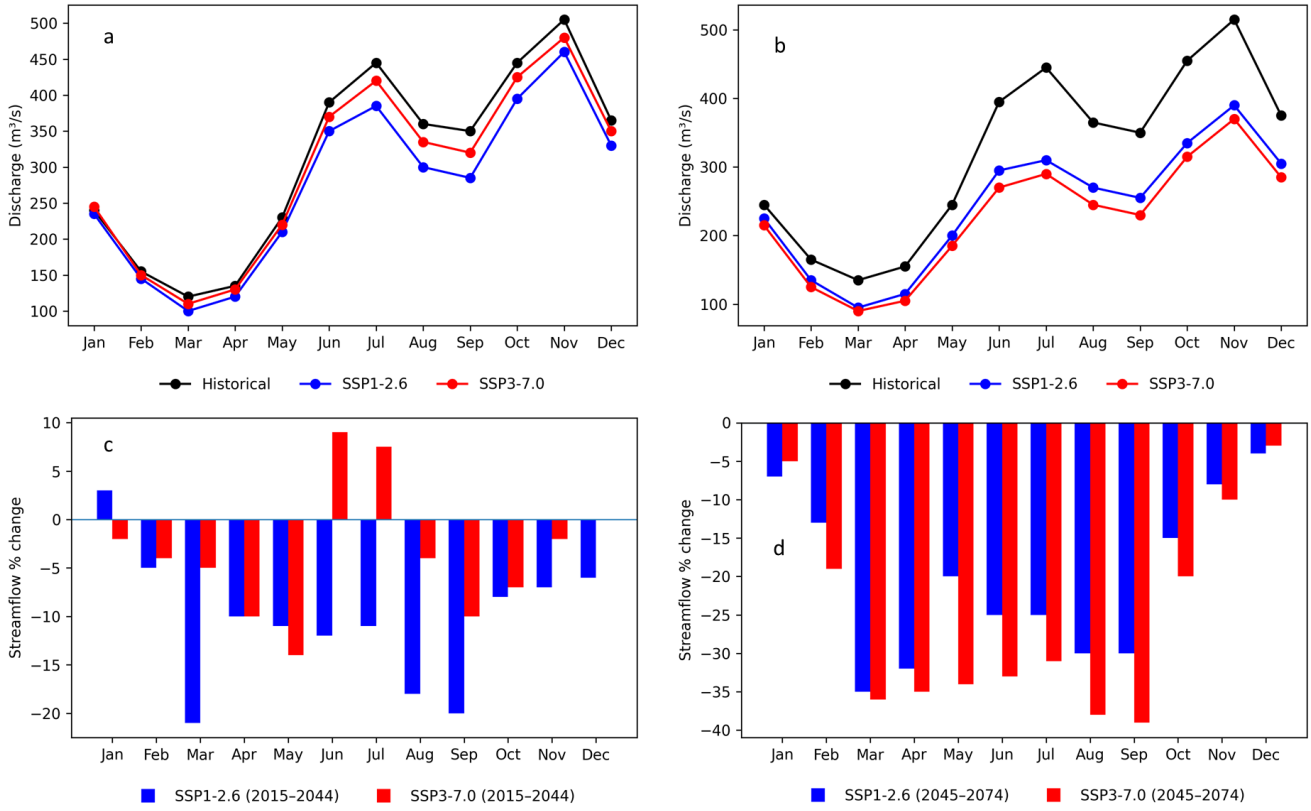

Figure 7.3: Change in seasonal streamflow for the (a) near-future (2015-2044) and (b) mid-future (2045-2074) period in relation to the historical period (1985-2014) over the Pra basin.

7.2 Discussion

7.2.1 Performance of the HBV Model in the Pra River Catchment

Application of the HBV hydrological model to the Pra River catchment demonstrated a generally satisfactory ability to reproduce observed streamflow behavior under data-scarce tropical conditions. Model calibration and validation results indicate moderate to good

performance, with efficiency metrics falling within ranges commonly reported for conceptual rainfall–runoff models applied in West African basins (Bizuneh et al., 2021; Tekleab et al., 2011). While the achieved performance does not reach the highest levels reported for more data-intensive semi-distributed models, it is consistent with expectations for lumped conceptual models operating under constrained observational inputs (Osei et al., 2019).

The level of agreement between simulated and observed discharge reflects the model's capacity to capture the dominant rainfall–runoff relationships governing the Pra basin. Similar performance levels have been reported in HBV applications across regions, where sparse rain gauge networks and reliance on satellite-derived precipitation products impose fundamental limits on achievable accuracy (Ahmad et al., 2020; Ali et al., 2018; Bizuneh et al., 2021; Grillakis et al., 2010). In this context, the Pra results confirm that HBV provides a defensible balance between predictive skill and data availability, reinforcing its suitability for hydrological analysis in the basin. Importantly, model performance remained stable across calibration and validation periods, indicating that the HBV structure was able to generalize beyond the calibration window and reproduce key flow characteristics under independent conditions. This temporal robustness strengthens confidence in the model's application for diagnostic and scenario-based analyses, particularly where relative changes in streamflow are of primary interest.

7.2.2 Representation of Streamflow Dynamics and Hydrological Processes

The HBV model reproduced the dominant seasonal streamflow dynamics of the Pra River system, including the characteristic bimodal flow regime linked to southern Ghana's rainfall climatology. Simulated hydrographs captured the timing of both the primary wet-season peak associated with the March–July monsoon and the secondary peak during September–October, indicating an appropriate response of soil moisture and runoff generation processes to cumulative precipitation. Peak flow timing showed strong agreement with observations, a key requirement for flood-related and water resources applications. This performance aligns with findings from monsoon-driven African basins, where seasonal timing is more reliably simulated than peak magnitude (Awotwi et al., 2019; Olofintoye et al., 2022; Tekleab et al., 2011; Wagner et al., 2006).Recession behaviour during wet-to-dry transitions was also realistically represented, reflecting groundwater drainage through the conceptual reservoir structure.

Evapotranspiration dominated the simulated water balance (Fig. 7.2), suggesting that land-use change, particularly forest conversion to agriculture, may be enhancing atmospheric water losses. Simulated surface runoff alone appears insufficient to explain observed sedimentation and erosion, including reported water treatment facility closures. This mismatch likely reflects localized disturbances such as small-scale illegal mining, which increase soil exposure and sediment transport independently of runoff volume.

Simulation of hydrological extremes showed limitations, with underestimation of some flood peaks and weaker representation of prolonged low-flow periods. Similar constraints have been reported in HBV applications to other tropical basins, including the Upper Blue Nile, where structural simplifications and input uncertainty affect extreme-flow (Bizuneh et al., 2021; Tekleab et al., 2011). Overall, the model provides a reliable representation of average seasonal behaviour and dominant processes but is less suited for precise extreme-event analysis.

7.2.3 Implications of Projected Climate Change on Streamflow

The projected reduction in streamflow across both emission scenarios and time slices reflects a broader response of the Pra Basin's hydrological system to future climatic changes. The persistence of a bimodal seasonal pattern suggests that the dominant regional rainfall mechanisms, particularly the migration of the Intertropical Convergence Zone and the West African monsoon, continue to shape the seasonal distribution of streamflow under future conditions. Similar bimodal behaviour has been reported for projected precipitation over the region (Osei et al., 2021). The magnitude of the projected decline in mean annual streamflow is consistent with previous climate impact studies conducted within the Pra Basin and its sub-basins. Kankam-Yeboah et al. (2013) reported reductions in simulated streamflow using an ensemble of global climate models over comparable future periods. Likewise, Osei et al. (2019) identified decreasing trends in projected streamflow for the Offin River Basin, a major tributary of the Pra. Bessah et al. (2020) also projected a decline in seasonal water yield across the Pra Basin using the INVEST model and an ensemble of climate models.

In contrast, some studies have reported increasing trends in projected precipitation over parts of the basin. Awotwi et al. (2021), using CMIP5 global climate model ensembles, observed an increase in precipitation, while Bessah et al. (2020) similarly noted increases when applying their best bias-corrected model. The divergence between precipitation and streamflow responses highlights the influence of additional hydrological processes, including

evapotranspiration, soil moisture dynamics, and catchment storage effects, which can offset increases in rainfall. The stronger and more uniform decline in streamflow projected for the mid-century period compared to the near-future period suggests an intensification of climate change impacts over time. Elevated temperatures under future scenarios are likely to enhance evaporative losses, thereby reducing effective runoff even in seasons with modest rainfall changes. The relatively linear response of streamflow to changes in precipitation, as noted by Gu & Adler (2003), further explains why reductions in rainfall translate into pronounced decreases in discharge. The consistent reduction in projected streamflow across seasons for the 2045–2074 period indicates a potential long-term decrease in water availability at the Pra Basin outlet. This trend has important implications for water resources management, ecosystem sustainability, and socio-economic activities dependent on surface water. The results, therefore, underscore the need for adaptive management strategies that account for reduced flows and increased climatic uncertainty under future conditions.

7.2.4 Implications for Water Resources Management and Basin Sustainability

The simulated streamflow regime highlights strong seasonal constraints on water availability in the Pra River Catchment. Vulnerability of dry-season flows indicates that irrigation, domestic supply, and potential hydropower development are primarily limited by low-flow conditions rather than mean annual runoff (Arthur et al., 2020; Jaramillo et al., 2020; Pluchinotta et al., 2018; Wriedt et al., 2009). The results suggest that irrigation expansion based on wet-season surplus alone is unlikely to be sustainable without storage, efficiency improvements, or conjunctive surface–groundwater use. Similar limitations have been observed in other tropical basins where dry-season flow reliability governs irrigation viability.

For domestic and urban water supply, the coincidence of minimum streamflow with peak dry-season demand explains recurrent water stress in Pra basin settlements dependent on surface abstractions (Osei & Amoakowaah, 2021; Osei et al., 2021). This structural vulnerability underscores the need for integrated management strategies combining regulation, groundwater development, and demand management. Although hydropower potential is currently limited, the simulated flow regime indicates strong intra-annual variability and restricted firm power during dry periods, consistent with findings from other monsoon-driven African basins (Awotwi et al., 2017, 2019). Overall, the HBV application supports the identification of management-relevant vulnerabilities under existing climatic and land-use conditions.

7.2.5 Influence of Catchment Characteristics, Data, and Uncertainties in Model Structure

Spatial heterogeneity within the Pra basin influenced model performance, as contrasting physiographic and land-use conditions were necessarily averaged within the lumped HBV structure. This spatial aggregation limits representation of sub-catchment-specific processes and may mask compensating errors at the basin outlet, a known trade-off in conceptual modeling (Gelete et al., 2023; Ningrum et al., 2024; Tibangayuka et al., 2022). Consequently, sub-basin-scale interpretations require caution.

Meteorological forcing uncertainty further constrained simulations. Reliance on gridded precipitation products introduced seasonal biases typical of satellite-based estimates over West Africa, particularly for convective rainfall, which propagate directly into runoff simulations (Atiah et al., 2020; Bagiliko et al., 2025; Dinku et al., 2018). In addition, parameter equifinality was evident, with multiple parameter sets yielding comparable calibration performance, indicating limited identifiability (Her et al., 2019; Shen et al., 2012). This non-uniqueness precludes deterministic interpretation of a single optimal parameter set, especially for extrapolation beyond observed conditions.

7.2.6 Partial conclusion

The HBV model application in the Pra River Catchment demonstrates that a lumped conceptual approach can adequately reproduce observed streamflow behaviour under data-scarce tropical conditions. Model calibration and validation yielded stable and defensible performance, indicating that the dominant rainfall–runoff relationships were captured and that the model structure generalized well beyond the calibration period. The simulated hydrographs successfully represented the characteristic bimodal seasonal regime of the basin, including the timing of major wet-season peaks and realistic recession behaviour during transitions to dry conditions. While the simulation of hydrological extremes showed some limitations, the model reliably reproduced average seasonal dynamics and key process controls.

Projected streamflow under future climate scenarios indicates a persistent reduction across both near- and mid-century periods, while maintaining the bimodal seasonal pattern. The magnitude and consistency of the projected decline highlight a likely reduction in basin-scale water availability, providing a quantitative basis for assessing future hydrological stress in the Pra River system.

CHAPTER 8: GENERAL CONCLUSION AND RECOMMENDATION

8.1 Conclusion

This study examined land use and land cover dynamics, rainfall extremes, and climate-driven hydrological responses in the Pra River Basin to establish a robust baseline for assessing future water resource impacts. By integrating historical analyses with future climate and land-use projections, the research provides a comprehensive understanding of how coupled climatic and anthropogenic drivers are reshaping hydrological processes within the basin.

A synthesis of thematic mapping and factor analysis of the Pra River Basin-related research reveals a steady expansion of scientific output, with an annual growth rate of 9.25% and a gradual shift from climate-centric investigations toward more multidimensional approaches. Despite this progress, the integration of climate change and land-use change research remains limited, highlighting a persistent gap in holistic basin-scale assessments.

Land use and land cover analysis indicate substantial deforestation driven primarily by agricultural expansion and the growth of settlements and bare land. Between 2007 and 2023, cultivated land increased by 33% and built-up or bare land by 8%, largely at the expense of forest cover (72.3%) and natural vegetation (10.4%). Projections for 2030 and 2063 suggest that forests and natural vegetation will continue to experience the largest net losses, exceeding approximately 3,300 km² and 2,200 km², respectively. These changes are likely to alter basin hydrology by enhancing surface runoff and evapotranspiration, with implications for increased flood susceptibility.

Analysis of rainfall seasonality shows a strong relationship between the Centre of Mass of rainfall and total annual precipitation, particularly at Assin-Praso, Daboasi, and Bunso. Wetter years are associated with delayed rainfall CoM, indicating a lengthening of the rainy season. Probability density functions further reveal an intensification of extreme rainfall events, especially under high-emission scenarios.

Future climate projections for 2021–2100 under SSP1-2.6 and SSP3-7.0 indicate increased uncertainty in rainfall onset and cessation, alongside spatially heterogeneous precipitation responses. Higher rainfall intensities are projected for the northwestern basin during the minor rainy season, while reduced precipitation is expected in the southern region during the major

rainy season over the long term. These shifts are accompanied by an increased likelihood of extreme drought and intense rainfall events, each increasing by approximately 20%. Projected temperature rises of 1–2°C under SSP1-2.6 and 3–4°C under SSP3-7.0 by 2100 are expected to exert strong control on basin water balance.

Finally, the combined effects of climate change and land-use transformation indicate sustained annual water losses through enhanced evapotranspiration and surface runoff under SSP3-7.0, with monthly variations reaching ±24% and 24% decrease in projected streamflow. Together, these findings underscore the growing vulnerability of the Pra River Basin to future hydroclimatic stress and highlight the need for integrated, forward-looking water resources management strategies.

8.2 Recommendations

Policy

i. Implementation of Climate-Smart Agriculture (CSA) by the Ministry of Food and Agriculture, working with the Ministry of Fisheries and Aquaculture. CSA builds resilience to onset/cessation variability via conservation agriculture, drought-tolerant crops, and flexible cropping calendars adjusted to forecasts.

ii. Government and extension agencies should provide farmers with seasonal outlooks and index-based insurance to reduce crop losses by 15-38%. Evidence from Uganda/Tanzania shows productivity gains and GHG reductions; scale via national policies.

iii. Promotion of Agroforestry Practices by the Ministry of Lands and Natural Resources through the integration of trees into farms for soil moisture buffering, biodiversity, and income amid land changes and rainfall uncertainty.

iv. Governments and farmer cooperatives should offer incentives, training programs, and region-specific systems (e.g., tree-crop-livestock) to counter heat/drought stresses. Studies confirm yield stability and carbon benefits in the tropics, like West Africa.

v. Strengthening Governance for Sustainable Land/Forest Management should be enforced through the collaboration of the Ministry of Lands and Natural Resources, the Ministry of Works, Housing and Water Resources, the Water Resources Commission, Environmental Protection Authority, Ghana Water Company, NGOs, and research institutes.

vi. The Government should secure tenure and participatory rules to curb deforestation, zone sensitive areas (e.g., riparian zones), and enable sustainable expansion, which will strengthen sustainable land management.

vii. National agencies and NGOs should link REDD+ incentives to local institutions for equitable enforcement. Brazil/Congo Basin examples highlight economic-environmental alignment.

Research

i. Integrated Assessment and Adaptive Management Planning led by the Water Resource Commission, the Ministry of Town and Country Planning, and research institutes.

ii. The use of science-backed tools (e.g., onset diagnostics, hydrological models) for iterative planning across scales will accelerate the assessment and adaptive management planning.

iii. Research institutes and Pra Basin Board authorities should invest in decentralized water storage (e.g., farm ponds) and real-time monitoring systems. This combines indigenous knowledge with data for enhanced food security in rainfed systems

iv. Alternative use of higher resolution satellite datasets, alternative land cover classification algorithms and multiple land change modelling approaches in future projections to verify and improve the robustness of scenario outcomes of this study.

8.3 Perspectives or Future Work (AGUA Project)

Based on the findings as a baseline on the current impact of climate and land use change in a nested tropical ecosystem, such as the Pra River Basin, the perspectives of this study are on the impact of these changes on streamflow dynamics using the Ecohydrological model (EcH_2O-iso) and coupling with isotope tracking to combat climate change and its impact. This has become urgent because science-based water resource management requires robust information on a catchment's hydrology and how global change alters streamflow that serves as the foundation for achieving Goals 6 and 13. The primary aim of the future project "AGUA" is to address the challenge of predicting global change impact on the hydrological cycle in a catchment in the Global South. In particular, in AGUA, we are (i) building and validating a distributed hydrological model (EcH_2O-iso) in a data-scarce tropical environment from the results of this dissertation and (ii) predicting global change impacts on streamflow through linking climate analysis to a distributed hydrological model. By addressing pressing scientific

challenges in hydrological modelling, AGUA will also provide the groundwork for sustainable management decisions in the Pra catchment and then replicate it for tropical regions.

Objectives, working hypotheses, and research questions

The research objective is to predict the impact of LULC-climate change on streamflow, aiding sustainable water management under change in the Pra River catchment. To overcome our current limitations in hydrological predictions, we will test the following **hypotheses** (H, linked to research objectives (RO)):

- H1: Climate change will decrease annual streamflow uniformly across all stream gauges in the Pra River catchment, with increased variability throughout the year.
- H2: LULCC will cause spatial variability in streamflow changes, in addition to climate change-driven alterations.
- H3: An innovative framework for ecohydrological modelling can effectively address data scarcity and provide a robust calibration strategy for regions experiencing LULCC.

Specific Objectives (SO):

- SO1: Setup and validate the most effective calibration strategies for the EcH2O-iso model (*focus on **model calibration and validation performance***).
- SO2: Evaluate the impact of climate-LULC Change, including downscaled climate and land-use scenarios, on streamflow dynamics (*focus on **data-model fusion***).

Deliverables:

A clear set of deliverables (D) will ensure our SOs are met, and hypotheses are tested. D1 linked to SO1; D2 linked to SO2.

- D1: Hydrological model calibration and validation.
- D2: Simulation of future hydrological conditions under Global Change.

Research Strategies and Methods

The strategy and methods will be in two categories using of EcH2O-iso model:

Data Analysis:

- Installing EcH2O-iso on a high-performance computer (HPC).
- Use of the EcH2O-iso model for hydrological simulations.
- Long-term hydrological and ecological data for model calibration and validation.

- Multiple objective functions (KGE, APB, NSE) for model performance assessment.

Impact Analysis:

- Coupling climate and land-use change models with EcH2O-iso to simulate streamflow dynamics.
- Climate scenarios from CMIP6 and socio-economic pathways (SSP1-2.6, SSP3-7.0) for future projections.
- Land-use maps for the period 2023-2063 to study LULCC effects on hydrology

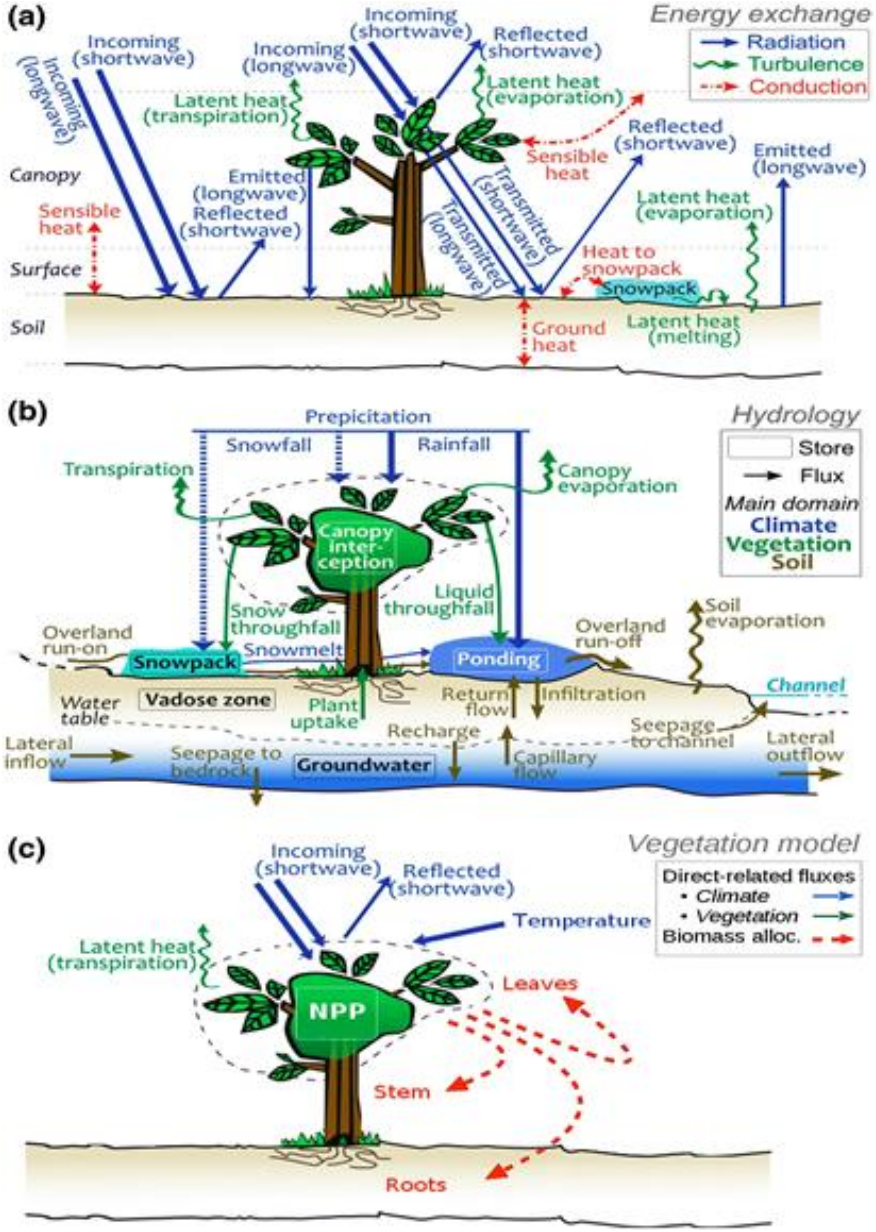

Figure 7.1: Schematic diagram of the processes simulated in (a) the energy balance, (b) the hydrologic, and (c) the vegetation modules of the EcH2O model (adapted from **Kuppel et al.**, *2018a)*

Work program - Summary of the research activities

To accomplish the objectives, three complementary work packages have been designed (WP): Hands-on training on high-performance computers (HPC) for computational analysis (WP1); simulating the impact of Global Change on streamflow through distributed hydrological modelling (WP2); and dissemination (WP3). Within these WPs, I will target the two specific objectives (SO):

Work Package 1: Hands-on training on HPC for computational analysis

- Task 1.1: Installation of Ech2O-iso model on the HPC.

Advance training on utilising high-performance computing (HPC) to handle complex simulations, installing the EcH2O-iso model on the HPC will enable the confident use of the physically distributed hydrological model, EcH2O-iso, to meet the project's scientific objectives. The downscaling process of large-scale climate data from CMIP6 models to a regional scale at a resolution of 0.25° (Koch et al., 2019), bridging the gap between global and local climatic effects by incorporating local data with larger-scale datasets. EcH2O-iso, developed by (Kuppel et al., 2018a), is a distributed, physically-based hydrological model that simulates water fluxes both at and below the surface. This model is essential for estimating the impacts of global change on hydrological processes, as evidenced by studies from Huang et al. (2020), Knighton et al. (2020), Kuppel et al. (2018a, 2018b).

Work Package 2: Simulating and analysing Global Change impacts on streamflow with EcH2O-iso.

- Task 2.1: Model calibration and validation.

The aim is to assess how appropriately the complex process-based model can be parameterised. The EcH2O-iso will be calibrated against long-term datasets that encompass hydrologic and energy exchanges, and ecological measurements with specific observations to reasonably reproduce storage dynamics. Applying diverse combinations of these constraints revealed that calibration against virtually all datasets enabled the model to reproduce streamflow reasonably well. Model performance will be assessed using multiple objective functions, including the Kling-Gupta Efficiency (KGE, (Gupta et al., 2020), the absolute percentage bias (APB), and the Nash-Sutcliffe Efficiency (NSE). These metrics will focus on different aspects of streamflow to ensure a comprehensive assessment of the model's accuracy and reliability.

- Task 2.2: Coupling climate and land-use change models with EcH2O-iso.

I aim to use the calibrated/validated EcH2O-iso model to simulate streamflow dynamics in the Pra catchment under global change scenarios. For the climate scenarios, I will utilise the global climate model (GCM) data series from the Coupled Model Intercomparison Project Phase 6 (CMIP6), downscaled to the study region at a resolution of 0.25° (cf. task 1.1). A minimum of 30 years of data is recommended for climate change impact analysis. Temperature and precipitation data from five CMIP6 models (ACCESS-CM2, EC-Earth3-Veg-LR, IPSL-CM6A-LR, MIROC-ES2L, MPI-ESM1-2-LR) and their ensemble mean will be selected. These parameters, based on two Shared Socioeconomic Pathway (SSP) emissions scenarios, SSP1-2.6 and SSP3-7.0, for the period 2021-2050, will be used to estimate and project the potential impact of global change on streamflow in the Pra catchment. For land-use and land-cover change (LULCC), I will use projected land-use maps for the period 2023-2063 (Agbenorhevi et al., 2024). In the EcH2O-iso model, changes in land use are represented by vegetation parameters documented in the literature. LULCC directly affects transpiration, soil water content, and groundwater recharge.

Work Package 3: Dissemination.

- Task 3.1: Journal publication preparation.

A key outcome of this project will be one anticipated journal publication on novel insights into streamflow dynamics predictions, mainly building on the modelling work. In this article, I will address the regional impact of climate scenarios in CMIP6 through multi-model ensembles and the impact of land-use scenarios on streamflow. The article will be submitted to a high-impact peer-reviewed journal of the water field, preferably open access (e.g. Hydrology and Earth System Sciences, Climatic Change, Journal of Hydrology: Regional Studies).

- Task 3.2: Dissemination through conferences, social media, and open science platforms.

Frequent communications at GIUB and the Geoverbund ABC/J are foreseen to disseminate the results in a local and regional context. Additionally, novel insights from modelling will be shared in English and German, through (i) the Graduate Research Program on Climate Change and Water Resources http://wascal-uac.org/), social media platforms, and the Department of Geography in Bonn. The aim is to disseminate the generated results and code in an Open Science approach through the Servicestelle Forschungsdaten and Servicestelle Open Access to

make the work and workflow fully reproducible. Results from the AGUA project will be disseminated at one International Conference in 2026/27 in person (e.g. American Geophysical Union, European Geoscience Union General Assembly, the International Association of Hydrological Sciences Conference. Besides that, the results will also be disseminated at the WASS conference, where he will disseminate the results to the communities of the tropical region

REFERENCES

Abu, I. O., Szantoi, Z., Brink, A., Robuchon, M., & Thiel, M. (2021). Detecting cocoa plantations in Côte d'Ivoire and Ghana and their implications on protected areas. *Ecological Indicators*, *129*. https://doi.org/10.1016/j.ecolind.2021.107863

Abungba, J. A., Adjei, K. A., Gyamfi, C., Odai, S. N., Pingale, S. M., & Khare, D. (2022). Implications of Land Use/Land Cover Changes and Climate Change on Black Volta Basin Future Water Resources in Ghana. *Sustainability (Switzerland)*, *14*(19). https://doi.org/10.3390/su141912383

Adib, M. N. M., Harun, S., & Rowshon, M. K. (2022). Long-term rainfall projection based on CMIP6 scenarios for Kurau River Basin of rice-growing irrigation scheme, Malaysia. *SN Applied Sciences*, *4*(3). https://doi.org/10.1007/s42452-022-04952-x

Adukpo, O. K., Faanu, A., Lawluvi, H., Tettey-Larbi, L., Emi-Reynolds, G., Darko, E. O., Kansaana, C., Kpeglo, D. O., Awudu, A. R., Glover, E. T., Amoah, P. A., Efa, A. O., Agyemang, L. A., Agyeman, B. K., Kpordzro, R., & Doe, A. I. (2015). Distribution and assessment of radionuclides in sediments, soil and water from the lower basin of river Pra in the Central and Western Regions of Ghana. *Journal of Radioanalytical and Nuclear Chemistry*, *303*(3), 1679–1685. https://doi.org/10.1007/s10967-014-3637-5

Agariga, F., Abugre, S., & Appiah, M. (2021). Spatio-temporal changes in land use and forest cover in the Asutifi North District of Ahafo Region of Ghana, (1986–2020). *Environmental Challenges*, *5*, 100209. https://doi.org/10.1016/J.ENVC.2021.100209

Agbenorhevi, A. E., Amekudzi, L. K., Kèlomé, N. C., Biney, E., & Annan, E. (2024). Analyzing land use and land cover change in the Pra River Basin: A multi-tool approach for informed decision-making. *Environmental Challenges*, *15*. https://doi.org/10.1016/j.envc.2024.100922

Agodzo, S. K., Bessah, E., & Nyatuame, M. (2023). *A review of the water resources of Ghana in a changing climate and anthropogenic stresses*. https://doi.org/https://doi.org/10.3389/frwa.2022.973825

Ahmad, B., Usman, M., Bukhari, S. A. A., & Sajjad, H. (2020). Contribution of Glacier, Snow and Rain Components in Flow Regime Projected with HBV Under AR5 Based Climate Change Scenarios Over Chitral River Basin (Hindukush Ranges, Pakistan). *International Journal of Climate Research*, *4*(1), 24–36. https://doi.org/10.18488/journal.112.2020.41.24.36

Ahmad, S., Kalra, A., & Stephen, H. (2010). Estimating soil moisture using remote sensing data: A machine learning approach. *Advances in Water Resources*, *33*(1), 69–80. https://doi.org/10.1016/j.advwatres.2009.10.008

Ahmed, M., Sultan, M., Wahr, J., & Yan, E. (2014). The use of GRACE data to monitor natural and anthropogenic induced variations in water availability across Africa. In *Earth-Science Reviews* (Vol. 136, pp. 289–300). Elsevier. https://doi.org/10.1016/j.earscirev.2014.05.009

Ajibola, F. O., Zhou, B., Gnitou, G. T., & Onyejuruwa, A. (2020). Evaluation of the performance of cmip6 highresmip on west african precipitation. *Atmosphere*, *11*(10). https://doi.org/10.3390/atmos11101053

Ajjur, S. B., & Al-Ghamdi, S. G. (2021). Evapotranspiration and water availability response to climate change in the Middle East and North Africa. *Climatic Change*, *166*(3–4). https://doi.org/10.1007/s10584-021-03122-z

Akpoti, K., Antwi, E. O., & Kabo-bah, A. T. (2016). Impacts of rainfall variability, land use and land cover change on stream flow of the Black Volta basin, West Africa. *Hydrology*, *3*(3). https://doi.org/10.3390/hydrology3030026

Akrasi, S. A., & Ansa-Asare, O. D. (2008). *Assessing Sediment and Nutrient Transport in the Pra Basin of Ghana*.

Alam, M. A., Emura, K., Farnham, C., & Yuan, J. (2018). Best-fit probability distributions and return periods for maximum monthly rainfall in Bangladesh. *Climate*, *6*(1). https://doi.org/10.3390/cli6010009

Aleissaee, A. A., Amandeep, K., Rao Muhammad, A., Salman, K., Hisham, C., Gui-Song, X., & Fahad Shahbaz Khan. (2023). Transformers in remote sensing: A survey. *Remote Sensing MDPI*, *15*(7), 1860.

Ali, A. F., Xiao, C. de, Zhang, X. peng, Adnan, M., Iqbal, M., & Khan, G. (2018). Projection of future streamflow of the Hunza River Basin, Karakoram Range (Pakistan) using HBV hydrological model. *Journal of Mountain Science*, *15*(10), 2218–2235. https://doi.org/10.1007/s11629-018-4907-4

Allan, R. P., Arias, P. A., Berger, S., Canadell, J. G., Cassou, C., Chen, D., ... & Zickfeld, K. (2023). Intergovernmental panel on climate change (IPCC). Summary for policymakers. In Climate change 2021: The physical science basis. Contribution of working group I to the sixth assessment report of the intergovernmental panel on climate change (pp. 3-32). Cambridge University Press. https://doi.org/10.1017/9781009157896.001.

Alley, W. M. (1984). The Palmer Drought Severity Index: Limitations and Assumptions. In *Source: Journal of Climate and Applied Meteorology* (Vol. 23, Issue 7).

Almazroui, M., Ashfaq, M., Islam, M. N., Rashid, I. U., Kamil, S., Abid, M. A., O'Brien, E., Ismail, M., Reboita, M. S., Sörensson, A. A., Arias, P. A., Alves, L. M., Tippett, M. K., Saeed, S., Haarsma, R., Doblas-Reyes, F. J., Saeed, F., Kucharski, F., Nadeem, I., … Sylla, M. B. (2021). Assessment of CMIP6 Performance and Projected Temperature and Precipitation Changes Over South America. *Earth Systems and Environment*, *5*(2), 155–183. https://doi.org/10.1007/s41748-021-00233-6

Almazroui, M., Saeed, F., Saeed, S., Nazrul Islam, M., Ismail, M., Klutse, N. A. B., & Siddiqui, M. H. (2020). Projected Change in Temperature and Precipitation Over Africa from CMIP6. *Earth Systems and Environment*, *4*(3), 455–475. https://doi.org/10.1007/s41748-020-00161-x

Almazroui, M., Saeed, S., Saeed, F., Islam, M. N., & Ismail, M. (2020). Projections of Precipitation and Temperature over the South Asian Countries in CMIP6. *Earth Systems and Environment*, *4*(2), 297–320. https://doi.org/10.1007/s41748-020-00157-7

Amekudzi, L. K., Bracher, A., Bramstedt, K., Rozanov, A., Bovensmann, H., & Burrows, J. P. (2008). Towards validation of SCIAMACHY lunar occultation NO2 vertical profiles. *Advances in Space Research*, *41*(11), 1921–1932. https://doi.org/10.1016/j.asr.2007.06.055

Amekudzi, L. K., Yamba, E. I., Preko, K., Asare, E. O., Aryee, J., Baidu, M., & Codjoe, S. N. A. (2015). Variabilities in rainfall onset, cessation and length of rainy season for the various agro-ecological zones of Ghana. *Climate*, *3*(2), 416–434. https://doi.org/10.3390/cli3020416

Amproche, A., Antwi, M., & Kabo-Bah, A. (2020). Geospatial Assessment of Land Use and Land Cover Patterns in the Black Volta Basin, Ghana. *Journal of Remote Sensing & GIS*, *09*(01). https://doi.org/10.35248/2469-4134.20.9.269

Antwi-Agyei, P., Dougill, A. J., & Stringer, L. C. (2015). Barriers to climate change adaptation: evidence from northeast Ghana in the context of a systematic literature review. *Climate and Development*, *7*(4), 297–309. https://doi.org/10.1080/17565529.2014.951013

Appiah, D. O., Schröder, D., Forkuo, E. K., & Bugri, J. T. (2015). Application of geo-information techniques in land use and land cover change analysis in a peri-urban district of Ghana. *ISPRS International Journal of Geo-Information*, *4*(3), 1265–1289. https://doi.org/10.3390/ijgi4031265

Araral, E., & Wang, Y. (2013). Water Governance 2.0: A Review and Second Generation Research Agenda. *Water Resources Management*, *27*(11), 3945–3957. https://doi.org/10.1007/s11269-013-0389-x

Aria, M., & Cuccurullo, C. (2017). bibliometrix: An R-tool for comprehensive science mapping analysis. *Journal of Informetrics*, *11*(4), 959–975. https://doi.org/10.1016/j.joi.2017.08.007

Armah, Y. S. (2010). Hydrochemical Analysis of Groundwater In The Lower Pra Basin of Ghana. *Journal of Water Resource and Protection*, *02*(10), 864–871. https://doi.org/10.4236/jwarp.2010.210103

Arthur, E., Anyemedu, F. O. K., Gyamfi, C., Asantewaa - Tannor, P., Adjei, K. A., Anornu, G. K., & Odai, S. N. (2020). Potential for small hydropower development in the Lower Pra River Basin, Ghana. *Journal of Hydrology: Regional Studies*, *32*, 100757. https://doi.org/10.1016/J.EJRH.2020.100757

Aryee, J. N. A., Amekudzi, L. K., Quansah, E., Klutse, N. A. B., Atiah, W. A., & Yorke, C. (2018). Development of high spatial resolution rainfall data for Ghana. *International Journal of Climatology*, *38*(3), 1201–1215. https://doi.org/10.1002/joc.5238

Asante, F. A., & Amuakwa-Mensah, F. (2015). Climate change and variability in Ghana: Stocktaking. In *Climate* (Vol. 3, Issue 1, pp. 78–99). MDPI AG. https://doi.org/10.3390/cli3010078

Asimah, E. (2013). *Report of the Commission on Environment Science and Technology on the 2014 Programme Based Budget Estimates of the Ministry of Environment, Science and Technology and Innovation (MESTI).*

Atiah, W. A., & Muthoni, F. K. (2023). *Trends and variability of rainfall seasonality indices in the Lao People's Democratic Republic (PDR)*.

Atiah, W. A., Amekudzi, L. K., Aryee, J. N. A., Preko, K., & Danuor, S. K. (2020). Validation of satellite and merged rainfall data over Ghana, West Africa. *Atmosphere*, *11*(8). https://doi.org/10.3390/ATMOS11080859

Atiah, W. A., Muthoni, F. K., Kotu, B., Kizito, F., & Amekudzi, L. K. (2021). Trends of rainfall onset, cessation, and length of growing season in northern ghana: Comparing the rain gauge, satellite, and farmer's perceptions. *Atmosphere*, *12*(12). https://doi.org/10.3390/atmos12121674

Attiogbe, F., & Nkansah, A. (2017). The Impact of Mining on the Water Resources in Ghana: Newmont Case Study at Birim North District (New Abirem). *Energy and Environment Research*, *7*(2), 27. https://doi.org/10.5539/eer.v7n2p27

Awotwi, A., Anornu, G. K., Quaye-Ballard, J. A., & Annor, T. (2018). Monitoring land use and land cover changes due to extensive gold mining, urban expansion, and agriculture in the Pra River Basin of Ghana, 1986–2025. *Land Degradation and Development*, *29*(10), 3331–3343. https://doi.org/10.1002/ldr.3093

Awotwi, A., Anornu, G. K., Quaye-Ballard, J. A., Annor, T., Forkuo, E. K., Harris, E., Agyekum, J., & Terlabie, J. L. (2019). Water balance responses to land-use/land-cover changes in the Pra River Basin of Ghana, 1986–2025. *CATENA*, *182*, 104129. https://doi.org/10.1016/J.CATENA.2019.104129

Awotwi, A., Anornu, G. K., Quaye-Ballard, J. A., Annor, T., Nti, I. K., Odai, S. N., Arhin, E., & Gyamfi, C. (2021). Impact of post- reclamation of soil by large-scale, small-scale and illegal mining on water balance components and sediment yield: Pra River Basin case study. *Soil and Tillage Research*, *211*. https://doi.org/10.1016/j.still.2021.105026

Awotwi, A., Kwame Anornu, G., Quaye-Ballard, J., Annor, T., & Kwabena Forkuo, E. (2017a). Analysis of climate and anthropogenic impacts on runoff in the Lower Pra River Basin of Ghana. *Heliyon*, *3*, 477. https://doi.org/10.1016/j.heliyon.2017

Awotwi, A., Kwame Anornu, G., Quaye-Ballard, J., Annor, T., & Kwabena Forkuo, E. (2017b). Analysis of climate and anthropogenic impacts on runoff in the Lower Pra River Basin of Ghana. *Heliyon*, *3*, 477. https://doi.org/10.1016/j.heliyon.2017

Awotwi, A., Kwame Anornu, G., Quaye-Ballard, J., Annor, T., & Kwabena Forkuo, E. (2017c). Analysis of climate and anthropogenic impacts on runoff in the Lower Pra River Basin of Ghana. *Heliyon*, *3*, 477. https://doi.org/10.1016/j.heliyon.2017

Bagiliko, J., Stern, D., Ndanguza, D., & Torgbor, F. F. (2025). *Validation of satellite and reanalysis rainfall products against rain gauge observations in Ghana and Zambia*. https://doi.org/10.1007/s00704-025-05462-7

Bailey, R. T., Park, S., Biegar, K., Arnold, J. G., & Allen, P. M. (2020). Enhancing SWAT+ Simulation of Groundwater Flow and Groundwater-surface Water Interactions using MODFLOW Routines. Environmental Modelling and Software. *126, 104660.*

Belgiu, M., & Drăgu, L. (2016). Random forest in remote sensing: A review of applications and future directions. In *ISPRS Journal of Photogrammetry and Remote Sensing* (Vol. 114, pp. 24–31). Elsevier B.V. https://doi.org/10.1016/j.isprsjprs.2016.01.011

Bell, B., Hersbach, H., Simmons, A., Berrisford, P., Dahlgren, P., Horányi, A., Muñoz-Sabater, J., Nicolas, J., Radu, R., Schepers, D., Soci, C., Villaume, S., Bidlot, J. R., Haimberger, L., Woollen, J., Buontempo, C., & Thépaut, J. N. (2021). The ERA5 global reanalysis: Preliminary extension to 1950. *Quarterly Journal of the Royal Meteorological Society*, *147*(741), 4186–4227. https://doi.org/10.1002/qj.4174

Bergström, S. (1976). *"Development and Applicationof a ConceptualRunoff Model for Scandinavian Catchments."*

Bessah, E., Raji, A. O., Taiwo, O. J., Agodzo, S. K., & Ololade, O. O. (2020a). The impact of varying spatial resolution of climate models on future rainfall simulations in the pra river basin (Ghana). *Journal of Water and Climate Change*, *11*(4), 1263–1283. https://doi.org/10.2166/wcc.2019.258

Bessah, E., Raji, A. O., Taiwo, O. J., Agodzo, S. K., & Ololade, O. O. (2020b). The impact of varying spatial resolution of climate models on future rainfall simulations in the pra river basin (Ghana). *Journal of Water and Climate Change*, *11*(4), 1263–1283. https://doi.org/10.2166/wcc.2019.258

Bessah, E., Raji, A. O., Taiwo, O. J., Agodzo, S. K., Ololade, O. O., & Strapasson, A. (2020). Hydrological responses to climate and land use changes: The paradox of regional and local climate effect in the Pra River Basin of Ghana. *Journal of Hydrology: Regional Studies*, *27*, 100654. https://doi.org/10.1016/J.EJRH.2019.100654

Beven, K. (2001). AGU Fellow, 1995, and the International Francqui Chair. In *Hydrology and Earth System Sciences* (Vol. 5, Number 1).

Biasutti, M. (2019). Rainfall trends in the African Sahel: Characteristics, processes, and causes. In Wiley Interdisciplinary Reviews: Climate Change (Vol. 10, Issue 4). Wiley-Blackwell. https://doi.org/10.1002/wcc.591

Bibi, U. M., Kaduk, J., & Balzter, H. (2014). Spatial-temporal variation and prediction of rainfall in Northeastern Nigeria. *Climate*, *2*(3), 206–222. https://doi.org/10.3390/cli2030206

Biney, E., Forkuo, E. K., Poku-Boansi, M., Hackman, K. O., Harris, E., Asare, Y. M., Yankey, D. B., Annan, E., & Agbenorhevi, A. E. (2024). Analyzing the spatio-temporal pattern of urban growth and its influence on urban heat islands in the Sekondi-Takoradi metropolis, Ghana. *Scientific African*, *26*. https://doi.org/10.1016/j.sciaf.2024.e02366

Bizuneh, B. B., Moges, M. A., Sinshaw, B. G., & Kerebih, M. S. (2021). SWAT and HBV models' response to streamflow estimation in the upper Blue Nile Basin, Ethiopia. *Water-Energy Nexus*, *4*, 41–53. https://doi.org/10.1016/j.wen.2021.03.001

Boakye, E., Anyemedu, F. O. K., Quaye-Ballard, J. A., & Donkor, E. A. (2020). Spatio-temporal analysis of land use/cover changes in the Pra River Basin, Ghana. *Applied Geomatics*, *12*(1), 83–93. https://doi.org/10.1007/s12518-019-00278-3

Bodjrènou, R., Sintondji, L. O., & Comandan, F. (2023). Hydrological modeling with physics-based models in the Ouémé basin: Issues and perspectives for simulation optimization. *Journal of Hydrology: Regional Studies. 4*.

Bormann, H., Breuer, L., Gräff, T., Huisman, J. A., & Croke, B. (2009). Assessing the impact of land use change on hydrology by ensemble modelling (LUCHEM) IV: Model sensitivity to data aggregation and spatial (re-)distribution. *Advances in Water Resources*, *32*(2), 171–192. https://doi.org/10.1016/j.advwatres.2008.01.002

Cai, Y., Yang, Y., Tan, Q., Dai, C., Zhu, Z., & Zhang, X. (2024). Impacts of temporal/spatial rainfall heterogeneities on peak runoff distribution and intensities for an urban river basin of south China. *River*, *3*(1), 24–37. https://doi.org/10.1002/rvr2.77

Caie, P. D., Dimitriou, N., & Arandjelović, O. (2020). Precision medicine in digital pathology via image analysis and machine learning. In *Artificial Intelligence and Deep Learning in Pathology* (pp. 149–173). Elsevier. https://doi.org/10.1016/B978-0-323-67538-3.00008-7

Camberlin, P., Janicot, S., & Poccard, I. (2001). Seasonality and atmospheric dynamics of the teleconnection between African rainfall and tropical sea-surface temperature: Atlantic vs. ENSO. *International Journal of Climatology*, *21*(8), 973–1005. https://doi.org/10.1002/joc.673

Cooper, R. (2018). *Water management/governance systems in Pakistan*.

Cornelissen, T., Diekkrüger, B., & Giertz, S. (2013). A comparison of hydrological models for assessing the impact of land use and climate change on discharge in a tropical catchment. *Journal of Hydrology*, *498*, 221–236. https://doi.org/10.1016/j.jhydrol.2013.06.016

Cruz, J., White, P. C. L., Bell, A., & Coventry, P. A. (2020). Effect of extreme weather events on mental health: A narrative synthesis and meta-analysis for the UK. In *International Journal of Environmental Research and Public Health* (Vol. 17, Issue 22, pp. 1–17). MDPI AG. https://doi.org/10.3390/ijerph17228581

Cui, W., Wei, Y., & Ji, N. (2024). Global trends of waste-to-energy (WtE) technologies in carbon neutral perspective: Bibliometric analysis. In *Ecotoxicology and Environmental Safety* (Vol. 270). Academic Press. https://doi.org/10.1016/j.ecoenv.2023.115913

Dahan, K. S., Kasei, R. A., Husseini, R., Sarr, M., & Said, M. Y. (2024). Analysis of the future potential impact of environmental and climate changes on wildfire spread in Ghana's ecological zones using a Random Forest (RF) machine learning approach. *Remote Sensing Applications: Society and Environment*, *33*. https://doi.org/10.1016/j.rsase.2023.101091

Darko, G., Obiri-Yeboah, S., Takyi, S. A., Amponsah, O., Borquaye, L. S., Amponsah, L. O., & Fosu-Mensah, B. Y. (2022). Urbanizing with or without nature: pollution effects of human activities on water quality of major rivers that drain the Kumasi Metropolis of Ghana. *Environmental Monitoring and Assessment*, *194*(1). https://doi.org/10.1007/s10661-021-09686-8

Darko, H. F., Karikari, A. Y., Duah, A. A., Akurugu, B. A., Mante, V., & Teye, F. O. (2023). Effect of small-scale illegal mining on surface water and sediment quality in Ghana. *International Journal of River Basin Management*, *21*(3), 375–386. https://doi.org/10.1080/15715124.2021.2002345

Dayinday, S. A. (2023). Assessment and Spatial Analysis of Land Use and Land Cover (LULC) Dynamics in the Black Volta Basin. *International Journal of Multidisciplinary Studies and Innovative Research*, *4*(4), 158–177. https://doi.org/10.53075/Ijmsirq/453636636363

Diatta, S., Diedhiou, C. W., Dione, D. M., & Sambou, S. (2020). Spatial variation and trend of extreme precipitation in West Africa and teleconnections with remote indices. *Atmosphere*, *11*(9). https://doi.org/10.3390/atmos11090999

Dibi-Anoh, P. A., Koné, M., Gerdener, H., Kusche, J., & N'Da, C. K. (2023). Hydrometeorological Extreme Events in West Africa: Droughts. In *Surveys in Geophysics* (Vol. 44, Issue 1, pp. 173–195). Springer Science and Business Media B.V. https://doi.org/10.1007/s10712-022-09748-7

Didi Sacré Regis, M., Mouhamed, L., Kouakou, K., Adeline, B., Arona, D., Saint, C. H. J., Claude, K. K. A., Jean, C. T. H., Salomon, O., & Issiaka, S. (2020). Using the CHIRPS dataset to investigate historical changes in precipitation extremes in West Africa. *Climate*, *8*(7). https://doi.org/10.3390/CLI8070084

Dinku, T., Funk, C., Peterson, P., Maidment, R., Tadesse, T., Gadain, H., & Ceccato, P. (2018). Validation of the CHIRPS satellite rainfall estimates over eastern Africa. *Quarterly Journal of the Royal Meteorological Society*, *144*. https://doi.org/10.1002/qj.3244

Dogar, M. M., Stenchikov, G., Osipov, S., Wyman, B., & Zhao, M. (2017). Sensitivity of the regional climate in the Middle East and North Africa to volcanic perturbations. *Journal of Geophysical Research*, *122*(15), 7922–7948. https://doi.org/10.1002/2017JD026783

Donat, M. G., Lowry, A. L., Alexander, L. V., O'Gorman, P. A., & Maher, N. (2016). More extreme precipitation in the worldâ €TM s dry and wet regions. *Nature Climate Change*, *6*(5), 508–513. https://doi.org/10.1038/nclimate2941

Donkor, A. K., Bonzongo, J. C., Nartey, V. K., & Adotey, D. K. (2006). Mercury in different environmental compartments of the Pra River Basin, Ghana. *Science of the Total Environment*, *368*(1), 164–176. https://doi.org/10.1016/j.scitotenv.2005.09.046

Dorleku, M. K., Nukpezah, D., & Carboo, D. (2018). Effects of small-scale gold mining on heavy metal levels in groundwater in the Lower Pra Basin of Ghana. *Applied Water Science*, *8*(5). https://doi.org/10.1007/s13201-018-0773-z

Dosio, A., & Panitz, H. J. (2016). Climate change projections for CORDEX-Africa with COSMO-CLM regional climate model and differences with the driving global climate models. *Climate Dynamics*, *46*(5–6), 1599–1625. https://doi.org/10.1007/s00382-015-2664-4

Dossou, J. F., Li, X. X., Kang, H., & Boré, A. (2021). Impact of climate change on the Oueme basin in Benin. *Global Ecology and Conservation*, *28*. https://doi.org/10.1016/j.gecco.2021.e01692

Dube, T., Dube, T., Dalu, T., Gxokwe, S., & Marambanyika, T. (2024). Assessment of land use and land cover, water nutrient and metal concentration related to illegal mining activities in an Austral semi–arid river system: A remote sensing and multivariate analysis approach. *Science of The Total Environment*, *907*, 167919. https://doi.org/10.1016/J.SCITOTENV.2023.167919

Duncan, A. E., de Vries, N., & Nyarko, K. B. (2018). Assessment of heavy metal pollution in the main Pra River and its tributaries in the Pra Basin of Ghana. *Environmental Nanotechnology, Monitoring and Management*, *10*, 264–271. https://doi.org/10.1016/j.enmm.2018.06.003

Dyrrdal, A. V., Médus, E., Dobler, A., Hodnebrog, Ø., Arnbjerg-Nielsen, K., Olsson, J., Thomassen, E. D., Lind, P., Gaile, D., & Post, P. (2023). Changes in design precipitation over the Nordic-Baltic region as given by convection-permitting climate simulations. *Weather and Climate Extremes*, *42*. https://doi.org/10.1016/j.wace.2023.100604

Enayati, M., Bozorg-Haddad, O., Bazrafshan, J., Hejabi, S., & Chu, X. (2021). Bias correction capabilities of quantile mapping methods for rainfall and temperature variables. *Journal of Water and Climate Change*, *12*(2), 401–419. https://doi.org/10.2166/wcc.2020.261

Essumang, D. K., Eshun, A., Hogarh, J. N., Bentum, J. K., Adjei, J. K., Negishi, J., Nakamichi, S., Habibullah-Al-Mamun, M., & Masunaga, S. (2017). Perfluoroalkyl acids (PFAAs) in the Pra and Kakum River basins and associated tap water in Ghana. *Science of the Total Environment*, *579*, 729–735. https://doi.org/10.1016/j.scitotenv.2016.11.035

Eyring, V., Bony, S., Meehl, G. A., Senior, C. A., Stevens, B., Stouffer, R. J., & Taylor, K. E. (2016). Overview of the Coupled Model Intercomparison Project Phase 6 (CMIP6) experimental design and organization. *Geoscientific Model Development*, *9*(5), 1937–1958. https://doi.org/10.5194/gmd-9-1937-2016

Falkenmark, M. (1989). The Massive Water Scarcity Now Threatening Africa: Why Isn't It Being Addressed? In *Source: Ambio* (Vol. 18, Issue 2).

Faramarzi, M., Abbaspour, K. C., Ashraf Vaghefi, S., Farzaneh, M. R., Zehnder, A. J. B., Srinivasan, R., & Yang, H. (2013). Modeling impacts of climate change on freshwater availability in Africa. *Journal of Hydrology*, *480*, 85–101. https://doi.org/10.1016/j.jhydrol.2012.12.016

Federal Ministry for Economic Cooperation and Development. (n.d.). Ghana. BMZ. Retrieved November 20, 2025, from https://www.bmz.de/en/countries/ghana

Field, C. B., Barros, V., Stocker, T. F., & Dahe, Q. (2012). *Managing the risks of extreme events and disasters to advance climate change adaptation: special report of the intergovernmental panel on climate change.* . Cambridge University Press.

Fisher, J. R. B., Acosta, E. A., Dennedy-Frank, P. J., Kroeger, T., & Boucher, T. M. (2018). Impact of satellite imagery spatial resolution on land use classification accuracy and modeled water quality. *Remote Sensing in Ecology and Conservation*, *4*(2), 137–149. https://doi.org/10.1002/rse2.61

Foody, G. M. (2010). Assessing the accuracy of land cover change with imperfect ground reference data. *Remote Sensing of Environment*, *114*(10), 2271–2285. https://doi.org/10.1016/j.rse.2010.05.003

Forkuor, G., Hounkpatin, O. K. L., Welp, G., & Thiel, M. (2017). High resolution mapping of soil properties using Remote Sensing variables in south-western Burkina Faso: A comparison of machine learning and multiple linear regression models. *PLoS ONE*, *12*(1). https://doi.org/10.1371/journal.pone.0170478

Fowler, H. J., Wasko, C., & Prein, A. F. (2021). Intensification of short-duration rainfall extremes and implications for flood risk: Current state of the art and future directions. In *Philosophical Transactions of the Royal Society A: Mathematical, Physical and Engineering Sciences* (Vol. 379, Issue 2195). Royal Society Publishing. https://doi.org/10.1098/rsta.2019.0541

Franzke, C. L. E. (2017). Impacts of a Changing Climate on Economic Damages and Insurance. *Economics of Disasters and Climate Change*, *1*(1), 95–110. https://doi.org/10.1007/s41885-017-0004-3

Fung, T., & LeDrew, E. (1988). For change detection using various accuracy. *Photogramm. Eng. Remote Sens 54, no. 10*, 1449–1454.

Funk, C., Peterson, P., Landsfeld, M., Pedreros, D., Verdin, J., Shukla, S., Husak, G., Rowland, J., Harrison, L., Hoell, A., & Michaelsen, J. (2015). The climate hazards infrared precipitation with stations - A new environmental record for monitoring extremes. *Scientific Data*, *2*. https://doi.org/10.1038/sdata.2015.66

Fuso, F., Bombelli, G. M., & Bocchiola, D. (2024). Ex-post assessment of climate and hydrological projections: reliability of CMPI6 outputs in Northern Italy. *Theoretical and Applied Climatology*, *155*(2), 1343–1362. https://doi.org/10.1007/s00704-023-04698-5

García-Álvarez, D., Camacho Olmedo, M. T., Van Delden, H., Mas, J. F., & Paegelow, M. (2022). Comparing the structural uncertainty and uncertainty management in four common Land Use Cover Change (LUCC) model software packages. *Environmental Modelling & Software*, *153*, 105411. https://doi.org/10.1016/J.ENVSOFT.2022.105411

Gbedzi, D. D., Ofosu, E. A., Mortey, E. M., Obiri-Yeboah, A., Nyantakyi, E. K., Siabi, E. K., Abdallah, F., Domfeh, M. K., & Amankwah-Minkah, A. (2022). Impact of mining on land use land cover change and water quality in the Asutifi North District of Ghana, West Africa. *Environmental Challenges*, *6*, 100441. https://doi.org/10.1016/J.ENVC.2022.100441

Gelete, G., Nourani, V., Gokcekus, H., & Gichamo, T. (2023). Physical and artificial intelligence-based hybrid models for rainfall–runoff–sediment process modelling. *Hydrological Sciences Journal*, *68*(13), 1841–1863. https://doi.org/10.1080/02626667.2023.2241850

Ghanim, A. A. J., Anjum, M. N., Rasool, G., Saifullah, Irfan, M., Alyami, M., Rahman, S., & Niazi, U. M. (2023). Analyzing Extreme Temperature Patterns in Subtropical Highlands Climates: Implications for Disaster Risk Reduction Strategies. *Sustainability (Switzerland)*, *15*(17). https://doi.org/10.3390/su151712753

Ghansah, B., Nyamekye, C., Owusu, S., & Agyapong, E. (2021). Mapping flood prone and Hazards Areas in rural landscape using landsat images and random forest classification: Case study of Nasia watershed in Ghana. *Cogent Engineering*, *8*(1). https://doi.org/10.1080/23311916.2021.1923384

Ghelani, R. P. S., Oliver, E. C. J., Holbrook, N. J., Wheeler, M. C., & Klotzbach, P. J. (2017). Joint Modulation of Intraseasonal Rainfall in Tropical Australia by the Madden-Julian Oscillation and El Niño-Southern Oscillation. *Geophysical Research Letters*, *44*(20), 10,754-10,761. https://doi.org/10.1002/2017GL075452

Gilmore Pontius, R., Millones, M., & Gilmore, R. (2011). Death to Kappa: Birth of quantity disagreement and allocation Death to Kappa: Birth of quantity disagreement and allocation disagreement for accuracy assessment disagreement for accuracy assessment Repository *Citation Repository Citation*. https://commons.clarku.edu/faculty_geography/760

Gomes, M. N., Jalihal, V., Castro, M., & Mendiondo, E. M. (2025). Exploring the impact of rainfall temporal distribution and critical durations on flood hazard modeling. *Natural Hazards, 121*(9), 10989–11012. https://doi.org/10.1007/s11069-025-07186-3

Gosling, S. N., Zaherpour, J., Mount, N. J., Hattermann, F. F., Dankers, R., Arheimer, B., Breuer, L., Ding, J., Haddeland, I., Kumar, R., Kundu, D., Liu, J., van Griensven, A., Veldkamp, T. I. E., Vetter, T., Wang, X., & Zhang, X. (2017). A comparison of changes in river runoff from multiple global and catchment-scale hydrological models under global warming scenarios of 1 °C, 2 °C and 3 °C. *Climatic Change*, *141*(3), 577–595. https://doi.org/10.1007/s10584-016-1773-3

Government of Ghana. (2007). *National Water Policy. Government of Ghana, Ministry of Water Resources, Works and Housing*.

Green, M. B., & Finlay, J. C. (2008). Detecting characteristic hydrological and biogeochemical signals through nonparametric scatter plot analysis of normalized data. *Water Resources Research*, *44*(8). https://doi.org/10.1029/2007WR006509

Grillakis, M. G., Koutroulis, A. G., Daliakopoulos, I. N., & Tsanis, I. K. (2017). A method to preserve trends in quantile mapping bias correction of climate modeled temperature. *Earth System Dynamics*, *8*(3), 889–900. https://doi.org/10.5194/esd-8-889-2017

Grillakis, M. G., Tsanis, I. K., & Koutroulis, A. G. (2010). Application of the HBV hydrological model in a flash flood case in Slovenia. *Natural Hazards and Earth System Science*, *10*(12), 2713–2725. https://doi.org/10.5194/nhess-10-2713-2010

Grose, M. R., Narsey, S., Delage, F. P., Dowdy, A. J., Bador, M., Boschat, G., Chung, C., Kajtar, J. B., Rauniyar, S., Freund, M. B., Lyu, K., Rashid, H., Zhang, X., Wales, S., Trenham, C., Holbrook, N. J., Cowan, T., Alexander, L., Arblaster, J. M., & Power, S. (2020). Insights From CMIP6 for Australia's Future Climate. *Earth's Future*, *8*(5). https://doi.org/10.1029/2019EF001469

Guidigan, M. L. G., Sanou, C. L., Ragatoa, D. S., Fafa, C. O., & Mishra, V. N. (2019). Assessing Land Use/Land Cover Dynamic and Its Impact in Benin Republic Using Land Change Model and CCI-LC Products. *Earth Systems and Environment*, *3*(1), 127–137. https://doi.org/10.1007/s41748-018-0083-5

Guo, D., & Wang, H. (2016). Comparison of a very-fine-resolution GCM with RCM dynamical downscaling in simulating climate in China. *Advances in Atmospheric Sciences*, *33*(5), 559–570. https://doi.org/10.1007/s00376-015-5147-y

Gupta, H. V., Kling, H., Yilmaz, K. K., & Martinez, G. F. (2009). Decomposition of the mean squared error and NSE performance criteria: Implications for improving hydrological modelling. *Journal of Hydrology*, *377*(1–2), 80–91. https://doi.org/10.1016/j.jhydrol.2009.08.003

Gupta, V., Singh, V., & Jain, M. K. (2020). Assessment of precipitation extremes in India during the 21st century under SSP1-1.9 mitigation scenarios of CMIP6 GCMs. *Journal of Hydrology*, *590*. https://doi.org/10.1016/j.jhydrol.2020.125422

Guttman, N. B. (1998). Comparing the palmer drought index and the standardized precipitation index'. In *Journal of the American Water Resources Association* (Vol. 34).

Gyamfi, C., Tindan, J. Z. O., & Kifanyi, G. E. (2021). Evaluation of CORDEX Africa multi-model precipitation simulations over the Pra River Basin, Ghana. *Journal of Hydrology: Regional Studies*, *35*. https://doi.org/10.1016/j.ejrh.2021.100815

Hakala, K., Addor, N., & Seibert, J. (2018). Hydrological modeling to evaluate climate model simulations and their bias correction. *Journal of Hydrometeorology*, *19*(8), 1321–1337. https://doi.org/10.1175/JHM-D-17-0189.1

Hamdy, O., Zhao, S., A. Salheen, M., & Eid, Y. Y. (2017). Analyses the Driving Forces for Urban Growth by Using IDRISI®Selva Models Abouelreesh - Aswan as a Case Study. *International Journal of Engineering and Technology*, *9*(3), 226–232. https://doi.org/10.7763/IJET.2017.V9.975

Hassan, Z., Shamsudin, S., & Harun, S. (2015). *Jurnal Teknologi Full Paper. Choosing the best fit distribution for rainfall event characteristics based on 6h-ietd within peninsular Malaysia* (Vol. 75). www.jurnalteknologi.utm.my

Haszpra, T., Herein, M., & Bodai, T. (2020). Investigating ENSO and its teleconnections under climate change in an ensemble view - A new perspective. *Earth System Dynamics*, *11*(1), 267–280. https://doi.org/10.5194/esd-11-267-2020

He, Z., Liu, H., Wang, Y., & Hu, J. (2017). Generative adversarial networks-based semi-supervised learning for hyperspectral image classification. *Remote Sensing*, *9*(10). https://doi.org/10.3390/rs9101042

Hegazy, I. R., & Kaloop, M. R. (2015). Monitoring urban growth and land use change detection with GIS and remote sensing techniques in Daqahlia governorate Egypt. *International Journal of Sustainable Built Environment*, *4*(1), 117–124. https://doi.org/10.1016/j.ijsbe.2015.02.005

Hengl, T., Heuvelink, G. B. M., Kempen, B., Leenaars, J. G. B., Walsh, M. G., Shepherd, K. D., Sila, A., MacMillan, R. A., De Jesus, J. M., Tamene, L., & Tondoh, J. E. (2015). Mapping soil properties of Africa at 250 m resolution: Random forests significantly improve current predictions. *PLoS ONE*, *10*(6). https://doi.org/10.1371/journal.pone.0125814

Her, Y., Yoo, S. H., Cho, J., Hwang, S., Jeong, J., & Seong, C. (2019). Uncertainty in hydrological analysis of climate change: multi-parameter vs. multi-GCM ensemble predictions. *Scientific Reports*, *9*(1). https://doi.org/10.1038/s41598-019-41334-7

Hernandez, D., Mendoza, P. A., Boisier, J. P., & Ricchetti, F. (2022). Hydrologic Sensitivities and ENSO Variability Across Hydrological Regimes in Central Chile (28°–41°S). *Water Resources Research*, *58*(9). https://doi.org/10.1029/2021WR031860

Hersbach, H., Bell, B., Berrisford, P., Hirahara, S., Horányi, A., Muñoz-Sabater, J., Nicolas, J., Peubey, C., Radu, R., Schepers, D., Simmons, A., Soci, C., Abdalla, S., Abellan, X., Balsamo, G., Bechtold, P., Biavati, G., Bidlot, J., Bonavita, M., … Thépaut, J. N. (2020). The ERA5 global

reanalysis. *Quarterly Journal of the Royal Meteorological Society*, *146*(730), 1999–2049. https://doi.org/10.1002/qj.3803

Höllermann, B., & Evers, M. (2017). Perception and handling of uncertainties in water management—A study of practitioners' and scientists' perspectives on uncertainty in their daily decision-making. *Environmental Science and Policy*, *71*, 9–18. https://doi.org/10.1016/j.envsci.2017.02.003

Höllermann, B., Giertz, S., & Diekkrüger, B. (2010). Benin 2025-Balancing Future Water Availability and Demand Using the WEAP "Water Evaluation and Planning" System. *Water Resources Management*, *24*(13), 3591–3613. https://doi.org/10.1007/s11269-010-9622-z

Houghton, J. (2000). The IPCC report 2001. *In The Solar Cycle and Terrestrial Climate, Solar and Space Weather*.

Hounkpè, J., & Diekkrüger, B. (2018). Challenges in calibrating hydrological models to simultaneously evaluate water resources and flood hazard: A case study of Zou basin, Benin. *Episodes*, *41*(2), 105–114. https://doi.org/10.18814/epiiugs/2018/018010

Hounkpè, J., Badou, D. F., Ahouansou, D. M. M., Totin, E., & Sintondji, L. O. C. (2022). Assessing observed and projected flood vulnerability under climate change using multi-modeling statistical approaches in the Ouémé River Basin, Benin (West Africa). *Regional Environmental Change*, *22*(4). https://doi.org/10.1007/s10113-022-01957-5

Hounkpè, J., Diekkrüger, B., Afouda, A. A., & Sintondji, L. O. C. (2019). Land use change increases flood hazard: a multi-modelling approach to assess change in flood characteristics driven by socio-economic land use change scenarios. *Natural Hazards*, *98*(3), 1021–1050. https://doi.org/10.1007/s11069-018-3557-8

Hounkpè, J., Merz, B., Badou, F. D., Bossa, A. Y., Yira, Y., & Lawin, E. A. (2022). Potential for seasonal flood forecasting in West Africa using climate indexes. *Journal of Flood Risk Management*. https://doi.org/10.1111/jfr3.12833

Howe, P. D., Marlon, J. R., Wang, X., & Leiserowitz, A. (2019). Public perceptions of the health risks of extreme heat across US states, counties, and neighborhoods. *PNAS*, *116*(14), 6743–6748. https://doi.org/10.26078/yr9w-n861).y

Hsu, H., Lo, M. H., Guillod, B. P., Miralles, D. G., & Kumar, S. (2017). Relation between precipitation location and antecedent/ subsequent soil moisture spatial patterns. *Journal of Geophysical Research*, *122*(12), 6319–6328. https://doi.org/10.1002/2016JD026042

Huang, J., Zhang, J., Zhang, Z., Xu, C. Y., Wang, B., & Yao, J. (2011). Estimation of future precipitation change in the Yangtze River basin by using statistical downscaling method. *Stochastic Environmental Research and Risk Assessment*, *25*(6), 781–792. https://doi.org/10.1007/s00477-010-0441-9

Huang, S., Shah, H., Naz, B. S., Shrestha, N., Mishra, V., Daggupati, P., Ghimire, U., & Vetter, T. (2020). Impacts of hydrological model calibration on projected hydrological changes under climate change—a multi-model assessment in three large river basins. *Climatic Change*, *163*(3), 1143–1164. https://doi.org/10.1007/s10584-020-02872-6

Hutchinson, C. F. (1982). *Techniques for Combining Landsat and Ancillary Data for Digital Classification improvement.*

Irizarry, R. A. (2001). Local regression with meaningful parameters. *American Statistician*, *55*(1), 72–79. https://doi.org/10.1198/000313001300339969

Jajarmizad, M., Harun, S., & Salarpour, M. (2012). A Review on Theoretical Consideration and Types of Models in Hydrology. . *Journal of Environmental Science and Technology. 5(5), 249–261*.

Jankowska, M. M., Lopez-Carr, D., Funk, C., Husak, G. J., & Chafe, Z. A. (2012). Climate change and human health: Spatial modeling of water availability, malnutrition, and livelihoods in Mali, Africa. *Applied Geography*, *33*(1), 4–15. https://doi.org/10.1016/j.apgeog.2011.08.009

Janssen, T. M. V., & Partee, B. H. (1997). Compositionality. *Handbook of Logic and Language*, 417–473. https://doi.org/10.1016/B978-044481714-3/50011-4

Jaramillo, S., Graterol, E., & Pulver, E. (2020). Sustainable Transformation of Rainfed to Irrigated Agriculture Through Water Harvesting and Smart Crop Management Practices. *Frontiers in Sustainable Food Systems*, *4*. https://doi.org/10.3389/fsufs.2020.437086

Kamruzzaman, M., Shahid, S., Towfiqul Islam, A., Hwang, S., Cho, J., Asad Uz Zaman, M., Ahmed, M., Mizanur Rahman, M., Belal Hossain, M., & Shahid sshahid, S. (2021). *Comparison of CMIP6 and CMIP5 model performance in simulating historical precipitation and temperature in Bangladesh: a preliminary study*. https://doi.org/10.1007/s00704-021-03691-0/Published

Kankam-Yeboah, K., Obuobie, E., Amisigo, B., & Opoku-Ankomah, Y. (2013). Impact du changement climatique sur les débits de plusieurs bassins au Ghana. *Hydrological Sciences Journal*, *58*(4), 773–788. https://doi.org/10.1080/02626667.2013.782101

Katiraie-Boroujerdy, P. S., Naeini, M. R., Asanjan, A. A., Chavoshian, A., Hsu, K. lin, & Sorooshian, S. (2020). Bias correction of satellite-based precipitation estimations using quantile mapping approach in different climate regions of Iran. *Remote Sensing*, *12*(13). https://doi.org/10.3390/rs12132102

Katzenberger, A., Schewe, J., Pongratz, J., & Levermann, A. (2021). Robust increase of Indian monsoon rainfall and its variability under future warming in CMIP6 models. *Earth System Dynamics*, *12*(2), 367–386. https://doi.org/10.5194/esd-12-367-2021

Kettle, N. P., Walsh, J. E., Heaney, L., Thoman, R. L., Redilla, K., & Carroll, L. (2020). Integrating archival analysis, observational data, and climate projections to assess extreme event impacts in Alaska. *Climatic Change*, *163*(2), 669–687. https://doi.org/10.1007/s10584-020-02907-y

Kim, C. (2016). Land use classification and land use change analysis using satellite images in Lombok Island, Indonesia. *Forest Science and Technology*, *12*(4), 183–191. https://doi.org/10.1080/21580103.2016.1147498

Kim, C., & Kim, D. H. (2020). Effects of rainfall spatial distribution on the relationship between rainfall spatiotemporal resolution and runoff prediction accuracy. *Water (Switzerland)*, *12*(3). https://doi.org/10.3390/w12030846

Kim, Y. H., Min, S. K., Zhang, X., Sillmann, J., & Sandstad, M. (2020). Evaluation of the CMIP6 multi-model ensemble for climate extreme indices. *Weather and Climate Extremes*, *29*. https://doi.org/10.1016/j.wace.2020.100269

Klubi, E., Abril, J. M., Nyarko, E., & Delgado, A. (2018). Impact of gold-mining activity on trace elements enrichment in the West African estuaries: The case of Pra and Ankobra rivers with the Volta estuary (Ghana) as the reference. *Journal of Geochemical Exploration*, *190*, 229–244. https://doi.org/10.1016/j.gexplo.2018.03.014

Klubi, E., Abril, J. M., Nyarko, E., Laissaoui, A., & Benmansour, M. (2017). Radioecological assessment and radiometric dating of sediment cores from dynamic sedimentary systems of Pra and Volta estuaries (Ghana) along the Equatorial Atlantic. *Journal of Environmental Radioactivity*, *178–179*, 116–126. https://doi.org/10.1016/j.jenvrad.2017.08.001

Knighton, J., Kuppel, S., Smith, A., Soulsby, C., Sprenger, M., & Tetzlaff, D. (2020). Using isotopes to incorporate tree water storage and mixing dynamics into a distributed ecohydrologic modelling framework. *Ecohydrology*, *13*(3). https://doi.org/10.1002/eco.2201

Koch, J., Berger, H., Henriksen, H. J., & Sonnenborg, T. O. (2019). Modelling of the shallow water table at high spatial resolution using random forests. *Hydrology and Earth System Sciences*, *23*(11), 4603–4619. https://doi.org/10.5194/hess-23-4603-2019

Kortei, N. K., Heymann, M. E., Essuman, E. K., Kpodo, F. M., Akonor, P. T., Lokpo, S. Y., Boadi, N. O., Ayim-Akonor, M., & Tettey, C. (2020). Health risk assessment and levels of toxic metals in fishes (Oreochromis noliticus and Clarias anguillaris) from Ankobrah and Pra basins: Impact of illegal mining activities on food safety. *Toxicology Reports*, *7*, 360–369. https://doi.org/10.1016/j.toxrep.2020.02.011

Koudahe, K., Kayode, A. J., Samson, A. O., Adebola, A. A., & Djaman, K. (2017). Trend Analysis in Standardized Precipitation Index and Standardized Anomaly Index in the Context of Climate Change in Southern Togo. *Atmospheric and Climate Sciences*, *07*(04), 401–423. https://doi.org/10.4236/acs.2017.74030

Kuhn, M., & Johnson, K. (2013). *Applied Predictive Modeling*. https://doi.org/10.1007/978-1-4614-6849-3

Kumar, R., Saxena, S., Kumar, V., Prabha, V., Kumar, R., & Kukreti, A. (2024). Service innovation research: a bibliometric analysis using VOSviewer. *Competitiveness Review*, *34*(4).

Kunstmann, H., Schneider, K., Forkel, R., & Knoche, R. (2004). Impact analysis of climate change for an Alpine catchment using high resolution dynamic downscaling of ECHAM4 time slices. In *Hydrology and Earth System Sciences* (Vol. 8, Issue 6).

Kuppel, S., Tetzlaff, D., Maneta, M. P., & Soulsby, C. (2018a). EcH2O-iso 1.0: Water isotopes and age tracking in a process-based, distributed ecohydrological model. *Geoscientific Model Development*, *11*(7), 3045–3069. https://doi.org/10.5194/gmd-11-3045-2018

Kuppel, S., Tetzlaff, D., Maneta, M. P., & Soulsby, C. (2018b). What can we learn from multi-data calibration of a process-based ecohydrological model? *Environmental Modelling and Software*, *101*, 301–316. https://doi.org/10.1016/j.envsoft.2018.01.001

Kusimi, J. M., Yiran, G. A. B., & Attua, E. M. (2015). Soil Erosion and Sediment Yield Modelling in the Pra River Basin of Ghana using the Revised Universal Soil Loss Equation (RUSLE). *Ghana Journal of Geography*, *7*(2), 38–57.

Lambin, E. F., Geist, H. J., & Lepers, E. (2003). Dynamics of land-use and land-cover change in tropical regions. *Annual Review of Environment and Resources*, *28*, 205–241. https://doi.org/10.1146/annurev.energy.28.050302.105459

Lange, S., Volkholz, J., Geiger, T., Zhao, F., Vega, I., Veldkamp, T., Reyer, C. P. O., Warszawski, L., Huber, V., Jägermeyr, J., Schewe, J., Bresch, D. N., Büchner, M., Chang, J., Ciais, P., Dury, M., Emanuel, K., Folberth, C., Gerten, D., … Frieler, K. (2020). Projecting Exposure to Extreme Climate Impact Events Across Six Event Categories and Three Spatial Scales. *Earth's Future*, *8*(12). https://doi.org/10.1029/2020EF001616

Lavaysse, C., Diedhiou, A., Laurent, H., & Lebel, T. (2006). African Easterly Waves and convective activity in wet and dry sequences of the West African Monsoon. *Climate Dynamics*, *27*(2–3), 319–332. https://doi.org/10.1007/s00382-006-0137-5

Lawin, A. E., Yèkambèssoun, N. T. M., & Biaou, C. A. (2019). *Mid-Century Daily Discharge Scenarios Based on Climate and Land Use Change in Ouémé River Basin at Bétérou Outlet*. 1–14.

Lennard, C. J., Nikulin, G., Dosio, A., & Moufouma-Okia, W. (2018). On the need for regional climate information over Africa under varying levels of global warming. In *Environmental Research Letters* (Vol. 13, Issue 6). Institute of Physics Publishing. https://doi.org/10.1088/1748-9326/aab2b4

Leta, M. K., Demissie, T. A., & Tränckner, J. (2021). Modeling and prediction of land use land cover change dynamics based on land change modeler (Lcm) in nashe watershed, upper blue nile basin, Ethiopia. *Sustainability (Switzerland)*, *13*(7). https://doi.org/10.3390/su13073740

Leube, A., Hirdes, W., Mauer, R., & Kesse, G. O. (1990). The early Proterozoic Birimian Supergroup of Ghana and some aspects of its associated gold mineralization. In *Precambrian Research* (Vol. 46).

Li, J., Linyi, L., Yanjiao, S., Jiaming, C., Zhe, W., Yi, B., Wen, Z., & Lingkui, M. (2023). A robust large-scale surface water mapping framework with high spatiotemporal resolution based on the fusion of multi-source remote sensing data. *International Journal of Applied Earth Observation and Geoinformation*, *118*.

Li, X., Ling, F., Cai, X., Ge, Y., Li, X., Yin, Z., Shang, C., Jia, X., & Du, Y. (2021). Mapping water bodies under cloud cover using remotely sensed optical images and a spatiotemporal dependence model. *International Journal of Applied Earth Observation and Geoinformation*, *103*(p. 102470).

Libanda, B., & Ngonga, C. (2018). Projection of frequency and intensity of extreme precipitation in Zambia: A CMIP5 study. *Climate Research*, *76*(1), 59–72. https://doi.org/10.3354/cr01528

Lieber, R., King, A., Brown, J., Ashcroft, L., Freund, M., & McMichael, C. (2022). ENSO Teleconnections More Uncertain in Regions of Lower Socioeconomic Development. In

Geophysical Research Letters (Vol. 49, Issue 21). John Wiley and Sons Inc. https://doi.org/10.1029/2022GL100553

Lillesand, T., Kiefer, R. W., & Chipman, J. (2015). *Remote sensing and image interpretation* (7th ed.). John Wiley & Sons.

Lin, L., Sills, E., & Cheshire, H. (2014). Targeting areas for Reducing Emissions from Deforestation and forest Degradation (REDD+) projects in Tanzania. *Global Environmental Change*, *24*(1), 277–286. https://doi.org/10.1016/j.gloenvcha.2013.12.003

Lobo, F., Costa, M., Novo, E., & Telmer, K. (2016). Distribution of Artisanal and Small-Scale Gold Mining in the Tapajós River Basin (Brazilian Amazon) over the Past 40 Years and Relationship with Water Siltation. *Remote Sensing*, *8*(7), 579. https://doi.org/10.3390/rs8070579

Loh, Y. S. A., Fynn, O. F., Manu, E., Afrifa, G. Y., Addai, M. O., Akurugu, B. A., & Yidana, S. M. (2022). Groundwater - surface water interactions: application of hydrochemical and stable isotope tracers to the lake bosumtwi area in Ghana. *Environmental*

Losada, T., Rodriguez-Fonseca, B., Mohino, E., Bader, J., Janicot, S., & Mechoso, C. R. (2012). Tropical SST and Sahel rainfall: A non-stationary relationship. *Geophysical Research Letters*, *39*(12). https://doi.org/10.1029/2012GL052423

Luna-Aranguré, C., Estrada, F., Velasco, J. A., Calderón-Bustamante, O., & Gonzalez-Salazar, C. (2025). Environmental exposure of terrestrial biomes to global climate change: An n-dimensional approach. *Ecosphere*, *16*(5). https://doi.org/10.1002/ecs2.70262

Madsen, H., Lawrence, D., Lang, M., Martinkova, M., & Kjeldsen, T. R. (2014). Review of trend analysis and climate change projections of extreme precipitation and floods in Europe. *Journal of Hydrology*, *519*(PD), 3634–3650. https://doi.org/10.1016/j.jhydrol.2014.11.003

Magang, D. S., Ojara, M. A., Yunsheng, L., & King'uza, P. H. (2024). Future climate projection across Tanzania under CMIP6 with high-resolution regional climate model. *Scientific Reports*, *14*(1). https://doi.org/10.1038/s41598-024-63495-w

Mann, H. B. (1945). *Nonparametric Tests Against Trend* (Vol. 13, Issue 3). https://www.jstor.org/stable/1907187

Manu, E., Kühn, M., Kempka, T., Goldberg, T., Vieth-Hillebrand, A., & Rach, O. (2021). *Hydrogeochemical modelling of origin, evolution and mechanisms controlling water resources quality in the Pra Basin (Ghana)*. https://doi.org/10.5194/egusphere-egu21-7800

Maraun, D. (2013). Bias correction, quantile mapping, and downscaling: Revisiting the inflation issue. *Journal of Climate*, *26*(6), 2137–2143. https://doi.org/10.1175/JCLI-D-12-00821.1

Markscheffel, B., & Schröter, F. (2021). Comparison of two science mapping tools based on software technical evaluation and bibliometric case studies. *COLLNET Journal of Scientometrics and Information Management*, *15*(2).

Mason, S. J., Waylen, P. R., Mimmack, G. M., Rajaratnam, B., & Harrison, J. M. (1999). *Changes in Extreme Rainfall Events in South Africa*.

Maxwell, A. E., Warner, T. A., & Fang, F. (2018). Implementation of machine-learning classification in remote sensing: An applied review. In *International Journal of Remote Sensing* (Vol. 39, Issue 9, pp. 2784–2817). Taylor and Francis Ltd. https://doi.org/10.1080/01431161.2018.1433343

Maybee, B., Ward, N., Hirons, L. C., & Marsham, J. H. (2023). Importance of Madden–Julian oscillation phase to the interannual variability of East African rainfall. *Atmospheric Science Letters*, *24*(5). https://doi.org/10.1002/asl.1148

McNicol, I. M., Ryan, C. M., & Mitchard, E. T. A. (2018). Carbon losses from deforestation and widespread degradation offset by extensive growth in African woodlands. *Nature Communications*, *9*(1). https://doi.org/10.1038/s41467-018-05386-z

Mcsweeney, C., New, M., Lizcano, G., & Lu, X. (2010). American Meteorological Society The UNDP Climate Change Country Profiles: Improving the Accessibility of Observed and Projected Climate Information for Studies of Climate Change in Developing Countries. *Source: Bulletin of the American Meteorological Society*, *91*(2), 157–166. https://doi.org/10.2307/26232858

Mensah, J. K., Ofosu, E. A., Akpoti, K., Kabo-Bah, A. T., Okyereh, S. A., & Yidana, S. M. (2022). Modeling current and future groundwater demands in the White Volta River Basin of Ghana under climate change and socio-economic scenarios. *Journal of Hydrology: Regional Studies*, *41*. https://doi.org/10.1016/j.ejrh.2022.101117

Meresa, H. K., & Gatachew, M. T. (2019). Climate change impact on river flow extremes in the upper blue nile river basin. *Journal of Water and Climate Change*, *10*(4), 759–781. https://doi.org/10.2166/wcc.2018.154

Momeni, R., Aplin, P., & Boyd, D. S. (2016). Mapping complex urban land cover from spaceborne imagery: The influence of spatial resolution, spectral band set and classification approach. *Remote Sensing*, *8*(2). https://doi.org/10.3390/rs8020088

Montanari, A., Young, G., Savenije, H. H. G., Hughes, D., Wagener, T., Ren, L. L., Koutsoyiannis, D., Cudennec, C., Toth, E., Grimaldi, S., Blöschl, G., Sivapalan, M., Beven, K., Gupta, H., Hipsey, M., Schaefli, B., Arheimer, B., Boegh, E., Schymanski, S. J., … Belyaev, V. (2013). "Panta Rhei-Everything Flows": Change in hydrology and society-The IAHS Scientific Decade 2013-2022. *Hydrological Sciences Journal*, *58*(6), 1256–1275. https://doi.org/10.1080/02626667.2013.809088

Mu, J., Huang, M., Hao, X., Chen, X., Yu, H., & Wu, B. (2022). Study on Waterlogging Reduction Effect of LID Facilities in Collapsible Loess Area Based on Coupled 1D and 2D Hydrodynamic Model. *Water (Switzerland)*, *14*(23). https://doi.org/10.3390/w14233880

Ndehedehe, C. E., Agutu, N. O., Ferreira, V. G., & Getirana, A. (2020). Evolutionary drought patterns over the Sahel and their teleconnections with low frequency climate oscillations. *Atmospheric Research*, *233*. https://doi.org/10.1016/j.atmosres.2019.104700

Ngoma, H., Ayugi, B., Onyutha, C., Babaousmail, H., Lim Kam Sian, K. T. C., Iyakaremye, V., Mumo, R., & Ongoma, V. (2022). Projected changes in rainfall over Uganda based on CMIP6 models. *Theoretical and Applied Climatology*, *149*(3–4), 1117–1134. https://doi.org/10.1007/s00704-022-04106-4

Ni, Y., & Hsu, P. C. (2018). Inter-annual variability of global monsoon precipitation in present-day and future warming scenarios based on 33 Coupled Model Intercomparison Project Phase 5 models. *International Journal of Climatology*, *38*(13), 4875–4890. https://doi.org/10.1002/joc.5704

Nicholson, S. E., & Grist, J. P. (2001). A conceptual model for understanding rainfall variability in the West African Sahel on interannual and interdecadal timescales. *International Journal of Climatology*, *21*(14), 1733–1757. https://doi.org/10.1002/joc.648

Nikulin, G., Lennard, C., Dosio, A., Kjellström, E., Chen, Y., Hansler, A., Kupiainen, M., Laprise, R., Mariotti, L., Maule, C. F., Van Meijgaard, E., Panitz, H. J., Scinocca, J. F., & Somot, S. (2018). The effects of 1.5 and 2 degrees of global warming on Africa in the CORDEX ensemble. *Environmental Research Letters*, *13*(6). https://doi.org/10.1088/1748-9326/aab1b1

Ningrum, W., Apip, & Narulita, I. (2024). Comparison of the application of HBV and HEC-HMS hydrology models for accessing climate change in the upper Citarum Watershed, Indonesia. *IOP Conference Series: Earth and Environmental Science*, *1314*(1). https://doi.org/10.1088/1755-1315/1314/1/012072

Nounangnonhou, T. C., Acakpovi, A., Lokonon, B. E., & Sanya, A. E. (2018). Modelling and Prediction of Ouémé (Benin) River Flows by 2040 based on GR2M Approach. Larhyss . *Journal. 33(2018), 71–91*.

Nsiah, J. J., Gyamfi, C., Anornu, G. K., & Odai, S. N. (2021). Estimating the spatial distribution of evapotranspiration within the Pra River Basin of Ghana. *Heliyon*, *7*(4). https://doi.org/10.1016/j.heliyon.2021.e06828

Nyadzi, E., Bessah, E., Kranjac-Berisavljevic, G., & Ludwig, F. (2021). Hydro-climatic and land use/cover changes in Nasia catchment of the White Volta basin in Ghana. *Theoretical and Applied Climatology*, *146*(3–4), 1297–1314. https://doi.org/10.1007/s00704-021-03772-0

O'Neill, B. C., Tebaldi, C., Van Vuuren, D. P., Eyring, V., Friedlingstein, P., Hurtt, G., Knutti, R., Kriegler, E., Lamarque, J. F., Lowe, J., Meehl, G. A., Moss, R., Riahi, K., & Sanderson, B. M. (2016). The Scenario Model Intercomparison Project (ScenarioMIP) for CMIP6. *Geoscientific Model Development*, *9*(9), 3461–3482. https://doi.org/10.5194/gmd-9-3461-2016

Obodai, J., Adjei, K. A., Odai, S. N., & Lumor, M. (2019). Land use/land cover dynamics using landsat data in a gold mining basin-the Ankobra, Ghana. *Remote Sensing Applications: Society and Environment*, *13*, 247–256. https://doi.org/10.1016/J.RSASE.2018.10.007

Odusanya, A. E., Schulz, K., Biao, E. I., Degan, B. A. S., & Mehdi-Schulz, B. (2021). Evaluating the performance of streamflow simulated by an eco-hydrological model calibrated and validated with global land surface actual evapotranspiration from remote sensing at a catchment scale in West Africa. *Journal of Hydrology: Regional Studies. 37*.

Okpara, J. N. , & Tarhule, A. (2015). Evaluation of Drought Indices in the Niger Basin, West Africa1. *Journal of Geography and Earth Sciences*, *3*(2). https://doi.org/10.15640/jges.v3n2a1

Okpara, J. N., Afiesimama, E. A., Anuforom, A. C., Owino, A., & Ogunjobi, K. O. (2017). The applicability of Standardized Precipitation Index: drought characterization for early warning system and weather index insurance in West Africa. *Natural Hazards*, *89*(2), 555–583. https://doi.org/10.1007/s11069-017-2980-6

Okyere, I. (2018). *Influence of diurnal tides and other physico-chemical factors on the assemblage and diversity of fish species in River Pra Estuary, Ghana*. https://www.researchgate.net/publication/325286408

Okyere, I., & Nortey, D. D. N. (2018). *Assessment of the Ecological Health Status of River Pra Estuary (Ghana) and Adjoining Wetland using Physico-chemical Conditions and Macroinvertebrate Bioindicators Women Shellfishers and Food Security Project-West Africa View project 1. Sustainable Fisheries Management Project View project*. https://www.researchgate.net/publication/330637459

Olofintoye, O. O., Ayanshola, A. M., Salami, A. W., Idrissiou, A., Iji, J. O., & Adeleke, O. O. (2022). A Study on the Applicability of a Swat Model in Predicting the Water Yield and Water Balance of the Upper Ouémé Catchment in the Republic of Benin. *Slovak Journal of Civil Engineering*, *30*(1), 57–66. https://doi.org/10.2478/sjce-2022-0007

Olofintoye, O. O., Ayanshola, A. M., Salami, A. W., Idrissiou, A., Iji, J. O., & Adeleke, O. O. (2022). A Study on the Applicability of a Swat Model in Predicting the Water Yield and Water Balance of the Upper Ouémé Catchment in the Republic of Benin. *Slovak Journal of Civil Engineering*, *30*(1), 57–66. https://doi.org/10.2478/sjce-2022-0007

Ongoma, V., Chena, H., & Gaoa, C. (2018). Projected changes in mean rainfall and temperature over east Africa based on CMIP5 models. *International Journal of Climatology*, *38*(3), 1375–1392. https://doi.org/10.1002/joc.5252

Oppong, S. O. B., Voegborlo, R. B., Agorku, S. E., & Adimado, A. A. (2010). Total Mercury in fish, sediments and soil from the River Pra Basin, Southwestern Ghana. *Bulletin of Environmental Contamination and Toxicology*, *85*(3), 324–329. https://doi.org/10.1007/s00128-010-0059-0

Oriakhi, O., Okonofua, E. S., Oriakhi, O., & Okonofua, E. S. (2021). Biogas Generation Using Solid Waste View project Determination of Area and Volume from Dredge Geodata Set View project Advective Particle Transport Modelling of Potential Contaminated Source Sites in the Lower Pra Basin of Ghana Article Information Abstract. In *Nigerian Research Journal of Engineering and Environmental Sciences* (Vol. 6, Issue 1). https://www.researchgate.net/publication/359380888

Osei, B., & Amoakowaah, M. (2021). *The Study of Atmospheric Dynamics on Rainfall and Spells over Pra Catchment of Ghana*.

Osei, M. A., Amekudzi, L. K., & Quansah, E. (2021). Characterisation of wet and dry spells and associated atmospheric dynamics at the Pra River catchment of Ghana, West Africa. *Journal of Hydrology: Regional Studies*, *34*, 100801. https://doi.org/10.1016/J.EJRH.2021.100801

Osei, M. A., Amekudzi, L. K., Wemegah, D. D., Preko, K., Gyawu, E. S., & Obiri-Danso, K. (2019). The impact of climate and land-use changes on the hydrological processes of Owabi catchment from SWAT analysis. *Journal of Hydrology: Regional Studies*, *25*. https://doi.org/10.1016/j.ejrh.2019.100620

Oti, J. O., Kabo-bah, A. T., & Ofosu, E. (2020). Hydrologic response to climate change in the Densu River Basin in Ghana. *Heliyon*, *6*(8). https://doi.org/10.1016/j.heliyon.2020.e04722

Owusu, C., Adjei, K. A., & Odai, S. N. (2019). Evaluation of Satellite Rainfall Estimates in the Pra Basin of Ghana. *Environmental Processes*, *6*(1), 175–190. https://doi.org/10.1007/s40710-018-0344-1

Owusu, G., Owusu, A. B., Amankwaa, E. F., & Eshun, F. (2017). Analyses of freshwater stress with a couple ground and surface water model in the Pra Basin, Ghana. *Applied Water Science*, *7*(1), 137–153. https://doi.org/10.1007/s13201-015-0279-x

Owusu, K., & Waylen, P. (2009). *Trends in spatio-temporal variability in annual rainfall in Ghana (1951-2000)* (Vol. 64, Issue 5). www.meteo.gov.gh/

Owusu, K., & Waylen, P. R. (2013). The changing rainy season climatology of mid-Ghana. *Theoretical and Applied Climatology*, *112*(3–4), 419–430. https://doi.org/10.1007/s00704-012-0736-5

Özerol, G., Vinke-De Kruijf, J., Brisbois, M. C., Flores, C. C., Deekshit, P., Girard, C., Knieper, C., Mirnezami, S. J., Ortega-Reig, M., Ranjan, P., Schröder, N. J. S., & Schröter, B. (2018). Comparative studies of water governance: A systematic review. *Ecology and Society*, *23*(4). https://doi.org/10.5751/ES-10548-230443

Padial-Iglesias, M., Serra, P., Ninyerola, M., & Pons, X. (2021). A framework of filtering rules over ground truth samples to achieve higher accuracy in land cover maps. *Remote Sensing*, *13*(14). https://doi.org/10.3390/rs13142662

Page, M. J., McKenzie, J. E., Bossuyt, P. M., Boutron, I., Hoffmann, T. C., Mulrow, C. D., Shamseer, L., Tetzlaff, J. M., Akl, E. A., Brennan, S. E., Chou, R., Glanville, J., Grimshaw, J. M., Hróbjartsson, A., Lalu, M. M., Li, T., Loder, E. W., Mayo-Wilson, E., McDonald, S., … Moher, D. (2021). The PRISMA 2020 statement: An updated guideline for reporting systematic reviews. *International Journal of Surgery*, *88*. https://doi.org/10.1016/j.ijsu.2021.105906

Pal, L., Ojha, C. S. P., Chandniha, S. K., & Kumar, A. (2019). Regional scale analysis of trends in rainfall using nonparametric methods and wavelet transforms over a semi-arid region in India. *International Journal of Climatology*, *39*(5), 2737–2764. https://doi.org/10.1002/joc.5985

Patakamuri, S. K., Muthiah, K., & Sridhar, V. (2020). Long-Term homogeneity, trend, and change-point analysis of rainfall in the arid district of ananthapuramu, Andhra Pradesh State, India. *Water (Switzerland)*, *12*(1). https://doi.org/10.3390/w12010211

Pearson, K., & Lee, A. (1903). Biometrika Trust On the Laws of Inheritance in Man: I. Inheritance of Physical Characters. In *Source: Biometrika* (Vol. 2, Issue 4).

Peng, S., Wang, C., Li, Z., Mihara, K., Kuramochi, K., Toma, Y., & Hatano, R. (2023). Climate change multi-model projections in CMIP6 scenarios in Central Hokkaido, Japan. *Scientific Reports*, *13*(1). https://doi.org/10.1038/s41598-022-27357-7

Penman, Jim. (2003). *Good practice guidance for land use, land-use change and forestry*. Published by the Institute for Global Environmental Strategies for the IPCC.

Pitman, W. V., & Bailey, A. K. (2021). Can chirps fill the gap left by the decline in the availability of rainfall stations in southern africa? *Water SA*, *47*(2). https://doi.org/10.17159/wsa/2021.v47.i2.10912

Pluchinotta, I., Pagano, A., Giordano, R., & Tsoukiàs, A. (2018). A system dynamics model for supporting decision-makers in irrigation water management. *Journal of Environmental Management*, *223*, 815–824. https://doi.org/10.1016/j.jenvman.2018.06.083

Pontius, G. R., & Malanson, J. (2005). Comparison of the structure and accuracy of two land change models. *International Journal of Geographical Information Science*, *19*(2), 243–265. https://doi.org/10.1080/13658810410001713434

Quansah, E., Amekudzi, L. K., Preko, K., Aryee, J., Boakye, O. R., Boli, D., & Salifu, M. R. (2014). Empirical Models for Estimating Global Solar Radiation over the Ashanti Region of Ghana. *Journal of Solar Energy*, *2014*, 1–6. https://doi.org/10.1155/2014/897970

Raziei, T. (2021). Revisiting the Rainfall Anomaly Index to serve as a Simplified Standardized Precipitation Index. *Journal of Hydrology*, *602*. https://doi.org/10.1016/j.jhydrol.2021.126761

Riahi, K., van Vuuren, D. P., Kriegler, E., Edmonds, J., O'Neill, B. C., Fujimori, S., Bauer, N., Calvin, K., Dellink, R., Fricko, O., Lutz, W., Popp, A., Cuaresma, J. C., KC, S., Leimbach, M., Jiang, L., Kram, T., Rao, S., Emmerling, J., … Tavoni, M. (2017). The Shared Socioeconomic Pathways and their energy, land use, and greenhouse gas emissions implications: An overview. *Global Environmental Change*, *42*, 153–168. https://doi.org/10.1016/j.gloenvcha.2016.05.009

Roshani, S. H., Kumar, P., Masroor, M., Rahaman, M. H., Rehman, S., Ahmed, R., & Sahana, M. (2022). Forest vulnerability to climate change: A review for future research framework. *Forest MDPI*, *13*(6), 917.

Rubel, F., & Kottek, M. (2010). Observed and projected climate shifts 1901-2100 depicted by world maps of the Köppen-Geiger climate classification. *Meteorologische Zeitschrift*, *19*(2), 135–141. https://doi.org/10.1127/0941-2948/2010/0430

Saharia, M., Kirstetter, P. E., Vergara, H., Gourley, J. J., Emmanuel, I., & Andrieu, H. (2021). On the Impact of Rainfall Spatial Variability, Geomorphology, and Climatology on Flash Floods. *Water Resources Research*, *57*(9). https://doi.org/10.1029/2020WR029124

Saini, A., Sahu, N., Duan, W., Kumar, M., Avtar, R., Mishra, M., Kumar, P., Pandey, R., & Behera, S. (2022). Unraveling Intricacies of Monsoon Attributes in Homogenous Monsoon Regions of India. *Frontiers in Earth Science*, *10*. https://doi.org/10.3389/feart.2022.794634

Sanogo, S., Fink, A. H., Omotosho, J. A., Ba, A., Redl, R., & Ermert, V. (2015). Spatio-temporal characteristics of the recent rainfall recovery in West Africa. *International Journal of Climatology*, *35*(15), 4589–4605. https://doi.org/10.1002/joc.4309

Sathya, R., & Abraham, A. (2013). Comparison of Supervised and Unsupervised Learning Algorithms for Pattern Classification. *International Journal of Advanced Research in Artificial Intelligence. 2(2).* www.ijarai.thesai.org

Schulla, J. (2014). *Model Description WaSiM (Water balance Simulation Model).*

Schuol, J., Abbaspour, K. C., Yang, H., Srinivasan, R., & Zehnder, A. J. B. (2008). Modeling blue and green water availability in Africa. *Water Resources Research*, *44*(7). https://doi.org/10.1029/2007WR006609

Seibert, J., & Vis, M. J. P. (2012). Teaching hydrological modeling with a user-friendly catchment-runoff-model software package. *Hydrology and Earth System Sciences*, *16*(9), 3315–3325. https://doi.org/10.5194/hess-16-3315-2012

Sen, P. K. (1968). Estimates of the Regression Coefficient Based on Kendall's Tau. *Journal of the American Statistical Association*, *63*(324), 1379–1389. https://doi.org/10.1080/01621459.1968.10480934

Shen, G., & Hwang, S. N. (2019). Spatial–Temporal snapshots of global natural disaster impacts Revealed from EM-DAT for 1900-2015. *Geomatics, Natural Hazards and Risk*, *10*(1), 912–934. https://doi.org/10.1080/19475705.2018.1552630

Shen, Z. Y., Chen, L., & Chen, T. (2012). Analysis of parameter uncertainty in hydrological and sediment modeling using GLUE method: A case study of SWAT model applied to Three Gorges Reservoir Region, China. *Hydrology and Earth System Sciences*, *16*(1), 121–132. https://doi.org/10.5194/hess-16-121-2012

Sheng, Y., Shah, C. A., & Smith, L. C. (2008). Automated image registration for hydrologic change detection in the lake-rich arctic. *IEEE Geoscience and Remote Sensing Letters*, *5*(3), 414–418. https://doi.org/10.1109/LGRS.2008.916646

Sillmann, J., Kharin, V. V., Zhang, X., Zwiers, F. W., & Bronaugh, D. (2013). Climate extremes indices in the CMIP5 multimodel ensemble: Part 1. Model evaluation in the present climate. *Journal of Geophysical Research Atmospheres*, *118*(4), 1716–1733. https://doi.org/10.1002/jgrd.50203

Sinharoy, S. S., Pittluck, R., & Clasen, T. (2019). Review of drivers and barriers of water and sanitation policies for urban informal settlements in low-income and middle-income countries. *Utilities Policy*, *60*. https://doi.org/10.1016/j.jup.2019.100957

Smith, J. A., Baeck, M. L., Miller, A. J., & Claggett, E. L. (2024). Rainfall Frequency Analysis Based on Long-Term High-Resolution Radar Rainfall Fields: Spatial Heterogeneities and Temporal Nonstationarities. *Water Resources Research*, *60*(3). https://doi.org/10.1029/2023WR035640

Snapir, B., Simms, D. M., & Waine, T. W. (2017). Mapping the expansion of galamsey gold mines in the cocoa growing area of Ghana using optical remote sensing. *International Journal of Applied Earth Observation and Geoinformation*, *58*, 225–233. https://doi.org/10.1016/J.JAG.2017.02.009

Sridhar, M. B., & Sathyanathan, R. (2020). Assessing the spatial impact of urbanization on surface water bodies using remote sensing and GIS. *IOP Conference Series: Materials Science and Engineering*, *912*(6). https://doi.org/10.1088/1757-899X/912/6/062069

Stanturf, J. A. (2015). Future landscapes: opportunities and challenges. *New Forests*, *46*(5–6), 615–644. https://doi.org/10.1007/s11056-015-9500-x

Tabari, H. (2020). Climate change impact on flood and extreme precipitation increases with water availability. *Scientific Reports*, *10*(1). https://doi.org/10.1038/s41598-020-70816-2

Tahiru, A. A., Doke, D. A., & Baatuuwie, B. N. (2020). Effect of land use and land cover changes on water quality in the Nawuni Catchment of the White Volta Basin, Northern Region, Ghana. *Applied Water Science*, *10*(8). https://doi.org/10.1007/s13201-020-01272-6

Tamoffo, A. T., Vondou, D. A., Pokam, W. M., Haensler, A., Yepdo, Z. D., Fotso-Nguemo, T. C., Tchotchou, L. A. D., & Nouayou, R. (2019). Daily characteristics of Central African rainfall in the REMO model. *Theoretical and Applied Climatology*, *137*(3–4), 2351–2368. https://doi.org/10.1007/s00704-018-2745-5

Tappan, G. G., Cushing, W. M., Cotillon, S. E., Mathis, M. L., Hutchinson, J. A., Herrmann, S. M., & Dalsted, K. J. (2016). *West Africa Land Use Land Cover Time Series: U.S. Geological Survey data release.*

Tarek, M., Brissette, F. P., & Arsenault, R. (2020). Evaluation of the ERA5 reanalysis as a potential reference dataset for hydrological modelling over North America. *Hydrology and Earth System Sciences*, *24*(5), 2527–2544. https://doi.org/10.5194/hess-24-2527-2020

Tay, C. (2015). *Hydrogeochemical Processes Influencing Groundwater Quality within the Lower Pra Basin, Ghana 2015 An appraisal of mercury (Hg) and Aluminium (Al) levels in treated drinking water supply in mining areas in Ghana: The case of Daboase and its environs View project Hydrogeochemical processes influencing groundwater quality within the Lower Pra Basin, Ghana. View project*. https://doi.org/10.13140/RG.2.2.25616.56320

Tay, C. K., Hayford, E. K., & Hodgson, I. O. A. (2017). Application of multivariate statistical technique for hydrogeochemical assessment of groundwater within the Lower Pra Basin, Ghana. *Applied Water Science*, *7*(3), 1131–1150. https://doi.org/10.1007/s13201-017-0540-6

Tay, C. K., Hayford, E., Hodgson, I. O., & Kortatsi, B. K. (2015). Hydrochemical appraisal of groundwater evolution within the Lower Pra Basin, Ghana: a hierarchical cluster analysis (HCA) approach. *Environmental Earth Sciences*, *73*(7), 3579–3591. https://doi.org/10.1007/s12665-014-3644-4

Tay, C. K., Kortatsi, B. K., Hayford, E., & Hodgson, I. O. (2014). Origin of major dissolved ions in groundwater within the Lower Pra Basin using groundwater geochemistry, source-rock deduction and stable isotopes of 2H and 18O. *Environmental Earth Sciences*, *71*(12), 5079–5097. https://doi.org/10.1007/s12665-013-2912-z

Taye, M. T., Ntegeka, V., Ogiramoi, N. P., & Willems, P. (2011). Assessment of climate change impact on hydrological extremes in two source regions of the Nile River Basin. *Hydrology and Earth System Sciences*, *15*(1), 209–222. https://doi.org/10.5194/hess-15-209-2011

Tekleab, S., Uhlenbrook, S., Mohamed, Y., Savenije, H. H. G., Temesgen, M., & Wenninger, J. (2011). Water balance modeling of Upper Blue Nile catchments using a top-down approach. *Hydrology and Earth System Sciences*, *15*(7), 2179–2193. https://doi.org/10.5194/hess-15-2179-2011

Tetzlaff, D., & Uhlenbrook, S. (2005). Hydrology and Earth System Sciences Significance of spatial variability in precipitation for process-oriented modelling: results from two nested catchments using radar and ground station data. In *Hydrology and Earth System Sciences* (Vol. 9). www.copernicus.org/EGU/hess/hess/9/29/SRef-ID:1607-7938/hess/2005-9-29EuropeanGeosciencesUnion

Thomas, M. L. H., Channon, A. A., Bain, R. E. S., Nyamai, M., & Wright, J. A. (2020). Household-reported availability of drinking water in Africa: A systematic review. In *Water (Switzerland)* (Vol. 12, Issue 9). MDPI AG. https://doi.org/10.3390/W12092603

Thorne, K. M., Elliott-Fisk, D. L., Freeman, C. M., Bui, T. V. D., Powelson, K. W., Janousek, C. N., Buffington, K. J., & Takekawa, J. Y. (2017). Are coastal managers ready for climate change? A case study from estuaries along the Pacific coast of the United States. *Ocean and Coastal Management*, *143*, 38–50. https://doi.org/10.1016/j.ocecoaman.2017.02.010

Thrasher, B., Maurer, E. P., McKellar, C., & Duffy, P. B. (2012). Technical Note: Bias correcting climate model simulated daily temperature extremes with quantile mapping. *Hydrology and Earth System Sciences*, *16*(9), 3309–3314. https://doi.org/10.5194/hess-16-3309-2012

Tibangayuka, N., Mulungu, D. M. M., & Izdori, F. (2022). Evaluating the performance of HBV, HEC-HMS and ANN models in simulating streamflow for a data scarce high-humid tropical catchment in Tanzania. *Hydrological Sciences Journal*, *67*(14), 2191–2204. https://doi.org/10.1080/02626667.2022.2137417

Tsakiris, G., Pangalou, D., & Vangelis, H. (2007). Regional drought assessment based on the Reconnaissance Drought Index (RDI). *Water Resources Management*, *21*(5), 821–833. https://doi.org/10.1007/s11269-006-9105-4

Tsunetaka, H., Murakami, W., Nakao, K., & Mtibaa, S. (2024). Evaluation of the impact of climate change on rainfall for potential landslide triggering in Japan. *Earth Surface Processes and Landforms*. https://doi.org/10.1002/esp.6050

Tufuor, J. K., Dodoo, D. K., Armah, A. K., Darpaah, G. A., & Essumang, D. K. (2007). Some chemical characteristics of the River Pra estuary in the western region of Ghana. *Bull. Chem. Soc. Ethiop*, *21*(3), 341–348.

Türkeğ, M., Serap Akgündüz, A., & Demirörs, Z. (2009). *Palmer Kuraklık Ġndisi'ne Göre Ġç Anadolu Bölgesi'nin Konya Bölümü'ndeki Kurak Dönemler ve Kuraklık ġiddeti Drought periods and severity over the Konya Sub-region of the Central Anatolia Region according to the Palmer Drought Index*.

Usman, M., Ndehedehe, C. E., Manzanas, R., Ahmad, B., & Adeyeri, O. E. (2021). Impacts of climate change on the hydrometeorological characteristics of the soan river basin, pakistan. *Atmosphere*, *12*(6). https://doi.org/10.3390/atmos12060792

Van Lanen, H. A. J., Laaha, G., Kingston, D. G., Gauster, T., Ionita, M., Vidal, J. P., Vlnas, R., Tallaksen, L. M., Stahl, K., Hannaford, J., Delus, C., Fendekova, M., Mediero, L., Prudhomme, C., Rets, E., Romanowicz, R. J., Gailliez, S., Wong, W. K., Adler, M. J., … Van Loon, A. F. (2016). Hydrology needed to manage droughts: the 2015 European case. In *Hydrological*

Processes (Vol. 30, Issue 17, pp. 3097–3104). John Wiley and Sons Ltd. https://doi.org/10.1002/hyp.10838

Vancutsem, C., Achard, F., Pekel, J.-F., Vieilledent, G., Carboni, S., Simonetti, D., Gallego, J., Aragão, L. E. O. C., & Nasi, R. (2021). Long-term (1990-2019) monitoring of forest cover changes in the humid tropics. In *Sci. Adv* (Vol. 7). https://www.science.org

Vandal, T., Kodra, E., & Ganguly, A. R. (2019). Intercomparison of machine learning methods for statistical downscaling: the case of daily and extreme precipitation. *Theoretical and Applied Climatology*, *137*(1–2), 557–570. https://doi.org/10.1007/s00704-018-2613-3

Vandal, T., Kodra, E., Ganguly, S., Michaelis, A., Nemani, R., & Ganguly, A. R. (2017). DeepSD: Generating high resolution climate change projections through single image super-resolution. *Proceedings of the ACM SIGKDD International Conference on Knowledge Discovery and Data Mining*, *Part F129685*, 1663–1672. https://doi.org/10.1145/3097983.3098004

Veldhuis, M. P., Martinez-Garcia, R., Deblauwe, V., & Dakos, V. (2022). Remotely-sensed slowing down in spatially patterned dryland ecosystems. *Ecography*, *2022*(10). https://doi.org/10.1111/ecog.06139

Vicente-Serrano, S. M., Beguería, S., & López-Moreno, J. I. (2010). A multiscalar drought index sensitive to global warming: The standardized precipitation evapotranspiration index. *Journal of Climate*, *23*(7), 1696–1718. https://doi.org/10.1175/2009JCLI2909.1

Wagner, S., Kunstmann, H., & Bárdossy, A. (2006). Model based distributed water balance monitoring of the White Volta catchment in West Africa through coupled meteorological-hydrological simulations. *Advances in Geosciences*, *9*, 39–44. https://doi.org/10.5194/adgeo-9-39-2006

Wanishsakpong, W., & Notodiputro, K. A. (2018). Locally weighted scatter-plot smoothing for analysing temperature changes and patterns in Australia. *Meteorological Applications*, *25*(3), 357–364. https://doi.org/10.1002/met.1702

Water Resource Commission. (2012). *Republic of Ghana Water Resources Commission National Integrated Water Resources Management (IWRM) Plan*.

Wemegah, C. S., Yamba, E. I., Aryee, J. N. A., Sam, F., & Amekudzi, L. K. (2020). Assessment of urban heat island warming in the greater accra region. *Scientific African*, *8*, e00426. https://doi.org/10.1016/J.SCIAF.2020.E00426

Werther, M., Spyrakos, E., Simis, S. G. H., Odermatt, D., Stelzer, K., Krawczyk, H., Berlage, O., Hunter, P., & Tyler, A. (2021). Meta-classification of remote sensing reflectance to estimate trophic status of inland and nearshore waters. . *ISPRS Journal of Photogrammetry and Remote Sensing. 176, 109–126.*

Westra, S., Fowler, H. J., Evans, J. P., Alexander, L. V., Berg, P., Johnson, F., Kendon, E. J., Lenderink, G., & Roberts, N. M. (2014). Future changes to the intensity and frequency of short-duration extreme rainfall. In *Reviews of Geophysics* (Vol. 52, Issue 3, pp. 522–555). Blackwell Publishing Ltd. https://doi.org/10.1002/2014RG000464

Wheeler, C. E., Omeja, P. A., Chapman, C. A., Glipin, M., Tumwesigye, C., & Lewis, S. L. (2016). Carbon sequestration and biodiversity following 18 years of active tropical forest restoration. *Forest Ecology and Management, 373,* 44–55. https://doi.org/10.1016/j.foreco.2016.04.025

Wilby, R. L., & Dawson, C. W. (2013). The statistical downscaling model: Insights from one decade of application. *International Journal of Climatology*, *33*(7), 1707–1719. https://doi.org/10.1002/joc.3544

Wilby, R. L., & Wigley, T. M. L. (1997). *Downscaling general circulation model output: a review of methods and limitations*.

Wilby, R. L., Dawson, C. W., Murphy, C., O'Connor, P., & Hawkins, E. (2014). The Statistical DownScaling Model -Decision Centric (SDSM-DC): Conceptual basis and applications. *Climate Research*, *61*(3), 251–268. https://doi.org/10.3354/cr01254

Winkler, K., Fuchs, R., Rounsevell, M., & Herold, M. (2021). Global land use changes are four times greater than previously estimated. *Nature Communications*, *12*(1). https://doi.org/10.1038/s41467-021-22702-2

WMO. (2012). *Standardized Precipitation Index User Guide* (M. Svoboda, M. Hayes, & D. Wood, Eds.; (WMO-No. 1090)). World Meteorological Organization. https://public.wmo.int/en/resources/library/standardized-precipitation-index-user-guide

Wood, A. W., Leung, L. R., Sridhar, V., & Lettenmaier, D. P. (2004). *Hydrologic implications of dynamical and statistical approaches to downscaling climate model outputs*.

World Bank. (2010). The Costs to Developing Countries of Adapting to Climate Change: New Methods and Estimates. Washington, DC: World Bank. Accessible at: http://www.worldbank.org/eacc.

World Bank. (2021). Climate Risk Country Profile-Ghana. Accessed on 20th November 2025 at: https://www.climateknowledgeportal.worldbank.org/sites/default/files/country-profiles/15857-WB_Ghana%20Country%20Profile-WEB.pdf

Wriedt, G., Van der Velde, M., Aloe, A., & Bouraoui, F. (2009). Estimating irrigation water requirements in Europe. *Journal of Hydrology*, *373*(3–4), 527–544. https://doi.org/10.1016/j.jhydrol.2009.05.018

Wu, L., Jiang, J., Li, G. X., & Ma, X. Y. (2018). Characteristics of pulsed runoff-erosion events under typical rainstorms in a small watershed on the Loess Plateau of China. *Scientific Reports*, *8*(1). https://doi.org/10.1038/s41598-018-22045-x

WWAP. (2020). *UNESCO, UN-Water, 2020: United Nations World Water Development Report 2020: Water and Climate Change, Paris, UNESCO.* https://unesdoc.unesco.org/ark:/48223/pf0000372882

Xin, X., Wu, T., Zhang, J., Yao, J., & Fang, Y. (2020). Comparison of CMIP6 and CMIP5 simulations of precipitation in China and the East Asian summer monsoon. *International Journal of Climatology*, *40*(15), 6423–6440. https://doi.org/10.1002/joc.6590

Yagbasan, O., Demir, V., & Yazicigil, H. (2020). Trend analyses of meteorological variables and lake levels for two shallow lakes in central Turkey. *Water (Switzerland)*, *12*(2). https://doi.org/10.3390/w12020414

Yeh, S. W., Wang, G., Cai, W., & Park, R. J. (2022). Diversity of ENSO-Related Surface Temperature Response in Future Projection in CMIP6 Climate Models: Climate Change Scenario Versus ENSO Intensity. *Geophysical Research Letters*, *49*(4). https://doi.org/10.1029/2021GL096135

Young, R., Chen, W., Quazi, A., Parry, W., Wong, A., & Poon, S. K. (2020). The relationship between project governance mechanisms and project success: An international data set. *International Journal of Managing Projects in Business*, *13*(7), 1496–1521. https://doi.org/10.1108/IJMPB-10-2018-0212

Yue, S., Pilon, P., & Cavadias, G. (2002). *Power of the Mann±Kendall and Spearman's rho tests for detecting monotonic trends in hydrological series*. www.elsevier.com/locate/jhydrol

APPENDIX

1. Probability density function of extreme event

Below are the results from the PDFs for all the stations with 1, 5, 15, and 20 days of aggregation using observed, historical, and future scenarios (SSP1-26 & SSP3-70, Figure 6.15A-Figure 6.15K). The plots are for the following stations: Sekyere-heman, Twifo-Praso, Offinso, Owabi, Mfensi, Daboasi, Dunkwa, Akim-Oda, Assin-Praso, Adiembra, and Kade.

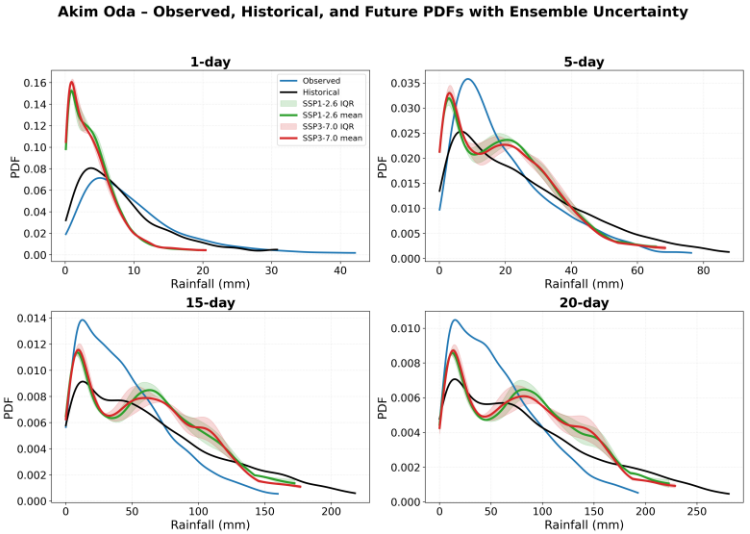

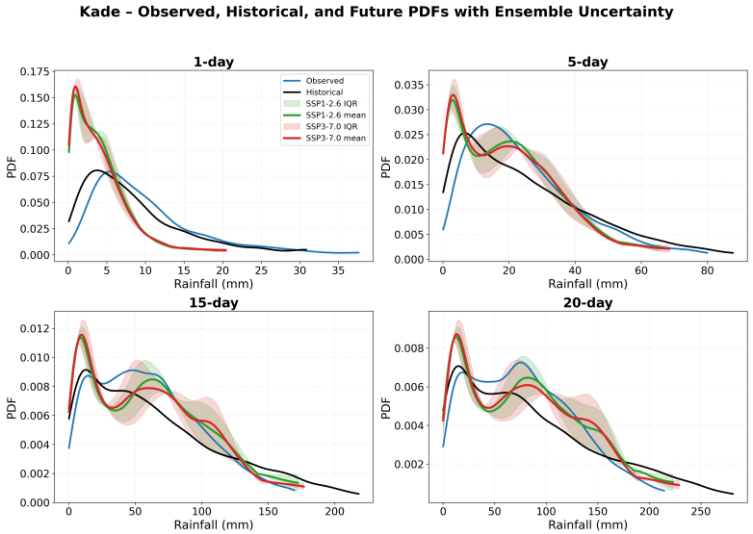

Adiembra – Observed, Historical, and Future PDFs with Ensemble Uncertainty

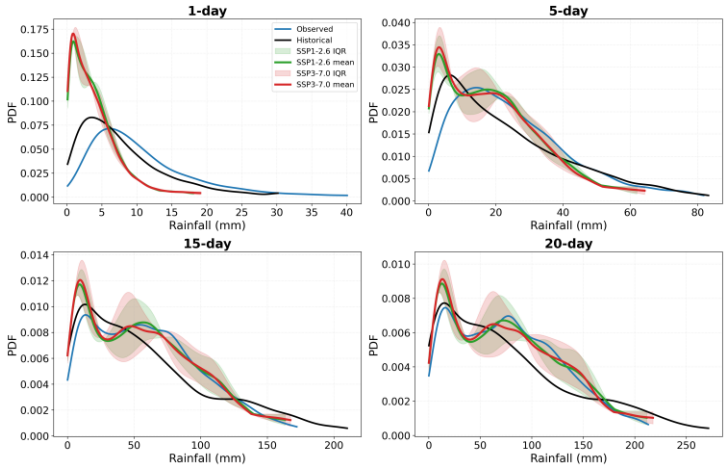

Assin-Praso – Observed, Historical, and Future PDFs with Ensemble Uncertainty

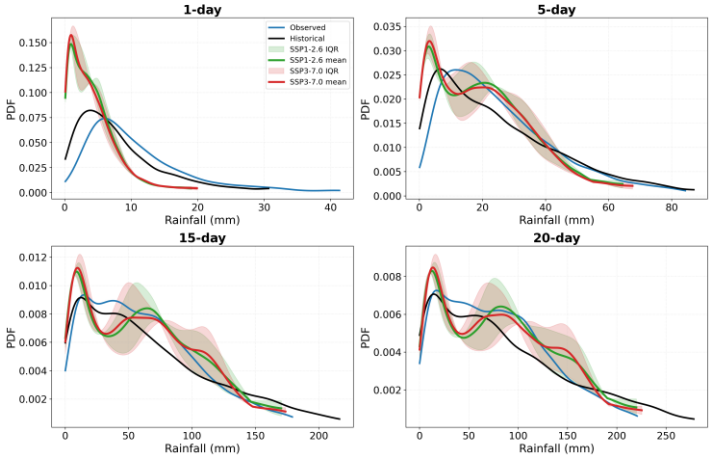

Twifo-Praso – Observed, Historical, and Future PDFs with Ensemble Uncertainty

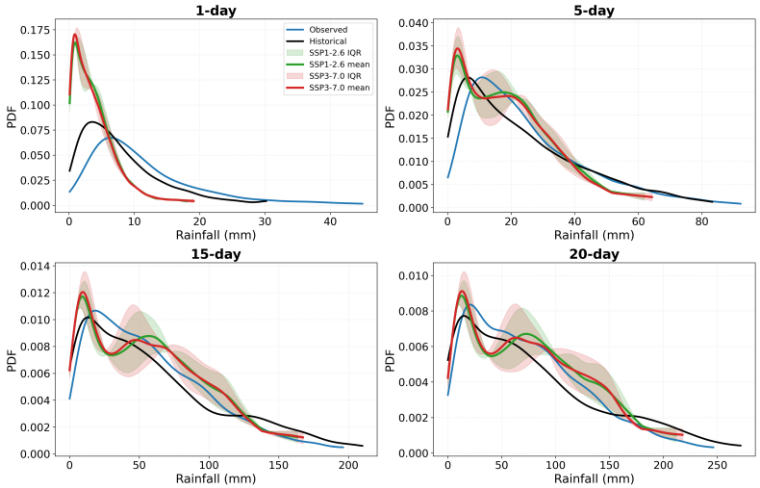

Daboasi – Observed, Historical, and Future PDFs with Ensemble Uncertainty

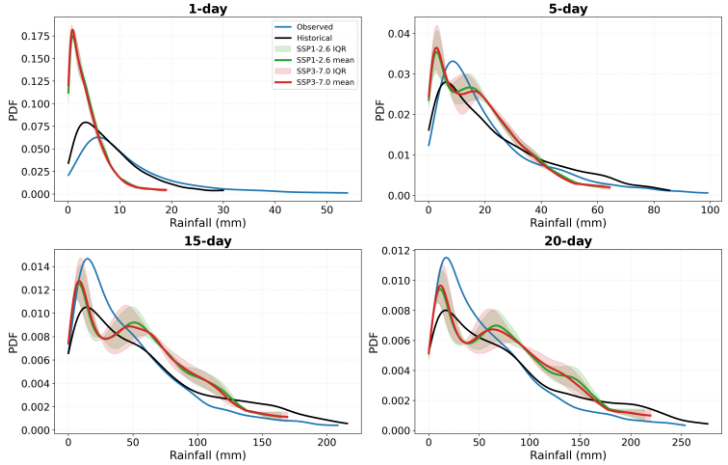

Dunkwa – Observed, Historical, and Future PDFs with Ensemble Uncertainty

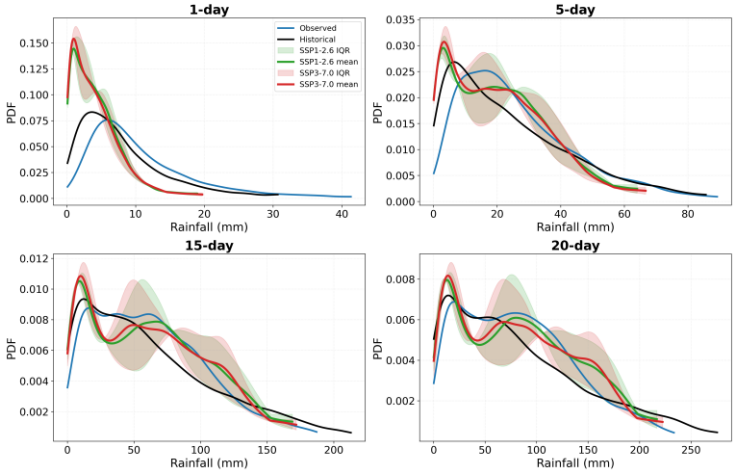

Mfensi – Observed, Historical, and Future PDFs with Ensemble Uncertainty

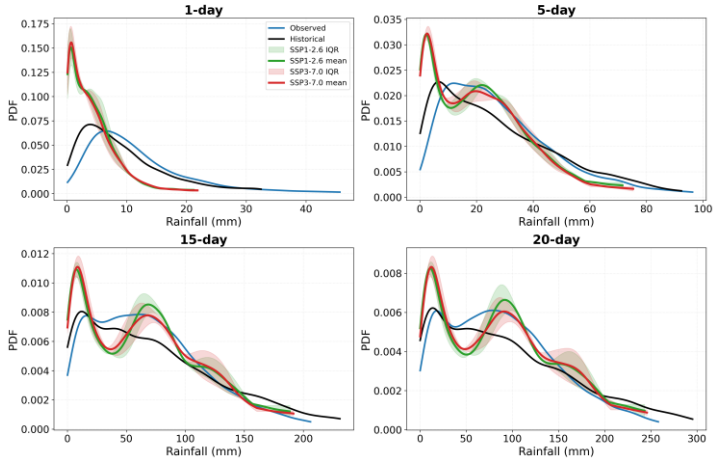

Offinso – Observed, Historical, and Future PDFs with Ensemble Uncertainty

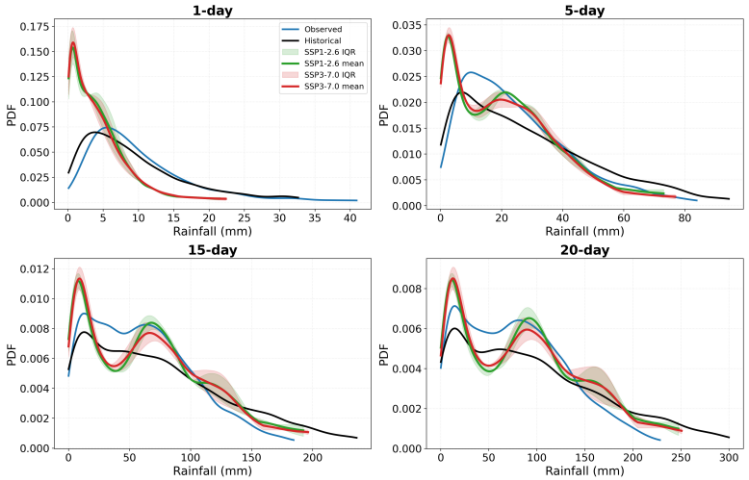

Owabi – Observed, Historical, and Future PDFs with Ensemble Uncertainty

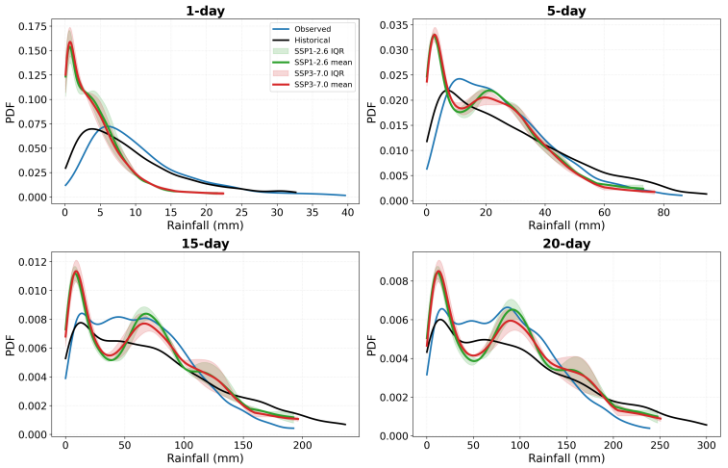

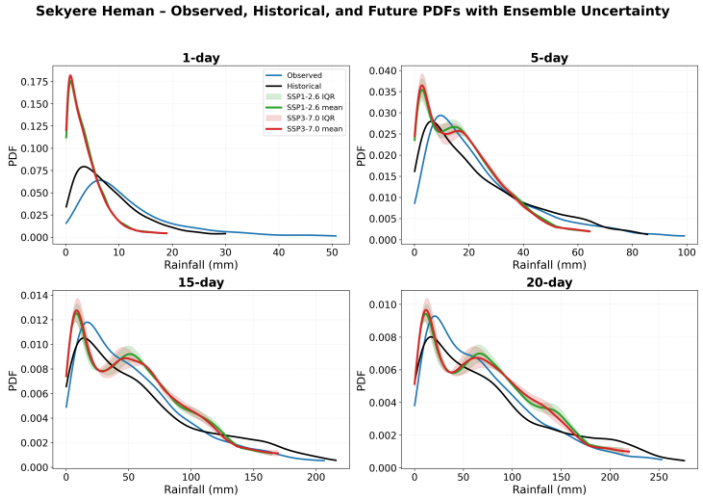

2. Rainfall variability and drought conditions

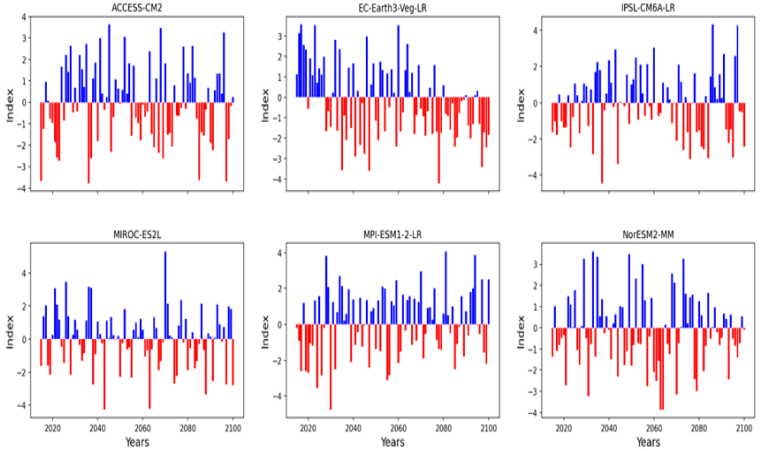

Figure 2A: Rainfall Anomaly Index (RAI) for the Pra River Basin under SSP1-2.6

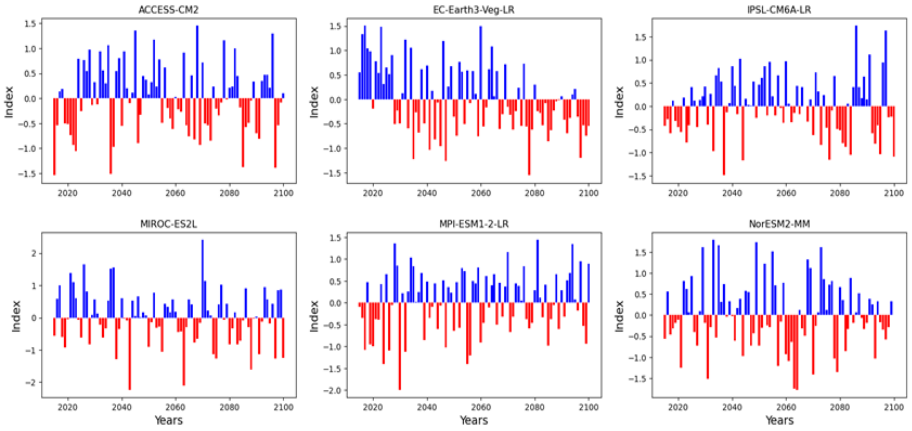

Figure 2B: Standard Precipitation Index (SP1-1) for the Pra River Basin (2015-2100) under SSP1.2-6.

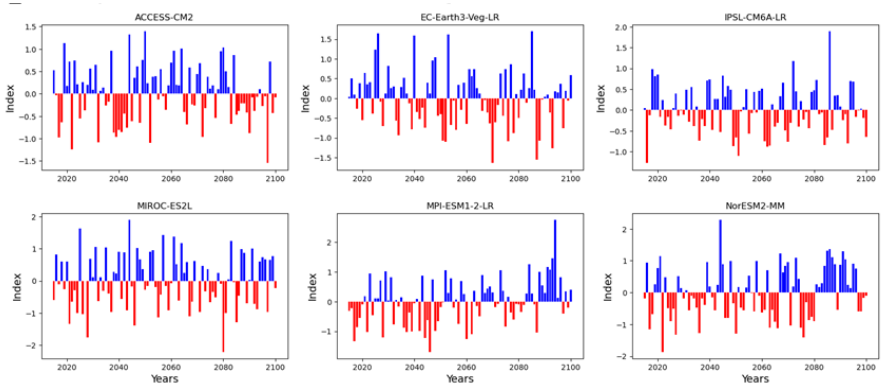

Figure 2C: Standard Precipitation Index (SP1-1) for the Pra River Basin (2015-2100) under under SSP3-7.0.

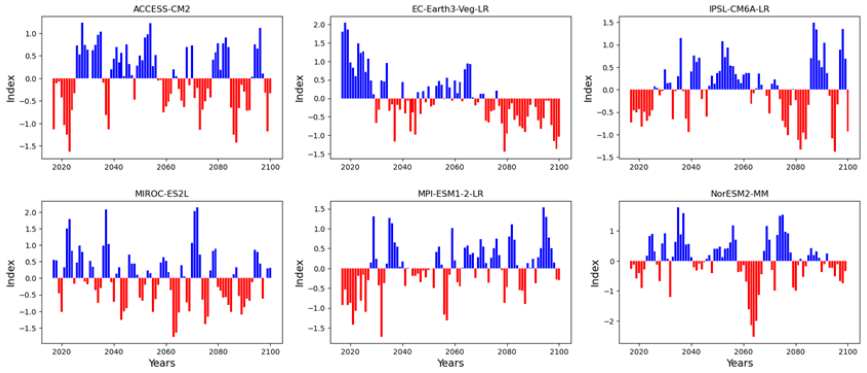

Figure 2D: Standard Precipitation Index (SP1-3) for the Pra River Basin (2015-2100) under SSP1-2.6.

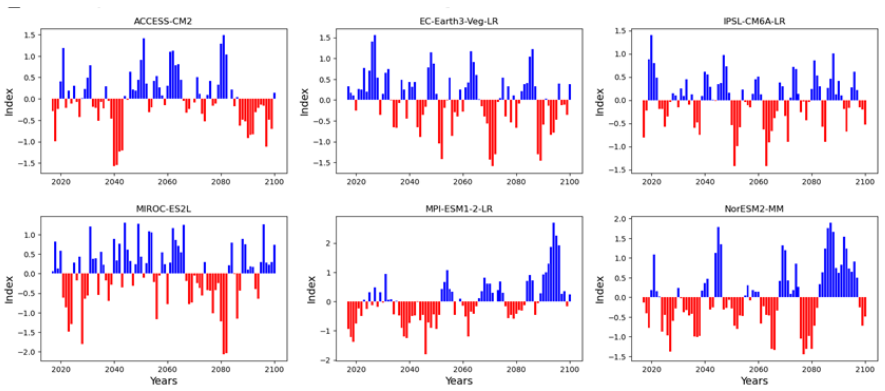

Figure 2E: Standard Precipitation Index (SP1-1) for the Pra River Basin (2015-2100) under SSP3-7.0

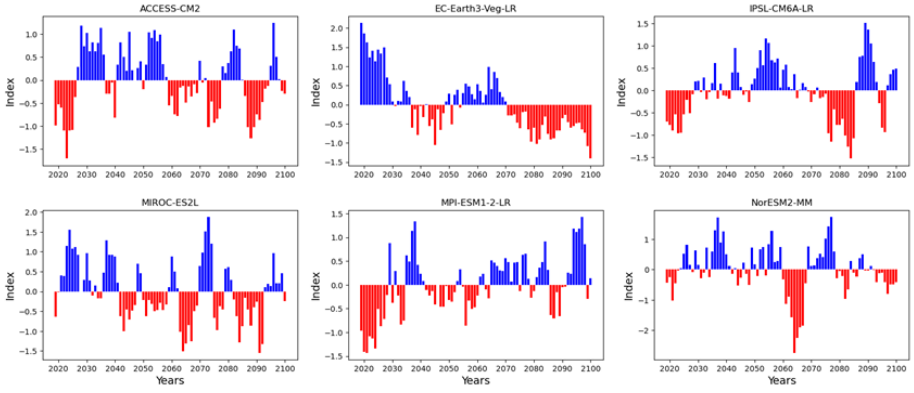

Figure 2F: Standard Precipitation Index (SP1-5) for the Pra River Basin (2015-2100) under SSP1-2.6.

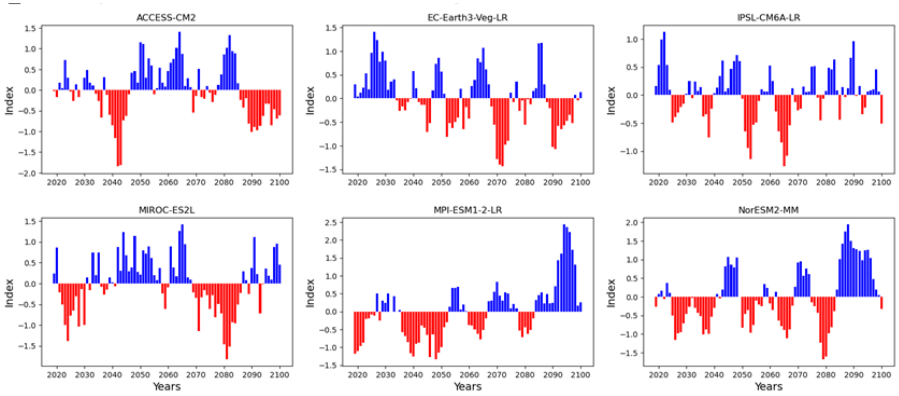

Figure 2G: Standard Precipitation Index (SP1-1) for the Pra River Basin (2015-2100) under SSP3-7.0.

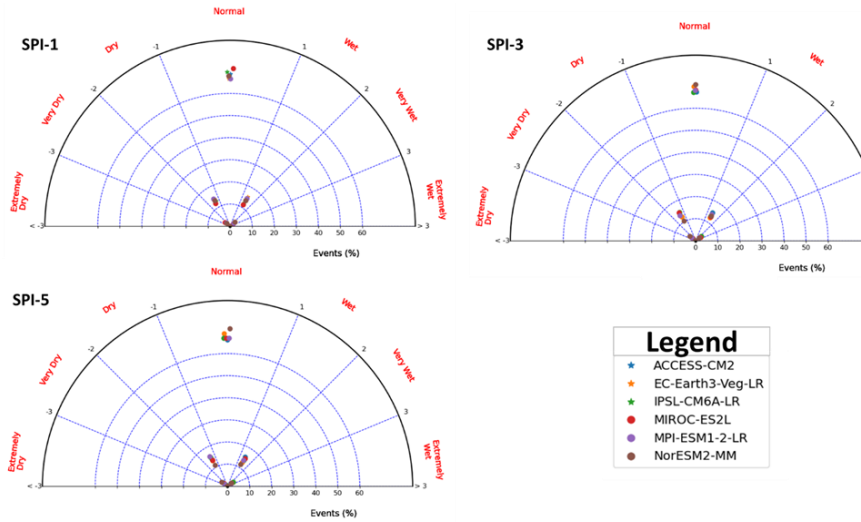

Figure 2H: A polar drought index projection (2015-2100) using the Standard Precipitation Index (SP1-1, SP1-3, SP1-5) for the Pra River Basin under SSP1-2.6.

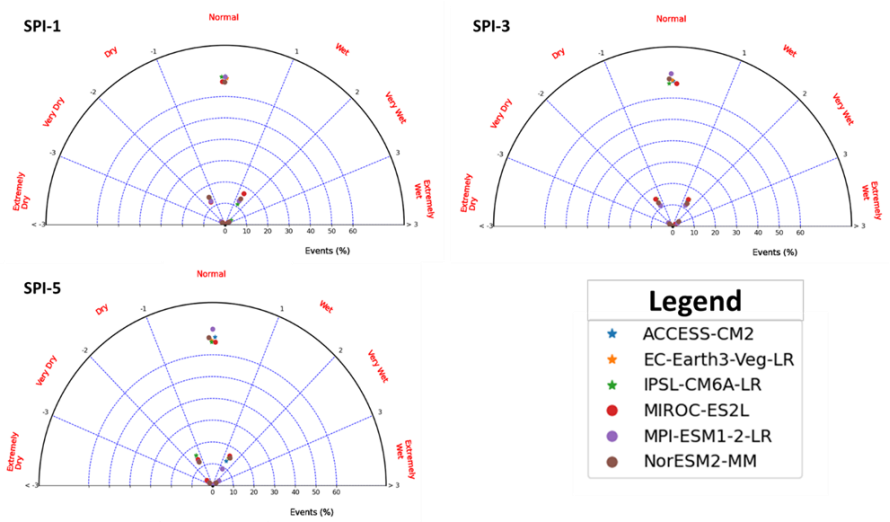

Figure 2H: A polar drought index projection (2015-2100) using the Standard Precipitation Index (SP1-1, SP1-3, SP1-5) for the Pra River Basin under SSP3-7.0

ANNEX

Annex 1: List of Publications

As the Main Author in the Framework of the Thesis

1. **Agbenorhevi, A. E.**, Klaus, J., Amekudzi, L.K., Kelome, N. C., Kouassi, V.B.S., Biney, E. (2025). Rainfall Onset Timing and Hydroclimatic Variability in a Tropical Catchment: Insights from Observations and Climate Projection **(submitted Article Paper, Meteorological Applications)**

2. **Agbenorhevi, A. E**., Amekudzi, L. K., Kèlomé, N. C., Biney, E., & Annan, E. (2024). Analyzing land use and land cover change in the Pra River Basin: A multi-tool approach for informed decision-making. *Environmental Challenges*, *15*, 100922. doi: https://doi.org/10.1016/j.envc.2024.100922

3. **Agbenorhevi, A. E,** Klaus, J., Amekudzi, L. K, Kelome, N. C, Biney, E., & Annan, E. (2024). Predicting Global Change impacts on streamflow dynamics using distributed hydrological modeling in a data-scarce nested tropical catchment in West Africa. In *EGU General Assembly Conference Paper* (p. 482). doi: 10.5194/egusphere-egu24-482

4. **Agbenorhevi, A E**; Annan, E; Biney, E (2024), "Spatio-temporal assessment of land use and cover classification with Google Earth Engine ", *Mendeley Data*, V1, doi: 10.17632/9hcwfgf6rs.1 https://data.mendeley.com/datasets/9hcwfgf6rs/1

5. **Agbenorhevi, A E**; Biney, E; Annan, E (2023), "Land Use land cover classification using Google Earth Engine ", *Mendeley Data*, V1, doi: 10.17632/cj3kg69psv.1 https://data.mendeley.com/datasets/cj3kg69psv/1

As Co-Author during the Ph.D period

1. Biney, E., Sakyi-Adjei, V., **Agbenorhevi, A.E.** (2025). Spatio-Temporal Dynamics of Urban Expansion and Ecosystem Service Value Decline in a Coastal Metropolis: Evidence from Sekondi–Takoradi, Ghana (1991–2023) **(Submitted, Sustainability**)

2. Sekyere, K.K.C., Odoi-Yorke, F., Baah, B., Oppon, J. A., **Agbenorhevi, A.E**., Atepor, L. (2025). Mapping urban climate change research: Insights from 20 years of global research trends, thematic evolution, and future perspectives. *Nature-Based Solutions* https://doi.org/10.1016/j.nbsj.2025.100271

3. Biney, E., Mintah, B. A., Ankomah, E., **Agbenorhevi, A. E**., Yankey, D. B., & Annan, E. (2024). Sustainability assessment of groundwater in south-eastern parts of the western region of Ghana for water supply. *Cleaner Water*, *1*, 100007. doi: https://doi.org/10.1016/j.clwat.2024.100007

4. Annan, E., Amponsah, W., Adjei, K. A., Disse, M., Hounkpè, J., Biney, E., **Agbenorhevi, A. E** & Agyare, W. A. (2024). Spatio-temporal Land Use and Land Cover Change Assessment: Insights from the Ouémé River Basin. *Scientific African*, e02262. doi: https://doi.org/10.1016/j.sciaf.2024.e02262

5. Biney, E., Forkuo, E. K., Poku-Boansi, M., Asare, Y. M., Hackman, K. O., Yankey, D. B., **Agbenorhevi, A. E** & Annan, E. (2024). A comprehensive analysis and future projection of land use and land cover dynamics in a fast-growing city: A case study of Sekondi-Takoradi metropolis, Ghana. *Scientific African*, *24*, e02207.doi: https://doi.org/10.1016/j.sciaf.2024.e02207

6. Biney, E., Forkuo, E. K., Poku-Boansi, M., Hackman, K. O., Harris, E., Asare, Y. M., ... & **Agbenorhevi, A. E**. (2024). Analyzing the spatio-temporal pattern of urban growth and its influence on urban heat islands in the Sekondi-Takoradi metropolis, Ghana. *Scientific African*, *26*, e02366. doi: https://doi.org/10.1016/j.sciaf.2024.e02366

7. Wooden, P., Lerback, J. C., & **Agbenorhevi, A. E**. (2024). International trends in authorship in AGU journals, 2010-2023. *AGU24 Conference paper.* https://agu.confex.com/agu/agu24/meetingapp.cgi/Paper/1761574

Annex 2: List of Conferences/Workshops/Training

Conferences Attended During Ph.D Period

1. **Agbenorhevi, E.A** (2024). *Evaluating Climate Projections to Mitigate Water Scarcity in Ghana's Pra River Basin under Climate Change.* World PhD Students and Postdoctoral Researchers Summit "Meeting the challenges of Climate Change 2024 on 27th November" Hamburg University of Applied Sciences, Hamburg, Germany (Online Presentation).

2. **Agbenorhevi, A.E**., Kelome, N.C., Amekudzi, K.L., Klaus, J. (2024). *Understanding Global Change Impact On Water Resources in a Tropical Ecosystem. A Catchment-scale Assessment of the Pra River*. GIUB Science Pitch 2024 on 6th November, University of Bonn, Germany (Oral Presentation).

3. **Agbenorhevi, A.E**., Klaus, J., Amekudzi, K.L., Kelome, N.C. (2024). *Predicting Global Change impacts on streamflow dynamics using EcH2O-iso model in a data-scarce nested tropical catchment in West Africa.* Hydrology Conference 2024 from 4th-6th June: Intermittency in Headwater Streams. University of Bonn, Germany (Poster Presentation).

4. **Agbenorhevi, A.E**., Klaus, J., Amekudzi, K.L., Kelome, N.C., Biney, E., Ernestina, A. (2024). *Predicting Global Change impacts on streamflow dynamics using distributed hydrological modeling in a data-scarce nested tropical catchment in West Africa.* European Geoscience Union (EGU) General Assembly 2024 from 14th -19th April, Vienna, Austria (Poster Presentation).

5. **Agbenorhevi, A.E**., Kelome, N.C., Amekudzi, K.L. (2023). *Preparing for the Hydroclimatic Impact on Water Resources of the Pra Basin: State-of-the-Art Review*. World Climate Research Programme. Open Science Conference from 23rd-27th October, Kigali, Rwanda (Online Presentation).

Workshops Attended During Ph.D Period

1. 1st African-European Workshop on Land Surface and Climate Change, University of Bonn, Germany, 05/2025
2. Ecohydrology Summer School 2024 (Eidgenössische Technische Hochschule (ETH)), Zürich, Switzerland 06/2024
3. ThESys-Situating Hydrological Modelling, Humboldt University, Berlin, Germany 09/2023
4. Climate Works Foundation on Just Transition Platform, Accra, Ghana 08/2022

Training Attended During Ph.D Period

1. Introduction to Supercomputing at JSC - Theory & Practice, Forschungszentrum Jülich, Germany 11/2024
2. Terrestrial Modelling and High-Performance Scientific Computing, Forschungszentrum Jülich, Germany 09/2024
3. Wheeler Institute GIS Workshop Series, Wheeler Institute for Business and Development, London, UK 05/2023.
4. WASCAL Training on Statistical Tool (R Studio), Accra, Ghana 03/2023
5. Joint WASCAL-ICTP Hands-on workshop on HPC technology for Climate Sciences. WASCAL Competence Center, Ouagadougou, Burkina Faso. 05/2022

Mr. Albert Elikplim Agbenorhevi is an early-career Ecohydrologist with a focus on climate science, land use change, and hydrology. Born in Ghana, a Christian, and married with one child. He got his Baccalaureate from Accra Academy in 2007. He earned a B.Sc. in Water and Sanitation from the University of Cape Coast, Ghana, in 2015, and an M.Sc. in Water Engineering from the Pan African University, Algeria, in 2018. Albert is a Ph.D. candidate at Université d'Abomey-Calavi, Benin, under the doctoral program in Climate Change and Water Resources of the West African Science Service Center on Climate Change and Adapted Land Use (WASCAL) since September 2022. Currently, he is a Research Fellow at the University of Bonn, Germany, and involved in the AGUA project: Assessing Global change impacts on streamflow dynamics. Albert has participated in international hydrological and GIS training programs, reviewer for Elsevier and the African Scientific Journals, and is actively engaged in professional organizations like AGU, EGU, IAHS, and WATSON. He has received scholarships, including the WASCAL Ph.D. Scholarship, Argelander Funding, Volkswagen Foundation, and Pan African Union Scholarship. He aims to contribute to sustainable water management and climate resilience in the tropics.

Abstract **:**

The impact of climate change (CC) and land use/cover (LULC) change in a data-scarce tropical catchment remains not fully understood. This poses a significant threat to progress toward achieving the UN Sustainable Development Goals on clean water and sanitation (Goal 6) and climate action (Goal 13). This study assesses their impact to provide a baseline for hydrological processes and sustainable water management. The study is carried out in the Pra River Basin by (i) applying the PRISMA, bibliometric and the VOSviewer systematic method to assess current knowledge on the CC and LULC at a basin scale (ii) utilising Google Earth Engine (GEE), Idrisi®Selva, and ArcMap to evaluate historical LULC (2007, 2015, and 2023) changes and project future (2030, 2063) trends across five land classification, and (iii) analysing climate change trends and projecting their impact on rainfall extremes and characterisation under the SSP1-2.6 and SSP3-7.0 climate scenarios. (iv) analysing the impact of LULC and CC on streamflow. Statistical metrics, including Overall accuracy, Kappa coefficient, Producer's Accuracy, User's Accuracy, NSE, MBE, and R, were used to evaluate the precision and performance of both land use change and climatic datasets of the basin. Findings indicate (i) an expected annual growth rate of 9.25% of research towards climate-land use-hydrology nexus (ii) an increasing deforestation and NV losses at the expense of CU/FL (13 %) and BU/BL (3%). Future projections point to continued conversion of NV and FO to CL and BU under the business-as-usual scenario, notably in the Northeast (Upper and Lower Offin, Twifo Praso) and South (Lower Pra) regions. (iii) Rainfall timing shows clear signals of wetter years delaying the centre of mass of rainfall at key stations, hinting at longer rainy seasons. The projected future climate for both SSP1-2.6 and SSP3-7.0 scenarios from 2021-2100 suggests uncertain onset and cessation dates in the Forest zones with short-duration events intensified. (iv) The combined effect of CC and LULC predicts annual water losses as a result of evapotranspiration and surface runoff under SSP3.7-0 throughout the century, with monthly variations up to ±24%. These findings highlight the urgent need for stringent management strategies to mitigate LULC

and climate change impacts on the PRB. It also provides a foundation for understanding the impact of these drivers on hydrological processes in water security and management planning for a basin that sustains 6.2 million people in Ghana.

***Keywords*:** Climate change, Hydrological extremes, Land use land cover change (LULC), Pra River Basin (PRB), Water Resource Management.